

Hyperglycemia-mediated onset of myocardial insulin resistance - unraveling molecular mechanisms and identifying therapeutic targets

by

Danzil Eugene Joseph

*Dissertation presented for the degree of Doctor of Philosophy
(Physiological Sciences) in the
Faculty of Natural Science at
Stellenbosch University*



Supervisor: Prof. M. Faadiel Essop

April 2014

Declaration

By submitting this thesis electronically, I declare that the entirety of the work contained therein is my own, original work, that I am the sole author thereof (save to the extent explicitly otherwise stated), that reproduction and publication thereof by Stellenbosch University will not infringe any third party rights and that I have not previously in its entirety or in part submitted it for obtaining any qualification.

April 2014

Copyright © 2014 Stellenbosch University

All rights reserved

Abstract

Background - Although acute hyperglycemic episodes are linked to lower glucose uptake, underlying mechanisms driving this process remain unclear. We hypothesized that acute hyperglycemia triggers reactive oxygen species (ROS) production and increases non-oxidative glucose pathway (NOGP) activation, i.e. stimulation of advanced glycation end products (AGE), polyol pathway (PP), hexosamine biosynthetic pathway (HBP) and protein kinase C (PKC) activation. These mechanisms attenuate cellular function, and may indeed decrease insulin-mediated cardiac glucose uptake. The role of the pentose phosphate pathway (PPP) under high glucose/diabetic conditions is a subject of contention. Activation of the PPP enzyme transketolase (TK) (by benfotiamine/BFT or thiamine) reduces flux via the other four NOGPs, and is associated with beneficial outcomes. Our aim was therefore to evaluate the effects of acute hyperglycemia on insulin-mediated glucose uptake in a cardiac-derived cell line. Specifically, we aimed to elucidate the role of ROS and NOGP induction under these conditions.

Methodology - H9c2 cardiomyoblasts were exposed to 25 mM glucose for 24 hr vs. 5.5 mM glucose controls \pm modulating agents during last hour of glucose exposure: a) antioxidant #1 for mitochondrial ROS (250 μ M 4-OHCA), b) antioxidant #2 for NADPH oxidase-generated ROS (100 μ M DPI), c) NOGP inhibitors – 100 μ M aminoguanidine (AGE), 5 μ M chelerythrine (PKC); 40 μ M DON (HBP); and 10 μ M zopolrestat (PP). We also employed BFT (50 and 100 μ M) *in vitro*, while the effects of *in vivo* thiamine administration were assessed in hearts of an obese/diabetic rat model of pre-diabetes and diabetes, the OLETF strain. We evaluated insulin

sensitivity by glucose uptake assay (flow cytometry), GLUT4 translocation (transfection of HA-GLUT4-GFP construct) and protein kinase B (Akt) activity assay. ROS levels (mitochondrial, intracellular) were measured by flow cytometry analysis of specific fluorescent probes. Markers of each NOGP were also assessed.

Results - Acute hyperglycemia elevated ROS, activated NOGPs and blunted glucose uptake. However, TK activity (marker of PPP) did not change. Respective 4-OHCA and DPI treatment blunted ROS production, diminished NOGP activation and normalized glucose uptake. NOGP inhibitory studies identified PKC β II as a key downstream player in lowering insulin-mediated glucose uptake. When we employed BFT (known to shunt flux away from NOGPs and into the PPP), it decreased ROS generation and NOGP activation, and restored glucose uptake under acute hyperglycemic conditions. *In vivo* thiamine administration reduced markers of the other NOGP, while it attenuated (mainly in the pre-diabetic phase) the metabolic dysfunction observed in the OLETF rats.

Conclusions - This study demonstrates that acute hyperglycemia elicits a series of maladaptive events that function in tandem to reduce glucose uptake, and that antioxidant treatment and/or attenuation of NOGP activation (PKC, polyol pathway) may limit the onset of insulin resistance.

Opsomming (Uittreksel)

Agtergrond – Alhoewel akute hiperglisemie voorvalle gekoppel is aan verlaagde glukose opname, is die onderliggende meganismes wat die proses dryf steeds onduidelik. Ons hipotetiseer dat akute hiperglisemie aanleiding gee tot die produksie van reaktiewe suurstofspesies (RSS) en toename in nie-oksidatiewe glukose weg (NOGW) aktivering, i.e. stimulering van gevorderde glukasie eindprodukte (GGE), poliolweg (PW), heksosamien biosintetiese weg (HBW) en proteïenkinase C (PKC) aktivering. Hierdie meganismes verminder sellulêre funksie, en mag inderdaad insulien-bemiddelde kardiêre glukose opname verlaag. Die rol van die pentosefosfaatweg (PFW) onder hoë glukose/diabetiese kondisies is 'n onderwerp van stryd. Aktivering van die PFW ensiem transketolase (TK) (deur benfotiamien/BFT of tiamien) verminder fluks deur die ander vier NOGWë, en is geassosieer met voordelige uitkomst. Ons doel was dus om die effekte van akute hiperglisemie op insulien-bemiddelde glukose opname te evalueer in 'n kardiaal-afkomstige sellyn. Meer bepaald het ons gepoog om die rol van RSS en NOGW induksie onder hierdie kondisies te verstaan.

Metode – H9c2 kardiomioblaste is aan 25 mM glukose vir 24 h blootgestel vs. 5.5 mM glukose kontroles ± moduleeragente tydens die laaste uur van glukose blootstelling: a) anti-oksidant #1 vir mitochondriese RSS (250 μ M 4-OHCA), b) anti-oksidant #2 vir NADPH oksidase-gegenereerde RSS (100 μ M DPI), c) NOGW inhibeerders – 100 μ M aminoguanidien (GGE), 5 μ M cheleritrien (PKC); 40 μ M DON (HBW); en 10 μ M zopolrestaat (PW). Ons het ook BFT (50 en 100 μ M) *in vitro*

aangewend, terwyl die effek van *in vivo* tiamien aanwending geassesseer is in die harte van 'n vetsugtige/diabetiese rotmodel van pre-diabetes en diabetes, die OLETF lyn. Ons het insulien sensitiwiteit deur 'n glukose opname toets (vloeisitometrie), GLUT4 translokasie (transfeksie van HA-GLUT4-GFP konstruk) en proteïenkinase B (Akt) aktiwiteitstoets, geëvalueer. RSS vlakke (mitochondries, intrasellulêr) is gemeet deur vloeisitometriese analise van spesifieke fluoresserende peilers. Merkers van elke NOGW is ook geassesseer.

Resultate - Akute hiperglisemie het RSS verhoog, NOGW geaktiveer en glukose opname versag. TK aktiwiteit (merker van PFW) het egter nie verander nie. Onderskeidelike 4-OHCA en DPI behandeling het RSS produksie versag, NOGW aktivering verminder en glukose opname genormaliseer. NOGW onderdrukking studies het PKC β II geïdentifiseer as 'n sleutel deelnemer in verlaging van insulien-bemiddelde glukose opname. Die aanwending van BFT (bekend vir die wegvoer van fluks vanaf NOGW na die PFW), het RSS skepping en NOGW aktivering verlaag, en glukose opname herwin onder akute hiperglisemiese kondisies. *In vivo* tiamien toediening het merkers van die ander NOGW verlaag, terwyl dit die metaboliese disfunksie waargeneem in die OLETF rotte (hoofsaaklik in die pre-diabetiese fase) verminder het.

Gevolgtrekking – Hierdie studie demonstreer dat akute hiperglisemie 'n reeks van wanaangepaste voorvalle ontlok wat gesamentlik funksioneer om glukose opname te verlaag, en dat anti-oksidant behandeling en/of vermindering van NOGW aktivering (PKC, polioliweg), die aanvang van insulien weerstand mag beperk.

Acknowledgements

I thank God for blessing me with the talent, personal attributes, strength and opportunities to pursue my academic career as a student.

I would also like to express my sincere gratitude to the following persons and institutions for their substantial contributions to me personally and to this study:

To my mentor and PhD supervisor, Professor M. Faadiel Essop: your incredible influence as roll model, supervisor, mentor, father figure, friend and colleague (each attribute employed in specific scenarios where they were required) have largely shaped my personal and professional life over the past six years. I thank you for your leadership, always by example, but also your willingness to let me express myself and listening to my side of the story while giving guidance and constructive criticism when necessary. Thank you for your commitment and willingness to put in extra work to help achieve my goals, and for your calming influence and valuable analogies, philosophies and life lessons when times get tough. Thank you for always putting the needs of others before your own. I hope that I have garnered some of your qualities, both professionally and personally.

I thank the Department of Physiological Sciences (my second home) for the opportunity to pursue my post-graduate studies here. Thank you to the staff for creating a friendly, positive and professional environment, and to the students for camaraderie and friendships. Specific thanks to Grazelda, Katrina, Jonnifer, Annadie, Lydia and Ashwin for ensuring the labs run smoothly.

Thank you to the CMRG for the friendships, teamwork and insightful and critical discussions during the Friday morning meetings. Thanks to Rudo and Charlene for adding a little laughter to life, but also for the advice and interesting discussions.

I wish to thank Prof. Takao Tanaka for kindly providing the OLETF rat heart tissues and Profs. Gavin Welsh and Jeremy Tavare for the HA-GLUT4-GFP construct.

To Dr. Ben Loos, thank you for your inputs, discussions and technical help, specifically for your help obtaining the HA-GLUT4-GFP construct and inputs regarding the optimization of transfection and imaging experiments. I also thank Dr. Craig Kinnear for amplification of the construct.

I wish to acknowledge the contributions of Charlene, Burger and Robyn towards some of the work.

I thank Lize and Rozanne for inputs regarding flow cytometry and fluorescence microscopy experiments and for running of samples.

My sincere thanks go to former staff and students of the department – Mark, Jamie, Uthra, James and Rob – who were always on hand to teach me techniques and discuss the science.

Also thanks to Theo and Ashwin for the much needed coffee breaks and interesting discussions and advice.

My family – al julle gebede, wense, liefde, ondersteuning en opoffering word opreg waardeer. Dankie aan Mary vir die proeflees en hulp met die tesis.

To Veronique – “What would I have done without you?” I thank you for your love and unwavering support throughout my studies. Thank you for your inputs and help with the corrections and proof reading of the thesis, for all the weekends and late nights spent at the lab and for believing in me when I questioned my own abilities.

Shandre - thank you for your support, proof reading and inputs with the thesis. Also thank you to the Human family for their support and prayers.

Importantly, my sincere gratitude goes to the National Research Foundation, Oppenheimer Trust and Stellenbosch University for financial support. I also thank the Post Graduate and International Office of Stellenbosch University, the SA Heart Association’s Louis Vogelpeel foundation and the American Physiological Society for travel grants.

Table of Contents

Declaration	ii
Abstract	iii
Opsomming (Uittreksel)	v
Acknowledgements	vii
Table of contents	ix
List of Tables	xiv
List of Figures	xiv
List of Abbreviations	xviii
Units of Measurements	xxiv
List of conference contributions	xxv
Chapter 1 Perspective	1
1.1. Metabolic dysfunction and lifestyle diseases	3
1.2. Risk factors	5
1.3. The obesity paradox	9
1.4. Metabolic syndrome, insulin resistance and type 2 diabetes	13
1.5. The South African context	14
1.6. Problem statement	17
1.7. References	19
Chapter 2 Cardiomyocyte metabolism in the physiological state	26
2.1. Introduction	26
2.2. Homeostatic metabolism in cardiomyocytes	28
2.2.1. Fuel substrates	28
2.2.2. Glucose uptake	30
2.2.2.1. Glucose transporter proteins	31
2.2.2.2. Insulin signaling mechanisms	35
2.2.2.3. Physiological regulation of glucose uptake	42

2.2.3.	Glycolysis	43
2.2.4.	Fatty acid uptake and fate	48
2.2.5.	Mitochondrial energetics.....	52
2.2.5.1.	Citric acid cycle.....	53
2.2.5.2.	Electron transport chain and oxidative phosphorylation.....	54
2.2.6.	The regulatory link for metabolic substrate switching – the Randle cycle	56
2.3.	References	59

Chapter 3 Metabolic alterations and myocardial insulin resistance.....74

3.1.	Principles and pathogenesis of insulin resistance and diabetes	74
3.1.1.	Introduction.....	74
3.1.2.	Diagnosis of insulin resistance and diabetes	76
3.1.3.	Etiology of insulin resistance	79
3.2.	Molecular mechanisms of insulin resistance.....	82
3.2.1.	Dysregulation of insulin action by fuel substrate overabundance – Randle cycle revisited.....	82
3.3.	Acute hyperglycemia	84
3.4.	Glucose-metabolic dysregulation and diabetic complications.....	86
3.4.1.	Oxidative stress	86
3.4.1.1.	ROS sources	87
3.4.1.2.	Intracellular antioxidant systems.....	90
3.4.1.3.	ROS and non-oxidative glucose pathways (NOGPs) – unifying hypothesis and its modifications	91
3.4.2.	Non-oxidative glucose pathways	93
3.4.2.1.	Advanced glycation end products.....	96
3.4.2.2.	Polyol pathway.....	97
3.4.2.3.	Protein kinase C activation	98
3.4.2.4.	Hexosamine biosynthetic pathway.....	99
3.4.2.5.	Pentose phosphate pathway	101
3.5.	Summary	104
3.6.	References	106

Chapter 4	Materials and methods	124
4.1.	Study design and research chapter layout.....	124
4.2.	Cell culture and maintenance	124
4.3.	Modulatory studies.....	125
4.4.	Otsuka Long-Evans Tokushima Fatty (OLETF) rat model of thiamine treatment.....	128
4.5.	Measurement of insulin action	130
4.5.1.	Glucose uptake assay	130
4.5.2.	GLUT4 translocation assay	134
4.5.2.1.	Transfection of HA-GLUT4-GFP	134
4.5.2.2.	Treatment and preparation for fluorescence microscopy.....	135
4.5.2.3.	Evaluation of HA:GFP ratio.....	135
4.5.3.	Protein kinase B (PKB/Akt) activity assay.....	136
4.5.3.1.	Preparation of cell lysate	136
4.5.3.2.	Immunoprecipitation of Akt	137
4.5.3.3.	Kinase assay	137
4.5.3.4.	Western blot analysis of phosphorylated GSK3 α	137
4.6.	Evaluation of oxidative stress mechanisms	138
4.6.1.	Total intracellular ROS levels – DCF fluorescence.....	138
4.6.1.1.	Fluorescence microscopy analysis of DCF staining.....	139
4.6.1.2.	Flow cytometry analysis of DCF staining	140
4.6.2.	Mitochondrial ROS levels	140
4.6.2.1.	Fluorescence microscopy analysis of MitoTracker CM-H2XRos staining	141
4.6.2.2.	Flow cytometry analysis of MitoTracker CM-H2XRos staining	141
4.6.3.	NADPH oxidase activation.....	142
4.6.4.	Aconitase activity	142
4.6.5.	Malondialdehyde (MDA) assay	143
4.6.6.	Superoxide dismutase (SOD) activity assay	145
4.6.7.	Glutathione levels	145
4.6.8.	NADPH levels and NADP ⁺ :NADPH ratio calculation	146
4.6.9.	Glucose-6-phosphate dehydrogenase (G6PD) activity assay	147
4.7.	Evaluation of metabolic alterations	148

4.7.1.	Measurement of intracellular ATP levels	148
4.7.2.	Evaluation of non-oxidative glucose metabolic pathways	149
4.7.2.1.	Sample preparation for NOGP analysis	150
4.7.2.2.	Methylglyoxal levels (AGE)	150
4.7.2.3.	Sorbitol levels (Polyol)	151
4.7.2.4.	PKC activity	151
4.7.2.5.	PKC isoform expression	152
4.7.2.6.	O-GlcNAc levels (HBP)	152
4.7.2.7.	Co-localization analysis of O-GlcNAc modifications	153
4.7.2.8.	Transketolase activity (PPP)	155
4.8.	Statistical analysis	156
4.9.	References	157

Chapter 5 Study I. Acute hyperglycemia induces oxidative stress-related insulin resistance in vitro.....158

5.1.	Introduction.....	158
5.2.	Aims.....	160
5.3.	Modulators and brief description of methodology	160
5.4.	Results.....	161
5.4.1.	Acute high glucose exposure upregulates ROS and reduces glucose transport capacity	161
5.4.2.	Mitochondrial and NOX-derived ROS mediates insulin resistance	167
5.4.3.	Attenuation of endogenous antioxidant systems under hyperglycemic conditions.....	171
5.5.	Discussion	175
5.6.	References	183

Chapter 6 Study II. Metabolic alterations of acute hyperglycemia – role of non-oxidative glucose pathways in insulin resistance.....188

6.1.	Introduction.....	188
6.2.	Aims.....	190

6.3.	Modulators	190
6.4.	Results.....	191
6.4.1.	Glucose metabolic alterations are mediated by mitochondrial and NOX-derived ROS	191
6.4.2.	The role of NOGP modulation on insulin and ROS signaling events	195
6.4.3.	Modulation of PPP diverts flux away from NOGPs – the role of benfotiamine <i>in vitro</i> and thiamine <i>in vivo</i>	205
6.4.4.	Molecular events downstream of NOGP activation in <i>in vitro</i> simulated hyperglycemia	220
6.5.	Discussion	224
6.6.	References	235
 Chapter 7 Concluding remarks		242
7.1.	Summary of findings	242
7.2.	Limitations	243
7.3.	Future directions	244
 Appendices		246

List of Tables

Table 1.1	Criteria for diagnosis of metabolic syndrome.....	14
Table 3.1	Criteria for diagnosis of insulin resistance and diabetes.....	77

List of Figures

Figure 2.1	Myocardial substrate utilization.....	28
Figure 2.2	Metabolic flux of myocardial substrate utilization.....	29
Figure 2.3	Sources of glucose and regulation of glycogen storage and breakdown.....	31
Figure 2.4	Schematic depiction of GLUT transporter proteins.....	32
Figure 2.5	Insulin signaling and GLUT4 translocation.....	40
Figure 2.6	Reactions and regulation of glycolysis.....	45
Figure 2.7	Regulation of the pyruvate dehydrogenase complex.....	48
Figure 2.8	Fatty acid uptake and metabolism.....	51
Figure 2.9	Reactions of the citric acid cycle.....	54
Figure 2.10	Electron transport chain.....	56
Figure 3.1	Glycolysis and NOGP branch points.....	95
Figure 3.2	AGE formation.....	97
Figure 3.3	Polyol pathway.....	98
Figure 3.4	PKC activation.....	99
Figure 3.5	Hexosamine biosynthetic pathway.....	100
Figure 3.6	Oxidative and non-oxidative branches of the pentose phosphate pathway.....	104
Figure 4.1	Timeline of experimental plan.....	127
Figure 4.2	Target sites for pharmacological modulators employed in this study.....	128
Figure 4.3	Flow cytometry analysis of 2-NBDG uptake in H9c2 cells – gating characteristics used to exclude non-viable cells.....	133

Figure 5.1	Modulators used to inhibit ROS from the mitochondria and NOX...161
Figure 5.2	Total intracellular ROS levels determined by CM-H ₂ DCFDA (DCF) fluorescence.....162
Figure 5.3	MitoTracker Red CMH ₂ XROS staining of cells to indicate mitochondrial ROS sources.....163
Figure 5.4	NADPH oxidase activity increased under high glucose conditions.....164
Figure 5.5	Impaired glucose uptake in response to high glucose conditions...165
Figure 5.6	High glucose treatment suppressed the translocation of HA-GLUT4-GFP to the sarcolemma.....166
Figure 5.7	Acute hyperglycemia downregulated the kinase activity of Akt.....167
Figure 5.8	Pharmacological attenuation of mitochondrial- and NOX-derived ROS.....168
Figure 5.9	Enhanced glucose uptake upon inhibition of mitochondrial and NOX-derived ROS.....169
Figure 5.10	Attenuation of ROS (mitochondrial and NOX-derived) restored GLUT4 translocation.....170
Figure 5.11	Regulation of Akt activity by mitochondrial and NOX-derived ROS.....171
Figure 5.12	High glucose attenuated superoxide dismutase (SOD) activity.....172
Figure 5.13	Attenuation of the glutathione replenishment system under high glucose conditions.....174
Figure 5.14	Intracellular markers of oxidative damage were unaltered.....175
Figure 6.1	Modulators used to inhibit NOGPs.....191
Figure 6.2	Intracellular ATP levels were reduced by ROS modulation.....192
Figure 6.3	Metabolic alterations under acute high glucose conditions were mediated by ROS.....194
Figure 6.4	Relative percentage induction of NOGP markers by high glucose treatment.....195
Figure 6.5	Inhibitory effect of NOGP inhibitors used in this study.....197
Figure 6.6	NOGP inhibition reversed high glucose-mediated inhibition of glucose uptake.....198

Figure 6.7	PKC inhibition outweighs that of the other NOGP inhibitors – upregulation of glucose uptake.....	199
Figure 6.8	NOGP modulation attenuated high glucose–induced ROS production.....	201
Figure 6.9	High glucose-mediated inhibition of SOD activity was reversed by NOGP inhibition.....	202
Figure 6.10	Regulation of the glutathione system by NOGP modulation.....	203
Figure 6.11	Levels of NOGP markers in high glucose treated cells subjected to pathway inhibition.....	204
Figure 6.12	Benfotiamine administration increased glucose uptake.....	206
Figure 6.13	Comparison of BFT <i>versus</i> the other NOGP inhibitors – effect on glucose uptake.....	207
Figure 6.14	BFT increased transketolase activity.....	207
Figure 6.15	BFT treatment reduced NOGP markers and ATP levels.....	209
Figure 6.16	Relative NOGP induction with BFT treatment compared to high glucose.....	210
Figure 6.17	BFT attenuated ROS production.....	211
Figure 6.18	BFT administration increased SOD activity.....	212
Figure 6.19	BFT upregulated GSH levels and increased NADPH utilization....	213
Figure 6.20	DON administration downregulated transketolase activity.....	214
Figure 6.21	Myocardial Akt activity is upregulated by thiamine in 25 week old OLETF rats.....	216
Figure 6.22	PPP enzymes are reduced in the 55 week old (diabetic) hearts and transketolase upregulated by thiamine <i>in vivo</i>	217
Figure 6.23	Methylglyoxal levels (marker of the AGE pathway) were decreased by thiamine treatment in pre-diabetic hearts <i>in vivo</i>	218
Figure 6.24	Sorbitol levels were decreased in the 25 week old animals.....	218
Figure 6.25	Thiamine treatment decreased PKC activity in the pre-diabetic OLETF rats.....	219
Figure 6.26	Thiamine treatment diminished O-GlcNAc levels in the pre-diabetic and diabetic OLETF rat hearts.....	220
Figure 6.27	Upregulation of PKC β II by acute hyperglycemia was reduced by 4-OHCA and DPI treatment.....	221

Figure 6.28	Co-localization of Akt and O-GlcNAc was elevated under high glucose conditions and reduced by inhibition of mitochondrial and NOX-derived ROS.....	222
Figure 6.29	Co-localization of AS160 and O-GlcNAc was elevated under high glucose conditions and reduced by inhibition of mitochondrial and NOX-derived ROS.....	224
Figure 6.30	Our proposed model for acute hyperglycemia-induced myocardial insulin resistance.....	234

List of Abbreviations

1,3-BPG	1,3-bisphosphoglycerate
2-NBDG	2-(<i>N</i> -(7-Nitrobenz-2-oxa-1,3-diazol-4-yl)amino)-2-deoxyglucose
3-KAT	3-ketoacyl-coenzyme A thiolase
4-OHCA	α -cyano-4-hydroxycinnamic acid
6-AN	6-aminonicotinamide
6-PG	6-phosphogluconolactone
6-PGL	6-phosphoglucono-1-5-lactone
A	Absorbance
ABSI	Body shape index
ACC	Acetyl co-enzyme A carboxylase
ADA	American Diabetes Association
ADP	Adenosine diphosphate
AGE	Advanced glycation end products
AHA	American Heart Association
AICAR	5-Aminoimidazole-4-carboxamide ribonucleotide
Akt	(also known as) Protein kinase B
AMG	Aminoguanidine
AMP	Adenosine monophosphate
AMPK	Adenosine monophosphate activated kinase
ANG II	Angiotensin II
ANOVA	One way analysis of variance
AR	Aldose reductase
AS160	Akt substrate of 160 kD
ATP	Adenosine triphosphate
BFT	Benfotiamine
BMI	Body mass index
Ca ²⁺	Calcium
CaCl ₂ (2H ₂ O)	Calcium chloride
CAT	Carnitine acyl translocase
cGMP	Cyclic guanine monophosphate
CHE	Chelerythrine

CM-H2XRos	carboxy-methyl dihydro-X-rosamine
CO ₂	Carbon dioxide
CoA	Co-enzyme A
CON	Control
COOH	Carboxy-terminal
CPT1	Carnitine palmatoyl transferase-1
CPT-II	Carnitine palmatoyl transferase-II
CVD	Cardiovascular disease
DAG	Diacylglycerol
DALYs	Death and years lived with disability
DAPI	4'-6' diamidino-2-phenylindole
DCF	Dichloro fluorescein
DHAP	Dihydroxy acetone phosphate
DMEM	Dulbecco's modified Eagle's medium
DMSO	Dimethyl sulfoxide
DNA	Deoxyribonucleic acid
DON	6-diazo-5-oxo-L-norleucine
DPI	Diphenylene iodonium
ECL	Enhanced chemiluminescence
EDTA	Ethylenediaminetetraacetic acid
ELISA	Enzyme-linked immunoadsorbent assay
eNOS	Endothelium nitric oxide synthase
EPIC	European Prospective Investigation into Cancer and Nutrition
ETC	Electron transport chain
F-1,6-BP	Fructose-1,6-bisphosphate
F-2,6-BP	Fructose-2,6-bisphosphate
F-6-P	Fructose-6-phosphate
FA	Fatty acid
FABPpm	Plasma membrane fatty acid binding protein
FACS	Fatty acyl-coenzyme A synthase
FAD	Flavin adenine dinucleotide
FADH ₂	Flavin adenine dinucleotide reduced
FAT	Fatty acid translocase
FATP	Fatty acid transport proteins

FATP-1	Fatty acid transport protein-1
FATP-6	Fatty acid transport protein-6
FFA	Free fatty acids
FITC	Fluorescein isothiocyanate
FPG	Fasting plasma glucose
G-3-P	Glyceraldehyde-3-phosphate
G-6-P	Glucose-6-phosphate
G6PD	Glucose-6-phosphate dehydrogenase
G6PDx	G6PD deficient
GAPDH	Glyceraldehyde-3-phosphate dehydrogenase
GBD 2010	Global Burden of Diseases, Injuries and Risk Factors Study 2010
GDP	Guanidine diphosphate
GFAT	Glutamine:fructose-6-phosphate amidotransferase
GFP	Green fluorescent protein
Gln-6-P	Glucosamine-6-phosphate
GLUT	Glucose transporter protein
GLUT4	Glucose transporter
GSH	Glutathione
GSK	Glycogen synthase kinase
GSK3 β	glycogen synthase kinase 3 β
GSSG	glutathione disulfide
GSVs	GLUT4 storage vesicles
GTP	Guanidine triphosphate
H ⁺	Proton
H ₂ DCFDA	2',7'-dichlorodihydrofluorescein diacetate stain
H ₂ O	Water
H ₂ O ₂	Hydrogen peroxide
HA-GLUT4-GFP	Hemagglutinin- and green fluorescent protein-tagged GLUT4
HbA1c	Glycated hemoglobin
HBP	Hexosamine biosynthetic pathway
HDL	High density lipoprotein
HEPES	4-(2-hydroxyethyl)-1-piperazineethanesulfonic acid
HG	High glucose

HIV	Human immune deficiency virus
HRP	Horse radish peroxidase
IDF	International Diabetes Federation
IFG	Impaired fasting glucose
IFM	Intramyofibrillar mitochondria
IGT	Impaired glucose tolerance
IR	Insulin receptor
IRAP	Insulin-regulated aminopeptidase
IRS1	Insulin receptor substrate 1
K _{ATP}	ATP-sensitive potassium channels
KCl	Potassium chloride
LDH	Lactate dehydrogenase
LETO	Long-Evans Tokushima Otsuka
LPL	Lipoprotein lipase
MAPK	Mitogen activated protein kinase
MCD	Malonyl co-enzyme A decarboxylase
MCT	Monocarboxylic acid transporter
MCT-1	Monocarboxylic acid transporter-1
MDA	Malondialdehyde
MG-BSA	Methylglyoxal (bovine serum albumin conjugated)
MgSO ₄ (7H ₂ O)	Magnesium sulphate
MnSOD	Manganese superoxide dismutase
mRNA	Messenger ribonucleic acid
mTOR	Mammalian target of rapamycin
NaCl	Sodium chloride
NAD	Nicotinamide adenine dinucleotide
NADH	Nicotinamide adenine dinucleotide reduced
NADP	Nicotinamide adenine dinucleotide phosphate
NADPH	Nicotinamide adenine dinucleotide phosphate hydrogen
NCDs	Non-communicable diseases
NEFAs	Non-esterified fatty acids
NF-κB	Nuclear factor κBr
NH ₂	Amino-terminal
NHANES	National Health and Nutrition Examination Survey

NOGP(s)	Non-oxidative glucose pathway(s)
NOX	NADPH oxidase
O ₂	Oxygen
OD	Optical density
O-GlcNAc	O-linked N-acetyl glucosamine
OGTT	Oral glucose tolerance test
OLETF	Otsuka Long-Evans Tokushima Fatty
PARP	Poly-ADP-ribose polymerase
PAS	Anti-pAkt substrates
PBS	Phosphate buffered saline
PDH	Pyruvate dehydrogenase
PDK1	PDH kinase-1
PDK-4	PDH kinase-4
PEP	Phosphoenolpyruvate
PFK-1	Phosphofructokinase-1
PFK-2	Phosphofructokinase-2
PH	Plecstrin homology
PI	Propidium iodide
Pi	Phosphate ion
PI3K	Phosphatidylinositol-3-kinase
PIP ₂	Phosphatidylinositol-4,5-biphosphate
PIP ₃	Phosphatidylinositol-3,4,5-triphosphate
PKA	Protein kinase A
PKB	Protein kinase B
PKC	Protein kinase C
PKC θ	Protein kinase C theta
PP	Polyol pathway
PPAR	Peroxisome proliferator-activated receptor
PPAR- α	Peroxisome proliferator activated receptor- α
PPP	Pentose phosphate pathway
PTEN	Phosphatase and tensin homolog deleted on chromosome 10
PTP1B	Protein tyrosine phosphatase 1B
PTPases	Tyrosine phosphatases
PVDF	Polyvinylidene fluoride

Q	Ubiquinol
R-5-P	Ribose 5-phosphate
RabGAP	Rab GTPase-activating protein
RACK	Receptors for activated protein kinase C proteins
RAGEs	Receptors for advanced glycation end product
ricTOR-mTORC2	Mammalian target of rapamycin in complex with rictor and SIN1
RIPA	Radio-immunoprecipitation assay buffer
RNAi	Ribonucleic acid interference
ROS	Reactive oxygen species
SDH	Sorbitol dehydrogenase
SDS-PAGE	Sodium dodecyl sulphate polyacrylamide gel electrophoresis
SEM	Standard error of the mean
SGLT1	Sodium-glucose co-transporter
SH2	Src homology two domains
SOD	Superoxide dismutase
SOD1	Superoxide dismutase 1
SR	Sarcoplasmic reticulum
SSM	Subsarcolemmal mitochondria
T2DM	Type 2 diabetes mellitus
TBS-T	Tris-buffered saline-tween
TIM	Triose phosphate isomerase.
TK	Transketolase
TMZ	Tetramethylbenzidine
TPP	Thiamine pyrophosphate
Tris-HCl	Tri-(hydroxyl-methyl)-aminomethane-hydrogen chloride
UN	United Nations
US	United States
VLDLs	Very low density lipoproteins
WHO	World Health Organization
WST-1	Water-soluble tetrazolium salt
X-5-P	Xylulose 5-phosphate
ZOP	Zopolrestat
β -NADH	β -nicotinamide adenine dinucleotide

Units of Measurement

%	percent/percentage
AU	arbitrary units
g	gram
g/L	grams per liter
h	hour/s
kcal	kilocalories
kDa	kilodalton
L	litre
M	molar
mg	milligram
min	minutes
ml	millilitres
mm	millimetre
mM	millimolar
mm/Hg	millimetres of mercury
mM/ μ g	millimolar per microgram
mmol/l	millimoles per liters
mU/ml	milliunits per milliliter
mU/ μ g	milliunits per microgram
ng	nanograms
ng/ μ g	nanograms per micrograms
ng/ μ l/min	nanograms per microliter per minute
nm	nanometre
nM	nanomolar
nmol	nanomoles
nmol/ μ g	nanomoles per micrograms
$^{\circ}$ C	degrees Celsius
w/v	weight per volume
μ g	microgram
μ g/ml	microgram per milliliter
μ l	microlitre

μm	micrometre
μM	micromolar

List of conference contributions

National conferences:

Joseph D, Essop MF. The detrimental effects of acute hyperglycemia on myocardial glucose uptake: a 'series of unfortunate events'. *Oral presentation presented in the Wyndham competition at the 41st annual congress of the Physiology Society of Southern Africa (PSSA), Roodevallei meetings and conference hotel, Pretoria, 15-18 September 2013*

Joseph D, Essop MF. Evaluation of novel therapeutic interventions to limit myocardial glucose toxicity. *Poster presented in the Johnny van der Walt competition at the 40th annual congress of the Physiology Society of Southern Africa (PSSA), Stellenbosch University, Stellenbosch, 10-13 September 2012*

Joseph D, Essop MF. Evaluation of novel therapeutic interventions to limit myocardial glucose toxicity. *Poster presented at the 47th annual congress of the Society for Endocrinology, Metabolism and Diabetes of South Africa (SEMDSA), Bantry Bay, Cape Town, 19-22 April 2012*

Joseph D, Essop MF. Hyperglycemia-mediated onset of myocardial insulin resistance: exploring novel therapeutic possibilities. *Oral presentation presented at the 39th annual congress of the Physiology Society of Southern Africa (PSSA), University of Western Cape, Cape Town, 29-31 August 2011*

Joseph D, Essop MF. Increased hexosamine biosynthetic pathway flux leads to PKB/Akt post-translational modification: implications for onset of insulin resistance. *Poster presented at the 45th annual congress of the Society for Endocrinology, Metabolism and Diabetes of South Africa (SEMDSA), Durban, 10-13 April 2010. (First prize winner in the poster competition for basic sciences)*

International conferences:

Joseph D, Kimar C, Essop MF. Exploring mechanisms that attenuate myocardial glucose uptake in response to acute hyperglycemia: identification of a vicious metabolic cycle. *Oral presentation presented at the 2013 Experimental Biology (EB) meeting, 20-24 April 2013, Boston convention and exhibition center, Boston, MA, USA.*

Joseph D, Essop MF. Exploring novel therapeutic targets to blunt hexosamine biosynthetic pathway-induced myocardial insulin resistance. *Poster presented at the 9th annual scientific sessions of the Society for Heart and Vascular Metabolism (SHVM), Brussels, Belgium, 18-21 June 2011*

CHAPTER 1

Perspective

Metabolic disorders, once considered diseases of wealthy, industrialized or westernized nations, are now becoming more prevalent globally. Developing nations now face daunting prospects in terms of disease prevalence, management and treatment. Moreover, future projections are alarming despite substantial efforts made to understand the pathophysiology, and also implementation of preventative or therapeutic possibilities. The umbrella term 'metabolic disorders' include the metabolic syndrome, insulin resistance and type 2 diabetes mellitus (T2DM), that are all complex, inter-linked and multi-factorial diseases with various secondary complications arising at different stages during the pathogenesis.

Treatment and management of such disorders are difficult and expensive, resulting in a significant economic and social burden on health care systems. Furthermore, therapeutic advances are relatively limited, with the majority of promising drugs triggering moderate to severe side-effects. Lifestyle interventions are also promising as a preventative strategy, but are generally difficult to adhere to. These problems augment the ever rising incidence in morbidity and mortality associated with such diseases.

Our current understanding of the pathogenesis of T2DM shows various stages of dysregulated glucose metabolism. Initially, glucose homeostasis becomes impaired at the cellular uptake level, resulting in elevated (compensatory) insulin secretion by the pancreas. Insulin signaling at the target organs becomes severely attenuated,

resulting in elevated blood glucose levels. The pancreatic islet β -cells eventually become impaired, leading to decreased insulin secretion.

The pathogenesis of human diabetes occurs over decades and affects adults during the latter stages of their lives. Secondary defects associated with diabetes, e.g. nephropathy, neuropathy and cardiovascular diseases also develop later-on during the disease progression. However, the first signs of reduced glucose metabolism (impaired glucose tolerance-IGT), occur during the early stages of T2DM pathogenesis. Furthermore, obesity and the metabolic syndrome (a cluster of metabolic risk factors – refer Section 1.4) are strongly implicated as precursors for the development of T2DM. Thus, metabolic alterations may also occur earlier-on in young and working age individuals; signaling the initial stages of T2DM disease progression.

Current therapeutic options target the management of blood glucose levels at a late stage (during overt diabetes). The primary goal of these therapies is to prevent secondary defects and limit cellular damage caused by hyperglycemia. The majority of such drugs act to limit glucose levels in the bloodstream by targeting one or more of the following mechanisms: reducing glucose absorption in the gut, increasing insulin output in the pancreas (or insulin treatment itself when pancreatic β -cell dysfunction occurs), elevating peripheral tissue glucose uptake, or reducing hepatic glucose output. Although many pharmacological treatments result in successful glucose control, their efficacy is lost over time, e.g. onset of hypoglycemia and weight gain are disease risk factors. Moreover, reducing the secondary disease burden can

still remain problematic. Thus research work to investigate alternative options to blunt the ever increasing incidence of metabolic disorders is imperative.

For this study, we endeavored to develop a deeper understanding of the molecular, cellular defects, and pathophysiology of insulin resistance at a relatively early stage. Our rationale was to identify maladaptive events during the early stages, and also to evaluate therapeutic targets to attenuate/reverse the development of insulin resistance. We are of the opinion that prevention of metabolic dysfunction/insulin resistance constitutes a useful approach. We focused on the effects of acute hyperglycemia *per se* as a risk factor for disrupted insulin action and glucose uptake, and suggest that this may lead to the pathogenic outcome of insulin resistance. As metabolic diseases impact on the heart's function, we focused on the effects on cardiac-derived cells.

This chapter reviews the current state of affairs and future projections of lifestyle-dependent metabolic diseases and associated risk factors, specifically in developing nations such as South Africa. We also explore the mechanisms and impact of the metabolic syndrome, obesity and diabetes, and conclude by providing a problem statement outlining the rationale for this study.

1.1. Metabolic dysfunction and lifestyle diseases

The growing contribution of non-communicable diseases (NCDs) to global cases of preventable mortality and disability recently came under the spotlight at the United Nations (UN) General Assembly (United Nations, 2011). Here, the contribution of

NCDs to preventable death and disability, and the resulting socio-economic and development burden were considered to be of epidemic proportions. The UN and the World Health Organization (WHO) proposed that urgent steps are taken to reduce NCD-related mortalities by 25% by the year 2025 among adults aged 30 to 70 years – adopting the slogan “25 by 25” (Hunter and Reddy, 2013; United Nations, 2011; World Health Organization, 2012). Furthermore, low- and middle-income countries are particularly affected as about 80% of deaths from NCDs occur in these countries, while a high proportion of mortality occurs in middle age (working) populations (World Health Organization, 2013). These factors may lead to dire economic consequences with the dual burden of inflated health care costs and significant loss of economic productivity. Indeed, global projections estimated a cumulative output loss of \$47 trillion between 2011 and 2030 (Bloom *et al.*, 2011). The Global Burden of Diseases, Injuries and Risk Factors Study 2010 (GBD 2010) calculated the sum of years of life lost from premature death and years lived with disability (DALY) (Murray *et al.*, 2012), and reported that DALYs increased from 43% in 1990 to 54% in 2010. Here, the largest increases in DALYs occurred due to cardiovascular diseases, cancer and diabetes.

These three disease clusters fall under the top four related to mortality, contributing to about 80% of deaths due to NCDs (Lozano *et al.*, 2012). The incidence and projections of diabetes is particularly alarming as it, along with obesity, is inextricably linked to a number of secondary complications, including cardiovascular diseases – the number one cause of mortality from NCDs. Previous estimations projected a rise in diabetes incidence from 135 million individuals affected in 1995 to 300 million by 2025 (King *et al.*, 1998), while the WHO extended this projection to ~366 million by

2030 (Wild *et al.*, 2004). However, the 366 million mark was already surpassed in 2011 and recent projections by the International Diabetes Federation (IDF) suggest this number could rise to 552 million by 2030 (International Diabetes Federation, 2011).

Type 1 (insulin-dependent) diabetes mellitus manifests mainly as an autoimmune disease leading to defective pancreatic β -cell function and impaired insulin secretion (Retnakaran and Zinman, 2008). T2DM is a complex, multifactorial condition mainly characterized by impaired insulin sensitivity and action that eventually develops into impaired insulin secretion (Kahn, 1998). Such metabolic dysfunction is strongly implicated as cardiovascular disease risk factors. Furthermore, obesity and metabolic syndrome incidence are also alarmingly high (discussed in Section 1.3 and 1.4). These facts highlight the need for implementation of urgent measures to blunt the epidemic of metabolic disorders. A more holistic understanding of the mediators of these disorders is however needed. We start by reviewing the risk factors associated with the pathogenesis of metabolic disorders next.

1.2. Risk factors

Metabolic syndrome, obesity and T2DM arise from common lifestyle-dependent risk factors, including poor dietary habits and physical inactivity. A salient feature of recent epidemiological research is that lifestyle risk factors increased globally, particularly in developing nations where the association between risk factors, their physiological mediators and disease incidence are well established (Danaei *et al.*, 2013; Ezzati and Riboli, 2013). Dietary patterns, specific foods and nutritional content

are indeed associated with cardiovascular diseases and diabetes (Mozaffarian *et al.*, 2011), and with intermediate outcomes including weight gain, hypertension, insulin resistance and hyperglycemia (He *et al.*, 2013; Mozaffarian *et al.*, 2011; Sacks *et al.*, 2009). For example, a number of observational studies and randomized trials highlight the benefit of lower salt intake, replacement of saturated fat with polyunsaturated fat and generally healthy dietary patterns (Estruch *et al.*, 2013; He *et al.*, 2013; Mozaffarian *et al.*, 2010; Rossi *et al.*, 2013; Sacks *et al.*, 2009). Conversely, low intake of fruits, vegetables, whole grain, nuts, seeds or high intake of salt contribute significantly to global disease burden (Lim *et al.*, 2012). Individuals adopting a high caloric, “Western” diet, have drastically increased serum cholesterol levels (Farzadfar *et al.*, 2011). Modulation of dietary intake can help to blunt such effects. For example, a recent prospective study on the Greek cohort of the European Prospective Investigation into Cancer and Nutrition (EPIC) study assessed the effect of adherence to the Mediterranean diet and glycemic load on T2DM risk (Rossi *et al.*, 2013) and found that adherence to the Mediterranean diet or a diet with a low glycemic load was associated with reduced risk for T2DM. Others also showed an association between consumption of a Mediterranean diet and prevention of cardiovascular diseases (Estruch *et al.*, 2013). By contrast, consumption of diets with a high glycemic load correlated positively with diabetes risk.

The intake of large amounts of sugar also increased substantially in recent decades, with consumption of added sugars contributing largely to such increases (Marriott *et al.*, 2010; Welsh *et al.*, 2011). Natural sugars, consisting of monosaccharides (glucose, fructose, galactose) and polysaccharides (sucrose and lactose) form part of a healthy diet and are found in fruit, vegetables, dairy products and cereals. Added

sugars – sugars or syrups added to food during preparation, processing or at the table – have drastically increased in diets since the introduction of modern food production methods (Johnson *et al.*, 2009). Sugars and sweeteners available for consumption in the United States increased from 25 teaspoons (400 calories) to 29.8 teaspoons (475 calories) per day, representing a 19% increase from 1970 to 2005 (Wells and Buzby, 2008). The National Health and Nutrition Examination Survey (NHANES) reported a mean intake of 22.2 teaspoons (355 calories) per day from 2001 to 2004 for all persons; while the estimated average intake for children aged 14 to 19 years was 34.5 teaspoons (549 calories) (Marriott *et al.*, 2009). These reported intakes far exceed the recommended allowance for discretionary calories proposed in the 2005 US Dietary Guidelines (Marriott *et al.*, 2010). Moreover, the American Heart Association (AHA) recently recommended that ingestion of added sugars be reduced to at least 80 calories (5 teaspoons) for a daily energy expenditure of 1,800 calories in an average adult woman, and to at least 144 calories (9 teaspoons) for a daily energy expenditure of 2,200 calories in an average adult man (Johnson *et al.*, 2009).

The primary source of added sugars comes in the form of sugar-sweetened beverages, including sodas, fruit juices, energy drinks and vitamin water drinks (Johnson *et al.*, 2009; Tappy and Lê, 2010). Recent data show that children and adults in the US consume 172 and 175 kcal per day, respectively, from sugar-sweetened beverages (Brownell *et al.*, 2009). High fructose corn syrup is the most common sugar used as sweetener for beverages. It is preferred by manufacturers due to its cost effectiveness and longer shelf life, and it exerts a higher perception of sweetness compared to sucrose (Tappy and Lê, 2010). Consumption of high fructose

corn syrup have increased drastically over the past thirty years and accounts for ~42% of total caloric sweetener consumption in the US (Marriott *et al.*, 2009).

A number of prospective studies show a link between sugar-sweetened beverage consumption and risk for T2DM, weight gain and risk for obesity, and the metabolic syndrome (Bray, 2012; Fung *et al.*, 2009; Mozaffarian *et al.*, 2011; Popkin *et al.*, 2012; Schulze *et al.*, 2004). Women consuming one serving of sugar-sweetened beverages per day gained significantly more weight and had an 83% greater risk for developing T2DM compared to those consuming one serving per month in an 8-year follow up study (Schulze *et al.*, 2004). Furthermore, data from the Framingham Offspring Study show that individuals (followed for four years) who consume one to two servings of soft drinks daily have about 40% greater risk of developing obesity and metabolic syndrome, and a 22% higher incidence of hypertension compared to those who do not consume soft drinks (Dhingra *et al.*, 2007). Additionally, soft drink consumers displayed elevated triglycerides and reduced high density lipoprotein cholesterol levels versus non-consumers. Data from the NHANES also show a significant correlation between dietary added sugars and dysregulated serum lipid levels (Welsh *et al.*, 2011), while sugar-sweetened beverage consumption is also implicated in the risk for coronary heart disease (Fung *et al.*, 2009).

Although high dietary lipid and sucrose may trigger metabolic abnormalities and result in myocardial dysfunction (Chess and Stanley, 2008; Gonsolin *et al.*, 2007; Sharma *et al.*, 2007a; Stanhope and Havel, 2008), fructose is thought to be a major contributor to pathogenic outcomes (Bray, 2013, 2012; Elliott *et al.*, 2002; Havel, 2005; Kasim-Karakas *et al.*, 1996; Sharma *et al.*, 2007b). For example, visceral

obesity was increased and insulin sensitivity decreased after consumption of fructose-sweetened, but not glucose-sweetened beverages in obese individuals (Stanhope *et al.*, 2009). Moreover, a high fructose diet resulted in increased mortality and decreased left-ventricular contractile function compared to high starch, high fat or "Western" diet in hypertensive rats (Sharma *et al.*, 2007b). Fructose also induced significantly greater obesity, hyperinsulinemia, hypertriglyceridemia and impaired glucose utilization versus high sucrose and control (where fructose and sucrose were substituted with corn starch and dextrinized corn starch) diets in hamsters (Kasim-Karakas *et al.*, 1996). Furthermore, individuals subjected to 100 grams sucrose, or 50 g glucose and 50 g fructose displayed higher triglyceride levels in the sucrose and fructose groups compared to the glucose alone, seven hours after ingestion (Cohen and Schall, 1988). These studies signify the importance of excess dietary sugar intake, specifically fructose, in developing metabolic dysfunction and subsequent disease phenotypes. Possible pathophysiological mechanisms resulting from dietary fuel overabundance will be discussed in Chapter 2.

1.3. The obesity paradox

The prevalence of obesity has drastically increased worldwide since 1980 (Ezzati and Riboli, 2013). Furthermore several observational studies related different measures of adiposity and excess body weight with increased mortality and increased risk of disease and death from diabetes, ischemic heart diseases and other pathologies (Ezzati and Riboli, 2013; Finucane *et al.*, 2011; Ni Mhurchu *et al.*, 2004; Pischon *et al.*, 2008; Renehan *et al.*, 2008; Stevens *et al.*, 2012; Whitlock *et al.*, 2009; Wormser *et al.*, 2011). Overweight and obesity are typically defined by the

body mass index (BMI; the weight of an individual in kilograms divided by the square of the height in meters), where individuals with a BMI 18.5 - 24.9 considered normal weight, those with a BMI of 25 - 29.9 overweight, and a BMI ≥ 30 considered as obese (Berrington de Gonzalez *et al.*, 2010; Flegal *et al.*, 2013; Whitlock *et al.*, 2009). Obesity is further classified (based on the BMI) into grade 1 (30 - 34.9), grade 2 (35 - 39.9) and grade 3 (≥ 40).

A U-shaped relationship between BMI and mortality have also been described, where BMI values higher than 30 and lower than 18.5 (obese and underweight, respectively) both contributed to disease and mortality (Berrington de Gonzalez *et al.*, 2010; Whitlock *et al.*, 2009). Although a high BMI is strongly related to detrimental outcomes, some studies suggested the converse, i.e. obesity improves survival associated with various chronic diseases (Carnethon *et al.*, 2012; Flegal *et al.*, 2013; Kokkinos *et al.*, 2012; Tseng, 2013). A recent study by Flegal and colleagues (2013) investigated the association between BMI and mortality and found increased all-cause mortality among obese individuals (grade 1, 2 and 3 combined) compared to normal weight individuals (Flegal *et al.*, 2013). However, grade 1 obesity (alone) and overweight individuals were associated with no increase or a decrease in mortality compared to normal weight individuals, respectively. Furthermore, others also found inverse correlations between BMI and mortality (Carnethon *et al.*, 2012; Kokkinos *et al.*, 2012; Tseng, 2013). For example, BMI was also inversely related to mortality in African-American and Caucasian males with diabetes (Kokkinos *et al.*, 2012). Of note, some individuals may display a normal weight BMI but are then “metabolically unhealthy”, i.e. characterized by hyperinsulinemia and insulin resistance and predisposed to T2DM and cardiovascular diseases (Wildman *et al.*, 2008).

The seemingly counterintuitive notion of overweight or obesity having positive effects on health and mortality can be explained by the difficulties of only relying on the BMI as a measure of obesity. However, the BMI fails to distinguish between muscle and fat accumulation, the distribution of fat, age and gender- and ethnic-based differences (Bray, 2012; Gómez-Ambrosi *et al.*, 2012; Heymsfield *et al.*, 2009; Kang *et al.*, 2011; Lumeng and Saltiel, 2011). Here fat localization is an important consideration, e.g. excess visceral (central or abdominal) fat may predispose individuals to the metabolic syndrome, and downstream outcomes such as insulin resistance, diabetes and cardiovascular diseases. By contrast, it is proposed that peripheral fat storage may be metabolically inert. Therefore, normal weight individuals who are metabolically unhealthy may present with excess (central) fat mass, together with lower muscle mass (Lee *et al.*, 2011). Loss of skeletal muscle as a result of aging or physical inactivity may also lead to impaired insulin sensitivity, as muscle is the major site of glucose disposal, resulting in adverse metabolic defects and cardiovascular outcomes (Fogelholm, 2010). A low BMI may also mask poor nutritional status that also has negative effects on health (Ahima and Lazar, 2013).

The validity of the notion that a low BMI can be associated with unhealthy metabolic status may come into question. A recent study by Wildman *et al.* (2008) investigated the prevalence of various body size phenotypes (based on BMI) and its link to cardiometabolic abnormalities in a cross-sectional sample of 5,440 participants of the NHANES 1999-2004 (a nationally representative sample of the adult US population) (Wildman *et al.*, 2008). The researchers estimated that ~10% of the US adult population display an obese BMI but are metabolically healthy, 8% have a normal

BMI but metabolically unhealthy, 21% have an obese BMI with metabolic abnormalities and 26% are lean (normal BMI) and display a metabolically healthy phenotype (Ahima and Lazar, 2013; Wildman *et al.*, 2008). Others found that more than 10% of participants in a Korean study of adults aged 40 or higher displayed normal weight with various metabolic derangements, and the researchers concluded that identification of the metabolically obese but normal weight subjects may aid in the early detection of groups with high risk for cardiovascular disease (Lee *et al.*, 2011).

These studies outline some of the uncertainties that may result when employing the BMI as a sole indicator of pathogenic obesity. Therefore, several additional factors should be taken into account when classifying individuals at risk for metabolic dysfunction. A number of studies have proposed waist circumference for indicating obesity as a leading complement to BMI and it may also be a better predictive tool for obesity-related mortality (Janssen *et al.*, 2005; Kuk and Ardern, 2009). In fact, a recent report by the WHO proposed that waist circumference could be used as an alternative predictive tool for disease to BMI (World Health Organization, 2012). The new body shape index (ABSI) was recently developed and tested on a US population sample of 14,105 individuals from the NHANES 1999-2004, with a follow-up period of five years (Krakauer and Krakauer, 2012). The ABSI calculation included waist circumference, weight and height, with a high ABSI indicating that waist circumference is higher for a given weight and height, corresponding to more central obesity. High ABSI may therefore correspond to higher visceral fat *versus* peripheral fat. The ABSI appeared to be a better predictor of mortality risk across age, gender and ethnicity in the US compared to BMI or waist circumference alone (Krakauer and

Krakauer, 2012). Using ABSI along with BMI and waist circumference may provide a more complete picture about the metabolic “fitness” and disease risk for a certain individual.

1.4. Metabolic syndrome, insulin resistance and type 2 diabetes

The metabolic syndrome is described by a cluster of metabolic aberrations, including dyslipidemia, hypertension, impaired glucose homeostasis and obesity (specifically visceral adiposity), and is associated with the risk for development of T2DM and cardiovascular disease (Reaven, 1988). These factors are inter-related and occur in tandem rather than individually, and the presence of an array of such factors is required to define the metabolic syndrome. Various criteria and definitions for the diagnosis of metabolic syndrome have surfaced since its original description. However, controversy surrounds the definitions of measurable factors, with differences in age, gender, ethnicity and lifestyle factors playing a role in one sense, while cut-off values and inclusion of certain factors (e.g. waist circumference) can also give rise to uncertainty. A recent joint statement¹ by a number of organizations¹ produced revised interim criteria for the definition and diagnosis of metabolic syndrome in an attempt to unify criteria (Alberti *et al.*, 2009). This statement suggested that any three out of five criteria constitutes diagnosis of the metabolic syndrome, and that a single set of cut-off points were defined for all components except waist circumference. More work is needed to evaluate waist circumference data and national or regional cut-off points should be used in the meantime. The researchers highlighted that the process of determining a unified definition and

¹ International Diabetes Federation Task Force on Epidemiology and Prevention; National Heart, Lung and Blood Institute; American Heart Association; World Health Federation; International Atherosclerosis Society; and International Association for the Study of Obesity.

criteria is an evolutionary process and requires further investigation. The criteria put forth in the statement are summarized in Table 1.1.

Table 1.1 Criteria for diagnosis of metabolic syndrome (Alberti *et al.*, 2009)

Metabolic risk factor	Suggested cut-off points
Elevated waist circumference	Population- and country-specific
Elevated serum triglycerides	≥1.7 mmol/l
Reduced HDL cholesterol	<1.0 mmol/l in males <1.3 mmol/l in females
Elevated blood pressure	Systolic ≥130 mm Hg and/or Diastolic ≥80 mm Hg
Elevated fasting plasma glucose	≥5.6 mmol/l

1.5. The South African context

Despite limited information available in reporting obesity-related diseases in developing nations, early work shows that obesity and poor lifestyle choices are at alarming levels and still increasing (Ezzati and Riboli, 2013). Moreover, Sub-Saharan Africa is facing a multiple disease burden, with metabolic diseases increasing concomitantly with epidemics of infectious diseases (e.g. HIV/AIDS, tuberculosis and malaria) (Levitt *et al.*, 2011). For example, South Africa has one of the largest populations of HIV-infected individuals, and here both HIV/AIDS and NCDs contribute largely to national mortality and disability figures (Norman *et al.*, 2007). Interestingly, the South African Burden of Diseases Study (2000) showed that

mortality and disability due to HIV/AIDS and other infectious diseases was higher in rural (and more impoverished) provinces compared to those with a higher average income (Bradshaw *et al.*, 2008). Conversely, NCDs accounted for high rates of death and disability across all provinces, rates of hypertension, diabetes, obesity and overweight and associated complications are on the rise. Recent evidence suggests that HIV-positive patients on antiretroviral therapy may be particularly susceptible to metabolic alterations, including dyslipidemia, diabetes and myocardial infarction (Bradbury and Samaras, 2008; Friis-Møller and Worm, 2007; Friis-Møller *et al.*, 2003). Indeed, our laboratory recently suggested experimental evidence for disrupted lipid metabolism accompanied by cardiac contractile dysfunction in a rat model exposed to the protease inhibitor class of antiretroviral therapy (Reyskens *et al.*, 2013).

The prevalence of metabolic risk factors is also alarmingly high among children and young adults. A 'nutrition paradox' exists, i.e. the simultaneous manifestation of under- and overweight in some sectors of the population. This may result in South African children exhibiting overweight and obesity on the one hand, and stunted on the other (Kimani-Murage, 2013; Steyn *et al.*, 2005). Such disparity in nutritional status may weigh heavily on future projections for metabolic disorders, and more attention is warranted to determine risk factor prevalence in children. Indeed, Matsha and colleagues recently investigated novel waist-to-hip ratio cut-off criteria to determine cardiovascular risk associated with overweight and obesity in children (Matsha *et al.*, 2013b). A study by our laboratory also showed that metabolic syndrome risk factors are high among young male and female university students (with gender-specific differences) and this may be attributable to poor eating habits

and a sedentary lifestyle (Smith and Essop, 2009). This serious situation will require creative, cost-effective interventions. For example, exercise intervention in the form of Tae-bo effectively reduced cardio-metabolic risk factors in obese/overweight and previously sedentary female university students (Mathunjwa *et al.*, 2013).

Determination of metabolic risk factor cut-off points, specifically waist circumference, is difficult owing to the ethnic diversity of South Africa. A number of studies attempted to define criteria for different ethnic populations to best predict metabolic syndrome and cardio-metabolic risk. However, differences in suggested cut-off points for the same populations still persist (Motala *et al.*, 2011; Prinsloo *et al.*, 2011). Nonetheless, the use of a variety of currently available definitions and criteria shows good concordance and agreement to determine the prevalence of metabolic risk factors in different South African populations in both the rural and urban settings (Erasmus *et al.*, 2012; Matsha *et al.*, 2013a; Motala *et al.*, 2011; Prinsloo *et al.*, 2011). Alarming, the prevalence of T2DM and impaired fasting glucose (IFG) has severely increased in the Mixed Ancestry community of the Western Cape, while a large proportion of cases are undiagnosed or newly diagnosed (Erasmus *et al.*, 2012). Recent data from the same study population also showed a drastic worsening of glucose tolerance in ~20% of participants over a follow-up period of three years (Matsha *et al.*, 2013b). These studies outline the growing burden of metabolic dysfunction and lifestyle diseases through a spectrum of the South African population.

1.6. Problem statement

In conclusion, metabolic dysfunction and lifestyle diseases contribute to a significant health care burden, morbidity and mortality. Of particular concern is the rising incidence in developing nations, including South Africa, and the higher level of young and middle-aged individuals affected. Poor dietary habits and physical inactivity are among the chief lifestyle factors influencing the negative medical outcomes. Such factors contribute to metabolic dysregulation and associated elevations in metabolites (hyperglycemia, hyperlipidemia), blood pressure, cholesterol and weight gain. Subsequent elevation in obesity, metabolic syndrome, pre-diabetes and insulin resistance give rise to development of diabetes and cardiovascular diseases later in life. Current diabetes medication succeed to an extent in meeting the main aims of treatment – curbing weight gain and reducing blood glucose levels – but fail to limit the associated secondary outcomes (e.g. cardiovascular diseases). Drug side-effects also limit development of successful treatment regimens for diabetic patients. Preventative measures including, national and individual restrictions on glycemetic intake, limiting refined foods and promoting healthy lifestyle are essential, but may also be hampered by several factors, including individual adherence.

It is therefore imperative to explore therapeutic and preventative strategies early on in the disease etiology. However, a better understanding of metabolic dysregulation and the associated molecular changes is first required. Acute hyperglycemic episodes may be prevalent in the early stages of diabetes development (pre-diabetes, metabolic syndrome, obesity) or “simply” as a result of high glycemetic dietary intake coupled to physical inactivity. Numerous studies underline molecular

alterations as a result of hyperglycemia (mainly in the chronic setting) and implicate these alterations in a wide variety of diabetic complications (reviewed in Chapter 2). For the present study, we proposed that similar molecular alterations may be at work as a result of acute hyperglycemic episodes. Here biochemical pathways of non-oxidative glucose metabolism and various sources of intracellular oxidative stress may be inter-linked and may exert molecular defects. We employed a novel, holistic approach to assess such mechanisms in a single model and propose a mechanism that may desensitize cardiac myocytes to insulin action. This may lead to insulin resistance if the acute hyperglycemic episodes manifests over a long period of time. The description of these mechanisms may open doors to new (affordable) preventative treatment options to help curb the growing burden of metabolic diseases in South Africa and other developing nations – thus contributing to the UN and WHO “25 by 25” initiative.

1.7. References

- Ahima, R.S., Lazar, M.A., 2013. Physiology. The health risk of obesity - better metrics imperative. *Science* 341, 856–8.
- Alberti, K.G.M.M., Eckel, R.H., Grundy, S.M., Zimmet, P.Z., Cleeman, J.I., Donato, K. a, Fruchart, J.-C., James, W.P.T., Loria, C.M., Smith, S.C., 2009. Harmonizing the metabolic syndrome: a joint interim statement of the International Diabetes Federation Task Force on Epidemiology and Prevention; National Heart, Lung, and Blood Institute; American Heart Association; World Heart Federation; *International Circulation* 120, 1640–5.
- Berrington de Gonzalez, A., Hartge, P., Cerhan, J.R., Flint, A.J., Hannan, L., MacInnis, R.J., Moore, S.C., Tobias, G.S., Anton-Culver, H., Freeman, L.B., Beeson, W.L., Clipp, S.L., English, D.R., Folsom, A.R., Freedman, D.M., Giles, G., Hakansson, N., Henderson, K.D., Hoffman-Bolton, J., Hoppin, J.A., Koenig, K.L., Lee, I.-M., Linet, M.S., Park, Y., Pocobelli, G., Schatzkin, A., Sesso, H.D., Weiderpass, E., Willcox, B.J., Wolk, A., Zeleniuch-Jacquotte, A., Willett, W.C., Thun, M.J., 2010. Body-mass index and mortality among 1.46 million white adults. *N Engl J Med* 363, 2211–9.
- Bloom, D.E., Cafiero, E.T., Jané-Llopis, E., Abrahams-Gessel, S., Bloom, L.R., Fathima, S., Feigl, A.B., Gaziano, T., Mowafi, M., Pandya, A., Prettner, K., Rosenberg, L., Seligman, B., Stein, A.Z., Weinstein, C., 2011. The Global Economic Burden of Non-communicable Diseases | World Economic Forum <http://www.weforum.org/reports/global-economic-burden-non-communicable-diseases>
- Bradbury, R.A., Samaras, K., 2008. Antiretroviral therapy and the human immunodeficiency virus--improved survival but at what cost? *Diabetes Obes Metab* 10, 441–50.
- Bradshaw, D., Nannan, N., Groenewald, P., Joubert, J., Laubscher, R., Nijilana, B., Norman, R., Pieterse, D., Schneider, M., 2008. Provincial mortality in South Africa, 2000 - priority-setting for now and benchmark for the future. *South African Med J*.
- Bray, G.A., 2012. Fructose and risk of cardiometabolic disease. *Curr Atheroscler Rep* 14, 570–8.
- Bray, G.A., 2013. Energy and fructose from beverages sweetened with sugar or high-fructose corn syrup pose a health risk for some people. *Adv Nutr* 4, 220–5.
- Brownell, K.D., Farley, T., Willett, W.C., Popkin, B.M., Chaloupka, F.J., Thompson, J.W., Ludwig, D.S., 2009. The public health and economic benefits of taxing sugar-sweetened beverages. *N Engl J Med* 361, 1599–605.
- Carnethon, M.R., De Chavez, P.J.D., Biggs, M.L., Lewis, C.E., Pankow, J.S., Bertoni, A.G., Golden, S.H., Liu, K., Mukamal, K.J., Campbell-Jenkins, B., Dyer, A.R., 2012. Association of weight status with mortality in adults with incident diabetes. *JAMA* 308, 581–90.
- Chess, D.J., Stanley, W.C., 2008. Role of diet and fuel overabundance in the development and progression of heart failure. *Cardiovasc Res* 269–278.

- Cohen, J.C., Schall, R., 1988. Reassessing the effects of simple carbohydrates on the serum triglyceride responses to fat meals. *Am J Clin Nutr* 48, 1031–4.
- Danaei, G., Singh, G.M., Paciorek, C.J., Lin, J.K., Cowan, M.J., Finucane, M.M., Farzadfar, F., Stevens, G.A., Riley, L.M., Lu, Y., Rao, M., Ezzati, M., 2013. The global cardiovascular risk transition: associations of four metabolic risk factors with national income, urbanization, and Western diet in 1980 and 2008. *Circulation* 127, 1493–502, 1502e1–8.
- Dhingra, R., Sullivan, L., Jacques, P.F., Wang, T.J., Fox, C.S., Meigs, J.B., D’Agostino, R.B., Gaziano, J.M., Vasan, R.S., 2007. Soft drink consumption and risk of developing cardiometabolic risk factors and the metabolic syndrome in middle-aged adults in the community. *Circulation* 116, 480–8.
- Elliott, S.S., Keim, N.L., Stern, J.S., Teff, K., Havel, P.J., 2002. Fructose, weight gain, and the insulin resistance syndrome. *Am J Clin Nutr* 76, 911–22.
- Erasmus, R.T., Soita, D.J., Hassan, M.S., Blanco-Blanco, E., Vergotine, Z., Kegne, A.P., Matsha, T.E., 2012. High prevalence of diabetes mellitus and metabolic syndrome in a South African coloured population: baseline data of a study in Bellville, Cape Town. *S Afr Med J* 102, 841–4.
- Estruch, R., Ros, E., Martínez-González, M.A., 2013. Mediterranean diet for primary prevention of cardiovascular disease. *N Engl J Med* 369, 676–7.
- Ezzati, M., Riboli, E., 2013. Behavioral and dietary risk factors for noncommunicable diseases. *N Engl J Med* 369, 954–64.
- Farzadfar, F., Finucane, M.M., Danaei, G., Pelizzari, P.M., Cowan, M.J., Paciorek, C.J., Singh, G.M., Lin, J.K., Stevens, G.A., Riley, L.M., Ezzati, M., 2011. National, regional, and global trends in serum total cholesterol since 1980: systematic analysis of health examination surveys and epidemiological studies with 321 country-years and 3·0 million participants. *Lancet* 377, 578–86.
- Finucane, M.M., Stevens, G.A., Cowan, M.J., Danaei, G., Lin, J.K., Paciorek, C.J., Singh, G.M., Gutierrez, H.R., Lu, Y., Bahalim, A.N., Farzadfar, F., Riley, L.M., Ezzati, M., 2011. National, regional, and global trends in body-mass index since 1980: systematic analysis of health examination surveys and epidemiological studies with 960 country-years and 9·1 million participants. *Lancet* 377, 557–67.
- Flegal, K.M., Kit, B.K., Graubard, B.I., 2013. Overweight, obesity, and all-cause mortality--reply. *JAMA* 309, 1681–2.
- Fogelholm, M., 2010. Physical activity, fitness and fatness: relations to mortality, morbidity and disease risk factors. A systematic review. *Obes Rev* 11, 202–21.
- Friis-Møller, N., Sabin, C.A., Weber, R., d’Arminio Monforte, A., El-Sadr, W.M., Reiss, P., Thiébaud, R., Morfeldt, L., De Wit, S., Pradier, C., Calvo, G., Law, M.G., Kirk, O., Phillips, A.N., Lundgren, J.D., 2003. Combination antiretroviral therapy and the risk of myocardial infarction. *N Engl J Med* 349, 1993–2003.
- Friis-Møller, N., Worm, S.W., 2007. Can the risk of cardiovascular disease in HIV-infected patients be estimated from conventional risk prediction tools? *Clin Infect Dis* 45, 1082–4.

- Fung, T.T., Malik, V., Rexrode, K.M., Manson, J.E., Willett, W.C., Hu, F.B., 2009. Sweetened beverage consumption and risk of coronary heart disease in women. *Am J Clin Nutr* 89, 1037–42.
- Gómez-Ambrosi, J., Silva, C., Galofré, J.C., Escalada, J., Santos, S., Millán, D., Vila, N., Ibañez, P., Gil, M.J., Valentí, V., Rotellar, F., Ramírez, B., Salvador, J., Frühbeck, G., 2012. Body mass index classification misses subjects with increased cardiometabolic risk factors related to elevated adiposity. *Int J Obes (Lond)* 36, 286–94.
- Gonsolin, D., Couturier, K., Garait, B., Rondel, S., Novel-Chaté, V., Peltier, S., Faure, P., Gachon, P., Boirie, Y., Keriél, C., Favier, R., Pepe, S., Demaison, L., Leverve, X., 2007. High dietary sucrose triggers hyperinsulinemia, increases myocardial beta-oxidation, reduces glycolytic flux and delays post-ischemic contractile recovery. *Mol Cell Biochem* 295, 217–28.
- Havel, P.J., 2005. Dietary Fructose: Implications for Dysregulation of Energy Homeostasis and Lipid/Carbohydrate Metabolism. *Nutr Rev* 63, 133–157.
- He, F.J., Li, J., Macgregor, G.A., 2013. Effect of longer term modest salt reduction on blood pressure: Cochrane systematic review and meta-analysis of randomised trials. *BMJ* 346, f1325.
- Heymsfield, S.B., Scherzer, R., Pietrobelli, A., Lewis, C.E., Grunfeld, C., 2009. Body mass index as a phenotypic expression of adiposity: quantitative contribution of muscularity in a population-based sample. *Int J Obes (Lond)* 33, 1363–73.
- Hunter, D.J., Reddy, K.S., 2013. Noncommunicable diseases. *N Engl J Med* 369, 1336–43.
- International Diabetes Federation, 2011. International Diabetes Federation. Diabetes Atlas: The Global Burden 2011 [WWW Document]. URL <http://www.idf.org/diabetesatlas/5e/the-global-burden>
- Janssen, I., Katzmarzyk, P.T., Ross, R., 2005. Body mass index is inversely related to mortality in older people after adjustment for waist circumference. *J Am Geriatr Soc* 53, 2112–8.
- Johnson, R.K., Appel, L.J., Brands, M., Howard, B. V, Lefevre, M., Lustig, R.H., Sacks, F., Steffen, L.M., Wylie-Rosett, J., 2009. Dietary sugars intake and cardiovascular health: a scientific statement from the American Heart Association. *Circulation* 120, 1011–20.
- Kahn, B.B., 1998. Type 2 Diabetes : When Insulin Secretion Fails to Compensate for Insulin Resistance. *Cell* 92, 593–596.
- Kang, S.M., Yoon, J.W., Ahn, H.Y., Kim, S.Y., Lee, K.H., Shin, H., Choi, S.H., Park, K.S., Jang, H.C., Lim, S., 2011. Android fat depot is more closely associated with metabolic syndrome than abdominal visceral fat in elderly people. *PLoS One* 6, e27694.
- Kasim-Karakas, S.E., Vriend, H., Almario, R., Chow, L.C., Goodman, M.N., 1996. Effects of dietary carbohydrates on glucose and lipid metabolism in golden Syrian hamsters. *J Lab Clin Med* 128, 208–13.
- Kimani-Murage, E.W., 2013. Exploring the paradox: double burden of malnutrition in rural South Africa. *Glob Health Action* 6, 19249.

- King, H., Aubert, R.E., Herman, W.H., 1998. Global Burden of Diabetes, 1995–2025. *Diabetes Care* 21, 1414–1431.
- Kokkinos, P., Myers, J., Faselis, C., Doulas, M., Kheirbek, R., Nylen, E., 2012. BMI-mortality paradox and fitness in African American and Caucasian men with type 2 diabetes. *Diabetes Care* 35, 1021–7.
- Krakauer, N.Y., Krakauer, J.C., 2012. A new body shape index predicts mortality hazard independently of body mass index. *PLoS One* 7, e39504.
- Kuk, J.L., Ardern, C.I., 2009. Influence of age on the association between various measures of obesity and all-cause mortality. *J Am Geriatr Soc* 57, 2077–84.
- Lee, S.-H., Ha, H.-S., Park, Y.-J., Lee, J.-H., Yim, H.-W., Yoon, K.-H., Kang, M.-I., Lee, W.-C., Son, H.-Y., Park, Y.-M., Kwon, H.-S., 2011. Identifying metabolically obese but normal-weight (MONW) individuals in a nondiabetic Korean population: the Chungju Metabolic disease Cohort (CMC) study. *Clin Endocrinol (Oxf)* 75, 475–81.
- Levitt, N.S., Steyn, K., Dave, J., Bradshaw, D., 2011. Chronic noncommunicable diseases and HIV-AIDS on a collision course: relevance for health care delivery, particularly in low-resource settings--insights from South Africa. *Am J Clin Nutr* 94, 1690S–1696S.
- Lim, S.S., Vos, T., Flaxman, A.D., Danaei, G., Shibuya, K., *et al.*, 2012. A comparative risk assessment of burden of disease and injury attributable to 67 risk factors and risk factor clusters in 21 regions, 1990-2010: a systematic analysis for the Global Burden of Disease Study 2010. *Lancet* 380, 2224–60.
- Lozano, R., Naghavi, M., Foreman, K., Lim, S., Shibuya, K., *et al.*, 2012. Global and regional mortality from 235 causes of death for 20 age groups in 1990 and 2010: a systematic analysis for the Global Burden of Disease Study 2010. *Lancet* 380, 2095–128.
- Lumeng, C.N., Saltiel, A.R., 2011. Inflammatory links between obesity and metabolic disease. *J Clin Invest* 121, 2111–7.
- Marriott, B.P., Cole, N., Lee, E., 2009. National estimates of dietary fructose intake increased from 1977 to 2004 in the United States. *J Nutr* 139, 1228S–1235S.
- Marriott, B.P., Olsho, L., Hadden, L., Connor, P., 2010. Intake of added sugars and selected nutrients in the United States, National Health and Nutrition Examination Survey (NHANES) 2003-2006. *Crit Rev Food Sci Nutr* 50, 228–58.
- Mathunjwa, M.L., Semple, S.J., du Preez, C., 2013. A 10-week aerobic exercise program reduces cardiometabolic disease risk in overweight/obese female African university students. *Ethn Dis* 23, 143–8.
- Matsha, T.E., Hassan, M.S., Hon, G.M., Soita, D.J., Kengne, A.P., Erasmus, R.T., 2013a. Derivation and validation of a waist circumference optimal cutoff for diagnosing metabolic syndrome in a South African mixed ancestry population. *Int J Cardiol* 168, 2954–5.
- Matsha, T.E., Soita, D.J., Hassan, M.S., Hon, G.M., Yako, Y.Y., Kengne, A.P., Erasmus, R.T., 2013b. Three-year's changes in glucose tolerance status in the Bellville South

- cohort: rates and phenotypes associated with progression. *Diabetes Res Clin Pract* 99, 223–30.
- Motala, A.A., Esterhuizen, T., Pirie, F.J., Omar, M.A.K., 2011. The prevalence of metabolic syndrome and determination of the optimal waist circumference cutoff points in a rural South african community. *Diabetes Care* 34, 1032–7.
- Mozaffarian, D., Hao, T., Rimm, E.B., Willett, W.C., Hu, F.B., 2011. Changes in diet and lifestyle and long-term weight gain in women and men. *N Engl J Med* 364, 2392–404.
- Mozaffarian, D., Micha, R., Wallace, S., 2010. Effects on coronary heart disease of increasing polyunsaturated fat in place of saturated fat: a systematic review and meta-analysis of randomized controlled trials. *PLoS Med* 7, e1000252.
- Murray, C.J.L., Vos, T., Lozano, R., Naghavi, M., Flaxman, A.D., *et al.*, 2012. Disability-adjusted life years (DALYs) for 291 diseases and injuries in 21 regions, 1990-2010: a systematic analysis for the Global Burden of Disease Study 2010. *Lancet* 380, 2197–223.
- Ni Mhurchu, C., Rodgers, A., Pan, W.H., Gu, D.F., Woodward, M., 2004. Body mass index and cardiovascular disease in the Asia-Pacific Region: an overview of 33 cohorts involving 310 000 participants. *Int J Epidemiol* 33, 751–8.
- Norman, A., Chopra, M., Kadiyala, S., 2007. Factors related to HIV disclosure in 2 South African communities. *Am J Public Health* 97, 1775–81.
- Pischon, T., Boeing, H., Hoffmann, K., Bergmann, M., Schulze, M.B., Overvad, K., van der Schouw, Y.T., Spencer, E., Moons, K.G.M., Tjønneland, A., Halkjaer, J., Jensen, M.K., Stegger, J., Clavel-Chapelon, F., Boutron-Ruault, M.-C., Chajes, V., Linseisen, J., Kaaks, R., Trichopoulou, A., Trichopoulos, D., Bamia, C., Sieri, S., Palli, D., Tumino, R., Vineis, P., Panico, S., Peeters, P.H.M., May, A.M., Bueno-de-Mesquita, H.B., van Duijnhoven, F.J.B., Hallmans, G., Weinehall, L., Manjer, J., Hedblad, B., Lund, E., Agudo, A., Arriola, L., Barricarte, A., Navarro, C., Martinez, C., Quirós, J.R., Key, T., Bingham, S., Khaw, K.T., Boffetta, P., Jenab, M., Ferrari, P., Riboli, E., 2008. General and abdominal adiposity and risk of death in Europe. *N Engl J Med* 359, 2105–20.
- Popkin, B.M., Adair, L.S., Ng, S.W., 2012. Global nutrition transition and the pandemic of obesity in developing countries. *Nutr Rev* 70, 3–21.
- Prinsloo, J., Malan, L., de Ridder, J.H., Potgieter, J.C., Steyn, H.S., 2011. Determining the waist circumference cut off which best predicts the metabolic syndrome components in urban Africans: the SABPA study. *Exp Clin Endocrinol Diabetes* 119, 599–603.
- Reaven, G.M., 1988. Banting lecture 1988. Role of insulin resistance in human disease. *Diabetes* 37, 1595–607.
- Renehan, A.G., Tyson, M., Egger, M., Heller, R.F., Zwahlen, M., 2008. Body-mass index and incidence of cancer: a systematic review and meta-analysis of prospective observational studies. *Lancet* 371, 569–78.
- Retnakaran, R., Zinman, B., 2008. Type 1 diabetes, hyperglycaemia, and the heart. *Lancet* 371, 1790–9.

- Reyskens, K.M.S.E., Fisher, T.-L., Schisler, J.C., O'Connor, W.G., Rogers, A.B., Willis, M.S., Planesse, C., Rondeau, P., Bourdon, E., Essop, M.F., 2013. The Maladaptive Effects of HIV Protease Inhibitors (Lopinavir/Ritonavir) on the Rat Heart. *PLoS One* 8, e73347.
- Rossi, M., Turati, F., Lagiou, P., Trichopoulos, D., Augustin, L.S., La Vecchia, C., Trichopoulou, A., 2013. Mediterranean diet and glycaemic load in relation to incidence of type 2 diabetes: results from the Greek cohort of the population-based European Prospective Investigation into Cancer and Nutrition (EPIC). *Diabetologia* 56, 2405–13.
- Sacks, F.M., Bray, G.A., Carey, V.J., Smith, S.R., Ryan, D.H., Anton, S.D., McManus, K., Champagne, C.M., Bishop, L.M., Laranjo, N., Leboff, M.S., Rood, J.C., de Jonge, L., Greenway, F.L., Loria, C.M., Obarzanek, E., Williamson, D.A., 2009. Comparison of weight-loss diets with different compositions of fat, protein, and carbohydrates. *N Engl J Med* 360, 859–73.
- Schulze, M.B., Manson, J.E., Ludwig, D.S., Colditz, G.A., Stampfer, M.J., Willett, W.C., Hu, F.B., 2004. Sugar-sweetened beverages, weight gain, and incidence of type 2 diabetes in young and middle-aged women. *JAMA* 292, 927–34.
- Sharma, N., Okere, I.C., Duda, M.K., Chess, D.J., O'Shea, K.M., Stanley, W.C., 2007a. Potential impact of carbohydrate and fat intake on pathological left ventricular hypertrophy. *Cardiovasc Res* 73, 257–68.
- Sharma, N., Okere, I.C., Duda, M.K., Johnson, J., Yuan, C.L., Chandler, M.P., Ernsberger, P., Hoit, B.D., Stanley, W.C., 2007b. High fructose diet increases mortality in hypertensive rats compared to a complex carbohydrate or high fat diet. *Am J Hypertens* 20, 403–9.
- Smith, C., Essop, M.F., 2009. Gender differences in metabolic risk factor prevalence in a South African student population. *Cardiovasc J Afr* 20, 178–82.
- Stanhope, K.L., Havel, P.J., 2008. Endocrine and metabolic effects of consuming beverages sweetened with fructose, glucose, sucrose, or high-fructose corn syrup. *Am J Clin Nutr* 88, 1733S–1737S.
- Stanhope, K.L., Schwarz, J.M., Keim, N.L., Griffen, S.C., Bremer, A.A., Graham, J.L., Hatcher, B., Cox, C.L., Dyachenko, A., Zhang, W., McGahan, J.P., Seibert, A., Krauss, R.M., Chiu, S., Schaefer, E.J., Ai, M., Otokozawa, S., Nakajima, K., Nakano, T., Beysen, C., Hellerstein, M.K., Berglund, L., Havel, P.J., 2009. Consuming fructose-sweetened, not glucose-sweetened, beverages increases visceral adiposity and lipids and decreases insulin sensitivity in overweight/obese humans. *J Clin Invest* 119, 1322–34.
- Stevens, G.A., Singh, G.M., Lu, Y., Danaei, G., Lin, J.K., Finucane, M.M., Bahalim, A.N., McIntire, R.K., Gutierrez, H.R., Cowan, M., Paciorek, C.J., Farzadfar, F., Riley, L., Ezzati, M., 2012. National, regional, and global trends in adult overweight and obesity prevalences. *Popul Health Metr* 10, 22.
- Steyn, N.P., Labadarios, D., Maunder, E., Nel, J., Lombard, C., 2005. Secondary anthropometric data analysis of the National Food Consumption Survey in South Africa: the double burden. *Nutrition* 21, 4–13.
- Tappy, L., Lê, K.-A., 2010. Metabolic effects of fructose and the worldwide increase in obesity. *Physiol Rev* 90, 23–46.

- Tseng, C.-H., 2013. Obesity paradox: differential effects on cancer and noncancer mortality in patients with type 2 diabetes mellitus. *Atherosclerosis* 226, 186–92.
- United Nations, 2011. Non-Communicable Diseases Deemed Development Challenge of “Epidemic Proportions” in Political Declaration Adopted During Landmark General Assembly Summit. United Nations Sixty-sixth General Assembly, GA/11138, September 2011. URL <http://www.un.org/News/Press/docs/2011/ga11138.doc.htm>
- Wells, H., Buzby, J., 2008. Dietary assessment of major trends in US food consumption, 1970-2005. *Economic Information Bulletin* No 33. URL <http://www.ers.usda.gov/publications/eib-economic-information-bulletin/eib33.aspx#.UnVtUXBmiSo> (accessed 11.2.13).
- Welsh, J.A., Sharma, A., Cunningham, S.A., Vos, M.B., 2011. Consumption of added sugars and indicators of cardiovascular disease risk among US adolescents. *Circulation* 123, 249–57.
- Whitlock, G., Lewington, S., Sherliker, P., Clarke, R., Emberson, J., Halsey, J., Qizilbash, N., Collins, R., Peto, R., 2009. Body-mass index and cause-specific mortality in 900 000 adults: collaborative analyses of 57 prospective studies. *Lancet* 373, 1083–96.
- Wild, S., Roglic, G., Green, A., Sicree, R., 2004. Global prevalence of diabetes: estimates for the year 2000 and projections for 2030. *Diabetes Care* 27, 1047–1053.
- Wildman, R.P., Muntner, P., Reynolds, K., McGinn, A.P., Rajpathak, S., Wylie-Rosett, J., Sowers, M.R., 2008. The obese without cardiometabolic risk factor clustering and the normal weight with cardiometabolic risk factor clustering: prevalence and correlates of 2 phenotypes among the US population (NHANES 1999-2004). *Arch Intern Med* 168, 1617–24.
- World Health Organization, 2012. 65th World Health Assembly closes with new global health measures
http://www.who.int/mediacentre/news/releases/2012/wha65_closes_20120526/en/index.html (accessed 10.31.13).
- World Health Organization, 2013. Noncommunicable diseases
<http://www.who.int/mediacentre/factsheets/fs355/en/> (accessed 10.31.13).
- Wormser, D., Kaptoge, S., Di Angelantonio, E., Wood, A.M., Pennells, L., Thompson, A., Sarwar, N., Kizer, J.R., Lawlor, D.A., Nordestgaard, B.G., Ridker, P., Salomaa, V., Stevens, J., Woodward, M., Sattar, N., Collins, R., Thompson, S.G., Whitlock, G., Danesh, J., 2011. Separate and combined associations of body-mass index and abdominal adiposity with cardiovascular disease: collaborative analysis of 58 prospective studies. *Lancet* 377, 1085–95.

CHAPTER 2

Cardiomyocyte metabolism in the physiological state

2.1. Introduction

Cardiovascular complications constitute a major cause of death and disability among individuals burdened with diabetes mellitus. Here myocardial insulin resistance may play an important role in the progression of diabetic cardiomyopathy and heart failure (Chavali *et al.*, 2013; Chiha *et al.*, 2012; Gustafsson *et al.*, 2004). Cardiac abnormalities may therefore be strongly linked to metabolic dysfunction. As outlined in Chapter 1, the detrimental consequences of lifestyle and metabolic diseases are taking its toll world-wide. There is a growing number of obese individuals, those presenting with metabolic syndrome risk factors and individuals with undiagnosed or newly diagnosed diabetes, IFG or IGT.

Hyperglycemia, a hallmark of diabetes, may in fact exert detrimental cardio-metabolic effects. For example chronic hyperglycemia is strongly correlated with higher incidence of myocardial infarction and markers of cardiac damage in humans (Barr *et al.*, 2007; Rubin *et al.*, 2012). Furthermore, effective glucose uptake and metabolism is particularly important in the ischemic heart (Tian and Abel, 2001), and also to prevent cardiac dysfunction associated with heart failure (Liao *et al.*, 2002). However, optimal glucose lowering interventions for the treatment of diabetic complications pose unique challenges within the clinical setting (Radke and Schunkert, 2008). Prevention of insulin resistance at an early stage is therefore of

utmost importance to help curb the growing global burden of cardio-metabolic complications.

Chronically elevated nutrients (hyperglycemia, hyperlipidemia) can initiate detrimental metabolic and molecular events. For example, increased hyperglycemia-induced production of reactive oxygen species (ROS) is considered a central factor in mediating damaging outcomes (Brownlee, 2005; Giacco and Brownlee, 2010). Oxidative stress may be linked to disrupted metabolic flux, particularly in the case of glucose metabolism. Here, a block in glycolytic flux may occur, leading to diversion of excess glucose-derived metabolites into alternative non-oxidative glucose pathways (NOGPs), resulting in harmful vascular complications associated with diabetes (Giaccari *et al.*, 2009).

Poor lifestyle and dietary habits can also give rise to the prevalence of acute hyperglycemic episodes (e.g. high postprandial excursions and impaired glucose tolerance) in diabetic and non-diabetic individuals. However, the role of ROS and associated activation of NOGPs under acute hyperglycemic conditions in insulin-responsive cells remains poorly understood. The focus of the current study was therefore to investigate the effects of ROS on NOGP activation and insulin-mediated glucose uptake within the setting of *in vitro* acute hyperglycemia. As the focus is on myocardial glucose uptake and cardio-metabolic dysfunction, we will review the physiological metabolic mechanisms of cardiomyocytes in this chapter. Mechanisms associated with perturbed metabolism in disease states will be addressed in Chapter 3.

2.2. Homeostatic metabolism in cardiomyocytes

2.2.1. Fuel substrates

The mammalian heart requires a continuous output to maintain blood flow and homeostasis throughout the body. Myocardial energy demands are therefore extremely high in order to maintain contractile function, ion pumps and general homeostasis of the heart. An intricate and well controlled series of biochemical mechanisms maintain optimal levels of adenosine triphosphate (ATP), the chemical energy “currency” of cells. The majority of ATP (~95%) is produced via oxidative phosphorylation in the mitochondrial electron transport chain, while glycolysis and guanine triphosphate (GTP) formation in the citric acid cycle contributes to a lesser extent to the ATP pool (reviewed in Stanley *et al.*, 2005). The energy required to fuel mitochondrial oxidative phosphorylation is supplied by electrons that are transferred from carbon fuel substrates to generate reducing equivalents, nicotinamide adenine dinucleotide reduced (NADH) and flavin adenine dinucleotide reduced (FADH₂) (Figure 2.1). The fatty acid (FA) β-oxidation pathway and the citric acid cycle contribute primarily to the pool of electrons used to fuel oxidative phosphorylation, with lesser contributions from the pyruvate dehydrogenase reaction and glycolysis (reviewed in Stanley *et al.*, 2005).

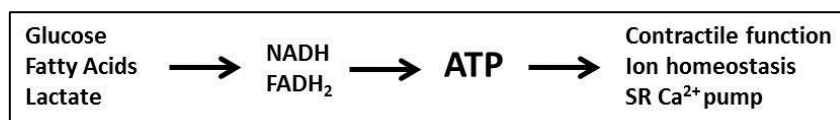


Figure 2.1 Myocardial substrated utilization. Metabolic fuel sources are converted to reducing equivalents that can be used for energy production in the form of ATP, that is subsequently utilized for myocardial functioning. ATP: adenosine triphosphate; FADH₂: flavin adenine dinucleotide reduced; NADH: nicotinamide adenine dinucleotide reduced; SR: sarcoplasmic reticulum.

The citric acid cycle can be viewed as a central mediator of energy metabolism. It is fueled by acetyl-CoA from the decarboxylation of pyruvate or from FA β -oxidation, resulting in the supply of reducing equivalents that are subsequently used for oxidative phosphorylation (Figure 2.2). Since the adult heart is capable of utilizing different substrates (therefore referred to as being “omnivorous”), the choice of substrate utilized at any given time depends on substrate availability, energy demand, rate of oxidation and hormonal concentrations (Atkinson *et al.*, 2002; Grynberg and Demaison, 1996; King *et al.*, 2005; Neely *et al.*, 1972; Opie, 1991; Stanley *et al.*, 1997b; Taegtmeyer, 1994).

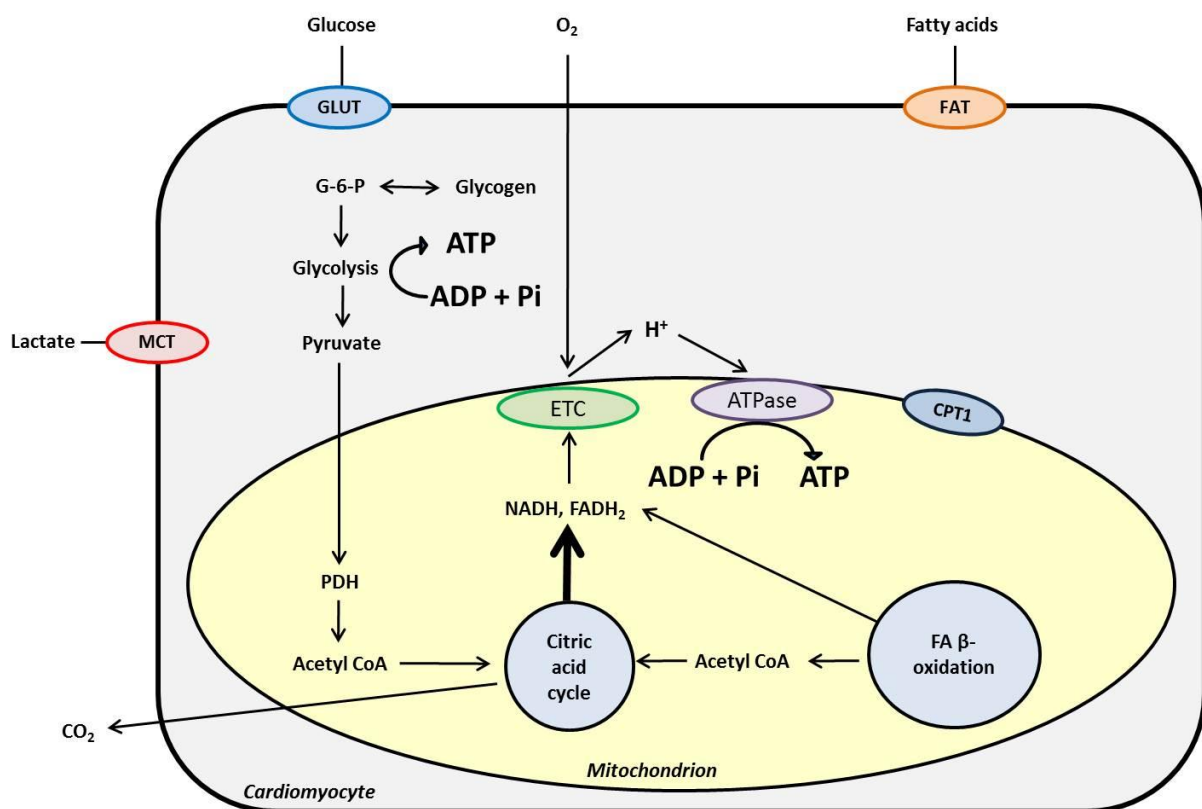


Figure 2.2 Metabolic flux of myocardial substrate utilization. Myocardial metabolic fuel sources (glucose, lactate and FAs) are transported into the cell. Metabolic breakdown of these substrates yield acetyl-CoA, which is in turn used for the production of reducing equivalents in the citric acid cycle, and finally coupled to ATP production in the mitochondrial ETC. GLUT: glucose transporter protein; G-6-P: glucose-6-phosphate; MCT: monocarboxylic acid transporter; PDH: pyruvate dehydrogenase; CoA; co-enzyme A; ETC: electron transport chain; H⁺: proton; FAT: fatty acid translocaser; CPT1: carnitine palmatoyl transferase-1; FA: fatty acid.

Under physiological conditions, the adult heart utilizes FAs as the major substrate, with ~60 to 90% of acetyl-CoA formed as a result of FA β -oxidation and ~10 to 40% from pyruvate oxidation via glycolysis and lactate oxidation (Gertz *et al.*, 1988; Stanley *et al.*, 1997a; Wisneski *et al.*, 1985a, 1985b, 1990). However, after consumption of a meal, the myocardium is exposed to elevated levels of glucose and insulin, resulting in increased glucose utilization that may account for ~60 to 70% of ATP production (Bertrand *et al.*, 2008). The next section will focus on the metabolic mechanisms required to utilize glucose and FA in myocardial cells.

2.2.2. Glucose uptake

Glucose is one of the primary carbohydrate fuel sources in the heart. It may be derived from the diet or endogenous sources (e.g. intracellular glycogen). A range of stimuli, including adrenergic stimulation, intense exercise, ischemia and a low level of myocardial ATP may stimulate glycogenolysis (Figure 2.3) (Goldfarb *et al.*, 1986; Hue *et al.*, 1995; Stanley *et al.*, 1997a). The myocardial glycogen pool is, however, relatively small compared to that of skeletal muscle, while the rate of its turnover is also high (Bøtker *et al.*, 1994; Stanley *et al.*, 1992). Intracellular glycogen concentrations are kept constant via replenishment by extracellular substrates or periods of hyperinsulinemia (Figure 2.3) (Henning *et al.*, 1996). Dietary carbohydrates contribute largely to elevated glucose availability, and glucose becomes the primary fuel substrate in the myocardium in the fed state.

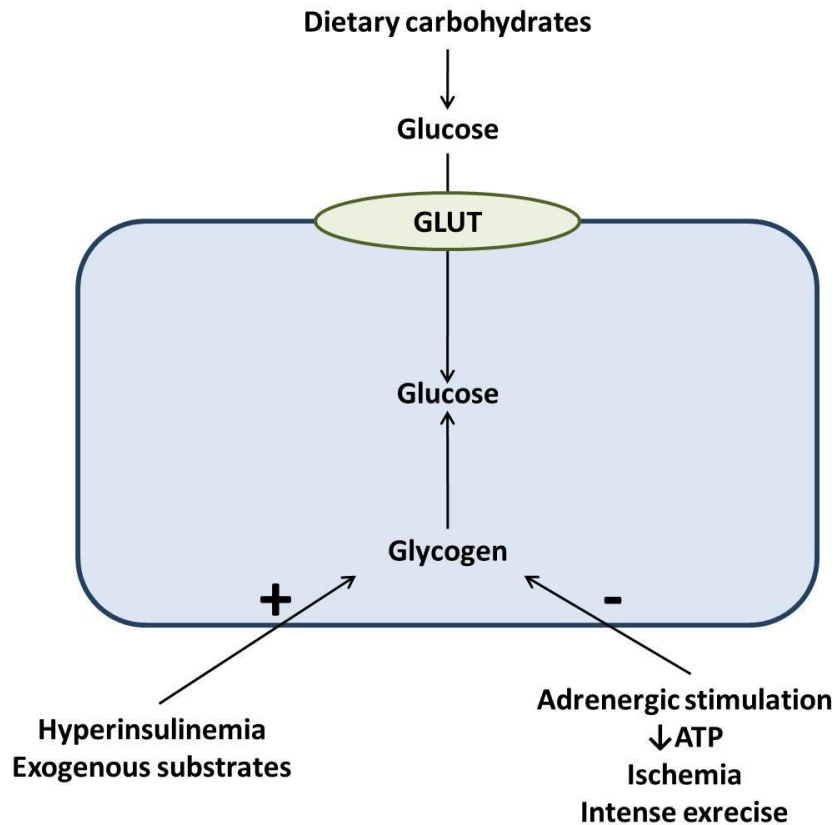


Figure 2.3 Sources of glucose and regulation of glycogen storage and breakdown. Glycogenolysis is stimulated by hyperinsulinemia and exogenous fuel substrates, and inhibited by adrenergic stimulation, low ATP levels, ischemia and intense exercise. ATP: adenosine triphosphate; GLUT: glucose transporter.

2.2.2.1. Glucose transporter proteins

Cardiomyocyte glucose uptake is dependent on its extracellular concentration, as well as the number, distribution and activity of glucose transporter proteins (Luiken *et al.*, 2004; Mueckler, 1994; Young *et al.*, 2000). Glucose metabolic flux is regulated at different steps, including uptake, glycolysis and pyruvate decarboxylation (An and Rodrigues, 2006). The metabolism of any nutrient substrate is, however, decidedly dependent on its uptake. Glucose is taken up into cardiomyocytes by facilitated diffusion via glucose transport proteins in the sarcolemma. The major role players in glucose uptake are the glucose transporters (GLUTs) – a family of 50 kDa proteins

with twelve membrane spanning domains and six extracellular loops (Figure 2.4) (Huang and Czech, 2007; Mueckler, 1994).

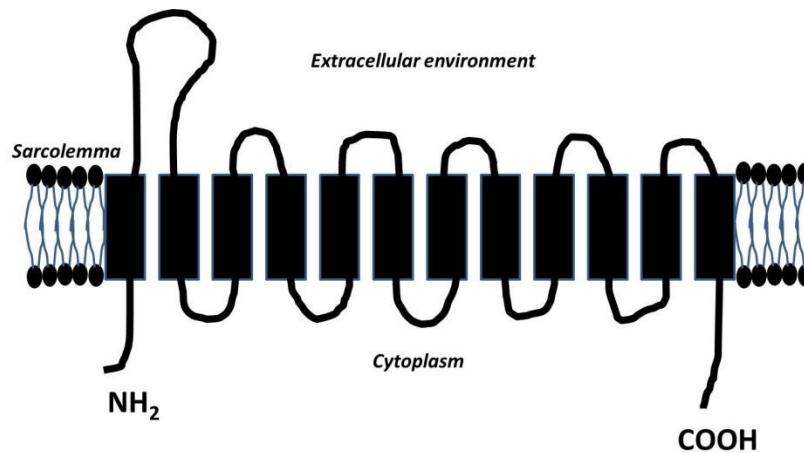


Figure 2.4 Schematic depictions of GLUT transporter proteins. GLUT transporters contain twelve membrane-spanning domains (indicated by the solid black bars) and six extracellular loops (indicated by the solid lines). The first exofacial loop is often used as a site for epitope labeling. COOH: carboxy-terminal; NH₂: amino-terminal.

A number of GLUT isoforms have been identified in cardiomyocytes. In the adult heart, GLUT1 and GLUT4 are responsible for the majority of glucose uptake. GLUT4 is the more abundant transporter, with the ratio of GLUT1/GLUT4 varying between 0.1 and 0.6 (Kraegen *et al.*, 1993). GLUT3 is highly expressed in the fetal heart, with expression levels peaking at embryonic day 15 (Santalucía *et al.*, 1999). However, its expression levels decline in the adult heart, pointing toward a possible role in cardiac development (Shepherd *et al.*, 1992). GLUT12 shares similar di-leucine motifs with that of GLUT4, with 29% sequence homology between the two proteins (reviewed in Abel, 2004). It is also expressed in adipose tissue and skeletal muscle, while its mRNA expression is high within the human heart (Rogers *et al.*, 2002). GLUT11 is present in cardiac and skeletal muscle, and is mainly located at the sarcolemma (Wu *et al.*, 2002). It is homologous to the fructose transporter, GLUT5, however its

glucose uptake function is not inhibited by fructose, pointing toward a possible dual role for glucose and fructose transport (Doege *et al.*, 2001; Wu *et al.*, 2002). GLUT8 may also be present in the myocardium, but together with GLUTs 5, 11 and 12, their function and prominence remains to be elucidated (Dawson *et al.*, 2001; Doege *et al.*, 2000). The sodium-glucose co-transporter (SGLT1) have recently been identified in the heart and may play a role in glucose uptake, however, the precise mechanisms involved need further elucidation (Balteau *et al.*, 2011).

Basal glucose uptake is primarily carried out via GLUT1, which is mainly present at the sarcolemma (Brosius *et al.*, 1997; Buchanan *et al.*, 2005). Insulin may play an important role in GLUT1 expression. This is evident in cardiomyocytes with deletion of the insulin receptor, where GLUT1 expression and basal glucose uptake was reduced (Belke *et al.*, 2002). GLUT4 is considered the most important regulator of myocardial glucose uptake. Indeed transgenic GLUT4^{+/-} mice displayed decreased GLUT4 protein levels and whole body insulin resistance (reviewed in Huang and Czech, 2007; Li *et al.*, 2000; Rossetti *et al.*, 1997). These effects were reversed by GLUT4 overexpression in the same model (Tsao *et al.*, 1999). Furthermore, GLUT4 whole body or cardiac-specific knockout, or transgenic animals developed deleterious cardiometabolic and functional derangements, including dysregulated energy metabolism, contractile dysfunction, hypertrophy and excessive ischemic damage (reviewed in Abel, 2004).

GLUT4 is stored in intracellular vesicles, termed GLUT4 storage vesicles (GSVs), around the perinuclear region in the basal state. Here GLUT4 is co-localized with insulin-regulated aminopeptidase (IRAP) in the same vesicles, residing in the

tubulovesicular structures (Hanpeter and James, 1985). This resembles GSVs from adipocytes and skeletal myocytes where GLUT4 and IRAP contained in the same GSVs possess similar di-leucine and acidic motifs in the carboxy- and amino terminals, features believed to play important roles in the kinetic aspects of GSV endocytosis and exocytosis (reviewed in Huang and Czech, 2007). Although it continuously cycles to and from the sarcolemma and T-tubules, only about 3 to 10% of GLUT4 is present at the sarcolemma with about 90% stored in GSVs in the basal state (Ishiki and Klip, 2005). Following a rise in extracellular glucose concentrations, insulin is secreted from the pancreas, travels to target cells and triggers greater mobilization of GSVs to the sarcolemma and T-tubules. This results in a significant increase in sarcolemmal GLUT4 content and subsequent uptake of glucose. Although it is primarily located at the sarcolemma and plays a prominent role in basal glucose uptake, GLUT1 may also be part of an intracellular storage pool and increases at the sarcolemma in response to insulin stimulation. Indeed, insulin stimulation results in increased GLUT1 and GLUT4 at the sarcolemma, which could be reversed by wortmannin (a PI3K inhibitor), suggesting a role for the phosphoinositol-3-kinase (PI3K) signaling pathway in this process (Egert *et al.*, 1999).

Similar to GSVs from adipocytes and skeletal muscle, cardiomyocyte GSVs contain the cellular machinery that governs their exocytosis, tethering, docking, fusion and endocytosis. These include v-snare protein cellubrevin/VAMP3 and the t-SNARE proteins SNAP25, syntaxin-1A and syntaxin-1B (Sevilla, 1997). Cardiomyocytes may contain two distinct pools of GLUT4. Pool 1, the large insulin responsive/storage pool mainly contains GLUT4 (reviewed in Abel, 2004). The second (endosomal) pool

consists of GLUT1, SCAMP39 and a small number of GLUT4. Insulin stimulation recruits all GLUT4 from pool 1 and all GLUT1 from pool 2, however, GLUT4 from pool 2 is only mobilized when the first insulin responsive pool is depleted. Furthermore, rotenone stimulates the recruitment of GLUT1 and GLUT4 from the endosomal pool, but not GLUT4 from the insulin responsive pool. Together, this suggests that a “reserve” of GLUT4 is stored in the endosomal pool, which may have migrated from the insulin responsive pool. Insulin withdrawal stimulates re-entry of GLUT1 and GLUT4 to their respective pools (Becker *et al.*, 2001; Doenst *et al.*, 2000; Kraegen *et al.*, 1993). This ensures availability of transporters for rapid upregulation of glucose uptake. Although tethering, docking and fusion events at the sarcolemma are integral to glucose uptake, the activation and translocation of GSVs are the primary events. This involves movement upon cytoskeletal proteins, including microtubules and cortical actin (Bose *et al.*, 2002; Semiz *et al.*, 2003; Thurmond *et al.*, 2003). Glucose uptake is terminated when GLUT4-containing GSVs are transported back to the site of storage via endocytosis.

2.2.2.2. Insulin signaling mechanisms

The anabolic hormone insulin promotes several cellular processes, including storage of nutrients from the circulation into various cell types (Koonen *et al.*, 2005). Insulin initiates two main intracellular signaling pathways – the mitogen activated protein kinase (MAPK) pathway and PI3K pathway (Coort *et al.*, 2007; Koonen *et al.*, 2005; Watson and Pessin, 2001). While the MAPK pathway is mainly involved in the regulation of gene expression, the PI3K is an essential regulator of metabolism.

Inhibition or expression of dominant negative PI3K may reduce the effects of insulin on glucose uptake and glycogen and lipid synthesis (Shepherd *et al.*, 1995).

Insulin is secreted from pancreatic β -cells when blood glucose levels rise following a meal. Here, glucose is taken up into the β -cells by insulin-independent GLUT1, GLUT2 and GLUT3. The increased oxidative metabolism of glucose results in elevated ATP/ADP ratios, leading to closure of ATP-sensitive potassium (K_{ATP}) channels. This in turn results in opening of voltage-gated calcium (Ca^{2+}) channels and a rapid influx of Ca^{2+} , which in turn stimulates the fusion of insulin-containing granules with the plasma membrane, leading to insulin exocytosis (Kahn *et al.*, 2006). Cyclic AMP, FA and protein kinase C(PKC)–mediated pathways may also contribute to release of intracellular Ca^{2+} stores and a global rise in β -cell Ca^{2+} levels, with the subsequent release of insulin into the bloodstream. The major targets of insulin-mediated glucose uptake are skeletal muscle, adipose tissue, the liver and the heart. For the purposes of this thesis, we will focus on insulin action at the cardiomyocyte.

Insulin signaling is initiated upon binding of the hormone with its receptor on the exofacial leaflet of the sarcolemma (Fig 2.5). The tetrameric insulin receptor consists of two extracellular α -subunits and two transmembrane β -subunits (Kasuga *et al.*, 1982). Upon binding, the receptor undergoes a conformational change that initiates the intrinsic tyrosine kinase activity of β -subunits. These events activate auto-phosphorylation of the tyrosine residues of the β -subunits, as well as those of insulin receptor substrate-1 (IRS-1), the downstream target of the insulin receptor (Bertrand *et al.*, 2008; Craparo *et al.*, 1997; Hotamisligil *et al.*, 1996). The activated IRS-1

subsequently binds to and activates PI3K. This is achieved by exposing and binding phospho-tyrosine binding sites on Src homology two (SH2) domains on adapter proteins or on the p85 regulatory subunit of PI3K directly (Wu *et al.*, 2007). The p85 regulatory subunit usually stabilizes and suppresses the catalytic activity of the p110 subunit of PI3K in unstimulated cells. Activation of the p85 subunit upon stimulation activates the catalytic action of the p110 subunit. This results in the phosphorylation of the D3 inositol ring of plasma membrane lipids, notably phosphatidylinositol-4,5-bisphosphate (PIP₂), generating phosphatidylinositol-3,4,5-triphosphate (PIP₃) (Cantrell, 2001). These lipids are generated in the inner leaflet of the sarcolemma, resulting in pools of second messengers present at this site upon insulin stimulation. Additional signaling cascades may also activate PI3K via recruitment and transphosphorylation of adapter proteins and stimulation of integrin dependent cell adhesion (Cantley, 2002).

The PIP₃ lipid mediators are able to interact with pleckstrin homology (PH) domain-containing proteins which are specialized to bind phosphoinositides (Vanhaesebroeck *et al.*, 2001). Many of these proteins, including protein kinase B (Akt) and 3-phosphoinositide-dependent kinase 1 (PDK1), associates with PIP₃ at the sarcolemma. These PH-domain containing proteins have a high affinity for phosphatidylinositol lipid products, and therefore accumulate in close proximity to the sarcolemma upon insulin stimulation (Vanhaesebroeck *et al.*, 2001). The serine/threonine kinase Akt (also known as protein kinase B or PKB) is an important effector of insulin signaling, with involvement in multiple cellular processes. These include cell survival, proliferation and growth, gene expression, angiogenesis and

metabolic regulation, among others. It is also a central effector of GLUT4 translocation to the sarcolemma and the subsequent uptake of glucose.

Activation of membrane-bound Akt is achieved through dual phosphorylation of serine 473 and threonine 308 residues by mammalian target of rapamycin (mTOR) in complex with rictor and SIN1 (also known as rictor-mTORC2) and PDK1, respectively (Sarbasov *et al.*, 2005). Both phosphorylation events are believed to be necessary for full activation of Akt. Rictor-mTORC2 and Akt are both recruited to the sarcolemma following PI3K-mediated PIP₃ formation, where they bind via their PH domains. As they are localized in close proximity, the rictor-mTORC2 phosphorylates Akt on the serine 473 residue of its C-terminal regulatory domain (Sarbasov *et al.*, 2005). Next, PDK1 phosphorylates the threonine 308 residue in the activation loop of the kinase domain, leading to complete activation of Akt (Stephens *et al.*, 1998). The distal signaling events involving Akt are diverse, with a number of Akt substrates involved. The phosphorylation of glycogen synthase kinase (GSK3 β) is among one of the substrates, promoting glycogen storage (Elchebly *et al.*, 1999; Stanley *et al.*, 1997a; Steinbusch *et al.*, 2011).

The recently identified Rab GTPase-activating protein (RabGAP) called Akt substrate of 160 kD (AS160, also known as TBC1D4), is believed to be directly involved in the mobilization of GSVs (Kane *et al.*, 2002; Sano *et al.*, 2003). Data generated thus far indicate that active (i.e. unphosphorylated) AS160 associates with GSVs and thereby keeps it immobilized in the basal condition, while insulin results in its phosphorylation and inhibition, leading to its dissociation from the GSV and dimerization with 14-3-3 proteins (Larance *et al.*, 2005; Peck *et al.*, 2006) (Fig 2.5). Phosphorylation occurs on

six sites *in vivo*, of which five are identical to the Akt substrate sequence. Cells expressing mutant AS160 lacking the Akt-specific phosphorylation sites inhibits insulin-mediated GLUT4 translocation, suggesting it acts as a negative regulator which is inactivated by insulin (Larance *et al.*, 2005; Peck *et al.*, 2006; Sano *et al.*, 2003). These studies therefore show that decreased Akt activity would also attenuate AS160 function, resulting in reduced GLUT4 translocation and glucose uptake. *In vitro* experiments show that AS160 catalyzes the inactivation of Rab proteins 2A, 8A, 10 and 14. Here the Rab proteins are inactivated by GDP binding (Fig 2.5). These Rab proteins are important regulators of intracellular vesicle trafficking (Zerial and McBride, 2001). Hence, the Akt-mediated phosphorylation of AS160 leads to its inactivation, thereby increasing the amount of active (GTP-bound) Rab proteins which in turn facilitates the mobilization of GSVs (refer red arrows in Fig 2.5). AS160 can also bind to IRAP, however, it is not clear whether this interaction is Akt-dependent (Larance *et al.*, 2005; Peck *et al.*, 2006). The interaction of AS160 with 14-3-3 proteins may be dependent on phosphorylation at threonine 642 (Ramm *et al.*, 2006). RNAi knockdown studies suggest that AS160 plays a role in GLUT4 mobilization to the sarcolemma, but not in its endocytosis (Eguez *et al.*, 2005; Larance *et al.*, 2005; Zeigerer *et al.*, 2004). Although insulin-stimulated AS160 phosphorylation is decreased by ~39% in skeletal muscle of diabetic patients (Karlsson *et al.*, 2005), overall myocyte GLUT4 translocation is reduced by ~90% (Ryder *et al.*, 2000). This may suggest that additional mechanisms are also impaired in diabetes.

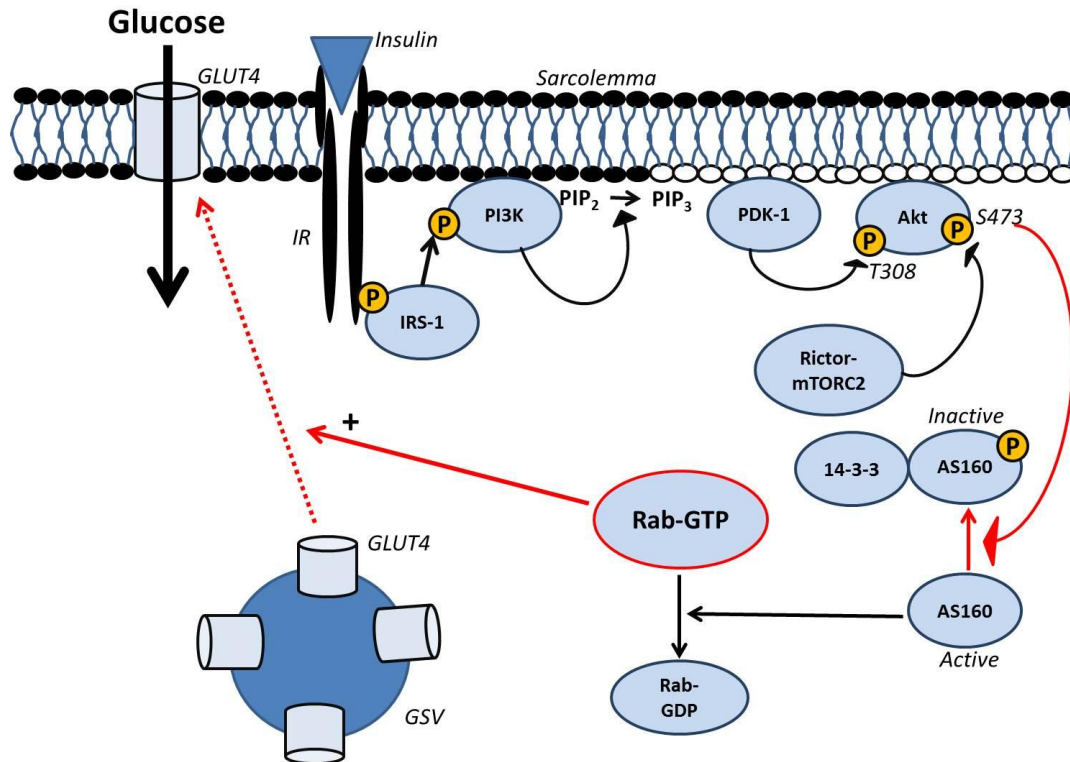


Figure 2.5 Insulin signaling and GLUT4 translocation. Insulin exerts a cascade of phosphorylation events upon binding to the insulin receptor. These phosphorylation events recruit PI3K and Akt to the sarcolemma, leading to its activation. Akt is a central mediator of insulin action, and inactivates AS160 by phosphorylation, followed by binding to 14-3-3 proteins. This leads to upregulation of active (GTP-bound) Rab proteins, which stimulates GSV mobilization. Akt: protein kinase B; AS160; Akt substrate of 160 kDa; GLUT4: glucose transporter 4; GSV; GLUT4 storage vesicle; IR: insulin receptor; IRS-1; insulin receptor substrate-1; mTOR; mammalian target of rapamycin; PI3K: phosphatidylinositol-3 kinase; PIP₂: phosphoinositide-3,4-diphosphate; PIP₃: phosphoinositide-3,4,5-triphosphate; PDK-1; 3-phosphoinositide-dependent kinase-1.

Termination of insulin signaling and glucose uptake can be mediated by endocytosis and degradation processes, as well as inhibitory phosphorylation events. Dephosphorylation of the insulin receptor and IRS-1 tyrosine residues is regulated by tyrosine phosphatases (PTPases). Protein tyrosine phosphatase 1B (PTP1B) has been identified to play a role, as transgenic mice lacking PTP1B showed prolonged insulin receptor and IRS-1 phosphorylation accompanied by higher insulin sensitivity (Elchebly *et al.*, 1999). Furthermore, serine/threonine kinases may attenuate the activity of the insulin receptor by interfering with tyrosine phosphorylation (Craparo *et al.*, 1997; Hotamisligil *et al.*, 1996). These inhibitory phosphorylation processes act

as negative feedback systems to insulin action, but may also be involved in attenuated signaling processes giving rise to insulin resistance (Saltiel and Kahn, 2001).

Signaling mechanisms in addition to the PI3K-Akt-AS160 axis have also been implicated in the translocation of GLUT4. The downstream activation of atypical PKC λ/ζ by PI3K is implicated in exerting insulin-mediated GLUT4 translocation (Bandyopadhyay *et al.*, 2002). However, the precise mechanisms involved and importance toward contributing to glucose uptake remain to be elucidated. A novel signaling pathway involving CAP/Cbl/TC10 may also exert GLUT4 translocation independent of and in concert with PI3K, downstream of IR tyrosine phosphorylation (Chiang *et al.*, 2001). Contraction of skeletal muscle is an important regulator of GLUT4 translocation and glucose uptake, independent of insulin action (Nesher *et al.*, 1985; Zorzano *et al.*, 1986).

Although this mechanism is difficult to determine in the heart due to its continuous contraction, some studies suggest it may play a role. For example, *in vivo* working heart experiments using mice with cardiomyocyte ablation of the IR showed a ~2-fold increase in GLUT4 levels and glucose uptake, despite decreased GLUT1 levels (Belke *et al.*, 2002). Overexpression of GLUT4 in transgenic mice showed an increase in glycolysis in working heart preparations (Belke *et al.*, 2001). Furthermore, field stimulation (*in vitro* contraction) of cardiomyocytes resulted in increased GLUT4 translocation and glucose uptake in the absence of insulin (Kolter *et al.*, 1992). This effect could be reversed by wortmannin treatment, contrasting findings to that in skeletal muscle (Wheeler *et al.*, 1994). As in skeletal muscle, contraction-mediated

GLUT4 translocation may be exerted via adenosine monophosphate protein kinase (AMPK) activation. Indeed, increased myocardial workload is associated with greater AMPK activity and GLUT4 translocation (Coven *et al.*, 2003). Here, higher intracellular Ca^{2+} concentrations and an increase in the AMP/ATP ratio may activate upstream kinases leading to AMPK activation, e.g. LKB-1 (reviewed in Huang and Czech, 2007). Myocardial ischemia may also upregulate GLUT1 and GLUT4 translocation by activation of AMPK (Egert *et al.*, 1999; Fuller *et al.*, 2001). Indeed, AICAR (a pharmacological activator of AMPK) increased GLUT4 translocation via PI3K independent mechanisms, while inhibition of AMPK decreased hypoxia-induced GLUT4 translocation and glucose uptake (Russell *et al.*, 1999). Furthermore, transgenic mice with AMPK inactivation were more prone to ischemic injury (Xing *et al.*, 2003). To summarize, glucose uptake is governed by multiple intracellular mechanisms, however insulin stimulated GLUT4 translocation represents the most prominent means of glucose transport.

2.2.2.3. Physiological regulation of glucose uptake

The regulation of glucose uptake is an important mechanism to control myocardial substrate usage. Elevated availability of various alternative substrates inhibits GLUT4 translocation and glucose uptake at the cardiomyocyte, e.g. high citrate and malate levels in response to increased metabolic flux from alternative fuel sources may negatively regulate cardiac glucose uptake (independent to the regulation of PDH) (Beauloye *et al.*, 2002). Long-chain FA, e.g. palmitate, resulted in the reduction of GLUT1 and GLUT4 at the sarcolemma (Wheeler *et al.*, 1994). The metabolism of lipids, amino acids and ketone bodies have also been associated with reduced

GLUT4 translocation (Tardif *et al.*, 2001; Terruzzi *et al.*, 2002). Additionally GLUT4 translocation may be promoted by α -lipoic acid, serotonin, bradykinin, endothelin-1, lactate and the intracellular pH, while cGMP impairs its translocation to the sarcolemma (Bergemann *et al.*, 2001; Dransfeld *et al.*, 2002; Fischer *et al.*, 1995; Medina *et al.*, 2002; Morin *et al.*, 2002; Ramrath *et al.*, 1999; Rett *et al.*, 1997, 1996; Wu-Wong *et al.*, 2000; Yang *et al.*, 2002). The information summarized here highlights the physiological mechanisms and regulation of myocardial glucose uptake. The next section reviews the fate of glucose upon entering cells under physiological conditions.

2.2.3. Glycolysis

Upon entry of glucose into the cell, it is rapidly phosphorylated to glucose-6-phosphate and enters the glycolytic pathway. Glycolysis is also the major metabolic pathway utilized within conditions of low oxygen availability (e.g. during ischemia). Exogenous glucose supply and glycogen stores are the major sources of glycolytic substrates. The rapid phosphorylation of glucose by hexokinase-2 produces glucose-6-phosphate (G-6-P), rendering it impermeable to the sarcolemma and hence trapping it inside the cell (Bouché *et al.*, 2004). Next, isomerase converts G-6-P to fructose-6-phosphate (F-6-P), followed by the phosphofructokinase-1 (PFK-1) reaction, resulting in the production of fructose-1,6-bisphosphate (F-1,6-BP). The hexokinase-2 and PFK-1 reactions each utilize one molecule of ATP. The myocardial glycolytic rate is controlled by several steps, including glucose uptake, its phosphorylation, and the PFK-1 catalyzed reaction (Rider *et al.*, 2004). PFK-1 is regulated by several stimuli. Here low pH, citrate, and ATP inhibits the enzyme, while

ADP, AMP, phosphate and fructose-2,6-bisphosphate(F-2,6-BP) stimulates its activity (Depre *et al.*, 1999; Rider *et al.*, 2004). Phosphofructokinase-2 (PFK-2) catalyzes the conversion of F-1,6-BP to F-2,6-BP (Hue and Rider, 1987). PFK-2 activity may alternatively be upregulated by PKC, protein kinase A (PKA) and PI3K (An and Rodrigues, 2006; Depre *et al.*, 1998; Marsin *et al.*, 2000). These stimulatory mechanisms lead to increased F-2,6-BP generation, which subsequently activates PFK-1 and promotes glycolysis.

The next step in glycolysis involves the splitting of the six-carbon F-1,6-BP into two triose phosphates, namely dihydroxy-acetone phosphate (DHAP) and glyceraldehyde-3-phosphate (G-3-P) in a reaction catalyzed by aldolase. Triose phosphate isomerase catalyzes the inter-conversion of DHAP and G-3-P; however G-3-P is rapidly utilized in the subsequent glycolytic reactions. It is converted to 1,3-bisphosphoglycerate(1,3-BPG) by glyceraldehyde-3-phosphate dehydrogenase (GAPDH). This is another regulatory step in glycolytic flux, and the regulation of GAPDH activity under increased nutrient conditions is an important factor. The GAPDH reaction results in the transfer of H^+ of NAD^+ molecules that results in the production of NADH. Next, phosphoglycerokinase transfers a phosphate from 1,3-BPG to ADP, forming ATP. As there are two molecules of 1,3-BPG, the net result of the reaction is two ATP and two 3-phosphoglycerate molecules. The enzyme phosphoglyceromutase relocates the phosphate from the third to the second carbon of 3-phosphoglycerate. The resulting 2-phosphoglycerate is then converted to phosphoenolpyruvate (PEP) by enolase. In the final step, PEP is converted to pyruvate by pyruvate kinase, a reaction that yields a further two ATP molecules. The main reactions and regulatory mechanisms of glycolysis are depicted in Figure 2.6.

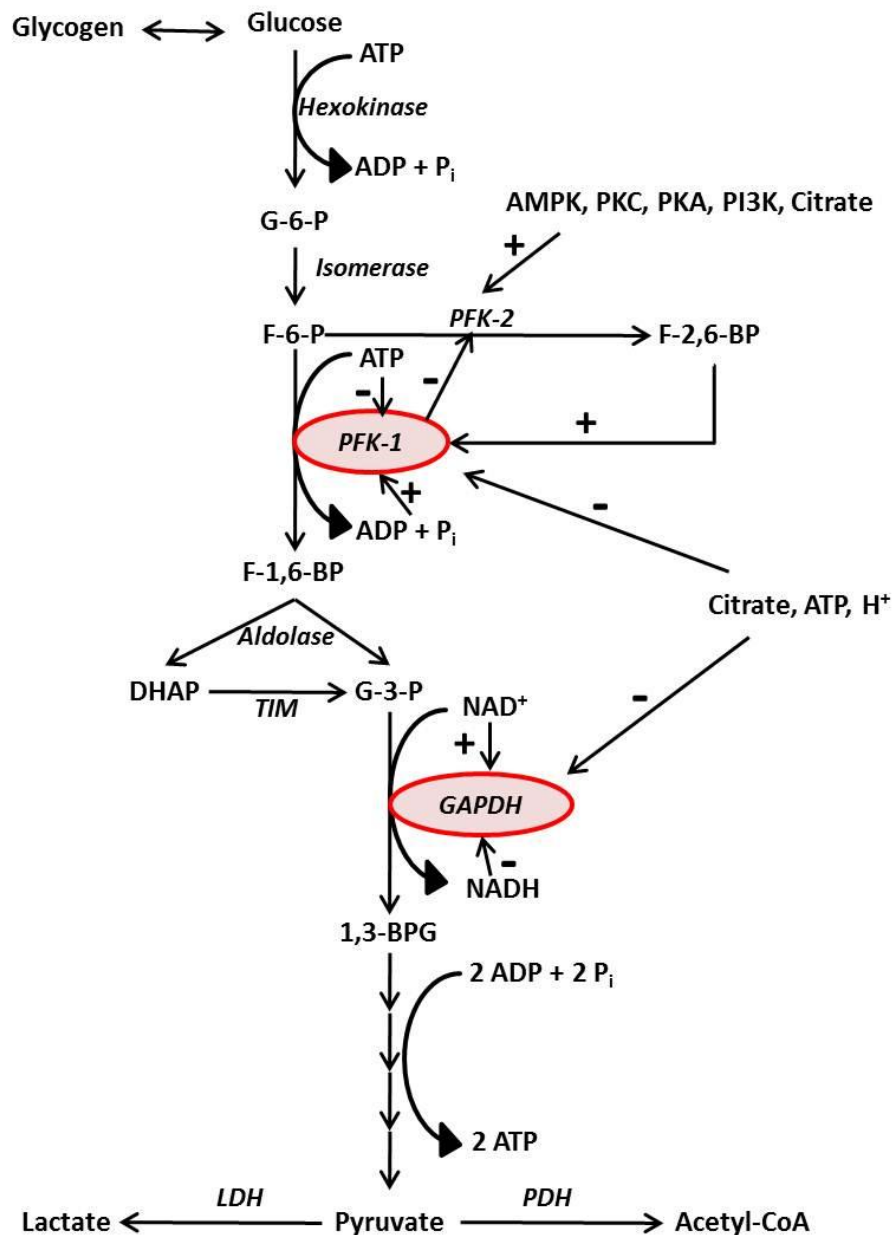


Figure 2.6 Reactions and regulation of glycolysis. Intracellular glucose (taken up from exogenous sources or from glycogen breakdown) is metabolized to pyruvate in a series of glycolytic steps. The reactions catalyzed by PFK-1 and GAPDH are regulated by various stimuli. AMPK: adenosine monophosphate (AMP) activated kinase; 1,3-BPG: 1,3-bisphosphoglycerate; DHAP: dihydroxy acetone phosphate; F-6-P: fructose-6-phosphate; F-1,6-BP: fructose-1,6-bisphosphate; F-2,6-BP: fructose-2,6-bisphosphate; G-6-P: glucose-6-phosphate; G-3-P: glyceraldehyde-3-phosphate; LDH: lactate dehydrogenase; PFK-1: phosphofructokinase-1; PFK-2: phosphofructokinase-2; PDH: pyruvate dehydrogenase; PKC: protein kinase C; PKA; protein kinase A; PI3K: phosphoinositide-3-kinase TIM: triose phosphate isomerase.

The net result of glycolytic flux yields two ATPs per glucose molecule under oxygen rich conditions, contributing to ~10% of total myocardial ATP production (Opie and

Knuuti, 2009). Glycolytic-derived ATP may play an important role in the maintenance of ion pumps, including sarcoplasmic reticulum ATPases (Hasin and Barry, 1984; Opie and Knuuti, 2009). This is highlighted by studies showing that glycolytic ATP may enhance sarcoplasmic calcium re-uptake and enhance diastolic relaxation in isolated heart tissues (Hasin and Barry, 1984; Jeremy *et al.*, 1992; Kusuoka and Marban, 1994; Schönekeess *et al.*, 1995; Weiss and Hiltbrand, 1985). Furthermore, glycolytic ATP may inhibit cardiac ATP-sensitive potassium channels, while it is important for optimal function of the Na⁺/K⁺ ATPase to prevent Na⁺ accumulation (Weiss and Lamp, 1989).

Glycolysis yields NADH and pyruvate, which can subsequently be shuttled into the mitochondrial matrix where these products can be further utilized for energy production via oxidative metabolic processes. When oxygen is limiting, pyruvate is converted to lactate by lactate dehydrogenase with the oxidation of NADH to NAD⁺. Lactate is taken up into the myocardium via the monocarboxylic acid transporter-1 (MCT-1). With tightly regulated energy metabolism and myocardial work in the healthy heart, the cardiomyocyte utilizes lactate as a substrate (Kaijser and Berglund, 1992; Massie *et al.*, 1995; Stanley, 1991). However, with impaired pyruvate oxidation and accelerated glycolysis it becomes a net producer of lactate, e.g. during ischemia or diabetes (Avogaro *et al.*, 1990; Hall *et al.*, 1996b; Stanley *et al.*, 1997a).

Upon entering the mitochondrial matrix, pyruvate may be decarboxylated to form acetyl-CoA or carboxylated to form oxaloacetate or malate. This anaplerotic reaction leads to maintenance of citric acid cycle intermediates (Comte *et al.*, 1997; England and Robinson, 1969; Gibala *et al.*, 2000; Paradies *et al.*, 2001; Vincent *et al.*, 2004).

The pyruvate dehydrogenase (PDH) complex located in the mitochondrial matrix is a key mediator of glucose metabolism, coupling glycolysis to oxidative phosphorylation by the irreversible conversion of pyruvate to acetyl-CoA (Randle, 1986). The enzyme complex consists of pyruvate decarboxylase, dihydrolipoyl transacetylase, dihydrolipoyl dehydrogenase and the co-factors thiamine pyrophosphate, lipoic acid, co-enzyme A, flavin adenine dinucleotide (FAD) and nicotinamide adenine dinucleotide (NAD) (reviewed in Taegtmeyer, 1994).

PDH is regulated by various mechanisms. Phosphorylation on the E1 subunit by PDH kinase-4 (PDK-4) inactivates the enzyme complex (Randle and Priesman, 1996). PDK-4 is the major PDK isoform in the heart and its expression and activity may be rapidly regulated by fasting, diabetes and ligands of the peroxisome proliferator-activated receptor- α (PPAR- α), a key FA transcriptional regulator (Bowker-Kinley *et al.*, 1998; Harris *et al.*, 2001; Wu *et al.*, 2001). Pyruvate itself together with decreases in acetyl-CoA/CoA and NADH/NAD⁺ ratios, also inhibit PDK-4 (Bowker-Kinley *et al.*, 1998; Holness and Sugden, 2003). The inhibition of PDH by increased FA metabolism (the Randle cycle) is another regulatory mechanism whereby FA oxidation inhibits glucose metabolism. This is discussed in Section 2.2.6. Activation of PDH occurs via de-phosphorylation by a PDH phosphatase contained within the PDH complex (Panchal *et al.*, 2000). The PDH phosphatase activity is in turn increased by elevated Ca²⁺ and Mg²⁺ levels as occurs during adrenergic stimulation of the myocardium (McCormack and Denton, 1989, 1984; McCormack *et al.*, 1990). The regulation of PDH is described in Figure 2.7 below.

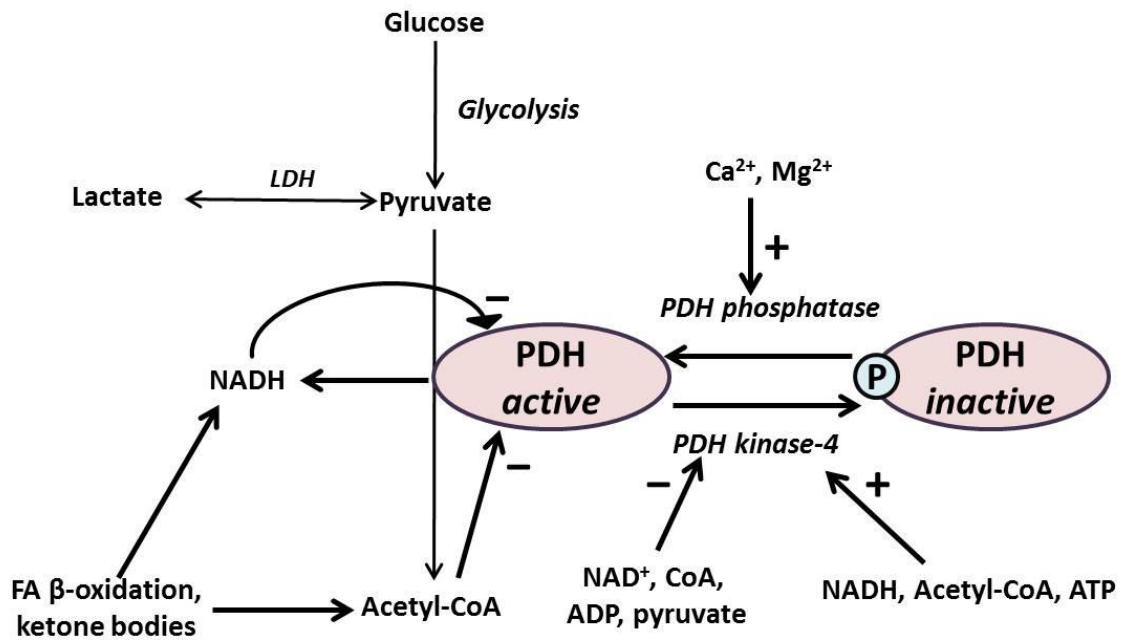


Figure 2.7 Regulation of the pyruvate dehydrogenase complex. PDH facilitates the conversion of pyruvate to acetyl-CoA in the mitochondria. PDH activity is controlled by phosphorylation/dephosphorylation events via PDK-4 and PDH phosphatase. These enzymes are in turn regulated by various stimuli. PDH activity is also directly inhibited by acetyl-CoA and NADH. ADP: adenosine diphosphate; ATP: adenosine triphosphate; Ca²⁺: calcium; CoA: co-enzyme A; FA: fatty acid; LDH: lactate dehydrogenase; Mg²⁺: magnesium; NAD⁺: nicotinamide adenine dinucleotide oxidized; NADH: nicotinamide adenine dinucleotide reduced; PDH: pyruvate dehydrogenase.

2.2.4. Fatty acid uptake and fate

Cardiomyocyte FA uptake is mainly dependent on the concentration of plasma FAs (Bing *et al.*, 1954; Lopaschuk *et al.*, 1994a; Wisneski *et al.*, 1987). FAs travel through the circulation as part of chylomicrons, bound to albumin or esterified in very low density lipoproteins (VLDLs) (Spector, 1984; Stremmel *et al.*, 1985). The concentration of FAs may increase by up to 5-fold during ischemia or in diabetes (Kurth-Kraczek *et al.*, 1999; Stanley *et al.*, 2005). FAs are released from storage during the fasted state, leading to elevated plasma levels, uptake and metabolism. Esterified FAs must be hydrolyzed by lipoprotein lipase, while those bound to

albumin can freely dissociate. FAs are mainly transported into cardiomyocytes with the aid of membrane transport proteins, although a small proportion is taken up by passive diffusion (Stahl *et al.*, 2002). Transporter-mediated FA uptake is regulated via fatty acid translocase (FAT), plasma membrane fatty acid binding protein (FABPpm) and fatty acid transport proteins (FATP-1 and FATP-6) (Coburn *et al.*, 2001; Coort *et al.*, 2007; Glatz *et al.*, 2002; Luiken *et al.*, 2001; Stahl *et al.*, 2001; Stanley *et al.*, 2005). The 88 kDa protein CD36 is the predominant FAT protein expressed in the heart, while FATP-6 is more abundant than FATP-1 in cardiomyocytes (Gimeno *et al.*, 2003; Schaap *et al.*, 1997). FATP co-localizes with CD36 at the sarcolemma and they are considered to act in concert to achieve FA uptake (Gimeno *et al.*, 2003). During uptake, FFA bind to FABPpm and are subsequently esterified to fatty acyl-CoA by fatty acyl-CoA synthase (FACS). CD36-associated FABP and FACS proteins may also be present in the cytoplasm, rapidly converting intracellular FFAs to fatty acyl-CoA (Schaffer, 2002). Insulin may increase the expression of CD36 and FATP (Egert *et al.*, 1999; Gimeno *et al.*, 2003; Kurth-Kraczek *et al.*, 1999; Stahl *et al.*, 2001). Additionally, CD36 may be located in intracellular storage vesicles and transported to the sarcolemma (similar to GLUT4), upon stimulation by insulin, increased energy demand or in response to contraction (Glatz *et al.*, 2002; Luiken *et al.*, 2001, 2003, 2004). These mechanisms are, however, not clear in the *in vivo* setting and warrants further investigation.

After uptake and esterification, fatty acyl-CoA may be utilized for metabolic conversion to ATP, for triglyceride synthesis or for incorporation into the intracellular lipid pool. Acyl-CoAs are transported across the outer mitochondrial membrane via CPT-1, forming fatty acylcarnitine in the intermembrane space. Indeed, studies using

radiolabeled oleate or palmitate suggest that (in the normal heart), 70 to 90% of FAs taken up are converted to acylcarnitine, while 10 to 30% are used for triglyceride storage (Lopaschuk *et al.*, 1994a; Saddik and Lopaschuk, 1992, 1991). CPT-1 is a key regulator of mitochondrial acylcarnitine uptake. The transporter itself is negatively regulated by malonyl-CoA, which is formed from the carboxylation of acetyl-CoA in a reaction catalyzed by acetyl-CoA carboxylase (ACC) (Goodwin and Taegtmeyer, 1999; Hall *et al.*, 1996a, 1996b; Kudo *et al.*, 1995; Ruderman *et al.*, 1999; Saddik *et al.*, 1993; Thampy, 1989). The amount of malonyl-CoA, and by extension the activity of CPT-1, is regulated by AMPK and the activities of ACC and malonyl-CoA decarboxylase (MCD). Here AMPK inhibits ACC activity driving the conversion of acetyl-CoA to malonyl-CoA resulting in the inhibition of CPT-1 and increased uptake of acyl-CoA into the mitochondria. MCD catalyzes the reverse reaction, i.e. conversion of malonyl-CoA to acetyl-CoA. Its inhibition would therefore increase malonyl-CoA and prolong CPT-I inhibition.

Acylcarnitine formed within the intermembrane space is transported across the inner mitochondrial membrane via carnitine acyl translocase (CAT), which exchanges acylcarnitine for free carnitine. Carnitine palmatoyl transferase-II (CPT-II) regenerates fatty acyl-CoA by transferring the acyl groups from acylcarnitine to free CoA, thereby replenishing carnitine that is shuttled back to the intermembrane space via CAT (Kerner and Hoppel, 2000; Lopaschuk *et al.*, 1994b; Schulz, 1994). Both CPT-II and CAT are located in the inner mitochondrial membrane. Upon entering the mitochondrial lumen, fatty acyl CoA is subjected to β -oxidation. This process involves repeated cleavage of two-carbon acetyl-CoA units, producing NADH and FADH₂. The final reaction catalyzed by 3-ketoacyl-CoA thiolase (3-KAT), regenerates acyl-CoA

that enters another round of β -oxidation, and releases acetyl-CoA for the citric acid cycle. NADH is formed by 3-hydroxyacyl-CoA dehydrogenase and FADH_2 by acyl-CoA dehydrogenase. FA uptake and utilization is outlined in Figure 2.8.

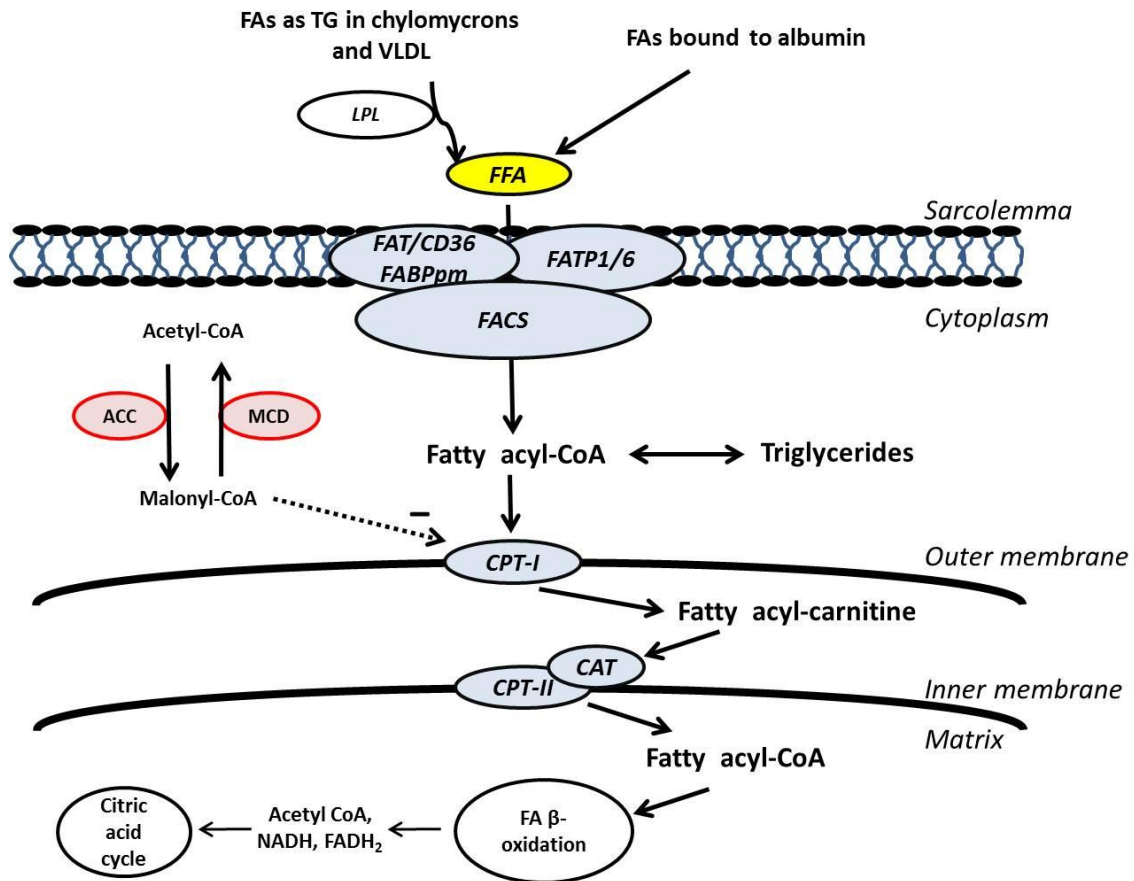


Figure 2.8 Fatty acid uptake and metabolism. FAs are transported into cells via transporter proteins and are converted into fatty acyl-CoA in the cytosol. Transport into the mitochondria is facilitated via CPT-1 (which is inhibited by malonyl-CoA) across the outer mitochondrial membrane. Fatty acyl-carnitine is formed in the inter-membrane space and transport across the inner membrane is facilitated by CPT-II. CAT plays a role here by removing and recycling the carnitine groups. Once in the matrix, fatty acyl-CoAs are utilized for β -oxidation. ACC: acetyl-CoA carboxylase; CAT: carnitine acyltransferase; CoA: co-enzyme A; CPT: carnitine palmitoyl transferase; FAs: fatty acids; FABPpm: plasma membrane fatty acid binding protein; FACS: fatty acyl-CoA synthase; FADH_2 : flavin adenine dinucleotide reduced; FAT/CD36: fatty acid translocase; FATP: fatty acid transport protein; LPL: lipoprotein lipase; MCD: malonyl-CoA decarboxylase; NADH: nicotinamide adenine dinucleotide reduced.

2.2.5. Mitochondrial energetics

Mitochondria are the major sites of ATP production in cells, hence it is often referred to as the “powerhouses” of the cell. These organelles possess tightly regulated and dynamic pathways and processes that facilitate the conversion of energy-rich substrates into electrons and, finally, ATP. Mitochondria are equipped with its own genome which supplies the necessary enzymes and regulatory proteins needed to operate efficient, “factory-like” work. Cardiomyocytes are enriched with mitochondria to maintain ATP levels. Mitochondria may in fact make up ~25 to 35% of total cardiomyocyte volume (Dobson and Himmelreich, 2002), and exist in two sub-populations, i.e. intramyofibrillar mitochondria (IFM) and subsarcolemmal mitochondria (SSM) (Palmer *et al.*, 1977). There are distinctive differences between the two sub-populations including structure of the cristae, respiration rates and expression patterns of metabolic proteins (Palmer *et al.*, 1977; Roden *et al.*, 1996). Both sub-populations supply energy for the maintenance of both ATP-dependent processes and of ion balance (Ishiki and Klip, 2005). The citric acid cycle and the electron transport chain (ETC) operate in tandem to turn metabolic substrates into energy. After converting acetyl-CoA (generated from glycolysis, lactate oxidation and FA β -oxidation) to reducing equivalents in the citric acid cycle, the electron transport chain uses the reducing equivalents to produce ATP. NADH derived from glycolysis enters the mitochondrion via the malate-aspartate shuttle, where aspartate is exchanged for malate (Kavazis *et al.*, 2009). The reactions occurring in the machinery of the mitochondria (the citric acid cycle and electron transport chain) will now be explained in detail below.

2.2.5.1. Citric acid cycle

The citric acid cycle (also known as the tricarboxylic acid cycle or Krebs cycle) is the first processing point for myocardial mitochondrial energy metabolism (Figure 2.9). The major products of the cycle include NADH, FADH₂ and GTP, which are used as electron donors to form ATP. The cycle is fueled by acetyl-CoA produced by upstream metabolism of carbohydrates, FAs and to a lesser extent, proteins (Gibala *et al.*, 2000; Neely *et al.*, 1972). Malate, 2-oxoglutarate, succinyl-CoA, oxaloacetate and fumarate are involved in anaplerotic reactions to replenish cycle intermediates (Gibala *et al.*, 2000; Russell and Taegtmeyer, 1991; Taegtmeyer *et al.*, 1980). The α -ketoglutarate dehydrogenase reaction converts α -ketoglutarate to succinyl-CoA, with the formation of NADH and CO₂. The NADH produced here is crucial for oxidative phosphorylation (Cooney *et al.*, 1981; Humphries and Szweda, 1998; Moreno-Sánchez *et al.*, 1990). The enzyme is highly regulated by the ATP/ADP and NADH/NAD⁺ ratios, calcium and substrate availability, and requires thiamine pyrophosphate as a co-factor. It may be a key regulatory point of control of citric acid cycle flux (Garland, 1964; Johnson and Hansford, 1975; Taegtmeyer *et al.*, 1980; Tretter and Adam-Vizi, 2000). The NADH and FADH₂ produced in the citric acid cycle are shifted to the electron transport chain, which is in close proximity in the inner mitochondrial membrane (Humphries and Szweda, 1998; Kerner and Hoppel, 2000). The cycle can thus be described as a metabolic link between the upstream breakdown of fuel substrates and downstream conversion of this fuel into energy. It thereby acts as an important cog in the chain of events governing energy metabolism.

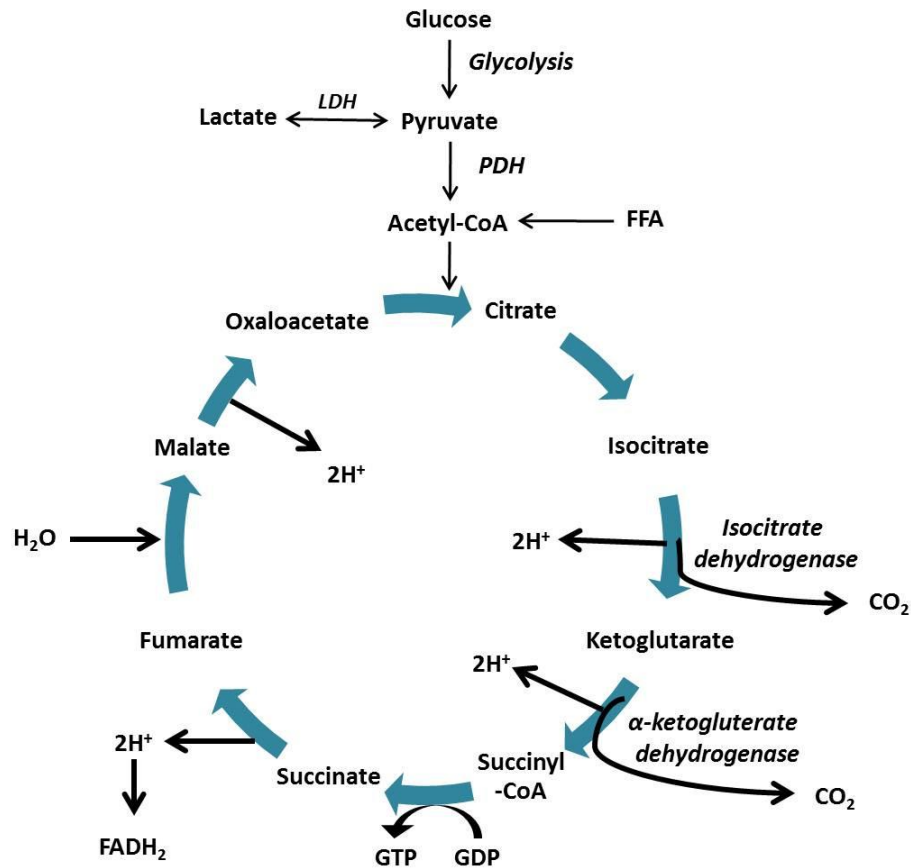


Figure 2.9 Reactions of the citric acid cycle. The acetyl group of acetyl-CoA is transferred to oxaloacetate in the initial reaction, generating citrate. The 6-carbon citrate is subsequently subjected to decarboxylation and oxidative reactions to generate the 4-carbon compound, malate, in a cyclic series of reactions. CoA: co-enzyme A; FADH₂: flavin adenine dinucleotide reduced; FFA: free fatty acids; GDP: guanidine diphosphate; GTP: guanidine triphosphate; LDH: lactate dehydrogenase; PDH: pyruvate dehydrogenase.

2.2.5.2. Electron transport chain and oxidative phosphorylation

The electron transport chain is composed of protein complexes in the inner mitochondrial membrane. The multi-unit complexes I, II, III and IV along with ATP synthase (complex V) transfers electrons provided by high-energy donors (reducing equivalents NADH and FADH₂) to molecular oxygen, with the formation of ATP and water (Figure 2.10). The entry point for electrons is NADH:ubiquinone oxidoreductase (complex I), a large multimeric protein complex consisting of at least

45 subunits (Carroll *et al.*, 2005, 2002; Cecchini, 2003). This complex catalyzes the transfer of electrons from NADH to ubiquinol (Q) via a series of redox centers, including a flavin moiety, seven to nine iron-sulfur clusters, and up to three ubisemiquinone species (Friedrich and Scheide, 2000; Koopman *et al.*, 2005; Ohnishi, 1998; Yano *et al.*, 2000). Four protons are translocated across the inner mitochondrial membrane, coupled to electron transfer in a process that conserves energy. The complex I reaction therefore contributes to the proton motive force required for ATP synthesis, maintaining the NAD⁺:NADH ratio in the matrix and providing ubiquinol to complex III (Hirst, 2005). The phospholipid cardiolipin may be essential for optimal functioning of complexes, specifically that of complex I (Dröse *et al.*, 2002; Fry and Green, 1981; Paradies *et al.*, 2001; Ragan, 1978; Robinson, 1993; Schlame *et al.*, 2000).

The multi-faceted succinate dehydrogenase (complex II, also known as succinate:ubiquinone oxidoreductase) contributes to the citric acid cycle and electron transport chain. The reduction of ubiquinone occurs in the inner mitochondrial membrane after complex II couples the oxidation of succinate to fumerate in the matrix (Cecchini *et al.*, 2002; Yankovskaya, 2003). Complexes I and II produces ubiquinol, which is oxidized by complex III (ubiquinol:cytochrome c oxidoreductase, also known as the cytochrome bc₁ complex). Here, the electrons from ubiquinol are transferred to cytochrome c, developing the proton motive Q cycle (Cecchini, 2003). Electrons from complexes I and III fuel the Q-cycle, while cytochrome b (a complex III subunit) transfers electrons to complex IV (di Rago *et al.*, 1990). Cytochrome c is a mobile electron carrier located between complexes II and IV (Gupte and Hackenbrock, 1988). The thirteen subunit complex IV generates a proton gradient

and ultimately reduces oxygen to two water molecules (Belevich *et al.*, 2006; Cecchini, 2003; Gupte and Hackenbrock, 1988; Ludwig *et al.*, 2001; Saraste, 1999; Yoshikawa, 2003; Yoshikawa *et al.*, 2006). ATP synthase (complex V or the F₁F₀ ATPase) forms the final component of the electron transport chain. The enzyme complex pumps protons against the electrochemical gradient, generating ATP in the process (Cecchini, 2003).

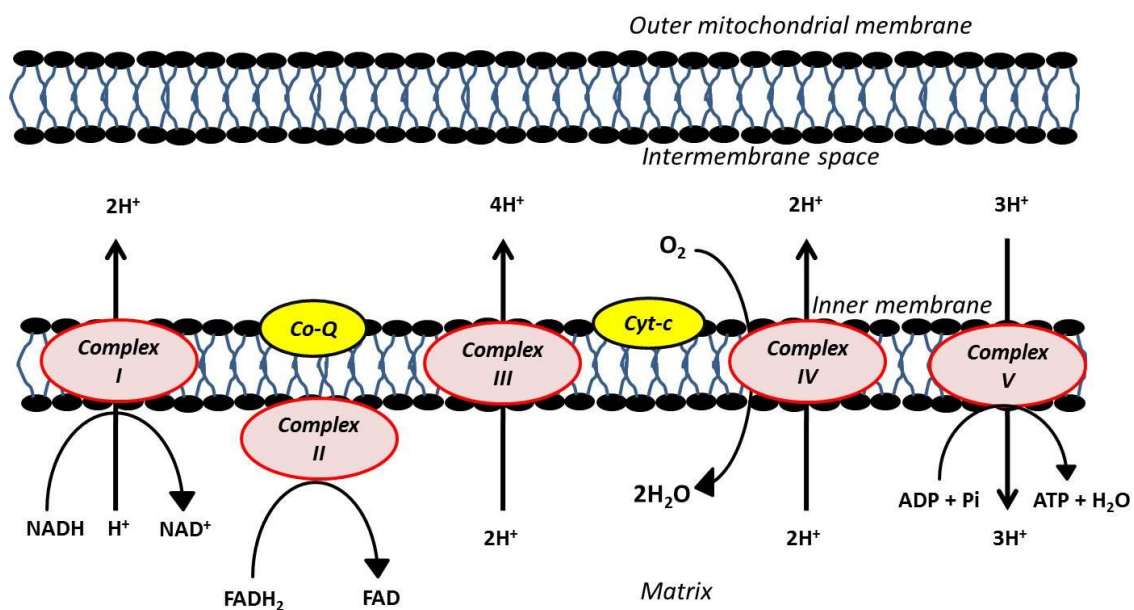


Figure 2.10 Electron transport chain.

2.2.6. The regulatory link for metabolic substrate switching – the Randle cycle

Metabolic substrate regulation, i.e. the preference between carbohydrate or FA metabolism, involves interlinked mechanisms. The preference of cardiomyocytes for FA oxidation may be explained by these mechanisms. Here, elevated FA metabolism may lead to the inhibition of glucose metabolic flux at various steps, including glucose uptake, glycogen synthesis and different glycolytic steps (Itani *et al.*, 2000;

Paz *et al.*, 1997). The metabolism of long-chain FA and ketone bodies can reduce glucose transport in isolated hearts (Paz *et al.*, 1997). FA β -oxidation produces citrate, which may downregulate glycolysis at the phosphofructokinase reaction (Randle *et al.*, 1964). The regulation of PDH, as first described by Randle and colleagues (Randle *et al.*, 1964) is one the best described mechanisms of fuel substrate regulation (refer Figure 2.7). Increased production of acetyl-CoA and NADH from FA β -oxidation may exert inhibitory effects on PDH, thereby promoting FA utilization and suppressing that of glucose (Stanley *et al.*, 2005). This is further demonstrated by experimental inhibition of FA oxidation (e.g. CPT-1 inhibition with etomoxir) resulting in improvement of glucose metabolism and cardiac function (An and Rodrigues, 2006; Campbell *et al.*, 2002; Stanley *et al.*, 2005). The negative regulator of PDH, PDK-4, may be transcriptionally upregulated by elevated circulating lipids and intracellular accumulation of FAs. Here PPAR- α mediates PDK-4 expression, resulting in increased phosphorylation and therefore inactivation of PDH (Huang *et al.*, 2002; Wu *et al.*, 2001). If uncontrolled, these mechanisms may lead to insulin resistance and impaired glucose uptake. The reverse scenario of elevated carbohydrates inhibiting FA metabolism may also play a role with excess substrate availability.

Chapter 2 provides as with the most important concepts of myocardial metabolism under physiological conditions. We reviewed the metabolism and regulation glucose and FA metabolic flux – important considerations when taking the homeostatic control of these substrates into account. For example, dysregulated glucose homeostasis is the core defect of insulin resistance (the focus of this thesis). The information reviewed in this chapter provides a basis to evaluate pathophysiological

mechanisms involving glucose dysregulation and insulin resistance – the topic of Chapter 3.

2.3. References

- Abel, E.D., 2004. Glucose transport in the heart. *Front Biosci* 9, 201–15.
- An, D., Rodrigues, B., 2006. Role of changes in cardiac metabolism in development of diabetic cardiomyopathy. *Am J Physiol Heart Circ Physiol* 291, H1489–506.
- Atkinson, L.L., Fischer, M.A., Lopaschuk, G.D., 2002. Leptin activates cardiac fatty acid oxidation independent of changes in the AMP-activated protein kinase-acetyl-CoA carboxylase-malonyl-CoA axis. *J Biol Chem* 277, 29424–30.
- Avogaro, A., Nosadini, R., Doria, A., Fioretto, P., Velussi, M., Vigorito, C., Saccà, L., Toffolo, G., Cobelli, C., Trevisan, R., 1990. Myocardial metabolism in insulin-deficient diabetic humans without coronary artery disease. *Am J Physiol* 258, E606–18.
- Balteau, M., Tajeddine, N., De Meester, C., Ginion, A., Des Rosiers, C., Brady, N.R., Sommereyns, C., Horman, S., Vanoverschelde, J.-L., Gailly, P., Hue, L., Bertrand, L., Beauloye, C., 2011. NADPH oxidase activation by hyperglycaemia in cardiomyocytes is independent of glucose metabolism but requires SGLT1. *Cardiovasc Res* 92, 237–46.
- Bandyopadhyay, G., Sajan, M.P., Kanoh, Y., Standaert, M.L., Quon, M.J., Lea-Currie, R., Sen, A., Farese, R. V, 2002. PKC-zeta mediates insulin effects on glucose transport in cultured preadipocyte-derived human adipocytes. *J Clin Endocrinol Metab* 87, 716–23.
- Barr, E.L.M., Zimmet, P.Z., Welborn, T.A., Jolley, D., Magliano, D.J., Dunstan, D.W., Cameron, A.J., Dwyer, T., Taylor, H.R., Tonkin, A.M., Wong, T.Y., McNeil, J., Shaw, J.E., 2007. Risk of cardiovascular and all-cause mortality in individuals with diabetes mellitus, impaired fasting glucose, and impaired glucose tolerance: the Australian Diabetes, Obesity, and Lifestyle Study (AusDiab). *Circulation* 116, 151–7.
- Beauloye, C., Marsin, A.S., Bertrand, L., Vanoverschelde, J.L., Rider, M.H., Hue, L., 2002. The stimulation of heart glycolysis by increased workload does not require AMP-activated protein kinase but a wortmannin-sensitive mechanism. *FEBS Lett* 531, 324–8.
- Becker, C., Sevilla, L., Tomàs, E., Palacin, M., Zorzano, A., Fischer, Y., 2001. The endosomal compartment is an insulin-sensitive recruitment site for GLUT4 and GLUT1 glucose transporters in cardiac myocytes. *Endocrinology* 142, 5267–76.
- Belevich, I., Verkhovskiy, M.I., Wikström, M., 2006. Proton-coupled electron transfer drives the proton pump of cytochrome c oxidase. *Nature* 440, 829–32.
- Belke, D.D., Betuing, S., Tuttle, M.J., Gravelleau, C., Young, M.E., Pham, M., Zhang, D., Cooksey, R.C., McClain, D.A., Litwin, S.E., Taegtmeyer, H., Severson, D., Kahn, C.R., Abel, E.D., 2002. Insulin signaling coordinately regulates cardiac size, metabolism, and contractile protein isoform expression. *J Clin Invest* 109, 629–639.
- Belke, D.D., Larsen, T.S., Gibbs, E.M., Severson, D.L., 2001. Glucose metabolism in perfused mouse hearts overexpressing human GLUT-4 glucose transporter. *Am J Physiol Endocrinol Metab* 280, E420–7.
- Bergemann, C., Löken, C., Becker, C., Graf, B., Hamidzadeh, M., Fischer, Y., 2001. Inhibition of glucose transport by cyclic GMP in cardiomyocytes. *Life Sci* 69, 1391–406.

- Bertrand, L., Horman, S., Beauloye, C., Vanoverschelde, J., 2008. Insulin signalling in the heart. *Cardiovasc Res* 79, 238–48.
- Bing, R.J., Siegel, A., Ungar, I., Gilbert, M., 1954. Metabolism of the human heart. II. Studies on fat, ketone and amino acid metabolism. *Am J Med* 16, 504–15.
- Bose, A., Guilherme, A., Robida, S.I., Nicoloso, S.M.C., Zhou, Q.L., Jiang, Z.Y., Pomerleau, D.P., Czech, M.P., 2002. Glucose transporter recycling in response to insulin is facilitated by myosin Myo1c. *Nature* 420, 821–4.
- Bøtker, H.E., Helligsø, P., Kimose, H.H., Thomassen, A.R., Nielsen, T.T., 1994. Determination of high energy phosphates and glycogen in cardiac and skeletal muscle biopsies, with special reference to influence of biopsy technique and delayed freezing. *Cardiovasc Res* 28, 524–7.
- Bouché, C., Serdy, S., Kahn, C.R., Goldfine, A.B., 2004. The cellular fate of glucose and its relevance in type 2 diabetes. *Endocr Rev* 25, 807–30.
- Bowker-Kinley, M.M., Davis, W.I., Wu, P., Harris, R.A., Popov, K.M., 1998. Evidence for existence of tissue-specific regulation of the mammalian pyruvate dehydrogenase complex. *Biochem J* 329 (Pt 1), 191–6.
- Brosius, F.C., Liu, Y., Nguyen, N., Sun, D., Bartlett, J., Schwaiger, M., 1997. Persistent myocardial ischemia increases GLUT1 glucose transporter expression in both ischemic and non-ischemic heart regions. *J Mol Cell Cardiol* 29, 1675–85.
- Brownlee, M., 2005. The pathobiology of diabetic complications: a unifying mechanism. *Diabetes* 54, 1615–25.
- Buchanan, J., Mazumder, P.K., Hu, P., Chakrabarti, G., Roberts, M.W., Yun, U.J., Cooksey, R.C., Litwin, S.E., Abel, E.D., 2005. Reduced cardiac efficiency and altered substrate metabolism precedes the onset of hyperglycemia and contractile dysfunction in two mouse models of insulin resistance and obesity. *Endocrinology* 146, 5341–9.
- Campbell, F.M., Kozak, R., Wagner, A., Altarejos, J.Y., Dyck, J.R.B., Belke, D.D., Severson, D.L., Kelly, D.P., Lopaschuk, G.D., 2002. A role for peroxisome proliferator-activated receptor alpha (PPARalpha) in the control of cardiac malonyl-CoA levels: reduced fatty acid oxidation rates and increased glucose oxidation rates in the hearts of mice lacking PPARalpha are associated with high. *J Biol Chem* 277, 4098–103.
- Cantley, L.C., 2002. The phosphoinositide 3-kinase pathway. *Science* 296, 1655–7.
- Cantrell, D.A., 2001. Phosphoinositide 3-kinase signalling pathways. *J Cell Sci* 114, 1439–45.
- Carroll, J., Fearnley, I.M., Skehel, J.M., Runswick, M.J., Shannon, R.J., Hirst, J., Walker, J.E., 2005. The post-translational modifications of the nuclear encoded subunits of complex I from bovine heart mitochondria. *Mol Cell Proteomics* 4, 693–9.
- Carroll, J., Shannon, R.J., Fearnley, I.M., Walker, J.E., Hirst, J., 2002. Definition of the nuclear encoded protein composition of bovine heart mitochondrial complex I. Identification of two new subunits. *J Biol Chem* 277, 50311–7.

- Cecchini, G., 2003. Function and structure of complex II of the respiratory chain. *Annu Rev Biochem* 72, 77–109.
- Cecchini, G., Schröder, I., Gunsalus, R.P., Maklashina, E., 2002. Succinate dehydrogenase and fumarate reductase from *Escherichia coli*. *Biochim Biophys Acta* 1553, 140–57.
- Chavali, V., Tyagi, S.C., Mishra, P.K., 2013. Predictors and prevention of diabetic cardiomyopathy. *Diabetes Metab Syndr Obes* 6, 151–60.
- Chiang, S.H., Baumann, C.A., Kanzaki, M., Thurmond, D.C., Watson, R.T., Neudauer, C.L., Macara, I.G., Pessin, J.E., Saltiel, A.R., 2001. Insulin-stimulated GLUT4 translocation requires the CAP-dependent activation of TC10. *Nature* 410, 944–8.
- Chiha, M., Njeim, M., Chedrawy, E.G., 2012. Diabetes and coronary heart disease: a risk factor for the global epidemic. *Int J Hypertens* 2012, 697240.
- Coburn, C.T., Hajri, T., Ibrahim, A., Abumrad, N.A., 2001. Role of CD36 in membrane transport and utilization of long-chain fatty acids by different tissues. *J Mol Neurosci* 16, 117–21; discussion 151–7.
- Comte, B., Vincent, G., Bouchard, B., Des Rosiers, C., 1997. Probing the origin of acetyl-CoA and oxaloacetate entering the citric acid cycle from the ¹³C labeling of citrate released by perfused rat hearts. *J Biol Chem* 272, 26117–24.
- Cooney, G.J., Taegtmeyer, H., Newsholme, E.A., 1981. Tricarboxylic acid cycle flux and enzyme activities in the isolated working rat heart. *Biochem J* 200, 701–3.
- Coort, S.L.M., Bonen, A., van der Vusse, G.J., Glatz, J.F.C., Luiken, J.J.F.P., 2007. Cardiac substrate uptake and metabolism in obesity and type-2 diabetes: role of sarcolemmal substrate transporters. *Mol Cell Biochem* 299, 5–18.
- Coven, D.L., Hu, X., Cong, L., Bergeron, R., Shulman, G.I., Hardie, D.G., Young, L.H., 2003. Physiological role of AMP-activated protein kinase in the heart: graded activation during exercise. *Am J Physiol Endocrinol Metab* 285, E629–36.
- Craparo, A., Freund, R., Gustafson, T.A., 1997. 14-3-3 (epsilon) interacts with the insulin-like growth factor I receptor and insulin receptor substrate I in a phosphoserine-dependent manner. *J Biol Chem* 272, 11663–9.
- Dawson, P.A., Mychaleckyj, J.C., Fossey, S.C., Mihic, S.J., Craddock, A.L., Bowden, D.W., 2001. Sequence and functional analysis of GLUT10: a glucose transporter in the Type 2 diabetes-linked region of chromosome 20q12-13.1. *Mol Genet Metab* 74, 186–99.
- Depre, C., Ponchaut, S., Deprez, J., Maisin, L., Hue, L., 1998. Cyclic AMP suppresses the inhibition of glycolysis by alternative oxidizable substrates in the heart. *J Clin Invest* 101, 390–7.
- Depre, C., Vanoverschelde, J.L., Taegtmeyer, H., 1999. Glucose for the heart. *Circulation* 99, 578–88.

- Di Rago, J.P., Netter, P., Slonimski, P.P., 1990. Intragenic suppressors reveal long distance interactions between inactivating and reactivating amino acid replacements generating three-dimensional constraints in the structure of mitochondrial cytochrome b. *J Biol Chem* 265, 15750–7.
- Dobson, G.P., Himmelreich, U., 2002. Heart design: free ADP scales with absolute mitochondrial and myofibrillar volumes from mouse to human. *Biochim Biophys Acta* 1553, 261–7.
- Doerge, H., Bocianski, A., Scheepers, A., Axer, H., Eckel, J., Joost, H.G., Schürmann, A., 2001. Characterization of human glucose transporter (GLUT) 11 (encoded by SLC2A11), a novel sugar-transport facilitator specifically expressed in heart and skeletal muscle. *Biochem J* 359, 443–9.
- Doerge, H., Schürmann, A., Bahrenberg, G., Brauers, A., Joost, H.G., 2000. GLUT8, a novel member of the sugar transport facilitator family with glucose transport activity. *J Biol Chem* 275, 16275–80.
- Doenst, T., Cedars, A.M., Taegtmeier, H., 2000. Insulin-stimulated glucose transport is dependent on Golgi function in isolated working rat heart. *J Mol Cell Cardiol* 32, 1481–8.
- Dransfeld, O., Rakatzi, I., Sasson, S., Eckel, J., 2002. Eicosanoids and the regulation of cardiac glucose transport. *Ann N Y Acad Sci* 967, 208–16.
- Dröse, S., Zwicker, K., Brandt, U., 2002. Full recovery of the NADH:ubiquinone activity of complex I (NADH:ubiquinone oxidoreductase) from *Yarrowia lipolytica* by the addition of phospholipids. *Biochim Biophys Acta* 1556, 65–72.
- Egert, S., Nguyen, N., Schwaiger, M., 1999. Myocardial glucose transporter GLUT1: translocation induced by insulin and ischemia. *J Mol Cell Cardiol* 31, 1337–44.
- Eguez, L., Lee, A., Chavez, J.A., Miinea, C.P., Kane, S., Lienhard, G.E., McGraw, T.E., 2005. Full intracellular retention of GLUT4 requires AS160 Rab GTPase activating protein. *Cell Metab* 2, 263–72.
- Elchebly, M., Payette, P., Michaliszyn, E., Cromlish, W., Collins, S., Loy, A.L., Normandin, D., Cheng, A., Himms-Hagen, J., Chan, C.C., Ramachandran, C., Gresser, M.J., Tremblay, M.L., Kennedy, B.P., 1999. Increased insulin sensitivity and obesity resistance in mice lacking the protein tyrosine phosphatase-1B gene. *Science* 283, 1544–8.
- England, P.J., Robinson, B.H., 1969. The permeability of rat heart mitochondria to citrate. *Biochem J* 112, 8P.
- Fischer, Y., Thomas, J., Kamp, J., Jüngling, E., Rose, H., Carpené, Kammermeier, H., 1995. 5-hydroxytryptamine stimulates glucose transport in cardiomyocytes via a monoamine oxidase-dependent reaction. *Biochem J* 311 (Pt 2), 575–83.
- Friedrich, T., Scheide, D., 2000. The respiratory complex I of bacteria, archaea and eukarya and its module common with membrane-bound multisubunit hydrogenases. *FEBS Lett* 479, 1–5.

- Fry, M., Green, D.E., 1981. Cardiolipin requirement for electron transfer in complex I and III of the mitochondrial respiratory chain. *J Biol Chem* 256, 1874–80.
- Fuller, W., Eaton, P., Medina, R.A., Bell, J., Shattock, M.J., 2001. Differential Centrifugation Separates Cardiac Sarcolemmal and Endosomal Membranes from Langendorff-Perfused Rat Hearts. *Anal Biochem* 293, 216–223.
- Garland, P.B., 1964. Some kinetic properties of pig-heart oxoglutarate dehydrogenase that provide a basis for metabolic control of the enzyme activity and also a stoichiometric assay for coenzyme A in tissue extracts. *Biochem J* 92, 10C–12C.
- Gertz, E.W., Wisneski, J.A., Stanley, W.C., Neese, R.A., 1988. Myocardial substrate utilization during exercise in humans. Dual carbon-labeled carbohydrate isotope experiments. *J Clin Invest* 82, 2017–25.
- Giaccari, A., Sorice, G., Muscogiuri, G., 2009. Glucose toxicity: the leading actor in the pathogenesis and clinical history of type 2 diabetes - mechanisms and potentials for treatment. *Nutr Metab Cardiovasc Dis* 19, 365–77.
- Giacco, F., Brownlee, M., 2010. Oxidative stress and diabetic complications. *Circ Res* 107, 1058–70.
- Gibala, M.J., Young, M.E., Taegtmeyer, H., 2000. Anaplerosis of the citric acid cycle: role in energy metabolism of heart and skeletal muscle. *Acta Physiol Scand* 168, 657–65.
- Gimeno, R.E., Ortegon, A.M., Patel, S., Punreddy, S., Ge, P., Sun, Y., Lodish, H.F., Stahl, A., 2003. Characterization of a heart-specific fatty acid transport protein. *J Biol Chem* 278, 16039–44.
- Glatz, J.F.C., Luiken, J.J.F.P., van Bilsen, M., van der Vusse, G.J., 2002. Cellular lipid binding proteins as facilitators and regulators of lipid metabolism. *Mol Cell Biochem* 239, 3–7.
- Goldfarb, A.H., Bruno, J.F., Buckenmeyer, P.J., 1986. Intensity and duration effects of exercise on heart cAMP, phosphorylase, and glycogen. *J Appl Physiol* 60, 1268–73.
- Goodwin, G.W., Taegtmeyer, H., 1999. Regulation of fatty acid oxidation of the heart by MCD and ACC during contractile stimulation. *Am J Physiol* 277, E772–7.
- Grynberg, A., Demaison, L., 1996. Fatty acid oxidation in the heart. *J Cardiovasc Pharmacol* 28 Suppl 1, S11–7.
- Gupte, S.S., Hackenbrock, C.R., 1988. The role of cytochrome c diffusion in mitochondrial electron transport. *J Biol Chem* 263, 5248–53.
- Gustafsson, I., Brendorp, B., Seibaek, M., Burchardt, H., Hildebrandt, P., Køber, L., Torp-Pedersen, C., 2004. Influence of diabetes and diabetes-gender interaction on the risk of death in patients hospitalized with congestive heart failure. *J Am Coll Cardiol* 43, 771–7.
- Hall, J.L., Lopaschuk, G.D., Barr, A., Bringas, J., Pizzurro, R.D., Stanley, W.C., 1996a. Increased cardiac fatty acid uptake with dobutamine infusion in swine is accompanied by a decrease in malonyl CoA levels. *Cardiovasc Res* 32, 879–85.

- Hall, J.L., Stanley, W.C., Lopaschuk, G.D., Wisneski, J.A., Pizzurro, R.D., Hamilton, C.D., McCormack, J.G., 1996b. Impaired pyruvate oxidation but normal glucose uptake in diabetic pig heart during dobutamine-induced work. *Am J Physiol* 271, H2320–9.
- Hanpeter, D., James, D.E., 1985. Characterization of the intracellular GLUT-4 compartment. *Mol Membr Biol* 12, 263–9.
- Harris, R.A., Huang, B., Wu, P., 2001. Control of pyruvate dehydrogenase kinase gene expression. *Adv Enzyme Regul* 41, 269–88.
- Hasin, Y., Barry, W.H., 1984. Myocardial metabolic inhibition and membrane potential, contraction, and potassium uptake. *Am J Physiol* 247, H322–9.
- Henning, S.L., Wambolt, R.B., Schönekeess, B.O., Lopaschuk, G.D., Allard, M.F., 1996. Contribution of glycogen to aerobic myocardial glucose utilization. *Circulation* 93, 1549–55.
- Hirst, J., 2005. Energy transduction by respiratory complex I—an evaluation of current knowledge. *Biochem Soc Trans* 33, 525–9.
- Holness, M.J., Sugden, M.C., 2003. Regulation of pyruvate dehydrogenase complex activity by reversible phosphorylation. *Biochem Soc Trans* 31, 1143–51.
- Hotamisligil, G.S., Peraldi, P., Budavari, A., Ellis, R., White, M.F., Spiegelman, B.M., 1996. IRS-1-mediated inhibition of insulin receptor tyrosine kinase activity in TNF- α - and obesity-induced insulin resistance. *Science* 271, 665–8.
- Huang, B., Wu, P., Bowker-Kinley, M.M., Harris, R.A., 2002. Regulation of pyruvate dehydrogenase kinase expression by peroxisome proliferator-activated receptor- α ligands, glucocorticoids, and insulin. *Diabetes* 51, 276–83.
- Huang, S., Czech, M.P., 2007. The GLUT4 Glucose Transporter. *Cell Metab* 5, 237–252.
- Hue, L., Depre, C., Lefebvre, V., Rider, M.H., Veitch, K., 1995. Regulation of glucose metabolism in cardiac muscle. *Biochem Soc Trans* 23, 311–4.
- Hue, L., Rider, M.H., 1987. Role of fructose 2,6-bisphosphate in the control of glycolysis in mammalian tissues. *Biochem J* 245, 313–24.
- Humphries, K.M., Szweda, L.I., 1998. Selective inactivation of alpha-ketoglutarate dehydrogenase and pyruvate dehydrogenase: reaction of lipoic acid with 4-hydroxy-2-nonenal. *Biochemistry* 37, 15835–41.
- Ishiki, M., Klip, A., 2005. Minireview: recent developments in the regulation of glucose transporter-4 traffic: new signals, locations, and partners. *Endocrinology* 146, 5071–8.
- Itani, S.I., Zhou, Q., Pories, W.J., MacDonald, K.G., Dohm, G.L., 2000. Involvement of protein kinase C in human skeletal muscle insulin resistance and obesity. *Diabetes* 49, 1353–8.
- Jeremy, R.W., Koretsune, Y., Marban, E., Becker, L.C., 1992. Relation between glycolysis and calcium homeostasis in postischemic myocardium. *Circ Res* 70, 1180–90.

- Johnson, R.N., Hansford, R.G., 1975. The control of tricarboxylate-cycle oxidations in blowfly flight muscle. The steady-state concentrations of citrate, isocitrate 2-oxoglutarate and malate in flight muscle and isolated mitochondria. *Biochem J* 146, 527–35.
- Kahn, S.E., Hull, R.L., Utzschneider, K.M., 2006. Mechanisms linking obesity to insulin resistance and type 2 diabetes. *Nature* 444, 840–6.
- Kaijser, L., Berglund, B., 1992. Myocardial lactate extraction and release at rest and during heavy exercise in healthy men. *Acta Physiol Scand* 144, 39–45.
- Kane, S., Sano, H., Liu, S.C.H., Asara, J.M., Lane, W.S., Garner, C.C., Lienhard, G.E., 2002. A method to identify serine kinase substrates. Akt phosphorylates a novel adipocyte protein with a Rab GTPase-activating protein (GAP) domain. *J Biol Chem* 277, 22115–8.
- Karlsson, H.K.R., Zierath, J.R., Kane, S., Krook, A., Lienhard, G.E., Wallberg-Henriksson, H., 2005. Insulin-stimulated phosphorylation of the Akt substrate AS160 is impaired in skeletal muscle of type 2 diabetic subjects. *Diabetes* 54, 1692–7.
- Kasuga, M., Karlsson, F., Kahn, C., 1982. Insulin stimulates the phosphorylation of the 95,000-dalton subunit of its own receptor. *Science* (80-) 215, 185–187.
- Kavazis, A.N., Alvarez, S., Talbert, E., Lee, Y., Powers, S.K., 2009. Exercise training induces a cardioprotective phenotype and alterations in cardiac subsarcolemmal and intermyofibrillar mitochondrial proteins. *Am J Physiol Heart Circ Physiol* 297, H144–52.
- Kerner, J., Hoppel, C., 2000. Fatty acid import into mitochondria. *Biochim Biophys Acta* 1486, 1–17.
- King, K.L., Okere, I.C., Sharma, N., Dyck, J.R.B., Reszko, A.E., McElfresh, T.A., Kerner, J., Chandler, M.P., Lopaschuk, G.D., Stanley, W.C., 2005. Regulation of cardiac malonyl-CoA content and fatty acid oxidation during increased cardiac power. *Am J Physiol Heart Circ Physiol* 289, H1033–7.
- Kolter, T., Uphues, I., Wichelhaus, A., Reinauer, H., Eckel, J., 1992. Contraction-induced translocation of the glucose transporter Glut4 in isolated ventricular cardiomyocytes. *Biochem Biophys Res Commun* 189, 1207–1214.
- Koonen, D.P.Y., Glatz, J.F.C., Bonen, A., Luiken, J.J.F.P., 2005. Long-chain fatty acid uptake and FAT/CD36 translocation in heart and skeletal muscle. *Biochim Biophys Acta* 1736, 163–80.
- Koopman, W.J.H., Verkaart, S., Visch, H.-J., van der Westhuizen, F.H., Murphy, M.P., van den Heuvel, L.W.P.J., Smeitink, J.A.M., Willems, P.H.G.M., 2005. Inhibition of complex I of the electron transport chain causes O₂-mediated mitochondrial outgrowth. *Am J Physiol Cell Physiol* 288, C1440–50.
- Kraegen, E.W., Sowden, J.A., Halstead, M.B., Clark, P.W., Rodnick, K.J., Chisholm, D.J., James, D.E., 1993. Glucose transporters and in vivo glucose uptake in skeletal and cardiac muscle: fasting, insulin stimulation and immunoisolation studies of GLUT1 and GLUT4. *Biochem J* 295 (Pt 1, 287–93.

- Kudo, N., Barr, A.J., Barr, R.L., Desai, S., Lopaschuk, G.D., 1995. High rates of fatty acid oxidation during reperfusion of ischemic hearts are associated with a decrease in malonyl-CoA levels due to an increase in 5'-AMP-activated protein kinase inhibition of acetyl-CoA carboxylase. *J Biol Chem* 270, 17513–20.
- Kurth-Kraczek, E.J., Hirshman, M.F., Goodyear, L.J., Winder, W.W., 1999. 5' AMP-activated protein kinase activation causes GLUT4 translocation in skeletal muscle. *Diabetes* 48, 1667–71.
- Kusuoka, H., Marban, E., 1994. Mechanism of the diastolic dysfunction induced by glycolytic inhibition. Does adenosine triphosphate derived from glycolysis play a favored role in cellular Ca²⁺ homeostasis in ferret myocardium? *J Clin Invest* 93, 1216–23.
- Larance, M., Ramm, G., Stöckli, J., van Dam, E.M., Winata, S., Wasinger, V., Simpson, F., Graham, M., Junutula, J.R., Guilhaus, M., James, D.E., 2005. Characterization of the role of the Rab GTPase-activating protein AS160 in insulin-regulated GLUT4 trafficking. *J Biol Chem* 280, 37803–13.
- Li, J., Houseknecht, K.L., Stenbit, A.E., Katz, E.B., Charron, M.J., 2000. Reduced glucose uptake precedes insulin signaling defects in adipocytes from heterozygous GLUT4 knockout mice. *FASEB J* 14, 1117–25.
- Liao, R., Jain, M., Cui, L., D'Agostino, J., Aiello, F., Luptak, I., Ngoy, S., Mortensen, R.M., Tian, R., 2002. Cardiac-specific overexpression of GLUT1 prevents the development of heart failure attributable to pressure overload in mice. *Circulation* 106, 2125–2131.
- Lopaschuk, G.D., Belke, D.D., Gamble, J., Itoi, T., Schönekeess, B.O., 1994a. Regulation of fatty acid oxidation in the mammalian heart in health and disease. *Biochim Biophys Acta* 1213, 263–76.
- Lopaschuk, G.D., Witters, L.A., Itoi, T., Barr, R., Barr, A., 1994b. Acetyl-CoA carboxylase involvement in the rapid maturation of fatty acid oxidation in the newborn rabbit heart. *J Biol Chem* 269, 25871–8.
- Ludwig, B., Bender, E., Arnold, S., Hüttemann, M., Lee, I., Kadenbach, B., 2001. Cytochrome C oxidase and the regulation of oxidative phosphorylation. *Chembiochem* 2, 392–403.
- Luiken, J.J., Willems, J., van der Vusse, G.J., Glatz, J.F., 2001. Electrostimulation enhances FAT/CD36-mediated long-chain fatty acid uptake by isolated rat cardiac myocytes. *Am J Physiol Endocrinol Metab* 281, E704–12.
- Luiken, J.J.F.P., Coort, S.L.M., Koonen, D.P.Y., van der Horst, D.J., Bonen, A., Zorzano, A., Glatz, J.F.C., Horst, D.J. Van Der, 2004. Regulation of cardiac long-chain fatty acid and glucose uptake by translocation of substrate transporters. *Pflugers Arch* 448, 1–15.
- Luiken, J.J.F.P., Coort, S.L.M., Willems, J., Coumans, W.A., Bonen, A., van der Vusse, G.J., Glatz, J.F.C., 2003. Contraction-induced fatty acid translocase/CD36 translocation in rat cardiac myocytes is mediated through AMP-activated protein kinase signaling. *Diabetes* 52, 1627–34.
- Marsin, a S., Bertrand, L., Rider, M.H., Deprez, J., Beauloye, C., Vincent, M.F., Van den Berghe, G., Carling, D., Hue, L., 2000. Phosphorylation and activation of heart PFK-2 by AMPK has a role in the stimulation of glycolysis during ischaemia. *Curr Biol* 10, 1247–55.

- Martin, D.B., Vagelos, P.R., 1962. The mechanism of tricarboxylic acid cycle regulation of fatty acid synthesis. *J Biol Chem* 237, 1787–92.
- Massie, B.M., Schaefer, S., Garcia, J., McKirnan, M.D., Schwartz, G.G., Wisneski, J.A., Weiner, M.W., White, F.C., 1995. Myocardial high-energy phosphate and substrate metabolism in swine with moderate left ventricular hypertrophy. *Circulation* 91, 1814–23.
- McCormack, J.G., Denton, R.M., 1984. Role of Ca²⁺ ions in the regulation of intramitochondrial metabolism in rat heart. Evidence from studies with isolated mitochondria that adrenaline activates the pyruvate dehydrogenase and 2-oxoglutarate dehydrogenase complexes by increasing the intramito. *Biochem J* 218, 235–47.
- McCormack, J.G., Denton, R.M., 1989. Influence of calcium ions on mammalian intramitochondrial dehydrogenases. *Methods Enzymol* 174, 95–118.
- McCormack, J.G., Halestrap, A.P., Denton, R.M., 1990. Role of calcium ions in regulation of mammalian intramitochondrial metabolism. *Physiol Rev* 70, 391–425.
- Medina, R.A., Southworth, R., Fuller, W., Garlick, P.B., 2002. Lactate-induced translocation of GLUT1 and GLUT4 is not mediated by the phosphatidylinositol-3-kinase pathway in the rat heart. *Basic Res Cardiol* 97, 168–76.
- Moreno-Sánchez, R., Hogue, B.A., Hansford, R.G., 1990. Influence of NAD-linked dehydrogenase activity on flux through oxidative phosphorylation. *Biochem J* 268, 421–8.
- Morin, N., Visentin, V., Calise, D., Marti, L., Zorzano, A., Testar, X., Valet, P., Fischer, Y., Carpené, C., 2002. Tyramine stimulates glucose uptake in insulin-sensitive tissues in vitro and in vivo via its oxidation by amine oxidases. *J Pharmacol Exp Ther* 303, 1238–47.
- Mueckler, M., 1994. Facilitative glucose transporters. *Eur J Biochem* 219, 713–25.
- Neely, J.R., Rovetto, M.J., Oram, J.F., 1972. Myocardial utilization of carbohydrate and lipids. *Prog Cardiovasc Dis* 15, 289–329.
- Nesher, R., Karl, I.E., Kipnis, D.M., 1985. Dissociation of effects of insulin and contraction on glucose transport in rat epitrochlearis muscle. *Am J Physiol* 249, C226–32.
- Ohnishi, T., 1998. Iron-sulfur clusters/semiquinones in complex I. *Biochim Biophys Acta* 1364, 186–206.
- Opie, L.H., 1991. *The heart. Physiology and metabolism*. Raven, New York.
- Opie, L.H., Knuuti, J., 2009. The adrenergic-fatty acid load in heart failure. *J Am Coll Cardiol* 54, 1637–46.
- Palmer, J.W., Tandler, B., Hoppel, C.L., 1977. Biochemical properties of subsarcolemmal and interfibrillar mitochondria isolated from rat cardiac muscle. *J Biol Chem* 252, 8731–9.

- Panchal, A.R., Comte, B., Huang, H., Kerwin, T., Darvish, A., des Rosiers, C., Brunengraber, H., Stanley, W.C., 2000. Partitioning of pyruvate between oxidation and anaplerosis in swine hearts. *Am J Physiol Heart Circ Physiol* 279, H2390–8.
- Paradies, G., Petrosillo, G., Pistolese, M., Ruggiero, F.M., 2001. Reactive oxygen species generated by the mitochondrial respiratory chain affect the complex III activity via cardiolipin peroxidation in beef-heart submitochondrial particles. *Mitochondrion* 1, 151–9.
- Paz, K., Hemi, R., LeRoith, D., Karasik, A., Elhanany, E., Kanety, H., Zick, Y., 1997. A molecular basis for insulin resistance. Elevated serine/threonine phosphorylation of IRS-1 and IRS-2 inhibits their binding to the juxtamembrane region of the insulin receptor and impairs their ability to undergo insulin-induced tyrosine phosphorylation. *J Biol Chem* 272, 29911–8.
- Peck, G.R., Ye, S., Pham, V., Fernando, R.N., Macaulay, S.L., Chai, S.Y., Albiston, A.L., 2006. Interaction of the Akt substrate, AS160, with the glucose transporter 4 vesicle marker protein, insulin-regulated aminopeptidase. *Mol Endocrinol* 20, 2576–83.
- Radke, P.W., Schunkert, H., 2008. Glucose-lowering therapy after myocardial infarction: more questions than answers. *Eur Hear J* 29, 141–143.
- Ragan, C.I., 1978. The role of phospholipids in the reduction of ubiquinone analogues by the mitochondrial reduced nicotinamide-adenine dinucleotide-ubiquinone oxidoreductase complex. *Biochem J* 172, 539–47.
- Ramm, G., Larance, M., Guilhaus, M., James, D.E., 2006. A role for 14-3-3 in insulin-stimulated GLUT4 translocation through its interaction with the RabGAP AS160. *J Biol Chem* 281, 29174–80.
- Ramrath, S., Tritschler, H.J., Eckel, J., 1999. Stimulation of cardiac glucose transport by thioctic acid and insulin. *Horm Metab Res* 31, 632–5.
- Randle, P.J., 1986. Fuel selection in animals. *Biochem Soc Trans* 14, 799–806.
- Randle, P.J., Newsholme, E.A., Garland, P.B., 1964. Regulation of glucose uptake by muscle. 8. Effects of fatty acids, ketone bodies and pyruvate, and of alloxan-diabetes and starvation, on the uptake and metabolic fate of glucose in rat heart and diaphragm muscles. *Biochem J* 93, 652–65.
- Rett, K., Maerker, E., Renn, W., van Gilst, W., Haering, H.U., 1997. Perfusion-independent effect of bradykinin and fosinoprilate on glucose transport in Langendorff rat hearts. *Am J Cardiol* 80, 143A–147A.
- Rett, K., Wicklmayr, M., Dietze, G.J., Häring, H.U., 1996. Insulin-induced glucose transporter (GLUT1 and GLUT4) translocation in cardiac muscle tissue is mimicked by bradykinin. *Diabetes* 45 Suppl 1, S66–9.
- Rider, M.H., Bertrand, L., Vertommen, D., Michels, P.A., Rousseau, G.G., Hue, L., 2004. 6-phosphofructo-2-kinase/fructose-2,6-bisphosphatase: head-to-head with a bifunctional enzyme that controls glycolysis. *Biochem J* 381, 561–79.

- Robinson, N.C., 1993. Functional binding of cardiolipin to cytochrome c oxidase. *J Bioenerg Biomembr* 25, 153–63.
- Roden, M., Price, T.B., Perseghin, G., Petersen, K.F., Rothman, D.L., Cline, G.W., Shulman, G.I., 1996. Mechanism of free fatty acid-induced insulin resistance in humans. *J Clin Invest* 97, 2859–65.
- Rogers, S., Macheda, M.L., Docherty, S.E., Carty, M.D., Henderson, M.A., Soeller, W.C., Gibbs, E.M., James, D.E., Best, J.D., 2002. Identification of a novel glucose transporter-like protein-GLUT-12. *Am J Physiol Endocrinol Metab* 282, E733–8.
- Rossetti, L., Stenbit, A.E., Chen, W., Hu, M., Barzilai, N., Katz, E.B., Charron, M.J., 1997. Peripheral but not hepatic insulin resistance in mice with one disrupted allele of the glucose transporter type 4 (GLUT4) gene. *J Clin Invest* 100, 1831–9.
- Rubin, J., Matsushita, K., Ballantyne, C.M., Hoogeveen, R., Coresh, J., Selvin, E., 2012. Chronic hyperglycemia and subclinical myocardial injury. *J Am Coll Cardiol* 59, 484–9.
- Ruderman, N.B., Saha, A.K., Vavvas, D., Witters, L.A., 1999. Malonyl-CoA, fuel sensing, and insulin resistance. *Am J Physiol* 276, E1–E18.
- Russell, R.R., Bergeron, R., Shulman, G.I., Young, L.H., 1999. Translocation of myocardial GLUT-4 and increased glucose uptake through activation of AMPK by AICAR. *Am J Physiol* 277, H643–9.
- Russell, R.R., Taegtmeyer, H., 1991. Changes in citric acid cycle flux and anaplerosis antedate the functional decline in isolated rat hearts utilizing acetoacetate. *J Clin Invest* 87, 384–90.
- Ryder, J.W., Yang, J., Galuska, D., Rincon, J., Bjornholm, M., Krook, A., Lund, S., Pedersen, O., Wallberg-Henriksson, H., Zierath, J.R., Holman, G.D., 2000. Use of a novel impermeable biotinylated photolabeling reagent to assess insulin- and hypoxia-stimulated cell surface GLUT4 content in skeletal muscle from type 2 diabetic patients. *Diabetes* 49, 647–654.
- Saddik, M., Gamble, J., Witters, L.A., Lopaschuk, G.D., 1993. Acetyl-CoA carboxylase regulation of fatty acid oxidation in the heart. *J Biol Chem* 268, 25836–45.
- Saddik, M., Lopaschuk, G.D., 1991. Myocardial triglyceride turnover and contribution to energy substrate utilization in isolated working rat hearts. *J Biol Chem* 266, 8162–70.
- Saddik, M., Lopaschuk, G.D., 1992. Myocardial triglyceride turnover during reperfusion of isolated rat hearts subjected to a transient period of global ischemia. *J Biol Chem* 267, 3825–31.
- Saltiel, A.R., Kahn, C.R., 2001. Insulin signalling and the regulation of glucose and lipid metabolism. *Nature* 414, 799–806.
- Sano, H., Kane, S., Sano, E., Miinea, C.P., Asara, J.M., Lane, W.S., Garner, C.W., Lienhard, G.E., 2003. Insulin-stimulated phosphorylation of a Rab GTPase-activating protein regulates GLUT4 translocation. *J Biol Chem* 278, 14599–602.

- Santalucía, T., Boheler, K.R., Brand, N.J., Sahye, U., Fandos, C., Viñals, F., Ferré, J., Testar, X., Palacín, M., Zorzano, A., 1999. Factors involved in GLUT-1 glucose transporter gene transcription in cardiac muscle. *J Biol Chem* 274, 17626–34.
- Saraste, M., 1999. Oxidative phosphorylation at the fin de siècle. *Science* 283, 1488–93.
- Sarbassov, D.D., Guertin, D.A., Ali, S.M., Sabatini, D.M., 2005. Phosphorylation and regulation of Akt/PKB by the rictor-mTOR complex. *Science* 307, 1098–101.
- Schaap, F.G., Hamers, L., Van der Vusse, G.J., Glatz, J.F., 1997. Molecular cloning of fatty acid-transport protein cDNA from rat. *Biochim Biophys Acta* 1354, 29–34.
- Schaffer, J.E., 2002. Fatty acid transport: the roads taken. *Am J Physiol Endocrinol Metab* 282, E239–46.
- Schlame, M., Rua, D., Greenberg, M.L., 2000. The biosynthesis and functional role of cardiolipin. *Prog Lipid Res* 39, 257–88.
- Schönekeess, B.O., Allard, M.F., Lopaschuk, G.D., 1995. Propionyl L-carnitine improvement of hypertrophied heart function is accompanied by an increase in carbohydrate oxidation. *Circ Res* 77, 726–34.
- Schulz, H., 1994. Regulation of fatty acid oxidation in heart. *J Nutr* 124, 165–71.
- Semiz, S., Park, J.G., Nicoloso, S.M.C., Furcinitti, P., Zhang, C., Chawla, A., Leszyk, J., Czech, M.P., 2003. Conventional kinesin KIF5B mediates insulin-stimulated GLUT4 movements on microtubules. *EMBO J* 22, 2387–99.
- Sevilla, L., 1997. Characterization of Two Distinct Intracellular GLUT4 Membrane Populations in Muscle Fiber. Differential Protein Composition and Sensitivity to Insulin. *Endocrinology* 138, 3006–3015.
- Shepherd, P.R., Gould, G.W., Colville, C.A., McCoid, S.C., Gibbs, E.M., Kahn, B.B., 1992. Distribution of GLUT3 glucose transporter protein in human tissues. *Biochem Biophys Res Commun* 188, 149–54.
- Shepherd, P.R., Navé, B.T., Siddle, K., 1995. Insulin stimulation of glycogen synthesis and glycogen synthase activity is blocked by wortmannin and rapamycin in 3T3-L1 adipocytes: evidence for the involvement of phosphoinositide 3-kinase and p70 ribosomal protein-S6 kinase. *Biochem J* 305 (Pt 1, 25–8.
- Spector, A.A., 1984. Plasma lipid transport. *Clin Physiol Biochem* 2, 123–34.
- Stahl, A., Evans, J.G., Pattel, S., Hirsch, D., Lodish, H.F., 2002. Insulin causes fatty acid transport protein translocation and enhanced fatty acid uptake in adipocytes. *Dev Cell* 2, 477–88.
- Stahl, A., Gimeno, R.E., Tartaglia, L.A., Lodish, H.F., 2001. Fatty acid transport proteins: a current view of a growing family. *Trends Endocrinol Metab* 12, 266–73.
- Stanley, W.C., 1991. Myocardial lactate metabolism during exercise. *Med Sci Sports Exerc* 23, 920–4.

- Stanley, W.C., Hall, J.L., Stone, C.K., Hacker, T.A., 1992. Acute myocardial ischemia causes a transmural gradient in glucose extraction but not glucose uptake. *Am J Physiol* 262, H91–6.
- Stanley, W.C., Lopaschuk, G.D., Hall, J.L., McCormack, J.G., 1997a. Regulation of myocardial carbohydrate metabolism under normal and ischaemic conditions. Potential for pharmacological interventions. *Cardiovasc Res* 33, 243–57.
- Stanley, W.C., Lopaschuk, G.D., McCormack, J.G., 1997b. Regulation of energy substrate metabolism in the diabetic heart. *Cardiovasc Res* 34, 25–33.
- Stanley, W.C., Recchia, F.A., Lopaschuk, G.D., 2005. Myocardial substrate metabolism in the normal and failing heart. *Physiol Rev* 85, 1093–129.
- Steinbusch, L.K.M., Schwenk, R.W., Ouwens, D.M., Diamant, M., Glatz, J.F.C., Luiken, J.J.F.P., 2011. Subcellular trafficking of the substrate transporters GLUT4 and CD36 in cardiomyocytes. *Cell Mol Life Sci* 68, 2525–38.
- Stephens, L., Anderson, K., Stokoe, D., Erdjument-Bromage, H., Painter, G.F., Holmes, A.B., Gaffney, P.R., Reese, C.B., McCormick, F., Tempst, P., Coadwell, J., Hawkins, P.T., 1998. Protein kinase B kinases that mediate phosphatidylinositol 3,4,5-trisphosphate-dependent activation of protein kinase B. *Science* 279, 710–4.
- Stremmel, W., Strohmeyer, G., Borchard, F., Kochwa, S., Berk, P.D., 1985. Isolation and partial characterization of a fatty acid binding protein in rat liver plasma membranes. *Proc Natl Acad Sci U S A* 82, 4–8.
- Taegtmeyer, H., 1994. Energy metabolism of the heart: from basic concepts to clinical applications. *Curr Probl Cardiol* 19, 59–113.
- Taegtmeyer, H., Hems, R., Krebs, H.A., 1980. Utilization of energy-providing substrates in the isolated working rat heart. *Biochem J* 186, 701–11.
- Tardif, A., Julien, N., Pelletier, A., Thibault, G., Srivastava, A.K., Chiasson, J.L., Coderre, L., 2001. Chronic exposure to beta-hydroxybutyrate impairs insulin action in primary cultures of adult cardiomyocytes. *Am J Physiol Endocrinol Metab* 281, E1205–12.
- Terruzzi, I., Allibardi, S., Bendinelli, P., Maroni, P., Piccoletti, R., Vesco, F., Samaja, M., Luzi, L., 2002. Amino acid- and lipid-induced insulin resistance in rat heart: molecular mechanisms. *Mol Cell Endocrinol* 190, 135–45.
- Thampy, K.G., 1989. Formation of malonyl coenzyme A in rat heart. Identification and purification of an isozyme of A carboxylase from rat heart. *J Biol Chem* 264, 17631–4.
- Thurmond, D.C., Gonelle-Gispert, C., Furukawa, M., Halban, P.A., Pessin, J.E., 2003. Glucose-stimulated insulin secretion is coupled to the interaction of actin with the t-SNARE (target membrane soluble N-ethylmaleimide-sensitive factor attachment protein receptor protein) complex. *Mol Endocrinol* 17, 732–42.
- Tian, R., Abel, E.D., 2001. Responses of GLUT4-Deficient Hearts to Ischemia Underscore the Importance of Glycolysis. *Circulation* 103, 2961–2966.

- Tretter, L., Adam-Vizi, V., 2000. Inhibition of Krebs cycle enzymes by hydrogen peroxide: A key role of [alpha]-ketoglutarate dehydrogenase in limiting NADH production under oxidative stress. *J Neurosci* 20, 8972–9.
- Tsao, T.S., Stenbit, A.E., Factor, S.M., Chen, W., Rossetti, L., Charron, M.J., 1999. Prevention of insulin resistance and diabetes in mice heterozygous for GLUT4 ablation by transgenic complementation of GLUT4 in skeletal muscle. *Diabetes* 48, 775–82.
- Vanhaesebroeck, B., Leeyers, S.J., Ahmadi, K., Timms, J., Katso, R., Driscoll, P.C., Woscholski, R., Parker, P.J., Waterfield, M.D., 2001. Synthesis and function of 3-phosphorylated inositol lipids. *Annu Rev Biochem* 70, 535–602.
- Vincent, G., Bouchard, B., Khairallah, M., Des Rosiers, C., 2004. Differential modulation of citrate synthesis and release by fatty acids in perfused working rat hearts. *Am J Physiol Heart Circ Physiol* 286, H257–66.
- Watson, R.T., Pessin, J.E., 2001. Intracellular organization of insulin signaling and GLUT4 translocation. *Recent Prog Horm Res* 56, 175–93.
- Weiss, J., Hiltbrand, B., 1985. Functional compartmentation of glycolytic versus oxidative metabolism in isolated rabbit heart. *J Clin Invest* 75, 436–47.
- Weiss, J.N., Lamp, S.T., 1989. Cardiac ATP-sensitive K⁺ channels. Evidence for preferential regulation by glycolysis. *J Gen Physiol* 94, 911–35.
- Wheeler, T.J., Fell, R.D., Hauck, M.A., 1994. Translocation of two glucose transporters in heart: effects of rotenone, uncouplers, workload, palmitate, insulin and anoxia. *Biochim Biophys Acta* 1196, 191–200.
- Wisneski, J.A., Gertz, E.W., Neese, R.A., Gruenke, L.D., Craig, J.C., 1985a. Dual carbon-labeled isotope experiments using D-[6-14C] glucose and L-[1,2,3-13C3] lactate: a new approach for investigating human myocardial metabolism during ischemia. *J Am Coll Cardiol* 5, 1138–46.
- Wisneski, J.A., Gertz, E.W., Neese, R.A., Gruenke, L.D., Morris, D.L., Craig, J.C., 1985b. Metabolic fate of extracted glucose in normal human myocardium. *J Clin Invest* 76, 1819–27.
- Wisneski, J.A., Gertz, E.W., Neese, R.A., Mayr, M., 1987. Myocardial metabolism of free fatty acids. Studies with 14C-labeled substrates in humans. *J Clin Invest* 79, 359–66.
- Wisneski, J.A., Stanley, W.C., Neese, R.A., Gertz, E.W., Nose, R.A., 1990. Effects of Acute Hyperglycemia on Myocardial Glycolytic Activity in Humans. *J Clin Invest* 85, 1648–1656.
- Wu, H., Yan, Y., Backer, J.M., 2007. Regulation of class IA PI3Ks. *Biochem Soc Trans* 35, 242–4.
- Wu, P., Peters, J.M., Harris, R.A., 2001. Adaptive increase in pyruvate dehydrogenase kinase 4 during starvation is mediated by peroxisome proliferator-activated receptor alpha. *Biochem Biophys Res Commun* 287, 391–6.

- Wu, X., Li, W., Sharma, V., Godzik, A., Freeze, H.H., 2002. Cloning and characterization of glucose transporter 11, a novel sugar transporter that is alternatively spliced in various tissues. *Mol Genet Metab* 76, 37–45.
- Wu-Wong, J.R., Berg, C.E., Kramer, D., 2000. Endothelin stimulates glucose uptake via activation of endothelin-A receptor in neonatal rat cardiomyocytes. *J Cardiovasc Pharmacol* 36, S179–83.
- Xing, Y., Musi, N., Fujii, N., Zou, L., Luptak, I., Hirshman, M.F., Goodyear, L.J., Tian, R., 2003. Glucose metabolism and energy homeostasis in mouse hearts overexpressing dominant negative alpha2 subunit of AMP-activated protein kinase. *J Biol Chem* 278, 28372–7.
- Yang, J., Gillingham, A.K., Hodel, A., Koumanov, F., Woodward, B., Holman, G.D., 2002. Insulin-stimulated cytosol alkalinization facilitates optimal activation of glucose transport in cardiomyocytes. *Am J Physiol Endocrinol Metab* 283, E1299–307.
- Yankovskaya, V., 2003. Architecture of Succinate Dehydrogenase and Reactive Oxygen Species Generation. *Science (80-)* 299, 700–704.
- Yano, T., Magnitsky, S., Ohnishi, T., 2000. Characterization of the complex I-associated ubisemiquinone species: toward the understanding of their functional roles in the electron/proton transfer reaction. *Biochim Biophys Acta* 1459, 299–304.
- Yoshikawa, S., 2003. A cytochrome c oxidase proton pumping mechanism that excludes the O₂ reduction site. *FEBS Lett* 555, 8–12.
- Yoshikawa, S., Muramoto, K., Shinzawa-Itoh, K., Aoyama, H., Tsukihara, T., Ogura, T., Shimokata, K., Katayama, Y., Shimada, H., 2006. Reaction mechanism of bovine heart cytochrome c oxidase. *Biochim Biophys Acta* 1757, 395–400.
- Young, L.H., Coven, D.L., Russell, R.R., 2000. Cellular and molecular regulation of cardiac glucose transport. *J Nucl Cardiol* 7, 267–76.
- Zeigerer, A., McBrayer, M.K., Mcgraw, T.E., 2004. Insulin stimulation of GLUT4 exocytosis, but not its inhibition of endocytosis, is dependent on RabGAP AS160. *Mol Biol Cell* 15, 4406–15.
- Zerial, M., McBride, H., 2001. Rab proteins as membrane organizers. *Nat Rev Mol Cell Biol* 2, 107–17.
- Zorzano, A., Balon, T.W., Goodman, M.N., Ruderman, N.B., 1986. Additive effects of prior exercise and insulin on glucose and AIB uptake by rat muscle. *Am J Physiol* 251, E21–6.

CHAPTER 3

Metabolic alterations and myocardial insulin resistance

3.1. Principles and pathogenesis of insulin resistance and diabetes

Having reviewed the mechanisms of myocardial metabolism under physiological conditions in Chapter 2, we now turn our attention to pathophysiological alterations during conditions of metabolic dysregulation. We place specific emphasis on literature outlining the etiology of insulin resistance – the topic of this thesis – and review the impact of metabolic fuel overabundance (specifically acute high glucose episodes) on this process. Lastly, we describe dysregulated glucose metabolic flux and its associated molecular defects, as put forth by the unifying hypothesis of diabetic complications. We propose that this may provide valuable insights and contribute to the development of hypotheses regarding the role of acute hyperglycemia in the onset of myocardial insulin resistance. However, we first pay attention to the description of insulin resistance, its diagnosis and etiology.

3.1.1. Introduction

The homeostatic control of glucose depends on its uptake and utilization by tissues, resulting in its clearance from the bloodstream. This process is chiefly governed by hormonal control by the release of insulin from the pancreatic β -cells (Kraegen *et al.*, 1993). Insulin exerts intracellular signaling cascades within target cells resulting in glucose uptake, storage or metabolic utilization (refer Chapter 2). The homeostatic mechanisms governing glucose utilization become impaired in conditions of insulin

resistance – the failure of insulin to effect the stimulation of glucose uptake in target cells. Insulin resistance is a complex, multifactorial and progressive condition that usually culminates in diabetes (reviewed in Petersen and Shulman, 2006; Stumvoll *et al.*, 2005). It is associated with various metabolic pathologies, and poor lifestyle/dietary habits contribute greatly to its progression. Skeletal muscle and adipose tissue are the main sites of glucose uptake, however, insulin resistance and the subsequent dysregulation of glucose homeostasis may impact cardiac metabolism and function (An and Rodrigues, 2006; Hu *et al.*, 2008; Leonard *et al.*, 2005; Ren *et al.*, 2003; Zhang *et al.*, 2011; Zhu *et al.*, 2013). The influence of insulin resistance in terms of defective glucose uptake in cardiomyocytes has not been given much attention in literature. A thorough understanding of the mechanisms of insulin resistance at play in the heart, and its consequences for cardiomyocyte function is therefore warranted. Furthermore, because insulin resistance develops gradually over time, it may be a beneficial approach to target an early time point for intervention during its pathogenesis. Here acute hyperglycemic episodes may play a role in exerting detrimental effects in the pre-diabetic state or as a result of increased dietary intake of sugars (Mapanga *et al.*, 2012; Parsons *et al.*, 2002; Williams *et al.*, 1998; Wisneski *et al.*, 1990; Yang *et al.*, 2009). The aim of this thesis is to investigate possible mechanisms of myocardial insulin resistance under acute hyperglycemic conditions. In light of this, we review mechanisms of metabolic alterations and myocardial insulin resistance in this chapter.

3.1.2. Diagnosis of insulin resistance and diabetes

The current diagnosis of insulin resistance and diabetes is based on the 2010 ADA recommendations and the 2011 WHO addendum report, using either glycosylated hemoglobin (HbA1c), fasting plasma glucose (FPG) or the oral glucose tolerance test (OGTT) (Malkani and DeSilva, 2012). Specific cut-off values for the outcome of each test defines glucose homeostasis in terms of normal (physiological/healthy), impaired fasting glucose (IFG – initial defect in the pathogenesis and indicative of pre-diabetes) and diabetes (severe loss of glucose homeostasis characterized by chronic hyperglycemia). The diagnostic criteria for diabetes and insulin resistance were developed over many years from different sets of criteria, as was the case for the diagnosis of the metabolic syndrome (refer Section 1.4). The currently used guidelines do not endorse any one specific detection method (Malkani and DeSilva, 2012) and specific cut-off values are continually revised to improve diagnostic utility across populations. However, despite the significant ground gained in the development of diagnostic criteria, current tests and criteria remain non-conforming and may result in inconsistencies when diagnosing insulin resistance and diabetes across populations (Borch-Johnsen and Colagiuri, 2009; Malkani and DeSilva, 2012). Each testing method also has peculiar features that may hamper efficient detection, while a significant number of individuals (mainly in developing countries) go undiagnosed due to various socio-economic factors (reviewed in Chapter 1). Nonetheless, to gain a better understanding of the etiology of insulin resistance, we will now briefly review the diagnostic screening methods, i.e. the OGTT, HbA1c and the FPG. The diagnostic criteria currently used are summarized in Table 3.1 below.

Table 3.1 Criteria for diagnosis of insulin resistance and diabetes (Malkani and DeSilva, 2012)

		2010 ADA criteria	2011 WHO guidelines
OGTT	Normal	<7.8 mmol/l	<7.8 mmol/l
	IFG	7.8-10.9 mmol/l	7.8-10.9 mmol/l
	Diabetes	≥11 mmol/l	≥11 mmol/l
FPG	Normal	<5.6 mmol/l	<6.1 mmol/l
	IFG	5.6-6.9 mmol/l	6.1-6.9 mmol/l
	Diabetes	≥7 mmol/l	≥7 mmol/l
HbA1c	Normal	<5.7%	Not specified
	IFG	5.7-6.4%	Not specified
	Diabetes	≥6.5%	≥6.5%

The OGTT is acknowledged as the 'gold standard' screening tool for the detection of diabetes (Park *et al.*, 2010) and is widely utilized in a range of different experimental studies (Barr *et al.*, 2002). However, the OGTT has several methodological and biological pitfalls. For example, individuals to be tested have to be available for more than 2 hours, while intra- individual variability and reproducibility are not optimal (Selvin *et al.*, 2007). The clinical utility of the OGTT is further hampered by differences in the rate of glucose absorption between males and females (Anderwald *et al.*, 2011).

HbA1c provides a measure of a person's average glucose metabolism over a longer time period (reviewed in Saudek *et al.*, 2006). Despite it being accredited as a highly

specific method for diabetes diagnosis, it has limited sensitivity and fails to detect short-term fluctuations in blood glucose (e.g. postprandial spikes and pre-diabetes) (reviewed in Derr *et al.*, 2003; Saudek *et al.*, 2008). The HbA1c tests are also more expensive compared to others, hampering the economic viability of its implementation (Bonora and Tuomilehto, 2011; George, 2011). Furthermore, several factors can influence HbA1c assay results and lead to misinterpretation, e.g. some hemoglobinopathies, iron deficiency, ageing, ethnicity and antiretroviral drugs (Amod, 2010; Bonora and Tuomilehto, 2011; Malkani and DeSilva, 2012).

The FPG test is frequently utilized as a diagnostic tool and is the most standardized and inexpensive means of diabetes identification (Malkani and DeSilva, 2012). However, it fails to specify daily glycemic fluctuations and excludes both the fasted and postprandial states as possible contributors to glucose levels observed (Wang *et al.*, 2009). This may lead to a lack of reproducibility and may result in day-to-day variation of results (Selvin *et al.*, 2007).

The pitfalls associated with the current diabetes diagnostic tests significantly hampers early and efficient detection of pre-diabetes and diabetes. This, together with the global prevalence of metabolic disorders, poor dietary and lifestyle habits and undiagnosed diabetes cases world-wide (reviewed in Chapter 1), makes the clinical identification of the etiology of insulin resistance difficult. It is therefore imperative that such measures are continuously re-evaluated and refined, but that the molecular events driving the etiology of insulin resistance are also better understood with the aim to enhance its detection. Although not all patients with impaired glucose tolerance (IGT) or impaired fasting glucose develop diabetes, it is

strongly associated with higher risk for development of diabetes, and patients in this group may be an important target for intervention (Edelstein *et al.*, 1997; Giugliano *et al.*, 2008; Tuomilehto *et al.*, 2001). In accordance, we are of the opinion that the transition from normal to IGT/IFG (a feature of pre-diabetes) may be an important time point to consider intervention, and that investigation of acute hyperglycemic episodes (which may be frequent during this transition) and its impact on myocardial glucose uptake is therefore an important pursuit. We next review literature concerning the etiology of insulin resistance to gain a better understanding of current knowledge in this regard.

3.1.3. Etiology of insulin resistance

Insulin resistance arises when physiological concentrations of insulin in response to increased blood glucose fail to exert its function. Pancreatic insulin release is subsequently elevated to attempt compensation for the loss of insulin sensitivity, developing into hyperinsulinemia. The pathophysiology of insulin resistance can be linked to mitochondrial dysfunction, glucocorticoids, inflammation, oxidative stress and the induction of non-oxidative glucose pathways (NOGPs) (to be discussed in section 3.4) (Ceriello and Motz, 2004; Hotamisligil *et al.*, 1993; Saini, 2010). Elevated metabolic fuel substrate availability (hyperglycemia, hyperlipidemia) may in itself contribute to the downregulation of insulin action (discussed in section 3.2.1 below) (Gao *et al.*, 2010; Marshall *et al.*, 1991; Petersen and Shulman, 2006; Ragheb *et al.*, 2009; Roden *et al.*, 1996).

The pathogenesis of diabetes progresses slowly over a long period and insulin resistance may precede full-blown diabetes by more than a decade (reviewed in Poornima *et al.*, 2006). Pancreatic β -cells upregulate insulin secretion in an attempt to maintain glucose homeostasis as the responsiveness to insulin decreases progressively (Stumvoll *et al.*, 2005). The elevated (supraphysiological) insulin concentrations effectively maintain normal glucose homeostasis during the early stages of insulin resistance (Dankner *et al.*, 2009; Savage *et al.*, 2007). This is evident by a normoglycemic-hyperinsulinemic state in which individuals are insulin resistant but display fasting plasma glucose levels in the normal range (Dankner *et al.*, 2009; Saltiel, 2001; Warram *et al.*, 1990). Pancreatic insulin secretion then progressively becomes impaired and β -cells fail to secrete the insulin concentrations required to maintain glucose homeostasis (Jurczak *et al.*, 2011; Lebovitz, 2011). Moreover, hyperinsulinemia contributes independently to the pathogenesis of insulin resistance (Shanik *et al.*, 2008; Weyer *et al.*, 2000). This leads to a pre-diabetic setting (displaying impaired glucose tolerance IGT/IFG) that is initially characterized by hyperinsulinemia and hyperglycemia (reviewed in Stolk *et al.*, 1997; Zimmet *et al.*, 1999). The function of β -cells decline progressively due to prolonged exposure to insulin resistance, hyperinsulinemia and glucolipotoxicity (Sicree *et al.*, 1987; Stumvoll *et al.*, 2005).

Although the pre-diabetic states of IFG and IGT are both characterized by insulin resistance (Qiao *et al.*, 2003), differences occur regarding the exact sites of decreased insulin sensitivity. Here IFG mainly presents as hepatic insulin resistance, while IGT is primarily characterized by muscle insulin resistance (Abdul-Ghani *et al.*, 2006; Nathan *et al.*, 2007). An understanding of the biphasic kinetics of insulin

secretion is important in order to evaluate the implications for insulin resistance (Gerich, 2002). The first phase lasting up to 15 min is a rapid release of insulin, peaking at 2-4 min after a glucose stimulus (Cavahan, 2004). The insulin secreted in this first phase is pre-formed and stored in granules within the β -cell (refer Chapter 2) (Cavahan, 2004). The second phase of insulin secretion is gradual and increases progressively for up to 3 h (Gerich, 2002). Individuals with IFG experience altered early-phase insulin response, while those with IGT show reduced first phase insulin secretion and a major reduction in the second phase (Nathan *et al.*, 2007). These features help to elucidate differences in glycemia between the two pre-diabetic states. Glycogenolysis in the liver together with defective early phase insulin release lead to excess hepatic glucose output and subsequent elevations in fasting plasma glucose levels observed in IFG (Nathan *et al.*, 2007). Conversely, decreased muscle glucose uptake and blunted late phase insulin secretion results in post-prandial hyperglycemia during IGT (Nathan *et al.*, 2007). Individuals with combined IFG/IGT experience both hepatic and muscle insulin resistance (Nathan *et al.*, 2007).

During the latter stages of insulin resistance, the steady decline in insulin secretion correlates with more severe hyperglycemia, raising glucose concentrations into the diabetic glucose range (Zimmet *et al.*, 1999). Overt type 2 diabetes is characterized by severe hyperglycemia and dysregulated glucose homeostasis coupled to drastically declined insulin levels (Mahler and Adler, 1999). Patients with established overt diabetes display complete β -cell failure (the major feature of type 1 diabetes) and therefore require insulin therapy (Lebovitz, 2011).

The review of the basic principles and features of insulin resistance, its diagnosis and etiology provides us with a foundation to next explore the molecular basis and mechanisms of insulin resistance.

3.2. Molecular mechanisms of insulin resistance

The physiological regulation of insulin action is reviewed in section 2.2.2. For the purpose of this study, we next review the pathophysiologic mechanisms contributing to insulin resistance. Specifically, we highlight the role metabolic fuel overabundance, the inter-relationship of lipid and glucose metabolism and mechanisms initiated by the (deranged) metabolism of hyperglycemia and hyperlipidemia leading to insulin resistance.

3.2.1. Dysregulation of insulin action by fuel substrate overabundance – Randle cycle revisited

Diabetes is characterized by hyperlipidemia, insulin resistance and compensatory hyperinsulinemia, and hyperglycemia (Poornima *et al.*, 2006). The excess fuel substrates in this state contribute to the etiology of insulin resistance. For example, hyperlipidemia usually presents with elevated blood levels of non-esterified fatty acids (NEFAs) and triglycerides (Poornima *et al.*, 2006). NEFAs play a significant role in the development of insulin resistance via several molecular mechanisms (Boden, 1997; Karpe *et al.*, 2011; Kelley *et al.*, 1993; Roden *et al.*, 1996). For example, increased citrate levels (as a result of high fatty acid β -oxidation) inhibit PFK-1, leading to an accumulation of glucose-6-phosphate and the inhibition of hexokinase II

activity. This causes elevated intracellular glucose concentrations and decreased GLUT4 translocation and glucose uptake (Randle *et al.*, 1963).

The Randle cycle (refer Chapter 2) describes the mechanisms of fuel substrate switching, where elevated fatty acid availability inhibits the metabolism of glucose by inhibition of PDH (Holness and Sugden, 2003; Randle *et al.*, 1963). Numerous studies have since revisited and further developed the Randle hypothesis (Boden, 1997; Dresner *et al.*, 1999; Griffin *et al.*, 1999; Roden *et al.*, 1996). For example, Shulman and colleagues (2000) suggest that elevated fatty acid metabolites (diacylglycerol, fatty acyl CoAs, ceramide) can disrupt insulin signaling pathways by activating PKC θ (Shulman, 2000). This in turn leads to the phosphorylation of serine residues on IRS-1. Normal insulin signaling requires tyrosine phosphorylation of the IRS-1 β -subunits (refer Chapter 2), while serine phosphorylation serves as a negative regulatory signal. PKC θ -mediated serine phosphorylation of IRS-1 therefore inhibits insulin action (Kim *et al.*, 2001; Shulman, 2000). This is supported by several rodent and human studies (Dresner *et al.*, 1999; Griffin *et al.*, 1999; Morino *et al.*, 2005; Yu *et al.*, 2002). Non-esterified fatty acids (NEFAs) can also regulate the expression of peroxisome proliferator-activated receptor γ (PPAR γ), thereby mediating the transcription of phosphatase and tensin homolog deleted on chromosome 10 (PTEN) (Schwartzbauer and Robbins, 2001). Subsequently PTEN catalyzes the dephosphorylation of PIP₃, thereby attenuating the insulin signaling cascade by limiting Akt activation (Poornima *et al.*, 2006). Additionally, FAs may reduce insulin action by attenuation of IR gene expression (Bhattacharya *et al.*, 2007).

High glucose levels may also play a significant role in the reduction of its own uptake, e.g. by the down regulation of AMPK, subsequently decreasing (specifically contraction-mediated) GLUT4 translocation (Itani *et al.*, 2003). In addition, increased glycolytic flux triggers greater oxidative stress production, thereby leading to downstream metabolic defects (discussed below). For example, induction of PKC isoforms and elevated hexosamine biosynthetic pathway (HBP) flux are important contributors to reduced glucose uptake under hyperglycemic conditions (Davidoff *et al.*, 2004; Park *et al.*, 2005; Ren *et al.*, 2013; Vosseller *et al.*, 2002) The mechanisms of high glucose-induced insulin resistance are further elucidated in this thesis. We will specifically focus on the role of acute hyperglycemia, a feature of the early events in the etiology of insulin resistance. The rationale here is that an understanding of the molecular events in the early phase of pathogenesis may provide insight regarding intervention strategies to stop the progression of insulin resistance. We therefore next review various aspects of acute hyperglycemia.

3.3. Acute hyperglycemia

Non-diabetic individuals may display acute hyperglycemia due to a combination of undiagnosed diabetes, IGT (Norhammar *et al.*, 2002) and a severe response to acute stress (Capes *et al.*, 2000; Lazzeri *et al.*, 2009; Oswald *et al.*, 1986). IGT precedes the progression to T2DM and is defined as having fasting plasma glucose levels below 7 mmol/l, and 2 hour post-prandial values between 7.8 mmol/l and 11.0 mmol/l (refer Section 3.1.2) (Mitrakou *et al.*, 1992). The ADA defines post-prandial hyperglycemia as blood glucose levels higher than 7.8 mmol/l in a 2 hour post-prandial period, with HbA1C <4% and normal FPG (Erlinger and Brancati, 2001).

Post-prandial hyperglycemia arises after glucose homeostasis becomes impaired and insulin fails to restore glucose levels after a meal. For example, in subjects with IGT insulin-mediated suppression of hepatic glucose production, enhancement of glucose uptake and reduction of FAs are impaired after consumption of a meal (Balkau *et al.*, 1999). Post-prandial hyperglycemia mainly manifests during the progression towards T2DM due to loss of the first phase of insulin secretion (Del Prato and Tiengo, 2001).

Fasting hyperglycemia results mainly from elevated glucose release (by gluconeogenesis) by the liver and kidneys (Dinneen *et al.*, 1992; Meyer *et al.*, 1998). Rates of glucose uptake are generally increased in individuals with fasting hyperglycemia, mainly because of the mass action effects of hyperglycemia. Moreover, fasting hyperglycemia may also occur due to precursor post-prandial hyperglycemia, i.e. the higher the hyperglycemia after an evening meal, the greater the hyperglycemia in the morning and *vice versa*. Hence treatment should therefore aim to control both post-prandial and fasting hyperglycemia.

Acute hyperglycemic episodes are major features of the early phases during the etiology of insulin resistance (e.g. pre-diabetes), while high dietary intake of sugars may also contribute to acute hyperglycemic episodes (Edelstein *et al.*, 1997; Tuomilehto *et al.*, 2001). A number of studies implicate acute hyperglycemia to cardio-metabolic derangements and vascular derangements (Ceriello *et al.*, 2002; Mapanga *et al.*, 2012; Parsons *et al.*, 2002; Williams *et al.*, 1998; Wisneski *et al.*, 1990; Yang *et al.*, 2009). For the current study, we propose that acute hyperglycemia may induce insulin resistance in cardiac-derived cells. We next review mechanisms

which mediate hyperglycemic (chronic and/or acute) derangements in an attempt to gain further insight.

3.4. Glucose-metabolic dysregulation and diabetic complications

Hyperglycemia (chronic and acute) contributes to various vascular complications by initiating detrimental molecular events. The upregulation of oxidative stress plays an important role in a diverse range of complications. Indeed, it may be a central factor governing the downstream metabolic dysregulation of glucose flux at the center of pathologies. Oxidative stress is also implicated in the etiology of insulin resistance. We now review various mechanisms of oxidative stress induction under hyperglycemic conditions in the next section.

3.4.1. Oxidative stress

Oxidative stress – the result of an imbalance between reactive oxygen species (ROS) generation and the intrinsic antioxidant capacity of a cell – is implicated in the pathogenesis of multiple diseases (Bonnetfont-Rousselot *et al.*, 2000; Khullar *et al.*, 2010; King and Loeken, 2004). ROS production may be triggered by multiple stimuli, including elevations in metabolic fuel substrate influx (Catherwood *et al.*, 2002; Finkel and Holbrook, 2000; Furukawa *et al.*, 2004; King and Loeken, 2004; Lindsay, 1999). For example, hyperglycemia is associated with increased superoxide levels, while hyperlipidemia may elevate superoxide and peroxynitrite levels (Baynes and Thorpe, 1999). The excess free radicals damage proteins, lipids and nucleic acids with detrimental outcomes.

Oxidative stress is also strongly implicated in the development of insulin resistance/diabetes and its complications, with diabetic patients and experimental models of diabetes (*in vitro* and *in vivo*) displaying increased oxidative stress compared to controls (Baynes and Thorpe, 1999; Brownlee, 2005, 2001; Catherwood *et al.*, 2002; Giardino *et al.*, 1996; King and Brownlee, 1996; Mapanga *et al.*, 2012; Nourooz-Zadeh *et al.*, 1997; Rösen *et al.*, 2001, 1998; Szaleczky *et al.*, 1999). Further evidence for this stems from studies which utilized antioxidants (e.g. vitamin E or C and α -lipoic acid) to attenuate diabetic complications (Jain *et al.*, 2004; Paolisso *et al.*, 1993; Ziegler *et al.*, 1995), while the overexpression of manganese superoxide dismutase (MnSOD) reduced oxidative stress in experimentally-induced diabetes (Chen *et al.*, 1998; Schwaiger *et al.*, 1989). Oxidative stress is also prominently implicated in the etiology of insulin resistance, and may play a role in the attenuation of pancreatic β -cell function and insulin secretion (Futamura *et al.*, 2012), as well as disruption of insulin signaling and glucose uptake in insulin responsive cells (Costford *et al.*, 2009; Gao *et al.*, 2010; Grimsrud *et al.*, 2007; Messner *et al.*, 2013; reviewed in Eriksson, 2007; Ruskovska and Bernlohr, 2013). The specific ROS producing mechanisms, sources involved and its link to insulin resistance and cardio-metabolic dysfunction are outlined below.

3.4.1.1. ROS sources

One of the primary sites for ROS generation is the mitochondrial electron transport chain. The metabolic utilization of glycolytic substrates and FA in mitochondria under physiological conditions was explained in Chapter 2. Briefly, the generation of electron donors (NADH and FADH₂) from the citric acid cycle and FA β -oxidation,

drive the flux of electrons from complexes I and II of the electron transport chain through complexes III and IV to oxygen, forming water and resulting in protons being pumped across the mitochondrial inner membrane with ATP synthesis (Cecchini, 2003; Hirst, 2005; Paradies *et al.*, 2001). Mitochondria respond to various signals by controlling ATP production, calcium homeostasis, ROS production and membrane permeability. Under conditions of metabolic stress, mitochondria can contribute to increased production of oxidants (Grivennikova and Vinogradov, 2006; Paradies *et al.*, 2001). This is evident from experimental studies demonstrating that mitochondrial damage is associated with diabetes (Ferreira *et al.*, 2003; Fitzl *et al.*, 2001; Shen *et al.*, 2004). Here, electrons may leak from the respiratory chain and react with oxygen to form free radicals which are highly reactive because of unpaired electrons in their structure. ROS are generated if the membrane potential across the inner mitochondrial membrane rises above a certain threshold (Korshunov *et al.*, 1997). Electrons mainly leak from complex I (Barja and Herrero, 1998; Barja, 1999; Chen *et al.*, 2005; Genova *et al.*, 2001; Herrero and Barja, 1997; Kudin *et al.*, 2004; Kushnareva *et al.*, 2002; Lambert and Brand, 2004; Ohnishi *et al.*, 2005) and complex III (Boveris *et al.*, 1976; Chen *et al.*, 2003; St-Pierre *et al.*, 2002). However, complex III is considered the major site of ROS production as a result of elevated substrate influx (e.g. hyperglycemia) (Brownlee 2001, 2005; Chen *et al.*, 2003). This is evident by excess production of superoxide ions in diabetic rats in response to glycation of complex III proteins (Rosca *et al.*, 2005).

Hyperglycemia causes higher mitochondrial ROS production via increased electron transfer donors (NADH and FADH₂), resulting in elevated electron flux through the mitochondrial ETC. This leads to a subsequent increase in the ATP/ADP ratio and

hyperpolarization of the mitochondrial membrane potential (Brand *et al.*, 2004; Korshunov *et al.*, 1997; Skulachev, 1999, 1996). The high electrochemical potential difference generated by the proton gradient leads to partial inhibition of the electron transport at complexes I and III. This results in accumulation of electrons at coenzyme Q, which in turn drives the partial reduction of oxygen to generate superoxide (Brownlee, 2001; Du *et al.*, 2003, 2000). The continual accelerated reduction of coenzyme Q and subsequent ROS generation may be an important causative factor for mitochondrial dysfunction and diabetes-related metabolic disorders. Moreover, mitochondrial ROS production is associated with insulin resistance, with hydrogen peroxide (H₂O₂) implicated in the disruption of insulin signaling intermediates (Anderson *et al.*, 2009; Fisher-Wellman and Neuffer, 2012). Mitochondrial dysfunction and defects in its morphology were found in muscle tissue of diabetic patients and animal models (reviewed in Cheng *et al.*, 2010; Rabøl, 2011). Whether defects at the mitochondrial level are causative factors, or a consequence of insulin resistance, is not yet clear (reviewed in Rabøl, 2011).

The mitochondrion is not the only site for intracellular ROS production. There is further evidence that elevated ROS generation from cytosolic sources may play central roles in pathogenic mechanisms (Garciaarena *et al.*, 2008; Zhou *et al.*, 2010). Additional sources of ROS generation include; glucose autoxidation, NADPH oxidase (NOX), lipoxygenases, cyclo-oxygenases, peroxidases, heme proteins, xanthine oxidase, peroxisomes, or the hepatic P-450 microsomal detoxifying system (Brownlee, 2001; Ceriello *et al.*, 2002; Desco *et al.*, 2002; Nishikawa *et al.*, 2000; Yamagishi *et al.*, 2001).

The role of ROS production via NOX and its part in cardiovascular complications recently gained considerable attention. For example, NOX activity and superoxide production is high in vascular tissue from diabetic patients (Guzik *et al.*, 2002), while it is a major producer of hyperglycemia-mediated ROS in cardiomyocytes (Brewer *et al.*, 2011; Li *et al.*, 2006; Santos *et al.*, 2011). NOX-derived ROS can also participate in myocardial apoptosis under hyperglycemic conditions (Balteau *et al.*, 2011), while NADPH from the pentose phosphate pathway (PPP) may be necessary to mediate NOX activity in obese and hyperglycemic rat hearts (Serpillon *et al.*, 2009). Angiotensin II (ANG II)-induced NOX activation also induced insulin resistance in *in vitro* and *in vivo* studies (Ogihara *et al.*, 2002; Sloniger *et al.*, 2005; Wei *et al.*, 2006). We are therefore particularly interested in NOX activation for the studies outlined in this thesis.

In summary, both mitochondrial and non-mitochondrial ROS are key players in the manifestation of cardio-metabolic pathophysiologies. Here the initiating event is mitochondrial superoxide production that triggers further ROS generation (other sources) thereby creating a vicious cycle.

3.4.1.2. Intracellular antioxidant systems

Mitochondria together with the other intracellular antioxidant systems have the capability of maintaining oxidative stress homeostasis by a balance between ROS production and its elimination (Dhar *et al.*, 2008). However, these endogenous oxidative stress defense mechanisms are overwhelmed during pathological conditions such as hyperglycemia and/or ischemia-induced oxidative stress.

Glutathione reductase and peroxidase play a key role in the recycling of glutathione between its reduced (GSH) and oxidized (GSSG) forms. Glutathione peroxidase removes H_2O_2 through the oxidation of GSH to GSSG, while glutathione reductase acts as an antioxidant by converting GSSG to GSH. Superoxide Dismutase (SOD) provides further defensive cover by conversion of superoxide to H_2O_2 that is then converted to water by catalase (another core antioxidant). SOD is present in three isoforms, i.e. SOD1; a dimer found in the cytoplasm, whereas SOD2 and SOD3 are tetramers found in the mitochondrion and extracellular matrix, respectively (McCord and Edeas, 2005).

3.4.1.3. ROS and non-oxidative glucose pathways (NOGPs) – unifying hypothesis and its modifications

The energy producing and fuel storage pathways of glucose metabolism are the chief avenues for glucose disposal in cells. However, small percentages of glucose-derived intermediates enter alternative pathways under physiological conditions. These pathways are, however, significantly activated under conditions of fuel substrate excess (e.g. hyperglycemia), and oxidative stress may play a central role in mediating this. A currently favored model suggests that superoxide produced in mitochondria under hyperglycemic conditions may be a central unifying factor underlying the induction of NOGPs and their detrimental downstream effects (Brownlee, 2005). ROS produced here leads to DNA damage and the subsequent activation of the DNA repair enzyme poly (ADP)-ribose polymerase (PARP) (Beneke and Bürkle, 2007; Bürkle, 2005; Colussi *et al.*, 2000; Diefenbach and Bürkle, 2005). PARP is recruited to catalyze the repair of single and double strand DNA breaks by

poly (ADP)-ribosylation. In addition to its DNA repair function, PARP activation results in the covalent linkage of ADP-ribose subunits to glutamate, aspartate and lysine residues of target proteins (Beneke and Bürkle, 2007; Bürkle, 2005). The glycolytic enzyme GAPDH is a PARP target, i.e. it can be inhibited by the action of PARP (Beneke and Bürkle, 2007; Bürkle, 2005; Du *et al.*, 2003; Nishikawa *et al.*, 2000). Subsequently, upstream glycolytic intermediates accumulate and are pushed into NOGPs, i.e. the pathways of advanced glycation end-product (AGE) formation and PKC activation, the polyol pathway and the hexosamine biosynthetic pathway (HBP) (Brownlee, 2005, 2001; Du *et al.*, 2003, 2000; Giacco and Brownlee, 2010; King and Brownlee, 1996; Nishikawa *et al.*, 2000). Elevated flux via these four pathways under hyperglycemic conditions is strongly implicated in a myriad of diabetic vascular complications. A fifth pathway, the pentose phosphate pathway (PPP) may also be altered under hyperglycemic conditions. However the fashion in which it is altered (increased or decreased with hyperglycemia/diabetes) remains controversial. However, a number of studies show that PPP activation under hyperglycemic/diabetic conditions reduced flux via the other NOGPs and this was associated with positive outcomes (Balakumar *et al.*, 2010; Beltramo *et al.*, 2008; Cameron *et al.*, 2005; Du *et al.*, 2008; Katare *et al.*, 2010a, 2010b; Mapanga *et al.*, 2013; Marchetti *et al.*, 2006). A more detailed description of the NOGPs is provided below (also refer Fig 3.1).

Although the unifying hypothesis gained strong experimental support and is a fairly widely accepted explanation for the vascular defects of hyperglycemia, recent studies show that additional factors may play more prominent roles in these mechanisms (reviewed in Schaffer *et al.*, 2012). Here intracellular source(s) of ROS production at

the center of hyperglycemia-induced detrimental effects, the contribution of other ROS species (not only mitochondrial superoxide), the role of antioxidant defense mechanisms and the regulation of glucose metabolism by these oxidative stress mechanisms, have been revisited. For example, decreased MnSOD activity and glutathione (GSH) levels may be the main mechanisms attributable to the elevated mitochondrial ROS observed (Kanwar *et al.*, 2007; Kowluru *et al.*, 2006). Furthermore, the transport of superoxide to the nucleus (where it exerts DNA damage) is improbable due its relatively short half-life and reactivity (reviewed in Schaffer *et al.*, 2012). It is thus plausible that other ROS species, e.g. cytosolic ROS sources may play more prominent roles in exerting damaging outcomes observed (Radi *et al.*, 2002; reviewed in Schaffer *et al.*, 2012). These concerns open up more possibilities for future work. In the case of this study, we considered the involvement of *both* mitochondrial- and NOX-derived ROS in activation of NOGPs, and the subsequent attenuation of insulin action. The next section provides a more in-depth discussion of the physiologic and pathophysiologic roles of the NOGPs.

3.4.2. Non-oxidative glucose pathways

As explained above, flux via the NOGPs is markedly upregulated when glucose fuel sources are in abundance and a number of these pathways are implicated in the pathogenesis of a wide array of diabetes-associated complications. Chronically elevated blood glucose levels under such conditions may contribute significantly to the observed adverse effects. Glucose metabolites may enter the pathways of advanced glycation-end products (AGE) formation, the polyol pathway, hexosamine

biosynthetic pathway (HBP), protein kinase C (PKC) activation and pentose phosphate (PPP) pathways (Fig 3.1). Each pathway will be described below.

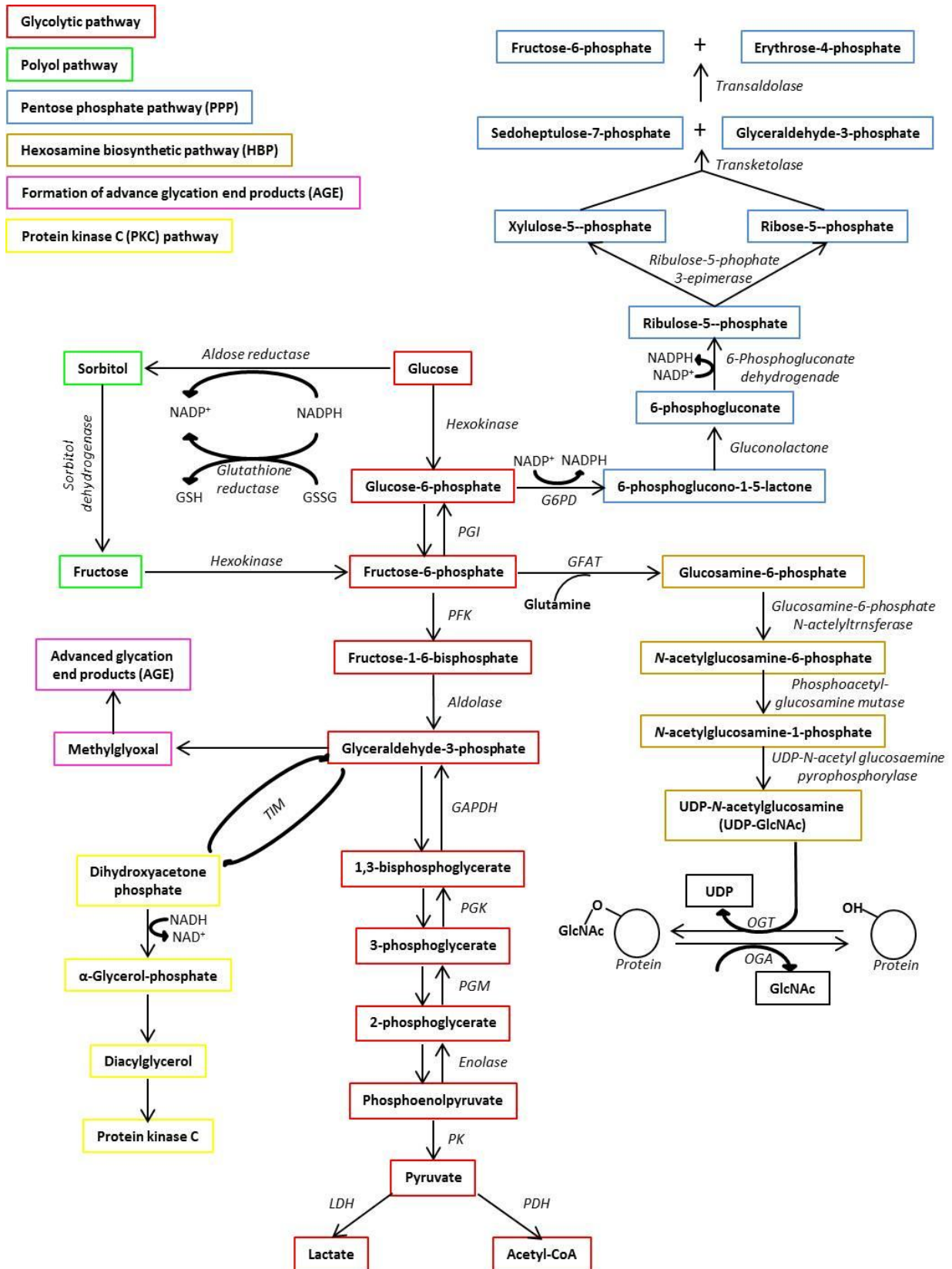


Figure 3.1 Glycolysis and NOGP branch points. The pathways of glycolysis (red blocks), AGE formation (pink blocks), polyol pathway (green blocks), PKC (yellow blocks), HBP (brown blocks) and PPP (blue blocks) are shown. (Modified from Brownlee, 2005 and Bolanos *et al.*, 2010)

3.4.2.1. Advanced glycation end products

The intracellular production of AGE precursors is an important mechanism of cellular stress. AGE molecules are formed during a non-enzymatic reaction between proteins and sugar residues, known as the Maillard reaction (Hartog *et al.*, 2007). AGE accumulates with aging and with conditions like diabetes, renal failure and oxidative stress. AGEs are formed when sugar residues react with the amino group of a protein to form a Schiff-base (Hartog *et al.*, 2007). This is a rapid and reversible reaction and the Schiff-base then forms a more stable Amadori product. Further steps result in the formation of irreversible and stable AGE compounds. High glucose levels may directly increase AGE precursors by accumulation of G-3-P in glycolysis, which is diverted to form methylglyoxal (Fig 3.2)

AGEs are also implicated in the development of heart failure in both diabetic and non-diabetic patients, i.e. it can increase rigidity of heart tissue leading to diastolic and systolic dysfunction through coronary artery disease and vascular dysfunction (Hartog *et al.*, 2007). AGE precursors may also exert cellular damage by modifying intracellular proteins (Giardino *et al.*, 1994; Shinohara *et al.*, 1998), extracellular matrix molecules (McLellan *et al.*, 1994), and circulating proteins such as albumin (Doi *et al.*, 1992). Modified circulating proteins can bind to and activate AGE receptors, hence causing an inflammatory response in the vasculature through the production of cytokines and growth factors (Abordo and Thornalley, 1997; Doi *et al.*, 1992; Kirstein *et al.*, 1992; Li *et al.*, 1996; Neeper *et al.*, 1992; Schmidt *et al.*, 1995; Skolnik *et al.*, 1991; Smedsrød *et al.*, 1997; Vlassara *et al.*, 1995, 1988). Through their receptors (RAGEs), AGEs inactivate enzymes by altering their structures and

functions (McCarthy *et al.*, 2001), promoting free radical formation (Baynes and Thorpe, 1999), and impair the anti-proliferative effects of nitric oxide (Vlassara, 1997). Moreover, AGEs increase intracellular oxidative stress thereby activating the transcription factor nuclear factor κ B (NF- κ B) and promoting up-regulation of its target genes (Mohamed *et al.*, 1999).

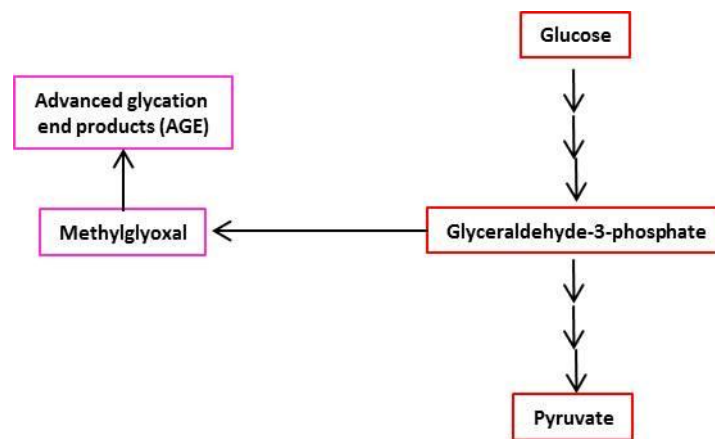


Figure 3.2 AGE formation

3.4.2.2. Polyol pathway

Polyol pathway flux is elevated up to ~10 fold under hyperglycemic conditions (Dunlop, 2000; González *et al.*, 1984; Sheetz and King, 2002; Travis *et al.*, 1971; Yabe-Nishimura, 1998). The pathway is initiated by aldose reductase reducing glucose to sorbitol, that is later oxidized to fructose (Fig 3.3). The aldose reductase reaction uses up intracellular NADPH (Lee and Chung, 1999). Since NADPH is also needed for the regeneration of GSH, a decrease in reduced glutathione levels due to lesser availability of NADPH, increases susceptibility to intracellular oxidative stress (Brownlee, 2005) and subsequent ROS-mediated effects. Hyperglycemia-mediated induction of the polyol pathway may therefore increase intracellular oxidative stress by limiting the antioxidant defense mechanism usually exerted by GSH (Fig 3.3).

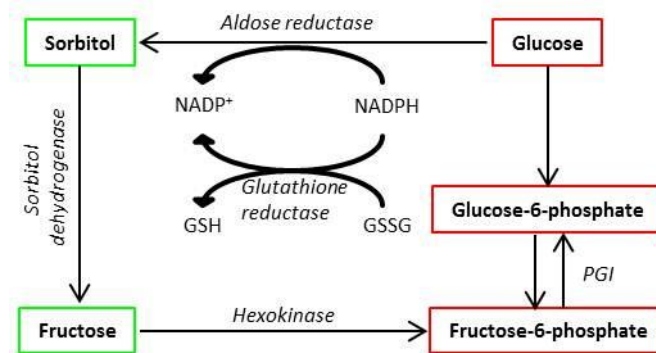


Figure 3.3 Polyol pathway

3.4.2.3. Protein kinase C activation

The PKC family consists of a diverse group of kinases that control the function of target proteins by phosphorylation of hydroxyl groups of serine and threonine residues. PKC enzymes are activated by upstream signals, e.g. diacylglycerol (DAG) (Koya *et al.*, 1997). Accumulation of triosephosphates as a result of hyperglycemia, increases the production of DAG, which in turn activates classic isoforms of PKC (Fig 3.4), i.e. β , δ , and α (Derubertis and Craven, 1994; Koya and King, 1998; Koya *et al.*, 1997; Xia *et al.*, 1994). Upon activation, PKC enzymes are translocated to the sarcolemma by membrane-bound receptor for activated protein kinase C proteins (RACK). This is achieved by DAG production from phosphatidylinositol (by a phospholipase). Moreover, FA may also play a role in long-term activation of PKC isoforms (Koya *et al.*, 1997). PKC activation exerts a number of downstream effects, including decreased endothelial nitric oxide synthase (eNOS), activation of NOX and subsequently increased ROS (Xia *et al.*, 2006). Indeed, intermittent high glucose challenge in endothelial cells resulted in NOX activation that was reduced by PKC

inhibition (Quagliaro *et al.*, 2003). Thus PKC activation may play an important role in the onset of insulin resistance (Davidoff *et al.*, 2004; Ren *et al.*, 2013).

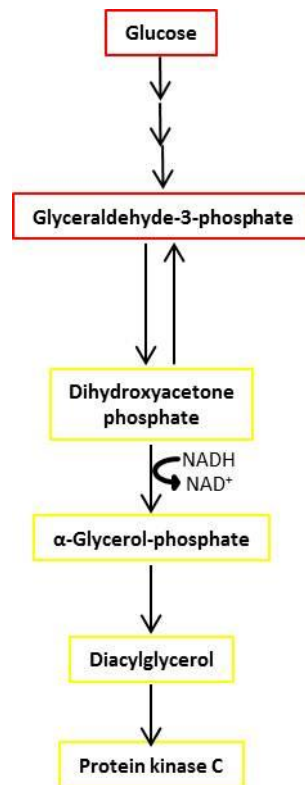


Figure 3.4 PKC activation

3.4.2.4. Hexosamine biosynthetic pathway

The HBP is regarded as an intracellular sensor of metabolic fuel substrates, resulting in partitioning of excess substrates to storage depots elsewhere in the body (reviewed in McClain, n.d.; Ravussin, 2002; Rossetti, 2000; Zachara and Hart, 2004). It utilizes approximately 3% of the total glucose available to the cell under normal circumstances, but is drastically increased by hyperglycemia (Hardie *et al.*, 2003; Tang *et al.*, 2000). Glutamine:fructose-6-phosphate amidotransferase (GFAT) is the rate-limiting enzyme of the HBP and responsible for the catalytic conversion of

fructose-6-phosphate to glucosamine-6-phosphate (Daniels *et al.*, 1996) (Fig 3.5). A series of successive reactions result in the post-translational modification of target proteins by addition of an O-GlcNAc moiety. During hyperglycemia increased O-GlcNAcylation of target proteins is strongly associated with the onset of cardiovascular disease (CVD) and insulin resistance (Jacobsen *et al.*, 1996). Moreover, the increased production of glucosamine-6-phosphate inhibits the activity of glucose-6-phosphate dehydrogenase (G6PD), the rate-limiting enzyme of the PPP (McDaniel *et al.*, 2002). This inhibition ultimately leads to a decrease in NADPH/NADP⁺ ratios since G6PD activity involves the reduction of NADP⁺ to NADPH (Li *et al.*, 1996). The HBP therefore plays a role in mitigating the PPP and thereby reduces the intracellular NADPH levels. The decreased availability of NADPH attenuates intracellular antioxidant capacity and further contributes to ROS production (decreased GSH and catalase activity) (Li *et al.*, 1996).

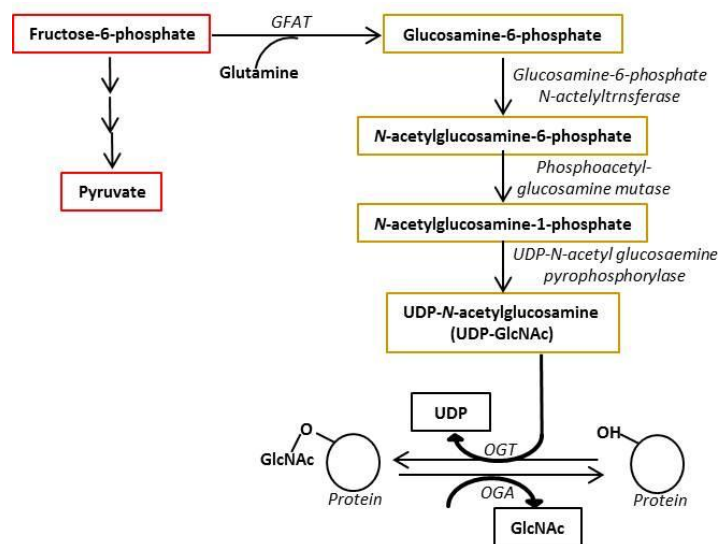


Figure 3.5 Hexosamine biosynthetic pathway

3.4.2.5. Pentose phosphate pathway

The pentose phosphate pathway (PPP) consists of two main branches, i.e. the oxidative and the non-oxidative branch, respectively. In addition to glucose oxidation, the PPP mainly generates reducing equivalents in the form of NADPH and pentoses (5-carbon sugars) such as ribose-5-phosphate and erythrose-4-phosphate used in the synthesis of nucleic acids and aromatic amino acids, respectively (Wamelink *et al.*, 2008).

For the oxidative PPP branch, glucose 6-phosphate is oxidized into 6-phosphogluconolactone (6PG) by the rate-limiting enzyme, G6PD (Fig 3.6). This reaction results in the production of the first NADPH molecule in the pathway. The end product of this pathway, ribulose 5-phosphate, can then be converted into ribose 5-phosphate in the non-oxidative pathway to yield nucleotides via the transketolase (TK) reaction. From these reactions it can be deduced that the main role of the oxidative PPP branch is to produce NADPH which functions in detoxification processes, i.e. reduced glutathione regeneration and lipid biosynthesis (Lonsdale, 2006; Riganti *et al.*, 2012) as well as provision of ribulose 5-phosphate for nucleotide synthesis.

There are conflicting reports whether G6PD activity is increased, decreased or not changed with insulin resistance/ diabetes. Some found that G6PD activity increases (Gupte *et al.*, 2009; Serpillon *et al.*, 2009) while others reported decreased activity (Cappai *et al.*, 2011; Carette *et al.*, 2011; Katare *et al.*, 2010a; Sudnikovich *et al.*, 2007; Yan *et al.*, 1994). Such conflicting data further extends to NADPH produced by

this pathway, i.e. whether it contributes to or blunts oxidative stress. In fact, almost all the studies show that increased G6PD activity enhances NOX-induced ROS production via PKC activation. Similar findings were observed in various heart failure studies where G6PD activity is increased to provide more NADPH possibly as a compensation mechanism to counter oxidative stress (Gupte *et al.*, 2007, 2006). However, the association of G6PD to increased NOX activity is disputed by Balteau *et al.* (2011) who suggested that this effect is independent of glucose metabolism but relies on glucose uptake via sodium glucose transporter 1 (SGLT1) (Balteau *et al.*, 2011). The differences observed may be attributed to variations of experimental approaches employed (*in vivo* and *in vitro*), species investigated (humans, rats and mice), and different tissues evaluated to measure G6PD (liver, cardiac, pancreas and neurons).

TK catalyzes several reactions in the non-oxidative PPP, and serves as a bridge between the oxidative PPP and the oxidative decarboxyl metabolism of glucose. This therefore allows the cell to adapt to a variety of metabolic needs under different environmental conditions (Horecker, 2002). TK recognizes D-xylulose 5-phosphate, D-fructose 6-phosphate and D-sedoheptulose 7-phosphate as donors while D-ribose 5-phosphate, D-erythrose 4-phosphate, D-glyceraldehyde 3-phosphate and glycoaldehyde as receptor substrates (Esakova *et al.*, 2004). The main function of the non-oxidative PPP branch is to convert hexoses into pentoses, particularly glyceraldehyde 3-phosphate into ribose-5-phosphate that is required for nucleic acid synthesis.

TK relies on thiamine pyrophosphate (a thiamine pyrophosphate [TPP] ester) as cofactor for its function. Here the main source is from Vitamin B1 (thiamine) a water-soluble compound that has been used for decades in the treatment of several disorders such as neurological, diabetic, and cardiovascular complications (Ang *et al.*, 2008; Beltramo *et al.*, 2009; Pomero *et al.*, 2001). More recently, studies found that thiamine can prevent diabetes and its associated complications (Haupt *et al.*, 2005; Pomero *et al.*, 2001; Stracke *et al.*, 1996).

The TK catalyzed reactions convert xylulose-5-phosphate and ribose-5-phosphate to glyceraldehyde-3-phosphate and sedoheptulose-7-phosphate, respectively. These are then converted to erythrose-4-phosphate and fructose-6-phosphate by transaldolase. In the second TK pathway, xylulose-5-phosphate and erythrose-4-phosphate are converted to glyceraldehyde 3-phosphate and sedoheptulose-7-phosphate. All the reactions are reversible and depend on substrate availability. Various studies reported reduced levels of thiamin, activity of transketolase (Babaei-Jadidi *et al.*, 2003; Havivi *et al.*, 1991) and beneficial effects of benfotiamine treatment with diabetes (Babaei-Jadidi *et al.*, 2003; Beltramo *et al.*, 2009, 2008; Haupt *et al.*, 2005; Katare *et al.*, 2010a, 2010b).

This section focused on the detrimental outcomes of hyperglycemia in terms of oxidative stress and NOGP induction. This analysis not only provides a sound foundation but also identifies current gaps and limited understanding regarding the role of acute hyperglycemia on insulin resistance in myocardial cells. We here employed a unique holistic approach by evaluating various aspects of ROS

production, scavenging mechanisms, sources and the relation to NOGP induction and insulin action.

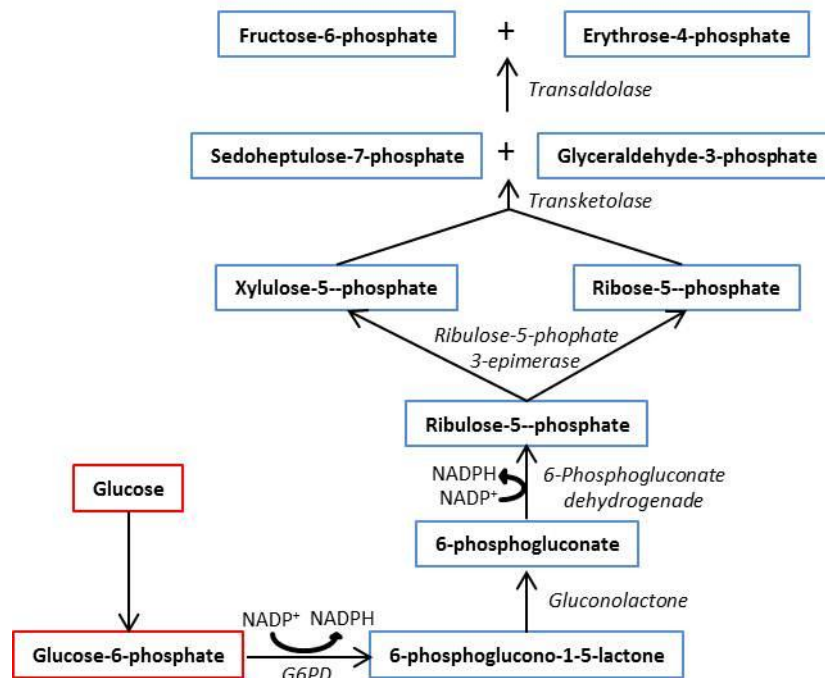


Figure 3.6 Oxidative and non-oxidative branches of the pentose phosphate pathway

3.5. Summary

In conclusion, elevated nutrient substrates play a significant role in the etiology of insulin resistance. Acute hyperglycemic episodes may be prominent in the pre-diabetic state, and contributes to the pathophysiology of glucose homeostatic dysregulation. However, mechanistic links between acute hyperglycemia and insulin resistance in this crucial window in the pathogenesis of insulin resistance, remain to be fully understood. Lessons from the role of chronic hyperglycemia in the diabetic state show that oxidative stress and the induction of NOGPs are central mediators of downstream complications. Many of these mechanisms may be involved in the

disruption of insulin action. We therefore propose that acute hyperglycemic conditions may induce similar alterations in insulin responsive myocardial cells. Such mechanisms and inter-pathway cross talk may contribute to the dysregulation of insulin action. In light of this, we therefore aim to investigate the role of oxidative stress (assessing sources and mechanisms of ROS production), NOGP activation, and the effect(s) of these events on insulin resistance using *in vitro* techniques to simulate acute hyperglycemia in a rat cardiac-derived cell line. The main objectives were to determine the insulin action (glucose uptake, GLUT4 translocation and Akt activity) in cells exposed to acute hyperglycemia, evaluate ROS levels and downstream effects on insulin action and assess the induction and role of each NOGP in mediating insulin resistance. The methodology is described in Chapter 4, while Chapters 5 and 6 describes our unique findings in this regard.

3.6. References

- Abdul-Ghani, M.A., Jenkinson, C.P., Richardson, D.K., Tripathy, D., DeFronzo, R.A., 2006. Insulin secretion and action in subjects with impaired fasting glucose and impaired glucose tolerance: results from the Veterans Administration Genetic Epidemiology Study. *Diabetes* 55, 1430–5.
- Abordo, E.A., Thornalley, P.J., 1997. Synthesis and secretion of tumour necrosis factor- α by human monocytic THP-1 cells and chemotaxis induced by human serum albumin derivatives modified with methylglyoxal and glucose-derived advanced glycation endproducts. *Immunol Lett* 58, 139–47.
- Amod, A., 2010. Position statement on the use of HbA1C assays for the diagnosis of diabetes mellitus (SEMDSA). *J Endocrinol Metab Diabetes South Africa*.
- An, D., Rodrigues, B., 2006. Role of changes in cardiac metabolism in development of diabetic cardiomyopathy. *Am J Physiol Heart Circ Physiol* 291, H1489–506.
- Anderson, E.J., Lustig, M.E., Boyle, K.E., Woodlief, T.L., Kane, D.A., Lin, C.-T., Price, J.W., Kang, L., Rabinovitch, P.S., Szeto, H.H., Houmard, J.A., Cortright, R.N., Wasserman, D.H., Neuffer, P.D., 2009. Mitochondrial H₂O₂ emission and cellular redox state link excess fat intake to insulin resistance in both rodents and humans. *J Clin Invest* 119, 573–81.
- Anderwald, C., Gastaldelli, A., Tura, A., Krebs, M., Promintzer-Schifferl, M., Kautzky-Willer, A., Stadler, M., DeFronzo, R.A., Pacini, G., Bischof, M.G., 2011. Mechanism and effects of glucose absorption during an oral glucose tolerance test among females and males. *J Clin Endocrinol Metab* 96, 515–24.
- Ang, C.D., Alviar, M.J.M., Dans, A.L., Bautista-Velez, G.G.P., Villaruz-Sulit, M.V.C., Tan, J.J., Co, H.U., Bautista, M.R.M., Roxas, A.A., 2008. Vitamin B for treating peripheral neuropathy. *Cochrane database Syst Rev* CD004573.
- Babaei-Jadidi, R., Karachalias, N., Ahmed, N., Battah, S., Thornalley, P.J., 2003. Prevention of incipient diabetic nephropathy by high-dose thiamine and benfotiamine. *Diabetes* 52, 2110–20.
- Balakumar, P., Rohilla, A., Krishan, P., Solairaj, P., Thangathirupathi, A., 2010. The multifaceted therapeutic potential of benfotiamine. *Pharmacol Res* 61, 482–8.
- Balkau, B., Bertrais, S., Ducimetiere, P., Eschwege, E., 1999. Is there a glycemic threshold for mortality risk? *Diabetes Care* 22, 696–9.
- Balteau, M., Tajeddine, N., De Meester, C., Ginion, A., Des Rosiers, C., Brady, N.R., Sommereyns, C., Horman, S., Vanoverschelde, J.-L., Gailly, P., Hue, L., Bertrand, L., Beauloye, C., 2011. NADPH oxidase activation by hyperglycaemia in cardiomyocytes is independent of glucose metabolism but requires SGLT1. *Cardiovasc Res* 92, 237–46.
- Barja, G., 1999. Mitochondrial oxygen radical generation and leak: sites of production in states 4 and 3, organ specificity, and relation to aging and longevity. *J Bioenerg Biomembr* 31, 347–66.

- Barja, G., Herrero, A., 1998. Localization at complex I and mechanism of the higher free radical production of brain nonsynaptic mitochondria in the short-lived rat than in the longevous pigeon. *J Bioenerg Biomembr* 30, 235–43.
- Barr, R.G., Nathan, D.M., Meigs, J.B., Singer, D.E., 2002. Tests of glycemia for the diagnosis of type 2 diabetes mellitus. *Ann Intern Med* 137, 263–72.
- Baynes, J.W., Thorpe, S.R., 1999. Role of oxidative stress in diabetic complications: a new perspective on an old paradigm. *Diabetes* 48, 1–9.
- Beltramo, E., Berrone, E., Tarallo, S., Porta, M., 2008. Effects of thiamine and benfotiamine on intracellular glucose metabolism and relevance in the prevention of diabetic complications. *Acta Diabetol* 45, 131–41.
- Beltramo, E., Nizheradze, K., Berrone, E., Tarallo, S., Porta, M., 2009. Thiamine and benfotiamine prevent apoptosis induced by high glucose-conditioned extracellular matrix in human retinal pericytes. *Diabetes Metab Res Rev* 25, 647–56.
- Beneke, S., Bürkle, A., 2007. Poly(ADP-ribosyl)ation in mammalian ageing. *Nucleic Acids Res* 35, 7456–65.
- Bhattacharya, S., Dey, D., Roy, S.S., 2007. Molecular mechanism of insulin resistance. *J Biosci* 32, 405–13.
- Boden, G., 1997. Role of fatty acids in the pathogenesis of insulin resistance and NIDDM. *Diabetes* 46, 3–10.
- Bolanos, J., Almeida A., Moncada, S., 2010. Glycolysis: a bioenergetic or survival pathway? *Trends Biochem Sci* 35, 145-9
- Bonnefont-Rousselot, D., Bastard, J.P., Jaudon, M.C., Delattre, J., 2000. Consequences of the diabetic status on the oxidant/antioxidant balance. *Diabetes Metab* 26, 163–76.
- Bonora, E., Tuomilehto, J., 2011. The pros and cons of diagnosing diabetes with A1C. *Diabetes Care* 34 Suppl 2, S184–90.
- Borch-Johnsen, K., Colagiuri, S., 2009. Diagnosing diabetes--time for a change? *Diabetologia* 52, 2247–50.
- Boveris, A., Cadenas, E., Stoppani, A.O., 1976. Role of ubiquinone in the mitochondrial generation of hydrogen peroxide. *Biochem J* 156, 435–44.
- Brand, M.D., Affourtit, C., Esteves, T.C., Green, K., Lambert, A.J., Miwa, S., Pakay, J.L., Parker, N., 2004. Mitochondrial superoxide: production, biological effects, and activation of uncoupling proteins. *Free Radic Biol Med* 37, 755–67.
- Brewer, A.C., Murray, T.V.A., Arno, M., Zhang, M., Anilkumar, N.P., Mann, G.E., Shah, A.M., 2011. Nox4 regulates Nrf2 and glutathione redox in cardiomyocytes in vivo. *Free Radic Biol Med* 51, 205–15.
- Brownlee, M., 2001. Biochemistry and molecular cell biology of diabetic complications. *Nature* 414, 813–20.

- Brownlee, M., 2005. The pathobiology of diabetic complications: a unifying mechanism. *Diabetes* 54, 1615–25.
- Bürkle, A., 2005. Poly(ADP-ribose). The most elaborate metabolite of NAD⁺. *FEBS J* 272, 4576–89.
- Cameron, N.E., Gibson, T.M., Nangle, M.R., Cotter, M. a, 2005. Inhibitors of advanced glycation end product formation and neurovascular dysfunction in experimental diabetes. *Ann N Y Acad Sci* 1043, 784–92.
- Capes, S.E., Hunt, D., Malmberg, K., Gerstein, H.C., 2000. Stress hyperglycaemia and increased risk of death after myocardial infarction in patients with and without diabetes: a systematic overview. *Lancet* 355, 773–8.
- Cappai, G., Songini, M., Doria, A., Cavallerano, J.D., Lorenzi, M., 2011. Increased prevalence of proliferative retinopathy in patients with type 1 diabetes who are deficient in glucose-6-phosphate dehydrogenase. *Diabetologia* 54, 1539–42.
- Carette, C., Dubois-Laforgue, D., Gautier, J.-F., Timsit, J., 2011. Diabetes mellitus and glucose-6-phosphate dehydrogenase deficiency: from one crisis to another. *Diabetes Metab* 37, 79–82.
- Catherwood, M.A., Powell, L.A., Anderson, P., McMaster, D., Sharpe, P.C., Trimble, E.R., 2002. Glucose-induced oxidative stress in mesangial cells. *Kidney Int* 61, 599–608.
- Cecchini, G., 2003. Function and structure of complex II of the respiratory chain. *Annu Rev Biochem* 72, 77–109.
- Ceriello, A., Motz, E., 2004. Is oxidative stress the pathogenic mechanism underlying insulin resistance, diabetes, and cardiovascular disease? The common soil hypothesis revisited. *Arterioscler Thromb Vasc Biol* 24, 816–23.
- Ceriello, A., Quagliaro, L., D'Amico, M., Di Filippo, C., Marfella, R., Nappo, F., Berrino, L., Rossi, F., Giugliano, D., 2002. Acute hyperglycemia induces nitrotyrosine formation and apoptosis in perfused heart from rat. *Diabetes* 51, 1076–82.
- Chen, Q., Vazquez, E.J., Moghaddas, S., Hoppel, C.L., Lesnfsky, E.J., 2003. Production of reactive oxygen species by mitochondria: central role of complex III. *J Biol Chem* 278, 36027–31.
- Chen, Y.-R., Chen, C.-L., Zhang, L., Green-Church, K.B., Zweier, J.L., 2005. Superoxide generation from mitochondrial NADH dehydrogenase induces self-inactivation with specific protein radical formation. *J Biol Chem* 280, 37339–48.
- Chen, Z., Siu, B., Ho, Y.S., Vincent, R., Chua, C.C., Hamdy, R.C., Chua, B.H., 1998. Overexpression of MnSOD protects against myocardial ischemia/reperfusion injury in transgenic mice. *J Mol Cell Cardiol* 30, 2281–9.
- Cheng, Z., Tseng, Y., White, M.F., 2010. Insulin signaling meets mitochondria in metabolism. *Trends Endocrinol Metab* 21, 589–98.

- Colussi, C., Albertini, M.C., Coppola, S., Rovidati, S., Galli, F., Ghibelli, L., 2000. H₂O₂-induced block of glycolysis as an active ADP-ribosylation reaction protecting cells from apoptosis. *FASEB J* 14, 2266–76.
- Costford, S.R., Crawford, S.A., Dent, R., McPherson, R., Harper, M.-E., 2009. Increased susceptibility to oxidative damage in post-diabetic human myotubes. *Diabetologia* 52, 2405–2415.
- Daniels, M.C., Ciaraldi, T.P., Nikoulina, S., Henry, R.R., McClain, D.A., 1996. Glutamine:fructose-6-phosphate amidotransferase activity in cultured human skeletal muscle cells: relationship to glucose disposal rate in control and non-insulin-dependent diabetes mellitus subjects and regulation by glucose and insulin. *J Clin Invest* 97, 1235–41.
- Dankner, R., Chetrit, A., Shanik, M.H., Raz, I., Roth, J., 2009. Basal-state hyperinsulinemia in healthy normoglycemic adults is predictive of type 2 diabetes over a 24-year follow-up: a preliminary report. *Diabetes Care* 32, 1464–6.
- Davidoff, A.J., Davidson, M.B., Carmody, M.W., Davis, M.E., Ren, J., 2004. Diabetic cardiomyocyte dysfunction and myocyte insulin resistance: role of glucose-induced PKC activity. *Mol Cell Biol* 26, 155–63.
- Del Prato, S., Tiengo, A., 2001. The importance of first-phase insulin secretion: implications for the therapy of type 2 diabetes mellitus. *Diabetes Metab Res Rev* 17, 164–74.
- Derr, R., Garrett, E., Stacy, G.A., Saudek, C.D., 2003. Is HbA(1c) affected by glycemic instability? *Diabetes Care* 26, 2728–33.
- Derubertis, F.R., Craven, P.A., 1994. Activation of protein kinase C in glomerular cells in diabetes. Mechanisms and potential links to the pathogenesis of diabetic glomerulopathy. *Diabetes* 43, 1–8.
- Desco, M.-C., Asensi, M., Márquez, R., Martínez-Valls, J., Vento, M., Pallardó, F. V, Sastre, J., Viña, J., 2002. Xanthine oxidase is involved in free radical production in type 1 diabetes: protection by allopurinol. *Diabetes* 51, 1118–24.
- Dhar, A., Desai, K., Kazachmov, M., Yu, P., Wu, L., 2008. Methylglyoxal production in vascular smooth muscle cells from different metabolic precursors. *Metabolism* 57, 1211–20.
- Diefenbach, J., Bürkle, A., 2005. Introduction to poly(ADP-ribose) metabolism. *Cell Mol Life Sci* 62, 721–30.
- Dinneen, S., Gerich, J., Rizza, R., 1992. Carbohydrate metabolism in non-insulin-dependent diabetes mellitus. *N Engl J Med* 327, 707–13.
- Doi, T., Vlassara, H., Kirstein, M., Yamada, Y., Striker, G.E., Striker, L.J., 1992. Receptor-specific increase in extracellular matrix production in mouse mesangial cells by advanced glycosylation end products is mediated via platelet-derived growth factor. *Proc Natl Acad Sci U S A* 89, 2873–7.

- Dresner, A., Laurent, D., Marcucci, M., Griffin, M.E., Dufour, S., Cline, G.W., Slezak, L.A., Andersen, D.K., Hundal, R.S., Rothman, D.L., Petersen, K.F., Shulman, G.I., 1999. Effects of free fatty acids on glucose transport and IRS-1-associated phosphatidylinositol 3-kinase activity. *J Clin Invest* 103, 253–9.
- Du, X., Edelstein, D., Brownlee, M., 2008. Oral benfotiamine plus alpha-lipoic acid normalises complication-causing pathways in type 1 diabetes. *Diabetologia* 51, 1930–2.
- Du, X., Matsumura, T., Edelstein, D., Rossetti, L., Zsengellér, Z., Szabó, C., Brownlee, M., 2003. Inhibition of GAPDH activity by poly(ADP-ribose) polymerase activates three major pathways of hyperglycemic damage in endothelial cells. *J Clin Invest* 112, 1049–57.
- Du, X.L., Edelstein, D., Rossetti, L., Fantus, I.G., Goldberg, H., Ziyadeh, F., Wu, J., Brownlee, M., 2000. Hyperglycemia-induced mitochondrial superoxide overproduction activates the hexosamine pathway and induces plasminogen activator inhibitor-1 expression by increasing Sp1 glycosylation. *Proc Natl Acad Sci U S A* 97, 12222–6.
- Dunlop, M., 2000. Aldose reductase and the role of the polyol pathway in diabetic nephropathy. *Kidney Int Suppl* 77, S3–12.
- Edelstein, S.L., Knowler, W.C., Bain, R.P., Andres, R., Barret-Conner, E.L., Dowse, G.K., Haffner, S.M., Pettitt, D.J., Sorkin, J.D., Muller, D.C., Collins, V.R., Hamman, R.F. 1997. Predictors of progression of impaired glucose tolerance to NIDDM: an analysis of six prospective studies. *Diabetes* 46, 701-10.
- Eriksson, J.W., 2007. Metabolic stress in insulin's target cells leads to ROS accumulation - a hypothetical common pathway causing insulin resistance. *FEBS Lett* 581, 3734–42.
- Erlinger, T.P., Brancati, F.L., 2001. Postchallenge hyperglycemia in a national sample of U.S. adults with type 2 diabetes. *Diabetes Care* 24, 1734–8.
- Esakova, O.A., Meshalkina, L.E., Golbik, R., Hübner, G., Kochetov, G.A., 2004. Donor substrate regulation of transketolase. *Eur J Biochem* 271, 4189–94.
- Ferreira, F.M., Palmeira, C.M., Seiça, R., Moreno, A.J., Santos, M.S., 2003. Diabetes and mitochondrial bioenergetics: alterations with age. *J Biochem Mol Toxicol* 17, 214–22.
- Finkel, T., Holbrook, N.J., 2000. Oxidants, oxidative stress and the biology of ageing. *Nature* 408, 239–47.
- Fisher-Wellman, K.H., Neuffer, P.D., 2012. Linking mitochondrial bioenergetics to insulin resistance via redox biology. *Trends Endocrinol Metab* 23, 142–53.
- Fitzl, G., Welt, K., Wassilew, G., Clemens, N., Penka, K., Mücke, N., 2001. The influence of hypoxia on the myocardium of experimentally diabetic rats with and without protection by Ginkgo biloba extract. III: Ultrastructural investigations on mitochondria. *Exp Toxicol Pathol* 52, 557–68.
- Furukawa, S., Fujita, T., Shimabukuro, M., Iwaki, M., Yamada, Y., Nakajima, Y., Nakayama, O., Makishima, M., Matsuda, M., Shimomura, I., 2004. Increased oxidative stress in obesity and its impact on metabolic syndrome. *J Clin Invest* 114, 1752–61.

- Futamura, M., Yao, J., Li, X., Bergeron, R., Tran, J.-L., Zycband, E., Woods, J., Zhu, Y., Shao, Q., Maruki-Uchida, H., Goto-Shimazaki, H., Langdon, R.B., Erion, M.D., Eiki, J., Zhou, Y.-P., 2012. Chronic treatment with a glucokinase activator delays the onset of hyperglycaemia and preserves beta cell mass in the Zucker diabetic fatty rat. *Diabetologia* 55, 1071–80.
- Gao, D., Nong, S., Huang, X., Lu, Y., Zhao, H., Lin, Y., Man, Y., Wang, S., Yang, J., Li, J., 2010. The effects of palmitate on hepatic insulin resistance are mediated by NADPH Oxidase 3-derived reactive oxygen species through JNK and p38MAPK pathways. *J Biol Chem* 285, 29965–73.
- Garciarena, C.D., Caldiz, C.I., Correa, M. V, Schinella, G.R., Mosca, S.M., Chiappe de Cingolani, G.E., Cingolani, H.E., Ennis, I.L., 2008. Na⁺/H⁺ exchanger-1 inhibitors decrease myocardial superoxide production via direct mitochondrial action. *J Appl Physiol* 105, 1706–13.
- Genova, M.L., Ventura, B., Giuliano, G., Bovina, C., Formiggini, G., Parenti Castelli, G., Lenaz, G., 2001. The site of production of superoxide radical in mitochondrial Complex I is not a bound ubisemiquinone but presumably iron-sulfur cluster N2. *FEBS Lett* 505, 364–8.
- George, J., 2011. Should haemoglobin A 1c be used for the diagnosis of diabetes mellitus in South Africa? *J Endocrinol Metab Diabetes South Africa*.
- Gerich, J.E., 2002. Is reduced first-phase insulin release the earliest detectable abnormality in individuals destined to develop type 2 diabetes? *Diabetes* 51 Suppl 1, S117–21.
- Giacco, F., Brownlee, M., 2010. Oxidative stress and diabetic complications. *Circ Res* 107, 1058–70.
- Giardino, I., Edelstein, D., Brownlee, M., 1994. Nonenzymatic glycosylation in vitro and in bovine endothelial cells alters basic fibroblast growth factor activity. A model for intracellular glycosylation in diabetes. *J Clin Invest* 94, 110–7.
- Giardino, I., Edelstein, D., Brownlee, M., 1996. BCL-2 expression or antioxidants prevent hyperglycemia-induced formation of intracellular advanced glycation endproducts in bovine endothelial cells. *J Clin Invest* 97, 1422–8.
- Giugliano, D., Ceriello, A., Esposito, K. 2008. Glucose metabolism and hyperglycemia. *Am J Clin Nutr* 87, 217S-22S.
- González, R.G., Barnett, P., Cheng, H.M., Chylack, L.T., 1984. Altered phosphate metabolism in the intact rabbit lens under high glucose conditions and its prevention by an aldose reductase inhibitor. *Exp Eye Res* 39, 553–62.
- Griffin, M.E., Marcucci, M.J., Cline, G.W., Bell, K., Barucci, N., Lee, D., Goodyear, L.J., Kraegen, E.W., White, M.F., Shulman, G.I., 1999. Free fatty acid-induced insulin resistance is associated with activation of protein kinase C theta and alterations in the insulin signaling cascade. *Diabetes* 48, 1270–4.
- Grimsrud, P.A., Picklo, M.J., Griffin, T.J., Bernlohr, D.A., 2007. Carbonylation of adipose proteins in obesity and insulin resistance: identification of adipocyte fatty acid-binding protein as a cellular target of 4-hydroxynonenal. *Mol Cell Proteomics* 6, 624–37.

- Grivennikova, V.G., Vinogradov, A.D., 2006. Generation of superoxide by the mitochondrial Complex I. *Biochim Biophys Acta* 1757, 553–61.
- Gupte, R.S., Floyd, B.C., Kozicky, M., George, S., Ungvari, Z.I., Neito, V., Wolin, M.S., Gupte, S.A., 2009. Synergistic activation of glucose-6-phosphate dehydrogenase and NAD(P)H oxidase by Src kinase elevates superoxide in type 2 diabetic, Zucker fa/fa, rat liver. *Free Radic Biol Med* 47, 219–28.
- Gupte, R.S., Vijay, V., Marks, B., Levine, R.J., Sabbah, H.N., Wolin, M.S., Recchia, F.A., Gupte, S.A., 2007. Upregulation of glucose-6-phosphate dehydrogenase and NAD(P)H oxidase activity increases oxidative stress in failing human heart. *J Card Fail* 13, 497–506.
- Gupte, S.A., Levine, R.J., Gupte, R.S., Young, M.E., Lionetti, V., Labinskyy, V., Floyd, B.C., Ojaimi, C., Bellomo, M., Wolin, M.S., Recchia, F.A., 2006. Glucose-6-phosphate dehydrogenase-derived NADPH fuels superoxide production in the failing heart. *J Mol Cell Cardiol* 41, 340–9.
- Guzik, T.J., Mussa, S., Gastaldi, D., Sadowski, J., Ratnatunga, C., Pillai, R., Channon, K.M., 2002. Mechanisms of increased vascular superoxide production in human diabetes mellitus: role of NAD(P)H oxidase and endothelial nitric oxide synthase. *Circulation* 105, 1656–62.
- Hardie, D.G., Scott, J.W., Pan, D.A., Hudson, E.R., 2003. Management of cellular energy by the AMP-activated protein kinase system. *FEBS Lett* 546, 113–20.
- Hartog, J.W.L., Voors, A.A., Bakker, S.J.L., Smit, A.J., van Veldhuisen, D.J., 2007. Advanced glycation end-products (AGEs) and heart failure: pathophysiology and clinical implications. *Eur J Heart Fail* 9, 1146–55.
- Haupt, E., Ledermann, H., Köpcke, W., 2005. Benfotiamine in the treatment of diabetic polyneuropathy--a three-week randomized, controlled pilot study (BEDIP study). *Int J Clin Pharmacol Ther* 43, 71–7.
- Havivi, E., Bar On, H., Reshef, A., Stein, P., Raz, I., 1991. Vitamins and trace metals status in non insulin dependent diabetes mellitus. *Int J Vitam Nutr Res* 61, 328–33.
- Herrero, A., Barja, G., 1997. Sites and mechanisms responsible for the low rate of free radical production of heart mitochondria in the long-lived pigeon. *Mech Ageing Dev* 98, 95–111.
- Hirst, J., 2005. Energy transduction by respiratory complex I--an evaluation of current knowledge. *Biochem Soc Trans* 33, 525–9.
- Holness, M.J., Sugden, M.C., 2003. Regulation of pyruvate dehydrogenase complex activity by reversible phosphorylation. *Biochem Soc Trans* 31, 1143–51.
- Horecker, B.L., 2002. The pentose phosphate pathway. *J Biol Chem* 277, 47965–71.
- Hotamisligil, G.S., Shargill, N.S., Spiegelman, B.M., 1993. Adipose expression of tumor necrosis factor- α : direct role in obesity-linked insulin resistance. *Science* 259, 87–91.

- Hu, J., Klein, J.D., Du, J., Wang, X.H., 2008. Cardiac muscle protein catabolism in diabetes mellitus: activation of the ubiquitin-proteasome system by insulin deficiency. *Endocrinology* 149, 5384–90.
- Itani, S.I., Saha, A.K., Kurowski, T.G., Coffin, H.R., Tornheim, K., Ruderman, N.B., 2003. Glucose autoregulates its uptake in skeletal muscle: involvement of AMP-activated protein kinase. *Diabetes* 52, 1635–40.
- Jacobsen, S.E., Binkowski, K.A., Olszewski, N.E., 1996. SPINDLY, a tetratricopeptide repeat protein involved in gibberellin signal transduction in Arabidopsis. *Proc Natl Acad Sci U S A* 93, 9292–6.
- Jain, M., Cui, L., Brenner, D. a, Wang, B., Handy, D.E., Leopold, J. a, Loscalzo, J., Apstein, C.S., Liao, R., 2004. Increased myocardial dysfunction after ischemia-reperfusion in mice lacking glucose-6-phosphate dehydrogenase. *Circulation* 109, 898–903.
- Jurczak, M.J., Lee, H.-Y., Birkenfeld, A.L., Jornayvaz, F.R., Frederick, D.W., Pongratz, R.L., Zhao, X., Moeckel, G.W., Samuel, V.T., Whaley, J.M., Shulman, G.I., Kibbey, R.G., 2011. SGLT2 deletion improves glucose homeostasis and preserves pancreatic beta-cell function. *Diabetes* 60, 890–8.
- Kanwar, M., Chan, P.-S., Kern, T.S., Kowluru, R.A., 2007. Oxidative damage in the retinal mitochondria of diabetic mice: possible protection by superoxide dismutase. *Invest Ophthalmol Vis Sci* 48, 3805–11.
- Karpe, F., Dickmann, J.R., Frayn, K.N., 2011. Fatty acids, obesity, and insulin resistance: time for a reevaluation. *Diabetes* 60, 2441–9.
- Katare, R., Caporali, A., Emanuelli, C., Madeddu, P., 2010a. Benfotiamine improves functional recovery of the infarcted heart via activation of pro-survival G6PD/Akt signaling pathway and modulation of neurohormonal response. *J Mol Cell Cardiol* 49, 625–38.
- Katare, R., Caporali, A., Oikawa, A., Meloni, M., Emanuelli, C., Madeddu, P., 2010b. Vitamin B1 analog benfotiamine prevents diabetes-induced diastolic dysfunction and heart failure through Akt/Pim-1-mediated survival pathway. *Circ Hear Fail* 3, 294–305.
- Kelley, D.E., Mokan, M., Simoneau, J.A., Mandarino, L.J., 1993. Interaction between glucose and free fatty acid metabolism in human skeletal muscle. *J Clin Invest* 92, 91–8.
- Khullar, M., Al-Shudiefat, A.A.-R.S., Ludke, A., Binopal, G., Singal, P.K., 2010. Oxidative stress: a key contributor to diabetic cardiomyopathy. *Can J Physiol Pharmacol* 88, 233–40.
- Kim, J.K., Kim, Y.J., Fillmore, J.J., Chen, Y., Moore, I., Lee, J., Yuan, M., Li, Z.W., Karin, M., Perret, P., Shoelson, S.E., Shulman, G.I., 2001. Prevention of fat-induced insulin resistance by salicylate. *J Clin Invest* 108, 437–46.
- King, G.L., Brownlee, M., 1996. The cellular and molecular mechanisms of diabetic complications. *Endocrinol Metab Clin North Am* 25, 255–70.
- King, G.L., Loeken, M.R., 2004. Hyperglycemia-induced oxidative stress in diabetic complications. *Histochem Cell Biol* 122, 333–8.

- Kirstein, M., Aston, C., Hintz, R., Vlassara, H., 1992. Receptor-specific induction of insulin-like growth factor I in human monocytes by advanced glycosylation end product-modified proteins. *J Clin Invest* 90, 439–46.
- Korshunov, S.S., Skulachev, V.P., Starkov, A.A., 1997. High protonic potential actuates a mechanism of production of reactive oxygen species in mitochondria. *FEBS Lett* 416, 15–8.
- Kowluru, R.A., Atasi, L., Ho, Y.-S., 2006. Role of mitochondrial superoxide dismutase in the development of diabetic retinopathy. *Invest Ophthalmol Vis Sci* 47, 1594–9.
- Koya, D., Jirousek, M.R., Lin, Y.W., Ishii, H., Kuboki, K., King, G.L., 1997. Characterization of protein kinase C beta isoform activation on the gene expression of transforming growth factor-beta, extracellular matrix components, and prostanoids in the glomeruli of diabetic rats. *J Clin Invest* 100, 115–26.
- Koya, D., King, G.L., 1998. Protein kinase C activation and the development of diabetic complications. *Diabetes* 47, 859–66.
- Kraegen, E.W., Sowden, J.A., Halstead, M.B., Clark, P.W., Rodnick, K.J., Chisholm, D.J., James, D.E., 1993. Glucose transporters and in vivo glucose uptake in skeletal and cardiac muscle: fasting, insulin stimulation and immunoisolation studies of GLUT1 and GLUT4. *Biochem J* 295 (Pt 1, 287–93.
- Kudin, A.P., Bimpong-Buta, N.Y.-B., Vielhaber, S., Elger, C.E., Kunz, W.S., 2004. Characterization of superoxide-producing sites in isolated brain mitochondria. *J Biol Chem* 279, 4127–35.
- Kushnareva, Y., Murphy, A.N., Andreyev, A., 2002. Complex I-mediated reactive oxygen species generation: modulation by cytochrome c and NAD(P)⁺ oxidation-reduction state. *Biochem J* 368, 545–53.
- Lambert, A.J., Brand, M.D., 2004. Inhibitors of the quinone-binding site allow rapid superoxide production from mitochondrial NADH:ubiquinone oxidoreductase (complex I). *J Biol Chem* 279, 39414–20.
- Lazzeri, C., Tarquini, R., Giunta, F., Gensini, G.F., 2009. Glucose dysmetabolism and prognosis in critical illness. *Intern Emerg Med* 4, 147–56.
- Lebovitz, H.E., 2011. Insulin: potential negative consequences of early routine use in patients with type 2 diabetes. *Diabetes Care* 34 Suppl 2, S225–30.
- Lee, A.Y., Chung, S.S., 1999. Contributions of polyol pathway to oxidative stress in diabetic cataract. *FASEB J* 13, 23–30.
- Leonard, B.L., Watson, R.N., Loomes, K.M., Phillips, a R.J., Cooper, G.J., 2005. Insulin resistance in the Zucker diabetic fatty rat: a metabolic characterisation of obese and lean phenotypes. *Acta Diabetol* 42, 162–70.
- Li, J., Stouffs, M., Serrander, L., Banfi, B., Bettiol, E., Charnay, Y., Steger, K., Krause, K., Jaconi, M.E., 2006. The NADPH oxidase NOX4 drives cardiac differentiation: role in regulating cardiac transcription factors and MAP kinase activation. *Mol Biol Cell* 17, 3978–3988.

- Li, Y.M., Mitsuhashi, T., Wojciechowicz, D., Shimizu, N., Li, J., Stitt, A., He, C., Banerjee, D., Vlassara, H., 1996. Molecular identity and cellular distribution of advanced glycation endproduct receptors: relationship of p60 to OST-48 and p90 to 80K-H membrane proteins. *Proc Natl Acad Sci U S A* 93, 11047–52.
- Lindsay, D.G., 1999. Diet and ageing: the possible relation to reactive oxygen species. *J Nutr Health Aging* 3, 84–91.
- Lonsdale, D., 2006. A review of the biochemistry, metabolism and clinical benefits of thiamin(e) and its derivatives. *Evid Based Complement Alternat Med* 3, 49–59.
- Mahler, R.J., Adler, M.L., 1999. Clinical review 102: Type 2 diabetes mellitus: update on diagnosis, pathophysiology, and treatment. *J Clin Endocrinol Metab* 84, 1165–71.
- Malkani, S., DeSilva, T., 2012. Controversies on how diabetes is diagnosed. *Curr Opin Endocrinol Diabetes Obes* 19, 97–103.
- Mapanga, R.F., Joseph, D., Symington, B., Garson, K.-L., Kimar, C., Kelly-Laubscher, R., Essop, M.F., 2013. Detrimental effects of acute hyperglycaemia on the rat heart. *Acta Physiol (Oxf)* (In press).
- Mapanga, R.F., Rajamani, U., Dlamini, N., Zungu-Edmondson, M., Kelly-Laubscher, R., Shafiullah, M., Wahab, A., Hasan, M.Y., Fahim, M. a, Rondeau, P., Bourdon, E., Essop, M.F., 2012. Oleanolic acid: a novel cardioprotective agent that blunts hyperglycemia-induced contractile dysfunction. *PLoS One* 7, e47322.
- Marchetti, V., Menghini, R., Rizza, S., Vivanti, A., Feccia, T., Lauro, D., Fukamizu, A., Lauro, R., Federici, M., 2006. Benfotiamine counteracts glucose toxicity effects on endothelial progenitor cell differentiation via Akt/FoxO signaling. *Diabetes* 55, 2231–7.
- Marshall, S., Bacote, V., Traxinger, R.R., 1991. Discovery of a metabolic pathway mediating glucose-induced desensitization of the glucose transport system. Role of hexosamine biosynthesis in the induction of insulin resistance. *J Biol Chem* 266, 4706–12.
- McCarthy, A.D., Etcheverry, S.B., Cortizo, A.M., 2001. Effect of advanced glycation endproducts on the secretion of insulin-like growth factor-I and its binding proteins: role in osteoblast development. *Acta Diabetol* 38, 113–22.
- McClain, D.A., n.d. Hexosamines as mediators of nutrient sensing and regulation in diabetes. *J Diabetes Complications* 16, 72–80.
- McCord, J.M., Edeas, M.A., 2005. SOD, oxidative stress and human pathologies: a brief history and a future vision. *Biomed Pharmacother* 59, 139–42.
- McDaniel, M.L., Marshall, C.A., Pappan, K.L., Kwon, G., 2002. Metabolic and autocrine regulation of the mammalian target of rapamycin by pancreatic beta-cells. *Diabetes* 51, 2877–85.
- McLellan, A.C., Thornalley, P.J., Benn, J., Sonksen, P.H., 1994. Glyoxalase system in clinical diabetes mellitus and correlation with diabetic complications. *Clin Sci (Lond)* 87, 21–9.

- Messner, D.J., Rhiu, B.H., Kowdley, K. V, 2013. Iron overload causes oxidative stress and impaired insulin signaling in AML-12 hepatocytes. *Dig Dis Sci* 58, 1899–908.
- Meyer, C., Stumvoll, M., Nadkarni, V., Dostou, J., Mitrakou, A., Gerich, J., 1998. Abnormal renal and hepatic glucose metabolism in type 2 diabetes mellitus. *J Clin Invest* 102, 619–24.
- Mitrakou, A., Kelley, D., Mookan, M., Veneman, T., Pangburn, T., Reilly, J., Gerich, J., 1992. Role of reduced suppression of glucose production and diminished early insulin release in impaired glucose tolerance. *N Engl J Med* 326, 22–9.
- Mohamed, A.K., Bierhaus, A., Schiekofer, S., Tritschler, H., Ziegler, R., Nawroth, P.P., 1999. The role of oxidative stress and NF-kappaB activation in late diabetic complications. *Biofactors* 10, 157–67.
- Morino, K., Petersen, K.F., Dufour, S., Befroy, D., Frattini, J., Shatzkes, N., Neschen, S., White, M.F., Bilz, S., Sono, S., Pypaert, M., Shulman, G.I., 2005. Reduced mitochondrial density and increased IRS-1 serine phosphorylation in muscle of insulin-resistant offspring of type 2 diabetic parents. *J Clin Invest* 115, 3587–93.
- Nathan, D.M., Davidson, M.B., DeFronzo, R.A., Heine, R.J., Henry, R.R., Pratley, R., Zinman, B., 2007. Impaired fasting glucose and impaired glucose tolerance: implications for care. *Diabetes Care* 30, 753–9.
- Neeper, M., Schmidt, A.M., Brett, J., Yan, S.D., Wang, F., Pan, Y.C., Elliston, K., Stern, D., Shaw, A., 1992. Cloning and expression of a cell surface receptor for advanced glycosylation end products of proteins. *J Biol Chem* 267, 14998–5004.
- Nishikawa, T., Edelstein, D., Du, X.L., Yamagishi, S., Matsumura, T., Kaneda, Y., Yorek, M.A., Beebe, D., Oates, P.J., Hammes, H.P., Giardino, I., Brownlee, M., 2000. Normalizing mitochondrial superoxide production blocks three pathways of hyperglycaemic damage. *Nature* 404, 787–90.
- Norhammar, A., Tenerz, Å., Nilsson, G., Hamsten, A., Efendíc, S., Rydén, L., Malmberg, K., Tenerz, A., 2002. Glucose metabolism in patients with acute myocardial infarction and no previous diagnosis of diabetes mellitus: a prospective study. *Lancet* 359, 2140–4.
- Nourooz-Zadeh, J., Rahimi, A., Tajaddini-Sarmadi, J., Tritschler, H., Rosen, P., Halliwell, B., Betteridge, D.J., 1997. Relationships between plasma measures of oxidative stress and metabolic control in NIDDM. *Diabetologia* 40, 647–53.
- Ogihara, T., Asano, T., Ando, K., Chiba, Y., Sakoda, H., Anai, M., Shojima, N., Ono, H., Onishi, Y., Fujishiro, M., Katagiri, H., Fukushima, Y., Kikuchi, M., Noguchi, N., Aburatani, H., Komuro, I., Fujita, T., 2002. Angiotensin II-induced insulin resistance is associated with enhanced insulin signaling. *Hypertension* 40, 872–9.
- Ohnishi, T., Johnson, J.E., Yano, T., Lobrutto, R., Widger, W.R., 2005. Thermodynamic and EPR studies of slowly relaxing ubisemiquinone species in the isolated bovine heart complex I. *FEBS Lett* 579, 500–6.
- Oswald, G.A., Smith, C.C., Betteridge, D.J., Yudkin, J.S., 1986. Determinants and importance of stress hyperglycaemia in non-diabetic patients with myocardial infarction. *Br Med J (Clin Res Ed)* 293, 917–22.

- Paolisso, G., D'Amore, A., Galzerano, D., Balbi, V., Giugliano, D., Varricchio, M., D'Onofrio, F., 1993. Daily vitamin E supplements improve metabolic control but not insulin secretion in elderly type II diabetic patients. *Diabetes Care* 16, 1433–7.
- Paradies, G., Petrosillo, G., Pistolese, M., Ruggiero, F.M., 2001. Reactive oxygen species generated by the mitochondrial respiratory chain affect the complex III activity via cardiolipin peroxidation in beef-heart submitochondrial particles. *Mitochondrion* 1, 151–9.
- Park, K., Saudek, C.D., Hart, G.W., 2010. Increased expression of beta-N-acetylglucosaminidase in erythrocytes from individuals with pre-diabetes and diabetes. *Diabetes* 59, 1845–50.
- Park, S.S.Y., Ryu, J., Lee, W., 2005. O-GlcNAc modification on IRS-1 and Akt2 by PUGNAc inhibits their phosphorylation and induces insulin resistance in rat primary adipocytes. *Exp Mol Med* 37, 220–9.
- Parsons, M.W., Barber, P.A., Desmond, P.M., Baird, T. a, Darby, D.G., Byrnes, G., Tress, B.M., Davis, S.M., 2002. Acute hyperglycemia adversely affects stroke outcome: a magnetic resonance imaging and spectroscopy study. *Ann Neurol* 52, 20–8.
- Petersen, K.F., Shulman, G.I., 2006. Etiology of insulin resistance. *Am J Med* 119, 10S–16S.
- Pomero, F., Molinar Min, A., La Selva, M., Allione, A., Molinatti, G.M., Porta, M., 2001. Benfotiamine is similar to thiamine in correcting endothelial cell defects induced by high glucose. *Acta Diabetol* 38, 135–8.
- Poornima, I.G., Parikh, P., Shannon, R.P., 2006. Diabetic cardiomyopathy: the search for a unifying hypothesis. *Circ Res* 98, 596–605.
- Qiao, Q., Jousilahti, P., Eriksson, J., Tuomilehto, J., 2003. Predictive properties of impaired glucose tolerance for cardiovascular risk are not explained by the development of overt diabetes during follow-up. *Diabetes Care* 26, 2910–4.
- Quagliaro, L., Piconi, L., Assaloni, R., Martinelli, L., Motz, E., Ceriello, A., 2003. Intermittent high glucose enhances apoptosis related to oxidative stress in human umbilical vein endothelial cells: the role of protein kinase C and NAD(P)H-oxidase activation. *Diabetes* 52, 2795–804.
- Rabøl, R., 2011. Mitochondrial function in skeletal muscle in type 2 diabetes. *Dan Med Bull* 58, B4272.
- Radi, R., Cassina, A., Hodara, R., Quijano, C., Castro, L., 2002. Peroxynitrite reactions and formation in mitochondria. *Free Radic Biol Med* 33, 1451–64.
- Ragheb, R., Shanab, G.M.L., Medhat, A.M., Seoudi, D.M., Adeli, K., Fantus, I.G., 2009. Free fatty acid-induced muscle insulin resistance and glucose uptake dysfunction: evidence for PKC activation and oxidative stress-activated signaling pathways. *Biochem Biophys Res Commun* 389, 211–6.
- Randle, P.J., Garland, P.B., Hales, C.N., Newsholme, E.A., 1963. The glucose fatty-acid cycle. Its role in insulin sensitivity and the metabolic disturbances of diabetes mellitus. *Lancet* 1, 785–9.

- Ravussin, E., 2002. Cellular sensors of feast and famine. *J Clin Invest* 109, 1537–40.
- Ren, J., Duan, J., Hintz, K.K., Ren, B.H., 2003. High glucose induces cardiac insulin-like growth factor I resistance in ventricular myocytes: role of Akt and ERK activation. *Cardiovasc Res* 57, 738–48.
- Ren, J., Gintant, G.A., Miller, R.E., Davidoff, A.J., Mellor, K.M., Wendt, I.R., Ritchie, R.H., Delbridge, L.M.D., Lima, V. V, Giachini, F.R., Hardy, D.M., Webb, R.C., Tostes, R.C., Physiol, A.J., Integr, R., Physiol, C., Tang, W.H., Cheng, W.T., Kravtsov, G.M., Tong, X.Y., Hou, X.Y., Chung, K., Sum, S., Chung, M., Laczy, B., Hill, B.G., Wang, K., Paterson, A.J., White, C.R., Xing, D., Chen, Y., Darley-usmar, V., Oparil, S., Chatham, J.C., Suarez, J., Hu, Y., Makino, A., Fricovsky, E., Wang, H., Wolfgang, H., Ren, J.U.N., Davidoff, A.M.Y.J., 2013. High extracellular glucose impairs cardiac E-C coupling in a glycosylation-dependent manner High extracellular glucose impairs cardiac E-C coupling in a glycosylation-dependent manner.
- Riganti, C., Gazzano, E., Polimeni, M., Aldieri, E., Ghigo, D., 2012. The pentose phosphate pathway: an antioxidant defense and a crossroad in tumor cell fate. *Free Radic Biol Med* 53, 421–36.
- Roden, M., Price, T.B., Perseghin, G., Petersen, K.F., Rothman, D.L., Cline, G.W., Shulman, G.I., 1996. Mechanism of free fatty acid-induced insulin resistance in humans. *J Clin Invest* 97, 2859–65.
- Rosca, M.G., Mustata, T.G., Kinter, M.T., Ozdemir, A.M., Kern, T.S., Szweda, L.I., Brownlee, M., Monnier, V.M., Weiss, M.F., 2005. Glycation of mitochondrial proteins from diabetic rat kidney is associated with excess superoxide formation. *Am J Physiol Renal Physiol* 289, F420–30.
- Rösen, P., Du, X., Tschöpe, D., 1998. Role of oxygen derived radicals for vascular dysfunction in the diabetic heart: prevention by alpha-tocopherol? *Mol Cell Biochem* 188, 103–11.
- Rösen, P., Nawroth, P.P., King, G., Möller, W., Tritschler, H.J., Packer, L., 2001. The role of oxidative stress in the onset and progression of diabetes and its complications: a summary of a Congress Series sponsored by UNESCO-MCBN, the American Diabetes Association and the German Diabetes Society. *Diabetes Metab Res Rev* 17, 189–212.
- Rossetti, L., 2000. Perspective: Hexosamines and nutrient sensing. *Endocrinology* 141, 1922–5.
- Ruskovska, T., Bernlohr, D.A., 2013. Oxidative stress and protein carbonylation in adipose tissue - Implications for insulin resistance and diabetes mellitus. *J Proteomics* 1820, 1–9.
- Saini, V., 2010. Molecular mechanisms of insulin resistance in type 2 diabetes mellitus. *World J Diabetes* 1, 68–75.
- Saltiel, A.R., 2001. New perspectives into the molecular pathogenesis and treatment of type 2 diabetes. *Cell* 104, 517–29.
- Santos, C.X.C., Anilkumar, N., Zhang, M., Brewer, A.C., Shah, A.M., 2011. Redox signaling in cardiac myocytes. *Free Radic Biol Med* 50, 777–93.

- Saudek, C.D., Derr, R.L., Kalyani, R.R., 2006. Assessing glycemia in diabetes using self-monitoring blood glucose and hemoglobin A1c. *JAMA* 295, 1688–97.
- Saudek, C.D., Herman, W.H., Sacks, D.B., Bergenstal, R.M., Edelman, D., Davidson, M.B., 2008. A new look at screening and diagnosing diabetes mellitus. *J Clin Endocrinol Metab* 93, 2447–53.
- Savage, D.B., Petersen, K.F., Shulman, G.I., 2007. Disordered lipid metabolism and the pathogenesis of insulin resistance. *Physiol Rev* 87, 507–20.
- Schaffer, S.W., Jong, C.J., Mozaffari, M., 2012. Role of oxidative stress in diabetes-mediated vascular dysfunction: unifying hypothesis of diabetes revisited. *Vasc Pharmacol* 57, 139–49.
- Schmidt, A.M., Hori, O., Chen, J.X., Li, J.F., Crandall, J., Zhang, J., Cao, R., Yan, S.D., Brett, J., Stern, D., 1995. Advanced glycation endproducts interacting with their endothelial receptor induce expression of vascular cell adhesion molecule-1 (VCAM-1) in cultured human endothelial cells and in mice. A potential mechanism for the accelerated vasculopathy of diabetes. *J Clin Invest* 96, 1395–403.
- Schwaiger, M., Neese, R.A., Araujo, L., Wyns, W., Wisneski, J.A., Sochor, H., Swank, S., Kulber, D., Selin, C., Phelps, M., 1989. Sustained nonoxidative glucose utilization and depletion of glycogen in reperfused canine myocardium. *J Am Coll Cardiol* 13, 745–54.
- Schwartzbauer, G., Robbins, J., 2001. The tumor suppressor gene PTEN can regulate cardiac hypertrophy and survival. *J Biol Chem* 276, 35786–93.
- Selvin, E., Crainiceanu, C.M., Brancati, F.L., Coresh, J., 2007. Short-term variability in measures of glycemia and implications for the classification of diabetes. *Arch Intern Med* 167, 1545–51.
- Serpillon, S., Floyd, B.C., Gupte, R.S., George, S., Kozicky, M., Neito, V., Recchia, F., Stanley, W., Wolin, M.S., Gupte, S.A., 2009. Superoxide production by NAD(P)H oxidase and mitochondria is increased in genetically obese and hyperglycemic rat heart and aorta before the development of cardiac dysfunction. The role of glucose-6-phosphate dehydrogenase-derived NADPH. *Am J Physiol Hear Circ Physiol* 297, H153–62.
- Shanik, M.H., Xu, Y., Skrha, J., Dankner, R., Zick, Y., Roth, J., 2008. Insulin resistance and hyperinsulinemia: is hyperinsulinemia the cart or the horse? *Diabetes Care* 31 Suppl 2, S262–8.
- Sheetz, M.J., King, G.L., 2002. Molecular understanding of hyperglycemia's adverse effects for diabetic complications. *JAMA* 288, 2579–88.
- Shen, X., Zheng, S., Thongboonkerd, V., Xu, M., Pierce, W.M., Klein, J.B., Epstein, P.N., 2004. Cardiac mitochondrial damage and biogenesis in a chronic model of type 1 diabetes. *Am J Physiol Endocrinol Metab* 287, E896–905.
- Shinohara, M., Thornalley, P.J., Giardino, I., Beisswenger, P., Thorpe, S.R., Onorato, J., Brownlee, M., 1998. Overexpression of glyoxalase-I in bovine endothelial cells inhibits intracellular advanced glycation endproduct formation and prevents hyperglycemia-induced increases in macromolecular endocytosis. *J Clin Invest* 101, 1142–7.

- Shulman, G.I., 2000. On diabetes: insulin resistance Cellular mechanisms of insulin resistance. *J Clin Invest* 106, 171–176.
- Sicree, R.A., Zimmet, P.Z., King, H.O., Coventry, J.S., 1987. Plasma insulin response among Nauruans. Prediction of deterioration in glucose tolerance over 6 yr. *Diabetes* 36, 179–86.
- Skolnik, E.Y., Yang, Z., Makita, Z., Radoff, S., Kirstein, M., Vlassara, H., 1991. Human and rat mesangial cell receptors for glucose-modified proteins: potential role in kidney tissue remodelling and diabetic nephropathy. *J Exp Med* 174, 931–9.
- Skulachev, V.P., 1996. Role of uncoupled and non-coupled oxidations in maintenance of safely low levels of oxygen and its one-electron reductants. *Q Rev Biophys* 29, 169–202.
- Skulachev, V.P., 1999. Anion carriers in fatty acid-mediated physiological uncoupling. *J Bioenerg Biomembr* 31, 431–45.
- Sloniger, J.A., Saengsirisuwan, V., Diehl, C.J., Dokken, B.B., Lailerd, N., Lemieux, A.M., Kim, J.S., Henriksen, E.J., 2005. Defective insulin signaling in skeletal muscle of the hypertensive TG(mREN2)27 rat. *Am J Physiol Endocrinol Metab* 288, E1074–81.
- Smedsrød, B., Melkko, J., Araki, N., Sano, H., Horiuchi, S., 1997. Advanced glycation end products are eliminated by scavenger-receptor-mediated endocytosis in hepatic sinusoidal Kupffer and endothelial cells. *Biochem J* 322 (Pt 2, 567–73.
- Stolk, R.P., Pols, H.A., Lamberts, S.W., de Jong, P.T., Hofman, A., Grobbee, D.E., 1997. Diabetes mellitus, impaired glucose tolerance, and hyperinsulinemia in an elderly population. The Rotterdam Study. *Am J Epidemiol* 145, 24–32.
- St-Pierre, J., Buckingham, J.A., Roebuck, S.J., Brand, M.D., 2002. Topology of superoxide production from different sites in the mitochondrial electron transport chain. *J Biol Chem* 277, 44784–90.
- Stracke, H., Lindemann, A., Federlin, K., 1996. A benfotiamine-vitamin B combination in treatment of diabetic polyneuropathy. *Exp Clin Endocrinol Diabetes* 104, 311–6.
- Stumvoll, M., Goldstein, B.J., van Haften, T.W., 2005. Type 2 diabetes: principles of pathogenesis and therapy. *Lancet* 365, 1333–46.
- Sudnikovich, E.J., Maksimchik, Y.Z., Zbrodskaya, S. V, Kubyshin, V.L., Lapshina, E.A., Bryszewska, M., Reiter, R.J., Zavodnik, I.B., 2007. Melatonin attenuates metabolic disorders due to streptozotocin-induced diabetes in rats. *Eur J Pharmacol* 569, 180–7.
- Szaleczky, E., Prechl, J., Fehér, J., Somogyi, A., 1999. Alterations in enzymatic antioxidant defence in diabetes mellitus—a rational approach. *Postgrad Med J* 75, 13–7.
- Tang, J., Neidigh, J.L., Cooksey, R.C., McClain, D.A., 2000. Transgenic mice with increased hexosamine flux specifically targeted to beta-cells exhibit hyperinsulinemia and peripheral insulin resistance. *Diabetes* 49, 1492–9.

- Travis, S.F., Morrison, A.D., Clements, R.S., Winegrad, A.I., Oski, F.A., 1971. Metabolic alterations in the human erythrocyte produced by increases in glucose concentration. The role of the polyol pathway. *J Clin Invest* 50, 2104–12.
- Tuomilehto, J., Lindstrom, J., Eriksson, J.G., Valle, T.T., Hamalainen, H., Ilanne-Parikka, P., Keinanen-Kiukaanniemi, S., Laakso, M., *et al.* 2001. Prevention of type 2 diabetes mellitus by changes in lifestyle among subjects with impaired glucose tolerance. *N Engl J Med* 344, 1343-50.
- Vlassara, H., 1997. Recent progress in advanced glycation end products and diabetic complications. *Diabetes* 46 Suppl 2, S19–25.
- Vlassara, H., Brownlee, M., Manogue, K.R., Dinarello, C.A., Pasagian, A., 1988. Cachectin/TNF and IL-1 induced by glucose-modified proteins: role in normal tissue remodeling. *Science* 240, 1546–8.
- Vlassara, H., Li, Y.M., Imani, F., Wojciechowicz, D., Yang, Z., Liu, F.T., Cerami, A., 1995. Identification of galectin-3 as a high-affinity binding protein for advanced glycation end products (AGE): a new member of the AGE-receptor complex. *Mol Med* 1, 634–46.
- Vosseller, K., Wells, L., Lane, M.D., Hart, G.W., 2002. Elevated nucleocytoplasmic glycosylation by O-GlcNAc results in insulin resistance associated with defects in Akt activation in 3T3-L1 adipocytes. *Proc Natl Acad Sci U S A* 99, 5313–8.
- Wamelink, M.M.C., Struys, E. a, Jakobs, C., 2008. The biochemistry, metabolism and inherited defects of the pentose phosphate pathway: a review. *J Inherit Metab Dis* 31, 703–17.
- Wang, Z., Park, K., Comer, F., Hsieh-Wilson, L.C., Saudek, C.D., Hart, G.W., 2009. Site-specific GlcNAcylation of human erythrocyte proteins: potential biomarker(s) for diabetes. *Diabetes* 58, 309–17.
- Warram, J.H., Martin, B.C., Krolewski, A.S., Soeldner, J.S., Kahn, C.R., 1990. Slow glucose removal rate and hyperinsulinemia precede the development of type II diabetes in the offspring of diabetic parents. *Ann Intern Med* 113, 909–15.
- Wei, Y., Sowers, J.R., Nistala, R., Gong, H., Uptergrove, G.M.-E., Clark, S.E., Morris, E.M., Szary, N., Manrique, C., Stump, C.S., 2006. Angiotensin II-induced NADPH oxidase activation impairs insulin signaling in skeletal muscle cells. *J Biol Chem* 281, 35137–46.
- Weyer, C., Hanson, R.L., Tataranni, P.A., Bogardus, C., Pratley, R.E., 2000. A high fasting plasma insulin concentration predicts type 2 diabetes independent of insulin resistance: evidence for a pathogenic role of relative hyperinsulinemia. *Diabetes* 49, 2094–101.
- Williams, S.B., Goldfine, A.B., Timimi, F.K., Ting, H.H., Roddy, M.A., Simonson, D.C., Creager, M.A., 1998. Acute hyperglycemia attenuates endothelium-dependent vasodilation in humans in vivo. *Circulation* 97, 1695–701.
- Wisneski, J.A., Stanley, W.C., Neese, R.A., Gertz, E.W., Nose, R.A., 1990. Effects of Acute Hyperglycemia on Myocardial Glycolytic Activity in Humans. *J Clin Invest* 85, 1648–1656.

- Xia, L., Wang, H., Goldberg, H.J., Munk, S., Fantus, I.G., Whiteside, C.I., 2006. Mesangial cell NADPH oxidase upregulation in high glucose is protein kinase C dependent and required for collagen IV expression. *Am J Physiol Renal Physiol* 290, F345–56.
- Xia, P., Inoguchi, T., Kern, T.S., Engerman, R.L., Oates, P.J., King, G.L., 1994. Characterization of the mechanism for the chronic activation of diacylglycerol-protein kinase C pathway in diabetes and hypergalactosemia. *Diabetes* 43, 1122–9.
- Yabe-Nishimura, C., 1998. Aldose reductase in glucose toxicity: a potential target for the prevention of diabetic complications. *Pharmacol Rev* 50, 21–33.
- Yamagishi, S.I., Edelstein, D., Du, X.L., Brownlee, M., 2001. Hyperglycemia potentiates collagen-induced platelet activation through mitochondrial superoxide overproduction. *Diabetes* 50, 1491–4.
- Yan, S.D., Schmidt, A.M., Anderson, G.M., Zhang, J., Brett, J., Zou, Y.S., Pinsky, D., Stern, D., 1994. Enhanced cellular oxidant stress by the interaction of advanced glycation end products with their receptors/binding proteins. *J Biol Chem* 269, 9889–97.
- Yang, Z., Laubach, V.E., French, B. a, Kron, I.L., 2009. Acute hyperglycemia enhances oxidative stress and exacerbates myocardial infarction by activating nicotinamide adenine dinucleotide phosphate oxidase during reperfusion. *J Thorac Cardiovasc Surg* 137, 723–9.
- Yu, C., Chen, Y., Cline, G.W., Zhang, D., Zong, H., Wang, Y., Bergeron, R., Kim, J.K., Cushman, S.W., Cooney, G.J., Atcheson, B., White, M.F., Kraegen, E.W., Shulman, G.I., 2002. Mechanism by which fatty acids inhibit insulin activation of insulin receptor substrate-1 (IRS-1)-associated phosphatidylinositol 3-kinase activity in muscle. *J Biol Chem* 277, 50230–6.
- Zachara, N.E., Hart, G.W., 2004. O-GlcNAc a sensor of cellular state: the role of nucleocytoplasmic glycosylation in modulating cellular function in response to nutrition and stress. *October* 1673, 13 – 28.
- Zhang, L., Ussher, J.R., Oka, T., Cadete, V.J.J., Wagg, C., Lopaschuk, G.D., 2011. Cardiac diacylglycerol accumulation in high fat-fed mice is associated with impaired insulin-stimulated glucose oxidation. *Cardiovasc Res* 89, 148–56.
- Zhou, L., Aon, M.A., Almas, T., Cortassa, S., Winslow, R.L., O'Rourke, B., 2010. A reaction-diffusion model of ROS-induced ROS release in a mitochondrial network. *PLoS Comput Biol* 6, e1000657.
- Zhu, Y., Pereira, R.O., O'Neill, B.T., Riehle, C., Ilkun, O., Wende, A.R., Rawlings, T. a, Zhang, Y.C., Zhang, Q., Klip, A., Shiojima, I., Walsh, K., Abel, E.D., 2013. Cardiac PI3K-Akt impairs insulin-stimulated glucose uptake independent of mTORC1 and GLUT4 translocation. *Mol Endocrinol* 27, 172–84.
- Ziegler, D., Hanefeld, M., Ruhnau, K.J., Meissner, H.P., Lobisch, M., Schütte, K., Gries, F.A., 1995. Treatment of symptomatic diabetic peripheral neuropathy with the anti-oxidant alpha-lipoic acid. A 3-week multicentre randomized controlled trial (ALADIN Study). *Diabetologia* 38, 1425–33.

Zimmet, P., Boyko, E.J., Collier, G.R., de Courten, M., 1999. Etiology of the metabolic syndrome: potential role of insulin resistance, leptin resistance, and other players. *Ann N Y Acad Sci* 892, 25–44.

CHAPTER 4

Materials and methods

4.1. Study design and research chapter layout

We aimed to evaluate the influence of acute hyperglycemia using an *in vitro* approach. Here, we simulated acute hyperglycemia in a cell culture model as this is a controllable experimental system. This approach allowed us to evaluate the role of acute hyperglycemia with minimal effect of other factors which may play a larger role in *in vivo* models. We could also manipulate various aspects of the experimental system through pharmacological intervention, while the measurement of certain parameters was accomplished by transfection experiments.

We initially aimed to evaluate the role of oxidative stress and downstream effects on insulin action (discussed in Chapter 5). Here, we determined the potential major sources of ROS production and their mechanisms involved in establishment or maintenance of an oxidative stress milieu. Our next aim was to investigate the involvement of NOGPs pathways and their possible links to oxidative stress and downstream disruption of insulin action (discussed in Chapter 6).

4.2. Cell culture and maintenance

H9c2 rat-derived cardiomyoblasts (ECACC No. 8809294) were cultured as monolayers at 37°C in a humidified atmosphere of 95% air and 5% CO₂. Cells were cultured in Dulbecco's modified Eagle's medium (DMEM) containing GlutaMAX™

and 5.5 mM glucose (Invitrogen, Carlsbad CA) as previously described by our laboratory (Rajamani and Essop 2010; Mapanga *et al.*, 2012). Media was supplemented with 10% fetal bovine serum (Invitrogen, Carlsbad CA) and 1% penicillin/streptomycin solution (Invitrogen, Carlsbad CA). Cells were cultured in T75 flasks and sub-cultured when they were ~80% confluent. Splitting was achieved by washing the cell monolayer with warm (37°C) phosphate buffered saline (PBS) and incubation in 4 ml 0.25% trypsin-EDTA (Invitrogen, Carlsbad CA) at 37°C until all cells have dislodged or for a maximum of 4 min. Cells were then diluted in a 2:1 ratio of DMEM:trypsin and centrifuged for 3 min at 1,358 x g in a Digicen 20-R Ortoalresa centrifuge (United Scientific, Cape Town, South Africa). Cell numbers were determined by counting using a hemocytometer (LASEC, Cape Town, South Africa). Cell pellets were resuspended in fresh 37°C DMEM and seeded in suitable culture flasks, plates or dishes for experiments or further passaging. Growth media were replaced every 48 h.

4.3. Modulatory studies

Cells were seeded at varying densities depending on the culture vessel for each experiment and allowed to plate and grow for 24 h prior to employment of modulators. Sub-confluent cells (~50%) were treated with high glucose (HG) DMEM (25 mM) (Invitrogen, Carlsbad CA) for 24 h to simulate acute hyperglycemia. The rationale for the high glucose (25 mM) concentration and time of exposure resulted from previous work in our laboratory, where high glucose (22 mM and 33 mM) were administered in a simulated chronic setting for 5 days (Mapanga *et al.*, 2012; Rajamani and Essop, 2010). We therefore aimed to expose the cells to high glucose

for a much shorter period. This exposure time is also in accordance with similar studies (Davidoff *et al.*, 2004; Park *et al.*, 2005). We chose 25 mM glucose as this is already the end concentration in DMEM used for routine maintenance of various cell types, and addition of more glucose would not be required. This ensured a higher level of standardization between independent experiments and ruled out possibilities of contamination associated with exogenously added glucose. The 25 mM concentration is also often used in similar studies (Davidoff *et al.*, 2004; Park *et al.*, 2005).

In separate treatment groups, cells were administered with pharmacological compounds (described below) \pm high glucose for the final hour of the simulated acute hyperglycemic period (i.e. 23 h HG + 1 h compounds with high glucose). A timeline for the experimental plan is illustrated in Fig 3.1. In order to assess the role of mitochondrial and NOX- derived ROS in our system, we employed 250 μ M α -cyano-4-hydroxycinnamic acid (4-OHCA, Sigma Aldrich, St Louis MO; inhibits mitochondrial ROS production) and 100 μ M diphenylene iodonium chloride (DPI, Sigma Aldrich, St Louis MO; NADPH oxidase inhibitor) (Fig 4.2). These ROS modulators were used for studies outlined in Chapter 4. The involvement of the four NOGPs was assessed using pharmacological inhibitors to target key mediators of each respective pathway. Here we employed 100 μ M aminoguanidine (AMG; inhibits AGE precursors), 5 μ M chelerythrine (CHE; PKC inhibitor), 40 μ M 6-diazo 5-oxo-L-norleucine (DON; HBP inhibitor), and 10 μ M zopolrestat (ZOP; polyol pathway inhibitor) (all from Sigma Aldrich, St. Louis MO). The transketolase co-factor and activator benfotiamine (BFT; Sigma Aldrich, St. Louis MO) was employed to evaluate the influence of the pentose phosphate pathway (PPP) (Fig. 4.2). The NOGP modulators were used for studies in

Chapter 5. Low glucose and high glucose controls were administered without any modulators. Acute high glucose treatments and modulatory studies were followed by molecular analyses for insulin action, oxidative stress and NOGPs using various experimental systems.

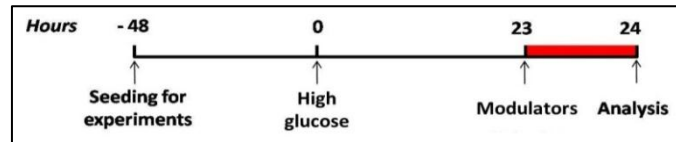


Figure 4.1 Timeline of experimental plan. Cells were seeded and allowed to plate and grow for 48 h prior to high glucose treatment for additional 24 h. Modulators were added (separate experimental groups) for the final hour prior to analysis.

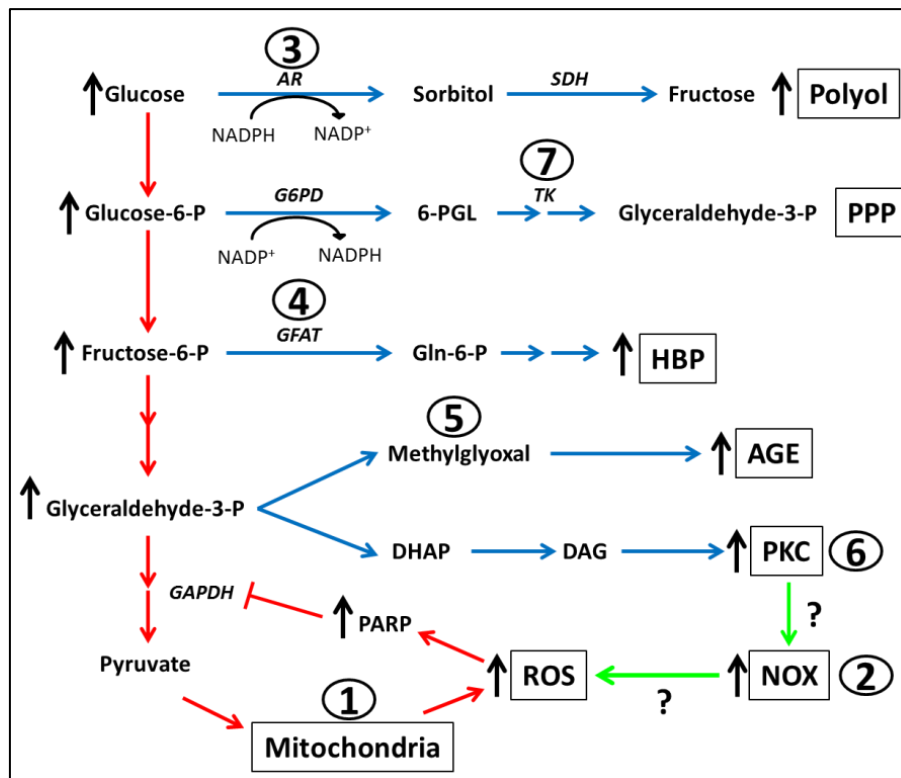


Figure 4.2 Target sites for pharmacological modulators employed in this study. Hyperglycemia leads to increased glycolytic flux and higher mitochondrial ROS production. PARP is released to repair the resulting DNA damage, but inhibits GAPDH in the process. This leads to accumulation of upstream metabolites (refer red arrows). Subsequently, non-oxidative glucose pathways (NOGPs) are activated: polyol pathway, PPP, HBP, AGE and PKC (refer blue arrows). This may result in NOX activation and further increased ROS production (refer green arrows). The following inhibitors were used: (1) α -cyano-4-hydroxycinnamic acid (4-OHCA) - mitochondrial ROS, (2) diphenylene iodonium (DPI) – NOX, (3) zopolrestat (ZOP) – polyol, (4) 6-diazo-5-oxo-L-norleucine (DON) – HBP, (5) aminoguanidine (AMG) – AGE, and (6) chelerythrine (CHE) – PKC. We also employed the transketolase activator benfotiamine (BFT) (7) to assess PPP involvement. AR: aldose reductase, SDH: sorbitol dehydrogenase, G6PD: glucose-6-phosphate dehydrogenase, 6-PGL: 6-phosphoglucono-1-5-lactone, TK: transketolase, GFAT: glutamine:fructose-6-phosphate amidotransferase, Gln-6-P: glucosamine-6-phosphate, DHAP: dihydroxy acetone phosphate, DAG: diacylglycerol, PARP: poly(ADP)ribose polymerase.

4.4. Otsuka Long-Evans Tokushima Fatty (OLETF) rat model of thiamine treatment

Previously collected heart tissues were kindly provided by Dr. Takao Tanaka (Osaka University of Pharmaceutical Sciences, Osaka, Japan). Here, four week old male OLETF rats (a model of obesity and insulin resistance) were randomly divided into

untreated and thiamine treated groups (n=16 per group) with the latter group receiving thiamine (2 g/L) in their drinking water (refer Tanaka *et al.*, 2010). Experimental groups were further divided according to treatment time, with one group sacrificed at 25 weeks (i.e. 21 weeks of thiamine) and the other at 55 weeks (i.e. 51 weeks thiamine). There were thus four groups of n=8 per group in total. Control OLETF rats displayed higher body and organ weights *versus* thiamine treated counterparts. Although control Long-Evans Tokushima Otsuka (LETO) rats (non-diabetic/lean counterparts to OLETF rats) were not assessed in the study by Tanaka *et al.* (2010), OLETF rats from the study and from breeder colonies exhibited obesity and insulin resistance phenotypes when compared to LETO breeders. Here, the researchers reported higher body weights and plasma glucose levels in the OLETF breeders and experimental animals. Thiamine administration reversed plasma glucose, insulin, triglycerides and HbA1c levels. Of note, the levels of plasma glucose and insulin were both higher in the 25 week OLETF controls relative to the thiamine treated group, while glucose levels remained high but insulin levels were reduced at 55 weeks in both untreated and treated groups. This was accompanied by enlarged pancreatic islets at 25 weeks, but severe morphologically altered islets at 55 weeks. The researchers suggested that these data may point to a hyperinsulinemic/hyperglycemic (pre-diabetic phenotype) state at 25 weeks, but a full blown diabetic state at 55 weeks. Thiamine treatment prevented development of insulin resistance and diabetes. Furthermore, echocardiographic assessment of 55 week-old OLETF rats showed reduced heart function which was attenuated by thiamine treatment (Tanaka *et al.*, 2010)

For the purposes of this thesis, we aimed to assess the role of *in vivo* hyperglycemia in the two different states of glucose metabolic dysregulation (i.e. 25 weeks - “pre-

diabetes” and 55 weeks – “overt diabetes”) and evaluate the molecular mechanisms underlying the thiamine-induced reversal of metabolic dysfunction in collected heart tissues. Here, we assessed the involvement of NOGPs (discussed in Section 6.4.3).

4.5. Measurement of insulin action

We employed different experimental approaches to evaluate insulin action. Here, we aimed to assess glucose uptake, GLUT4 translocation and activity of the proximal insulin signaling cascade. These events occur in a sequential manner upon insulin stimulation and directly results in the uptake of glucose.

4.5.1. Glucose uptake assay

Insulin-mediated glucose uptake was assessed by labeling cells with the fluorescent glucose analog 2-(*N*-(7-Nitrobenz-2-oxa-1,3-diazol-4-yl)amino)-2-deoxyglucose (2-NBDG; Invitrogen, Carlsbad CA). Cells were seeded in T25 culture flasks at 300,000 cells per flask and treated as described in Section 4.3. Serum free DMEM was employed for 3 h prior to preparation for analysis to achieve a basal condition. This is routinely done in similar experiments to evaluate the effect of insulin *per se* on downstream mechanisms such as glucose uptake (Bogan *et al.*, 2001; Gonzales *et al.*, 2011; Welsh *et al.*, 2007; Zeigerer *et al.*, 2004). Cells were trypsinized and centrifuged at 1,358 x g for 3 min. The pellets were washed in warm PBS (1 ml) and the resulting suspension divided into two separate tubes (i.e. two tubes per treatment condition). Here, one tube would serve as a basal control while the other would be exposed to insulin. The following working solutions were prepared - reaction buffer A:

100 μ M 2-NBDG and 10 μ g/ml propidium iodide (PI; Invitrogen, Carlsbad CA); and reaction buffer B: 100 μ M 2-NBDG, 10 μ g/ml PI and 100 nM insulin (Sigma Aldrich, St. Louis MO). Aliquots of 500 μ l of the appropriate buffer (A for basal and B for insulin groups) were added to respective cell pellets for 20 min prior to analysis by flow cytometry (BD FACSAria, Becton Dickinson, San Jose CA). A minimum of 10,000 events were analyzed per sample using the 488 nm laser. PI and 2-NBDG fluorescence intensities were detected using the PE-Texas Red and FITC emission filters, respectively. Four independent experiments were performed.

PI-positive (non-viable) cells were identified in order to be excluded from analysis for glucose uptake. Initial optimization experiments were performed to determine the scatter characteristics of PI-positive cells (Fig. 4.3). Here, a positive control sample tube containing cells with compromised membranes (methanol treated) were analyzed for both PI and 2-NBDG uptake (Fig. 4.3 A-D). Population P1 (A) represents all cells analyzed. Sub-population P2 is a daughter population of P1 and is gated from the intensity histogram (B) which represents PI fluorescence intensity. The large peak to the right of the gate P2 (indicated by the arrow) represents PI positive cells, allowing gate P2 to be set to the left of the base of this peak. All cells falling in gate P2 would thus be considered PI-negative and viable. Sub-population P3 (C) is a daughter population of P2 and represents the 2-NBDG fluorescence intensity of (only) the viable cell population. Figure 3.3 (D) represents the fluorescence intensities of PI-PE-Texas Red (y-axis) and 2-NBDG-FITC (x-axis), and shows the large PI-positive population (red dots indicated with black arrow) with a small PI-negative (blue dots) population. Figure 3.3 (E-H) represents a normal experimental sample. The gating parameters set up using the positive control sample

were applied to identify and exclude PI positive cells in experimental samples. Here, a large population of PI-negative cells fall inside gate P2 (F) and is included in the analysis of 2-NBDG uptake (the peak inside gate P3 at G and population of blue dots in H). The smaller peak in F and small population of red dots in H (indicated by the arrows) are the PI-positive cells excluded from analysis. The appropriate timepoint for incubation in reaction buffer was also optimized during an initial set of experiments (refer Fig 5.5).

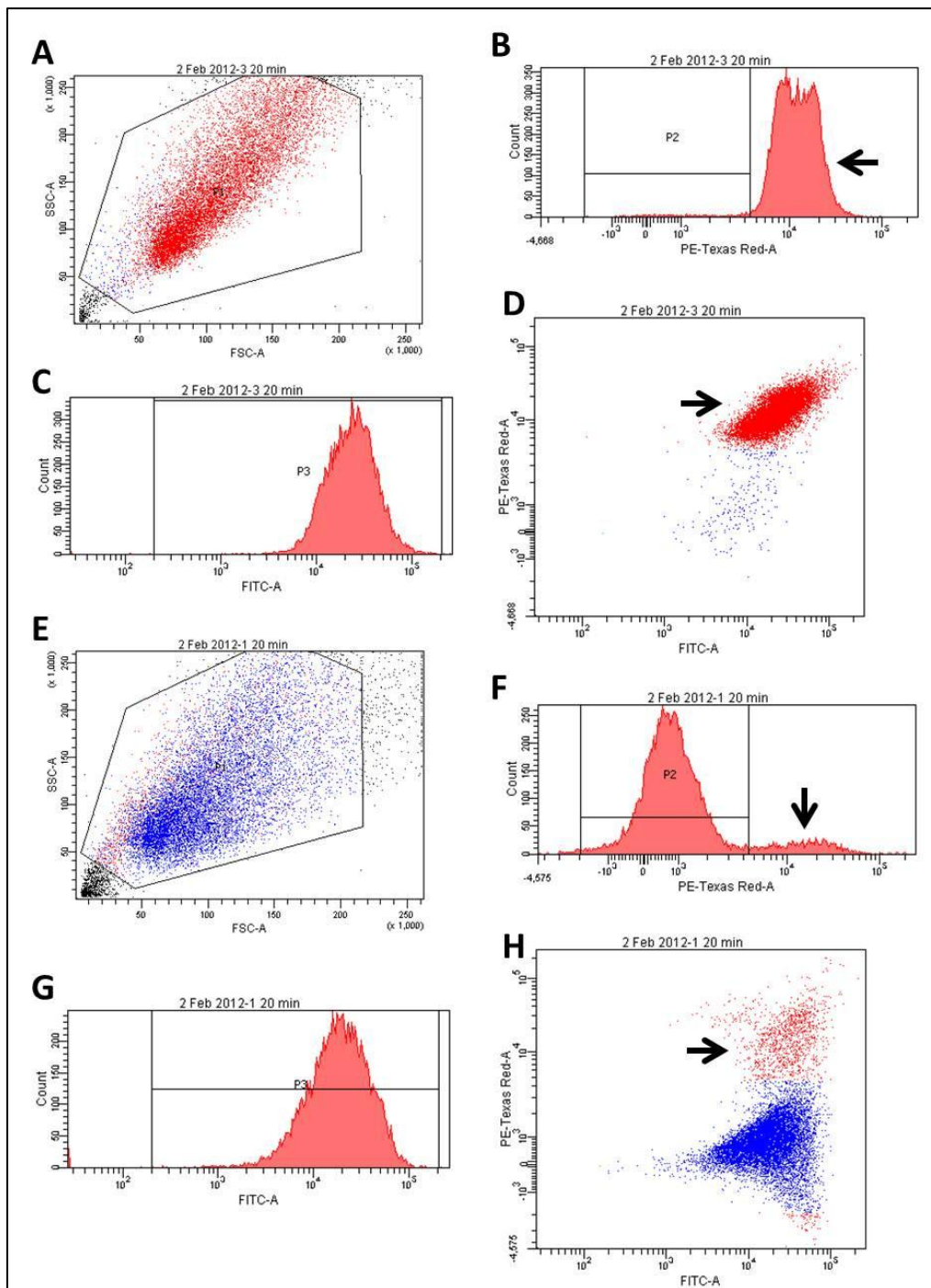


Figure 4.3 Flow cytometry analysis of 2-NBDG uptake in H9c2 cells – gating characteristics used to exclude non-viable cells. Cells were stained with 100 μ M 2-NBDG and 10ng/ml PI. Non-viable (PI-positive) cells were identified by inclusion of a positive control sample containing cells with comprised membranes (A-D). Parameters from a normal experimental sample are indicated (E-F). A and E: Parent populations falling in gate P1 with side scatter (SSC-A) on the y-axis and forward scatter (FSC-A) on the x-axis. B and F: PI intensity histograms indicated by PE-Texas Red-A showing PI-negative populations in gate P2. C and G: 2-NBDG intensity histograms indicated by FITC-A. D and H: Scatter plots of PI-PE-Texas Red (y-axis) and 2-NBDG-FITC (x-axis) showing PI-positive cells (red dots) and 2-NBDG-positive cells (blue dots). Arrows indicate PI-positive cells B, D, F and H.

4.5.2. GLUT4 translocation assay

Insulin-stimulated translocation of GLUT4 transporters was determined by expressing the HA-GLUT4-GFP fusion protein (a kind gift from Drs. G. Welsh and J.M. Tavarè, University of Bristol, UK) in H9c2 cells.

4.5.2.1. Transfection of HA-GLUT4-GFP

H9c2 cells were seeded in 8-chamber coverslides (Nalge Nunc, Roschester NY) at 10,000 cells per well and allowed to plate for 24 h. Transfection of HA-GLUT4-GFP was achieved using Lipofectamine LTX™ transfection reagent (Invitrogen, Carlsbad CA). Per sample well, 3 µl of Lipofectamine transfection reagent was diluted in 50 µl serum and antibiotic free DMEM in a sterile microcentrifuge tube. A second solution, 800 ng DNA in 50 µl serum and antibiotic free DMEM was prepared in separate tubes. The two solutions were gently vortexed and mixed together to form 100 µl of DNA-Lipofectamine complexes. The solution was incubated at room temperature for 15 min and added in a drop wise manner to each well. The plates were gently rocked and cells were incubated for 24 h at 37°C and 5% CO₂. Expression of GLUT4 was determined in cells exhibiting positive GFP fluorescence. After establishing successful transfection and expression of HA-GLUT4-GFP, cells were exposed to treatment protocols as described above and the effect of insulin was determined by labeling HA tags using immunofluorescence.

4.5.2.2. Treatment and preparation for fluorescence microscopy

After 24 h, cells were treated with pharmacological compounds (4-OHCA, DPI), serum starved for 3 h and treated with 100 nM insulin for 10 min. Cell monolayers were then washed with cold PBS and fixed in 4% paraformaldehyde followed by immunostaining with 10 µg/ml anti-HA mouse monoclonal antibody (Cell Signaling, Danvers MA) and anti-mouse Texas Red secondary antibody (Invitrogen, Carlsbad CA). This approach allows the detection of HA tags which would be exposed on the outer face of the sarcolemma when HA-GLUT4-GFP molecules have translocated, docked and fused. Fluorescence microscopy was performed using an Olympus Cell[^]R IX-81 fluorescence inverted microscope (Olympus Biosystems, Germany). All images were acquired using a 60X oil immersion objective. Multicolor images were acquired for both the Texas Red (HA) and GFP channels. Fluorescence in each channel was corrected for background by subtracting the fluorescence from untransfected cells.

4.5.2.3. Evaluation of HA: GFP ratio

The HA:GFP ratio was calculated for each cell to determine the membrane-to-total GLUT4 (the relative amount of GLUT4 at the membrane as a measure of GLUT4 translocation), as done before (Welsh *et al.*, 2007). This also served to normalize for differences in expression levels between cells. Results were derived from at least 150 cells per treatment group from five independent experiments.

4.5.3. Protein kinase B (PKB/Akt) activity assay

The activity of protein kinase B (PKB), also known as Akt, was determined by employing an Akt kinase activity assay kit (Abcam, Cambridge MA). Akt was isolated by immunoprecipitation from lysates of treated cells and incubated with a mixture of recombinant glycogen synthase kinase (GSK) 3 α (a known Akt substrate) and ATP. Akt activity was determined by the degree of GSK3 α phosphorylation as detected by Western blotting. The kit components included: kinase extraction buffer, kinase assay buffer, anti-Akt antibody, protein-A sepharose beads, GSK3 α peptide-ATP mixture and phospho-GSK3 α specific antibody. The protocol consisted of the following steps: preparation of cell lysate, immunoprecipitation of Akt, kinase assay and Western blotting. A detailed description is outlined below.

4.5.3.1. Preparation of cell lysate

Cells were grown in T25 flasks and treated according to the protocols described in Section 3.3. Monolayers were then washed with warm PBS, trypsinized and centrifuged (1,358 x g, 3 min). Pellets were washed with cold (4°C) PBS and subsequently lysed in 200 μ l cold kinase extraction buffer for 5 min on ice. The lysed cells were centrifuged (5,000 x g, 10 min at 4°C) and supernatant (cell lysate) transferred to new pre-chilled microcentrifuge tubes. Protein content was assayed using the Bradford protein determination method (Appendix B). Cell lysates were kept on ice and immunoprecipitation carried out immediately.

4.5.3.2. Immunoprecipitation of Akt

Akt was immunoprecipitated from cell lysates by incubation of 200 μ l lysate (containing 400 μ g total protein) with 2 μ l anti-Akt antibody per reaction for 45 min at room temperature while gently rotating. Protein A sepharose beads were gently resuspended and 50 μ l of the slurry was added to each sample. Rotation of tubes was continued at room temperature for 1 h. Samples were then centrifuged at 8,000 x g for 2 min and the supernatant removed. Protein A beads were washed twice with 500 μ l kinase extraction buffer and once with 500 μ l kinase assay buffer.

4.5.3.3. Kinase assay

Kinase assay buffer (50 μ l) was added to the washed beads, followed by 2 μ l of the GSK3 α -ATP mixture per sample and incubated at 30°C for 4 h. Samples were then centrifuged to pellet beads and 30 μ l supernatant collected into new microcentrifuge tubes. Next, 15 μ l Laemmli sample buffer (3X concentrated) was added and samples boiled at 95°C for 3 min. Samples were microcentrifuged to pellet any remaining beads and 20 μ l aliquots of the supernatant were transferred to new tubes for Western blot analysis.

4.5.3.4. Western blot analysis of phosphorylated GSK3 α

Samples were subjected to 12% SDS-PAGE and semi-dry transfer onto PVDF membranes (a full Western blotting protocol is described in Appendix C). Membranes were blocked with 5% non-fat milk in TBS-T and incubated with the rabbit anti-

phospho-GSK3 α antibody (1:1,000) overnight at 4°C. This was followed by incubation with anti-rabbit HRP-conjugated secondary antibody (1:10,000) for 1 h at room temperature and detection using ECL (Bio-Rad, Hercules CA).

4.6. Evaluation of oxidative stress mechanisms

We aimed to evaluate the role of oxidative stress mechanisms under acute hyperglycemic conditions. Here, we employed various techniques to determine the levels of total intracellular ROS, mitochondrial-derived ROS and activity of NADPH oxidase. We further assessed intracellular damage associated with oxidative stress by evaluation of aconitase activity and malondialdehyde (MDA) adduct formation. Finally, we also determined the intracellular antioxidant systems by evaluation of superoxide dismutase (SOD) activity, formation of reduced glutathione (GSH) and catalase activity. As the replenishment of GSH pools require NADPH, we also assessed its levels and turnover (NADP⁺:NADPH ratio), and the activity of glucose-6-phosphate dehydrogenase (G6PD), a major supplier of intracellular NADPH.

4.6.1. Total intracellular ROS levels – DCF fluorescence

We employed the cell permeant ROS indicator 2',7'-dichlorodihydrofluorescein diacetate stain (H₂DCFDA or DCF; Molecular Probes, Eugene OR) for detection of relative changes in intracellular ROS. These dyes are non-fluorescent, chemically reduced and acetylated compounds which become fluorescent when the acetate groups are removed upon oxidation. An increase in fluorescein (FITC) fluorescence is observed, which in turn can be related to ROS levels within the cell.

DCF stock solutions were prepared by dissolving lyophilized reagent in DMSO to a concentration of 10 mM. Single use aliquots were stored at -20°C protected from light and air. Fresh working solutions were prepared for every experiment by diluting stocks in warm (37°C) PBS to a final concentration of 50 µM (1:200 dilution). We employed fluorescence microscopy to qualitatively evaluate intracellular localization and fluorescence intensity of DCF in single cells, while flow cytometry was employed to quantitatively evaluate relative changes of cell populations per treatment group.

4.6.1.1. Fluorescence microscopy analysis of DCF staining

Cells were seeded in 8-well chambered coverslides (Nalgene Nunc, Rochester NY) at 15,000 cells per well in 400 µl DMEM for fluorescence microscopy experiments. High glucose and modulator treatments were performed as described in Section 4.2. After treatments, cell monolayers were washed with warm (37°C) PBS and incubated in 100 µl of freshly prepared dye solution (50 µM DCF) for 10 min at 37°C in the dark. Cells were also stained with 1:200 dilution of DAPI (Molecular Probes, Eugene OR) to detect nuclei. After 10 min, dye solutions were removed and cells washed with warm PBS. The cell layers were covered with 100 µl warm PBS, followed by fluorescence microscopy using an Olympus Cell^R IX-81 fluorescence inverted microscope (Olympus Biosystems, Germany) equipped with an F-view-II cooled CCD camera. All images were acquired using a 60X oil immersion objective. Cells were maintained at 37°C using the heating chamber while images were acquired. Multicolor images were acquired for both the DAPI and FITC channels. At least three random fields of view were acquired per treatment group per experiment and four

independent experiments were performed. Images were used for qualitative data while flow cytometry analysis served as a quantitative measure of DCF fluorescence.

4.6.1.2. Flow cytometry analysis of DCF staining

For flow cytometry experiments, cells were seeded in T25 flasks and treated as described in Section 3.2. Cells were washed with warm PBS and trypsinized using 2 ml warm Trypsin-EDTA (Invitrogen, Carlsbad CA) and incubated at 37°C until cells have dislodged. Cell suspensions were diluted with 4 ml warm DMEM, collected in 15 ml centrifuge tubes and centrifuged at 1,358 x g for 3 min in a Digicen 20-R Ortoalresa centrifuge (United Scientific, Cape Town, South Africa). Cells were incubated for 10 min at 37°C with the freshly prepared dye working solution, centrifuged (1,358 x g, 2 min) and pellets washed with warm PBS before flow cytometry analysis (BD FACSAria™, Becton Dickinson, San Jose CA). Positive control samples were treated with 100 µM H₂O₂. A 488 nm laser and 502LP, 530/30 BP emission filters were used. Fluorescence intensity was determined using the geometric mean. A minimum of 10 000 events were analyzed per sample tube. Experiments were repeated at least nine times and population data for treatment groups were normalized to relative control population data.

4.6.2. Mitochondrial ROS levels

In separate experiments, MitoTracker Red™ carboxy-methyl dihydro-X-rosamine (CM-H2XRos) dye (Molecular Probes, Eugene OR) was employed to detect mitochondrial ROS sources. As with DCF, this dye is chemically reduced and non-

fluorescent. It readily diffuses across cell membranes and accumulates in mitochondria of live and actively respiring cells. It becomes fluorescent when it is oxidized in the mitochondria, with Ex/Em wavelengths at 579/599 nm.

Stock solutions were prepared by dissolving the lyophilized product in DMSO to a concentration of 1 mM. Single use aliquots were stored at -20°C protected from light and air. Fresh working solutions were prepared for every experiment by diluting stocks in warm (37°C) PBS to a final concentration of 20 nM (1:500 dilution). We employed fluorescence microscopy to qualitatively evaluate intracellular localization and fluorescence intensity of MitoTracker in single cells, while flow cytometry was employed to quantitatively evaluate relative changes of cell populations per treatment group.

4.6.2.1. Fluorescence microscopy analysis of MitoTracker CM-H2XRos staining

Cell treatment, staining and microscopy analysis were performed as described in Section 4.6.1.1, with the following exceptions: cells were stained with 20 nM MitoTracker and 1:200 DAPI (Molecular Probes, Eugene OR) and images were acquired for the Texas Red and DAPI channels.

4.6.2.2. Flow cytometry analysis of MitoTracker CM-H2XRos staining

Flow cytometry protocols for MitoTracker detection were as described in Section 4.6.1.2, with the following exceptions: cells were incubated for 10 min at 37°C with 20 nM MitoTracker and a minimum of 10,000 events were analyzed per sample tube

using a 488 nm laser and 610LP, 616/23 BP emission filters. Experiments were repeated at least twelve times and population data for treatment groups were normalized to relative control population data.

4.6.3. NADPH oxidase activation

The activity of NADPH oxidase was evaluated using a modified assay (Abid *et. Al.*, 2007). Lucigenin emits photons upon acceptance of electrons generated by the NADPH oxidase complex. Briefly, lysates of treated cells were prepared and protein content determined using the Bradford method. Assay buffer containing 250 mM HEPES (pH 7.4), 120 mM NaCl, 5.9 mM KCl, 1.2 mM MgSO₄(7H₂O), 1.75 mM CaCl₂(2H₂O), 11 mM glucose, 0.5 mM EDTA, 100 μM NADH and 5 μM lucigenin was added to the samples and light emission measured over a 20 min period using a Glomax-96 luminometer (Promega, Madison WI). Data was converted to relative light units/min/μg protein and expressed as percentage (%) of control cells.

4.6.4. Aconitase activity

Aconitase is a citric acid cycle intermediate that catalyzes the stereospecific isomerization of citrate to isocitrate. We employed a colorimetric aconitase activity assay kit (Abcam, Cambridge MA) to monitor relative changes in cytosolic aconitase activity in our cell system. In the assay, aconitase converts citrate to isocitrate and a subsequent reaction results in a product that converts a colorless probe into a colored form with λ_{\max} at 450 nm.

Cells were cultured in T25 flasks and treated as described in Section 4.3. Cell monolayers were washed with cold PBS and scraped in 100 µl cold assay buffer, followed by sonication and centrifugation at 800 x g for 10 min at 4°C. The supernatant was transferred to new tubes, followed by addition of 10 µl activation solution and kept on ice for 1 h to activate aconitase. Fifty microliters of activated samples were added to duplicate wells of a 96-well plate. A 2 mM isocitrate standard solution was prepared and 0, 2, 4, 6, 8 and 10 µl added to triplicate wells to respectively generate 0, 4, 8, 12, 16 and 20 nmol/well standard curve. The volumes in each well were adjusted to 50 µl with assay buffer. Reaction mixture containing assay buffer, enzyme mixture and substrate were prepared and 50 µl added to each well and the contents mixed well. Plates were incubated at 25°C for 60 min followed by addition of 10 µl developer and further incubation at 25°C for 10 min. Optical density (OD) was measured at 450 nm in a microplate reader (EL 800 KC Junior Universal Microplate reader, Bio-Tek Instruments, Winooski VT). OD values from blank wells were subtracted from sample and standard curve wells and isocitrate content per well determined from the standard curve. Aconitase activity was calculated as follows: Aconitase activity = $B/(T \times V) \times \text{sample dilution factor}$, where B = nmol isocitrate per well; T = time incubated (60 min) and V = final sample volume assayed. Data was calculated as nmol/min/ml and expressed as percentage (%) of control. An n=3 was generated.

4.6.5. Malondialdehyde (MDA) assay

Lipid peroxidation is a detrimental modification of lipids exerted by oxidative stress. Malondialdehyde (MDA) adducts are among the products of lipid peroxidation and a

measure of MDA adduct formation can serve as an indication of oxidative stress. We employed the Oxiselect MDA adduct ELISA kit (Cell Biolabs, San Diego CA) to assess levels of MDA adducts. Briefly, cells treated as described in Section 4.3 were lysed using cold modified RIPA buffer and protein concentrations determined using the Bradford method. Protein samples were diluted to 10 µg/ml in 1X PBS and kept on ice. MDA-BSA standards were prepared according to kit instructions and serial dilutions were prepared in duplicate to create a range of standards. Protein samples (triplicates) and standards with blank controls (duplicates) were pipetted into wells of a 96-well protein binding plate (included in the kit) and incubated at 4°C overnight. Wells were washed with 250 µl 1X PBS the next day, followed by addition of 200 µl assay diluent and incubated for 2 h at room temperature. This was followed by washing with 1X wash buffer and addition of 100 µl 1:1,000 anti-MDA antibody for 1 h at room temperature. Wells were thoroughly washed and incubated with 100 µl 1:1,000 secondary HRP-conjugated antibody for 1 hour at room temperature. This was followed by thorough washing as before and addition of 100 µl substrate solution to all wells and incubation for 30 min at room temperature. The enzyme reaction was terminated by adding 100 µl stop solution to each well and absorbance was immediately read at 450 nm using a microplate reader (EL 800 KC Junior Universal Microplate reader, Bio-Tek Instruments, Winooski VT). MDA adduct levels were determined by calculating sample values from the standard curve after subtracting blank OD values.

4.6.6. Superoxide dismutase (SOD) activity assay

Total SOD activity was assessed by using the Biovision SOD activity assay kit (Biovision, Mountain View CA). The kit utilizes a water-soluble tetrazolium salt (WST-1) which is reduced by superoxide radicals to a water soluble and colored WST1-formazan product. The reaction is inhibited by SOD and the inhibition activity of SOD can therefore be determined colorimetrically. Protein samples were prepared from treated cells using cold modified RIPA buffer and protein concentration determined by the Bradford method. Protein samples, controls and blanks were pipetted into wells of a 96-well plate, 20 µl per well, followed by addition of 200 µl WST working solution and 20 µl SOD enzyme working solution to all wells. Plates were incubated at 37°C for 20 min. Absorbance was read at 450 nm using a microplate reader (EL 800 KC Junior Universal Microplate reader, Bio-Tek Instruments, Winooski VT). SOD activity was calculated by determining the % inhibition as follows: % inhibition = $(A_{\text{control}} - A_{\text{sample}})/A_{\text{control}} \times 100$.

4.6.7. Glutathione levels

Intracellular glutathione (GSH) levels were determined by employing the DetectX glutathione colorimetric detection kit (Arbor Assays, Ann Arbor MI). A colorimetric substrate provided with the kit reacts with free thiol groups on GSH, resulting in a colored product. Samples were prepared by lysing cells in cold 100 mM phosphate buffer, pH 7. An aliquot of the cell lysate was used for protein determination, while a second aliquot was treated with an equal volume of cold 5% sulfosalicylic acid and incubated at 4°C for 10 min to deproteinize the sample. Samples were centrifuged for

10 min at 10,000 x g at 4°C to remove precipitated protein. Supernatants were collected in new microcentrifuge tubes and diluted 1:5 with assay buffer. A serial dilution of the supplied GSH standard was prepared in sample diluent. Prepared samples and standards were pipetted into duplicate wells of a 96-well plate (50 µl each) and sample diluent served as a reaction blank. Colorimetric detection reagent (25 µl per well) was added to all wells followed by the addition of 25 µl reaction mixture (NADPH concentrate and glutathione reductase concentrate diluted in assay buffer). Plates were tapped gently to mix the contents and incubated for 20 min at room temperature. Absorbance was measured at 405 nm using a microplate reader (EL 800 KC Junior Universal Microplate reader, Bio-Tek Instruments, Winooski VT). GSH levels in samples were calculated from the standard curve.

4.6.8. NADPH levels and NADP⁺: NADPH ratio calculation

We employed a NADP/NADPH assay kit (Abcam, Cambridge MA) to determine the levels of NADPH and the ratio of NADP: NADPH in treated cells. Samples were prepared by washing cell monolayers (cells grown in T25 flasks) with PBS followed by trypsinization. Cell pellets were treated with 400 µl NADP/NADPH extraction buffer and exposed to two freeze-thaw cycles (20 min on dry ice followed by 10 min at room temperature). Extractions were vortexed for 10 sec and centrifuged at 10,000 x g for 5 min. Supernatants were transferred to new tubes and kept on ice – this contained total NADP (NADPH and NADP). In order to determine NADPH levels, an aliquot of the extracted samples was decomposed by heating at 60°C for 30 min. A serial dilution was prepared using the supplied NADPH standard to generate a standard curve. Samples and standards (50 µl) were added to duplicate wells of a 96-well

plate followed by addition of 100 µl NADP cycling mix (NADP cycling enzyme diluted in NADP cycling buffer). Plates were gently rocked and incubated for 5 min at room temperature. This was followed by addition of 10 µl NADPH developer to each well and incubation for 4 h at room temperature. Absorbance was read at 450 nm using a microplate reader (EL 800 KC Junior Universal Microplate reader, Bio-Tek Instruments, Winooski VT), before and after the addition of 10 µl stop solution. Total NADP and NADPH values were calculated from the standard curve using blanked absorbance values. The ratio of NADP: NADPH was calculated as follows: Ratio = $(\text{NADP}_t - \text{NADPH})/\text{NADPH}$, where NADP_t is the total NADP (i.e. NADP and NADPH combined).

4.6.9. Glucose-6-phosphate dehydrogenase (G6PD) activity assay

We employed a commercially obtained colorimetric assay kit to determine the activity of G6PD (Biovision, Mountain View CA). In the assay, the oxidation of glucose-6-phosphate is accompanied by the conversion of a colorless probe into a colored product. Protein samples were prepared from treated cells using cold modified RIPA buffer (Appendix A) and protein concentrations determined using the Bradford method. Fifty microliters of the prepared protein samples, a G6PD positive control and serial dilution of NADH standards were pipetted in duplicate wells of a 96-well plate. This was followed by addition of 50 µl reaction mix (G6PD substrate and developer diluted in assay buffer). The plate was immediately read at 450 nm using a microplate reader (EL 800 KC Junior Universal Microplate reader, Bio-Tek Instruments, Winooski VT) at timepoint T1, followed by incubation at 37°C for 30 min. Thereafter, the plate was read again at 450 nm (timepoint T2). The change in

absorbance (ΔA_{450}) was determined by subtracting OD values of T1 from that of T2. After correcting for background by subtracting blank OD values, the NADH amount between T1 and T2 (B) was calculated from the standard curve by applying ΔA_{450} . G6PD activity was calculated as follows: $G6PD \text{ activity} = [B/(T2 - T1) \times V] \times \text{sample dilution}$; V is the pre-treated sample volume added to wells.

4.7. Evaluation of metabolic alterations

We aimed to evaluate metabolic alterations by measuring intracellular ATP levels and several markers of the NOGPs.

4.7.1. Measurement of intracellular ATP levels

Intracellular ATP levels were determined using the ENLITEN® ATP bioluminescent assay kit (Promega, Madison WI). Here, the ATP-dependent oxidation of luciferin by luciferase results in light emission, which could be quantitatively measured using a luminometer. The assay includes recombinant luciferase which is used to catalyze the reaction:



The light emission is directly proportional to the ATP amount since ATP is the limiting factor.

Cells were grown in T25 flasks and treated as outlined in Section 4.2. Monolayers were washed and trypsinized (4 ml Trypsin-EDTA, 37°C) until cells detached. Cells were collected, centrifuged (1,350 x g, 3 min at 4°C) and pellets washed in sterile

PBS. The suspension was centrifuged again and resulting pellets were resuspended in 50 μ l ice cold lysis buffer (100 mM Tris-HCl, 4 mM EDTA, pH 7.75) (Essmann *et al.*, 2003). This was immediately followed by the addition of 150 μ l boiling lysis buffer and incubation at 99°C for 2 min. Samples were then centrifuged at 8,000 x g, 4°C for 1 min and supernatant collected for ATP assay and protein determination.

A volume of 50 μ l samples were added to duplicate wells of a white 96-well luminometer plate (Glomax Promega, Madison WI). ATP-free water served as a negative control and ATP standard as a positive control. These reagents were added to triplicate wells (50 μ l). The luciferase reagent was prepared as per the kit instructions, and 50 μ l added to samples followed by immediate analysis using a Glomax-96 luminometer (Promega, Madison WI).

4.7.2. Evaluation of non-oxidative glucose metabolic pathways

We employed commercial kits to evaluate markers of NOGPs as follows: polyol pathway using a D-sorbitol colorimetric detection kit (Biovision, Mountain View CA), PKC kinase activity (Enzo Life Sciences, Farmingdale NY), AGE precursors using the OxiSelect™ Methylglyoxal ELISA kit (Cell Biolabs, San Diego CA) and oxidative PPP using the G6PD assay kit (Biovision, Mountain View CA). O-GlcNAc levels (HBP marker) were determined by immunofluorescence microscopy and Western blotting. Transketolase activity (non-oxidative PPP) was assessed by using a modified enzyme assay. These procedures were as described by us before (Mapanga *et al.*, 2012).

4.7.2.1. Sample preparation for NOGP analysis

Cells were grown and treated in T25 flasks as described in Section 4.3. Monolayers were washed with cold PBS followed by the addition of 500 µl cold freshly prepared modified RIPA buffer (see Appendix) and scraped using a pre-chilled sterile cell scraper. The suspension was transferred to pre-chilled microcentrifuge tubes, sonicated and centrifuged at 4,300 x g at 4°C for 10 min. The supernatant (cell lysate) was transferred to new tubes and kept on ice. Protein concentrations were determined using the Bradford method (refer Appendix B).

4.7.2.2. Methylglyoxal levels (AGE)

Methylglyoxal-BSA (MG-BSA) standards and a blank (triplicate wells) and 100 µl of 10 µg/ml protein samples (duplicate wells) were pipetted into a pre-adsorbed 96-well ELISA plate (component of the kit), and incubated overnight at 4°C with gentle agitation. Wells were washed with 1X PBS the following day and 250 µl assay diluent added for 2 h at room temperature. The plate was subsequently washed with wash buffer and probed with 100 µl of anti-MG monoclonal antibody (1:1,000 dilution) for 60 min at room temperature. Primary antibody was then removed, wells washed and 100 µl of secondary HRP-conjugated antibody (1:1,000 dilution) added and incubated for 60 min at room temperature. After an additional series of wash steps, 100 µl of substrate solution was added to each well and the plate incubated for 20 min at room temperature. The enzyme reaction was stopped by adding 100 µl of stop solution to each well. Absorbance was read immediately at 450 nm using a microplate reader (EL 800 KC Junior Universal Microplate reader, Bio-Tek Instruments, Winooski VT).

Optical densities were normalized by subtracting values of the blank from those of samples and standards. MG levels were calculated from the standard curve as nmol/ μ g protein and data normalized to relevant controls. A minimum of six independent sample preparations were performed and each assayed in duplicate.

4.7.2.3. Sorbitol levels (Polyol)

A working solution of sorbitol standards (1 mM) was prepared using the stock solution provided in the kit. Standards (including reaction blanks) were pipetted into triplicate wells of a 96-well microtitre plate to generate 0, 2, 4, 6, 8 and 10 nmol/well by dilution in assay buffer. A volume of 50 μ l protein samples was pipetted into duplicate wells. This was followed by addition of 50 μ l reaction mix (enzyme mix, developer and probe diluted in assay buffer) to all wells and incubation at 37°C for 30 min. Absorbance was read at 560 nm using a microplate reader (EL 800 KC Junior Universal Microplate reader, Bio-Tek Instruments, Winooski VT). Sorbitol concentration (C) was calculated by using the sample amount from the standard curve (S_a) in nmol, sample volume (S_v) and dilution factor (D) in the following equation: $C = S_a / S_v * D$.

4.7.2.4. PKC activity

Duplicates of prepared protein samples (refer Section 4.6.2.2) and triplicates of serially diluted PKC standards were pipetted (30 μ l per well) into wells of the PKC substrate microtitre plate provided with the kit. The kinase reaction was initiated by addition of 10 μ l ATP to each well and incubation at 30°C for 90 min. The reaction

was stopped by emptying the wells, followed by addition of 40 μ l phospho-specific substrate antibody to each well and incubation for 60 min at room temperature. Wells were then emptied and, after a series of wash steps using 100 μ l wash buffer, secondary HRP-conjugated anti-rabbit antibody (40 μ l) added to each well. Plates were incubated at room temperature for a further 30 min. Wells were again emptied and washed as before. The assay was developed by adding 60 μ l of tetramethylbenzidine (TMZ) substrate and incubation for 60 min at room temperature. Twenty microliters of acid stop solution was then added to each well and absorbance measured at 450 nm using a microplate reader (EL 800 KC Junior Universal Microplate reader, Bio-Tek Instruments, Winooski VT). The relative PKC kinase activity was calculated from the standard curve and expressed per μ g protein for each well. Values were normalized to relative controls.

4.7.2.5. PKC isoform expression

Western blots were performed to investigate the expression levels of PKC β II in total cell lysate after treatment. Membranes were probed with an antibody against PKC β II (Abcam, Cambridge MA) and quantified by densitometric analysis - values normalized to β -actin.

4.7.2.6. O-GlcNAc levels (HBP)

O-GlcNAc levels were determined using immunofluorescence microscopy as described by us before (Rajamani and Essop, 2010) (Rajamani and Essop.,2010). Briefly, treated cells were fixed and permeabilized in cold (-20°C) methanol, blocked

in 5% donkey serum (Sigma Aldrich, St. Louis MO) and probed overnight at 4°C with the anti-O-GlcNAc CTD110.6 monoclonal antibody (Santa Cruz Biotechnology, Santa Cruz CA). This was followed by staining with a donkey anti-mouse Texas Red secondary antibody (Invitrogen, Carlsbad CA) and imaging done by fluorescence microscopy (Olympus Biosystems, Germany) using the Texas Red filter.

Cells were grown and treated in T25 flasks as described. Monolayers were washed with cold PBS followed by addition of 500 µl cold freshly prepared modified RIPA buffer (see Appendix A) and scraped using a pre-chilled sterile cell scraper. The suspension was transferred to pre-chilled microcentrifuge tubes, sonicated and centrifuged at 4,300 x g at 4°C for 10 min. The supernatant (cell lysate) was transferred to new tubes and kept on ice. Protein concentrations were determined using the Bradford method (refer Appendix B).

4.7.2.7. Co-localization analysis of O-GlcNAc modifications

Co-localization allows the visualization of proteins in close proximity using immunocytochemistry and fluorescence microscopy techniques. Using this approach, molecular interactions e.g. protein dimerization, post-translational modifications, intracellular localization, etc. may be determined and quantified by calculating the area of co-localization, as previously done by us (Rajamani and Essop, 2010). We aimed to determine the O-GlcNAc modification of insulin signaling intermediates Akt and AS160 by using double antibody staining and determining co-localization of O-GlcNAc with each of these intermediates in separate experiments.

H9c2 cells were seeded in 8-well chambered coverslides (Nalgene Nunc, Rochester NY) at 10,000 cells per well and allowed to proliferate. High glucose and pharmacological treatments were administered as described in Section 3.2. Upon completion of the treatment protocols, media was removed and wells were washed with 300 μ l cold (4°C) PBS. Cells were then fixed by adding cold 1:1 methanol:acetone solution (100 μ l per well) for 10 min at 4°C. Non-specific sites were blocked by incubating the cells in 50 μ l 5% donkey serum solution (Sigma, St. Louis MO) for 20 min at 4°C. This was followed by addition of a primary antibody cocktail (100 μ l per well) at 4°C overnight. The primary antibody cocktails consisted of the following combinations: a) 1:50 anti-O-GlcNAc CTD110.6 mouse monoclonal antibody (Santa Cruz Biotechnology, Santa Cruz CA) and 1:200 anti-Akt rabbit polyclonal primary antibody (Cell Signaling, Danvers MA); or b) 1:50 anti-O-GlcNAc CTD110.6 mouse monoclonal antibody (Santa Cruz Biotechnology, Santa Cruz CA) and 1:200 anti-AS160 rabbit primary antibody (Cell Signaling, Danvers MA). Antibody solutions were removed the following day and wells thoroughly washed with 300 μ l cold PBS. A cocktail of secondary antibodies was then added (1:200 anti-mouse Texas Red conjugated – for O-GlcNAc detection; and 1:200 anti-rabbit FITC conjugated – for Akt or AS160 detection) and plates incubated for a further 30 min at 4°C in the dark. We also included DAPI to stain the nuclei. The anti-mouse Texas Red conjugated antibody and DAPI were from Invitrogen (Carlsbad CA) and the anti-rabbit FITC conjugated secondary antibody was from Santa Cruz Biotechnology (Santa Cruz CA). Wells were subsequently washed up to six times with cold PBS to remove excess antibodies, and coated with layer of fluorescence mounting medium (DAKO, Glostrup, Denmark) followed by analysis using an Olympus Cell^R fluorescence IX-81 inverted microscope (Olympus Biosystems, Germany) equipped

with an F-view-II cooled CCD camera. All images were acquired using a 60X oil immersion objective. Multicolor images were acquired for the DAPI, Texas Red and FITC channels. Images were acquired through z-stacks with the top and bottom dimensions selected beforehand and a step width of 0.26 μm between image frames were used for all experiments. At least four random fields of view were acquired per treatment group per experiment and four independent experiments were performed. Images were processed for background subtraction and maximum intensity projections used for co-localization analysis using the Cell[^]R software (Olympus Biosystems, Germany). The area of co-localization was determined and data expressed relative to control values per experiment.

4.7.2.8. Transketolase activity (PPP)

Transketolase activity (non-oxidative PPP) was measured using a modified protocol (EC 2.2.1.1) from Sigma Aldrich (St. Louis MO). All chemicals used were of analytical grade and from Sigma Aldrich (St. Louis MO). An assay buffer containing 216 mM glycylglycine buffer, 3.3 mmol/l xylulose 5-phosphate (X-5-P), 1.7 mmol/l ribose 5-phosphate (R-5-P), 0.002% (w/v) cocarboxylase (thiamine pyrophosphate solution) (TPP), 0.14 mmol/l reduced β -nicotinamide adenine dinucleotide (β -NADH), 15 mmol/l MgCl_2 , 20 units α -glycerophosphate dehydrogenase/triophosphate isomerase enzyme solution (α -GDH/TPI) were added to a 96-well plate. Absorbance was monitored until constant using a microplate reader (EL 800 KC Junior Universal Microplate reader, Bio-Tek Instruments, Winooski VT), whereafter cell samples and transketolase enzyme solution (positive control) were added to triplicate wells and

the relative decrease in absorbance monitored for 10 min. Transketolase activity was calculated as follows:

$$\text{Units/ml of enzyme} = \frac{(\Delta A_{340\text{nm}} / \text{min test} - \Delta A_{340\text{nm}} / \text{min blank}) (0.3) (\text{df})}{(6.22) (0.01)}$$

$$\text{The values were presented as units/mg protein} = \frac{\text{units / ml enzyme}}{\text{mg protein / ml enzyme}}$$

(Δ - change increment; A-absorbance; df-dilution factor; ml-milliliter; mg-milligram)

4.8. Statistical analysis

Data are presented as mean \pm standard error of the mean (SEM). Two-way ANOVA was used to determine changes between basal and insulin stimulated groups for the glucose uptake and GLUT4 translocation experiments. One-way ANOVA was used to assess differences between more than two groups. A Bonferroni *post hoc* test was performed when significant differences were observed. All statistical analyses were performed using Graphpad Prism version 5.01 (Graphpad Software Inc., San Diego CA). Values were considered significant when $p < 0.05$.

4.9. References

- Bogan, J.S., McKee, A.E., Lodish, H.F., 2001. Insulin-responsive compartments containing GLUT4 in 3T3-L1 and CHO cells: regulation by amino acid concentrations. *Mol Cell Biol* 21, 4785-806.
- Davidoff, A.J., Davidson, M.B., Carmody, M.W., Davis, M.E., Ren, J., 2004. Diabetic cardiomyocyte dysfunction and myocyte insulin resistance: role of glucose-induced PKC activity. *Mol Cell Biol* 262, 155-63.
- Essmann, F., Bantel, H., Totzke, G., Engels, I.H., Sinha, B., Schulze-Osthoff, K., Jänicke, R.U., 2003. Staphylococcus aureus alpha-toxin-induced cell death: predominant necrosis despite apoptotic caspase activation. *Cell Death Differ* 10, 1260-72.
- Gonzales, E., Flier, E., Molle, D., Accili D., McGraw, T., 2011. Hyperinsulinemia leads to uncoupled insulin regulation of the GLUT4 glucose transporter and the FoxO1 transcription factor. *Proc Natl Acad Sci USA* 108, 10162-7
- Mapanga, R.F., Rajamani, U., Dlamini, N., Zungu-Edmondson, M., Kelly-Laubscher, R., Shafiullah, M., Wahab, A., Hasan, M.Y., Fahim, M. a, Rondeau, P., Bourdon, E., Essop, M.F., 2012. Oleanolic acid: a novel cardioprotective agent that blunts hyperglycemia-induced contractile dysfunction. *PLoS One* 7, e47322.
- Park, S.S.Y., Ryu, J., Lee, W., 2005. O-GlcNAc modification on IRS-1 and Akt2 by PUGNAc inhibits their phosphorylation and induces insulin resistance in rat primary adipocytes. *Exp Mol Med* 37, 220-9.
- Rajamani, U., Essop, M.F., 2010. Hyperglycemia-mediated activation of the hexosamine biosynthetic pathway results in myocardial apoptosis. *Am J Physiol Cell Physiol* 299, C139-47.
- Tanaka, T., Kono, T., Terasaki, F., Yasui, K., Soyama, A., Otsuka, K., Fujita, S., Yamane, K., Manabe, M., Usui, K., Kohda, Y., 2010. Thiamine prevents obesity and obesity-associated metabolic disorders in OLETF rats. *J Nutr Sci Vitaminol (Tokyo)* 56, 335-46.
- Welsh, G.I., Leney, S.E., Lloyd-Lewis, B., Wherlock, M., Lindsay, A.J., McCaffrey, M.W., Tavaré, J.M., 2007. Rip11 is a Rab11 and AS160-RabGAP-binding protein required for insulin-stimulated glucose uptake in adipocytes. *J Cell Sci* 120, 4197-208.
- Zeigerer, A., McBrayer, M.K., McGraw T.E., 2004. Insulin stimulation of GLUT4 exocytosis, but not its inhibition of endocytosis, is dependent on Rab-GAP AS160. *Mol Biol Cell* 15, 4406-15.

CHAPTER 5

Study I: Acute hyperglycemia induces oxidative stress-related insulin resistance *in vitro*.

5.1. Introduction

Cardiovascular complications constitute a major cause of death and disability among individuals burdened with diabetes mellitus. Here myocardial insulin resistance may play an important role in the progression of diabetic cardiomyopathy and heart failure (Chavali *et al.*, 2013; Chiha *et al.*, 2012; Gustafsson *et al.*, 2004). Chronic hyperglycemia, a hallmark of diabetes, is strongly correlated with higher incidence of myocardial infarction and markers of cardiac damage in humans (Barr *et al.*, 2007; Rubin *et al.*, 2012). Furthermore, effective glucose uptake and metabolism is particularly important in the ischemic heart (Tian and Abel, 2001), and also in preventing cardiac dysfunction associated with heart failure (Liao *et al.*, 2002). However, optimal glucose lowering interventions for the treatment of diabetic complications pose unique challenges within the clinical setting (Radke and Schunkert, 2008). Thus prevention of insulin resistance at an early stage is of utmost importance to help curb the growing global burden of cardio-metabolic complications.

Chronically elevated nutrients (hyperglycemia, hyperlipidemia) can initiate detrimental metabolic and molecular events. For example, increased hyperglycemia-induced production of reactive oxygen species (ROS) is considered a central factor in mediating damaging outcomes (Brownlee, 2005; Giacco and Brownlee, 2010). Here, the current paradigm is that elevation of mitochondrial-derived ROS causes DNA damage and the subsequent release of poly-ADP-ribose polymerase (PARP) as a restorative mechanism (Nishikawa *et al.*, 2000). However, PARP can also inhibit glyceraldehyde-3-phosphate dehydrogenase (GAPDH), thereby reducing glycolytic flux (Du *et al.*, 2003). Glucose metabolites are subsequently

diverted into non-oxidative glucose metabolic pathways (NOGP) – the formation of advanced glycation end products (AGE), activation of protein kinase C (PKC), polyol pathway and hexosamine biosynthetic pathway (HBP) - resulting in harmful vascular complications associated with diabetes (Giaccari *et al.*, 2009).

It is plausible that oxidative stress also plays a prominent part in the etiology of insulin resistance, i.e. not only does it attenuate pancreatic β -cell function and insulin secretion (Futamura *et al.*, 2012), but it can also disrupt insulin signaling and glucose uptake in skeletal muscle, adipose tissue and the liver (Costford *et al.*, 2009; Gao *et al.*, 2010; Grimsrud *et al.*, 2007; Messner *et al.*, 2013; reviewed in Eriksson, 2007; Ruskovska and Bernlohr, 2013). Although mitochondrial-derived ROS are generally considered chief participants in exerting such detrimental effects, the impact of additional sources of ROS production and downstream mechanisms needs further elucidation. For example, the NADPH oxidase (NOX) complex is emerging as an important producer of hyperglycemia-mediated ROS in cardiomyocytes (Brewer *et al.*, 2011; Li *et al.*, 2006; Santos *et al.*, 2011). Furthermore, hyperglycemia-mediated NOX-derived ROS can participate in myocardial apoptosis (Balteau *et al.*, 2011), while NADPH from the pentose phosphate pathway (PPP) may be a crucial mediator of NOX activity in obese/hyperglycemic rat hearts (Serpillon *et al.*, 2009). Angiotensin II (ANG II)-induced NOX activation also induced insulin resistance in *in vitro* and *in vivo* studies, including the TG(mRen-2)²⁷ rat model of ANG II overexpression (Ogihara *et al.*, 2002; Sloniger *et al.*, 2005; Wei *et al.*, 2006).

Poor lifestyle and dietary habits can give rise to the prevalence of acute hyperglycemic episodes (e.g. high postprandial excursions and impaired glucose tolerance) in diabetic and non-diabetic individuals. However, the role of ROS and associated activation of NOGPs under acute hyperglycemic conditions in insulin-responsive cells remains poorly understood. In light of this, we investigated the effects of ROS on NOGP activation and insulin-mediated glucose uptake within the setting of *in vitro* acute hyperglycemia. We hypothesized that

mitochondria and NOX are major sources of ROS production and function in tandem to modulate NOGPs, resulting in reduced cardiac glucose uptake with acute hyperglycemia. The first study (this chapter) focuses on oxidative stress mechanisms and the effect of elevated intracellular ROS on insulin-mediated glucose uptake. NOGP activation and their downstream effects are described in Chapter 6.

5.2. Aims

We aimed to evaluate the effect of simulated acute hyperglycemia on intracellular ROS production *in vitro*. Here specific emphasis was placed on ROS sources, focusing on mitochondrial and NOX-derived ROS. We also aimed to elucidate mechanisms of oxidative stress by evaluating intracellular antioxidant systems and markers of oxidative damage. More importantly, we aimed to assess the impact of ROS from both sources on insulin action and glucose uptake by employing inhibitors to reduce mitochondrial ROS output and NOX activation.

5.3. Modulators and brief description of methodology

The first phase of experiments focused on elucidating the effect of high glucose on ROS production and insulin action. This was followed by phase two – assessing the role of mitochondrial and NOX-derived ROS in insulin action. In order to achieve this, we employed 250 μM α -cyano-4-hydroxycinnamic acid (4-OHCA, inhibits mitochondrial ROS production) and 100 μM diphenylene iodonium chloride (DPI; NOX inhibitor) (Fig 5.1 refer Section 4.3 and Figs 4.1 and 4.2 for description of the methodology employed) (Cross and Jones, 1986; Halestrap and Denton, 1975; O'Donnell *et al.*, 1993; Rajamani and Essop, 2010). We utilized fluorescent markers

to detect total intracellular ROS (CM-H₂DCF) and mitochondrial ROS levels (MitoTracker Red CMH₂XRos), and a luminescence assay to evaluate NOX activity. Insulin action was assessed by 1) glucose uptake using the fluorescent glucose analog 2-NBDG; 2) GLUT4 translocation in cells expressing the HA-GLUT4-GFP construct and 3) Akt kinase activity. Oxidative stress mechanisms were further evaluated by ascertaining the intracellular antioxidant capacity (superoxide dismutase activity, replenishment of glutathione) and assessing markers of oxidative damage (aconitase activity and malondialdehyde levels). The detailed methodology is described in Chapter 4.

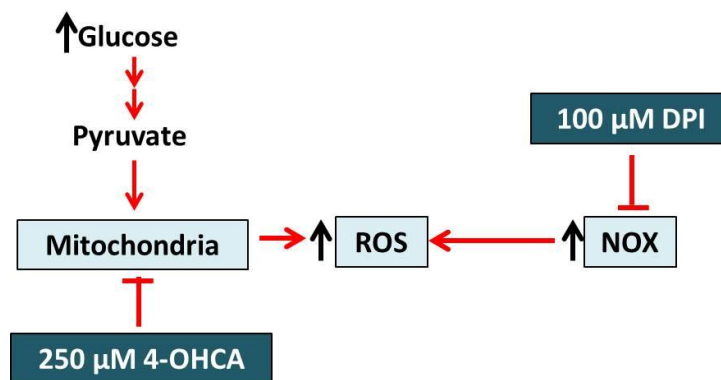


Figure 5.1 Modulators used to inhibit ROS from the mitochondria and NOX. 4-OHCA: α -cyano-4-hydroxy cinnamic acid; DPI: diphenylene iodonium chloride; NOX: NADPH oxidase.

5.4. Results

5.4.1. Acute high glucose exposure upregulates ROS and reduces glucose transport capacity

Total intracellular ROS levels were determined by DCF fluorescence. Qualitative analysis by fluorescence microscopy revealed a dispersed cytoplasmic signal which increased in

intensity in the high glucose group compared to controls (Fig 5.2A). Flow cytometric analysis showed that DCF fluorescence was markedly upregulated (~58%) with high glucose treatment ($P < 0.001$ vs. control) (Fig 5.2 B and C). MitoTracker Red CMH2XRos fluorescence signal was localized within mitochondria, with increased intensity in the high glucose group (Fig 5.3A). Flow cytometry data showed a moderate increase of mitochondrial ROS levels by $9.6 \pm 2.6\%$ ($P < 0.05$ vs. control) in the high glucose group (Fig 5.3 B and C). NOX activity was robustly upregulated by high glucose treatment (by ~49%) ($P < 0.001$ vs. control) (Fig 5.4).

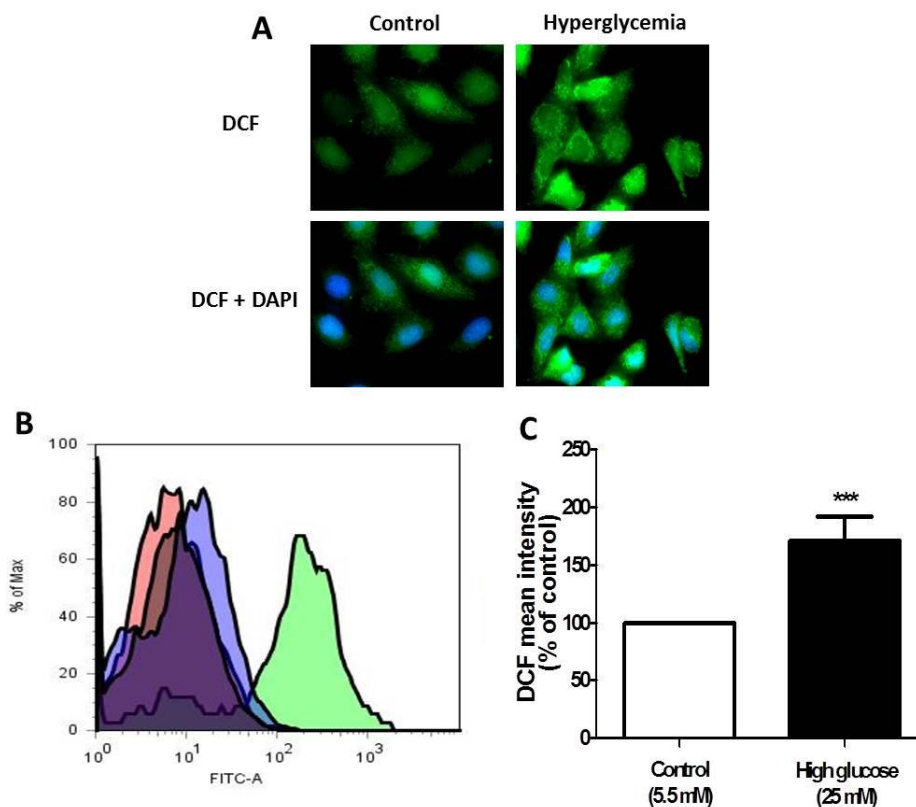


Figure 5.2 Total intracellular ROS levels determined by CM-H₂DCFDA (DCF) fluorescence. H9c2 cells were subjected to 24 h high glucose conditions vs. controls. (A) Qualitative analysis of DCF fluorescence (FITC-green, top panel) by microscopy with nuclei stained with DAPI (blue fluorescence, bottom panel); (B) Fluorescence intensity histogram indicating DCF signal (FITC channel) as measured by flow cytometry with controls indicated in the red peak, high glucose treated cells in the blue peak and a positive control (50 μ M H₂O₂) in green; (C) Statistical analysis of flow cytometry population data (10,000 events analyzed per treatment condition), expressed as percentage (%) of control. Values are expressed as mean \pm SEM (n=3 for microscopy; n=9 for flow cytometry analysis). *** $P < 0.001$ vs. control.

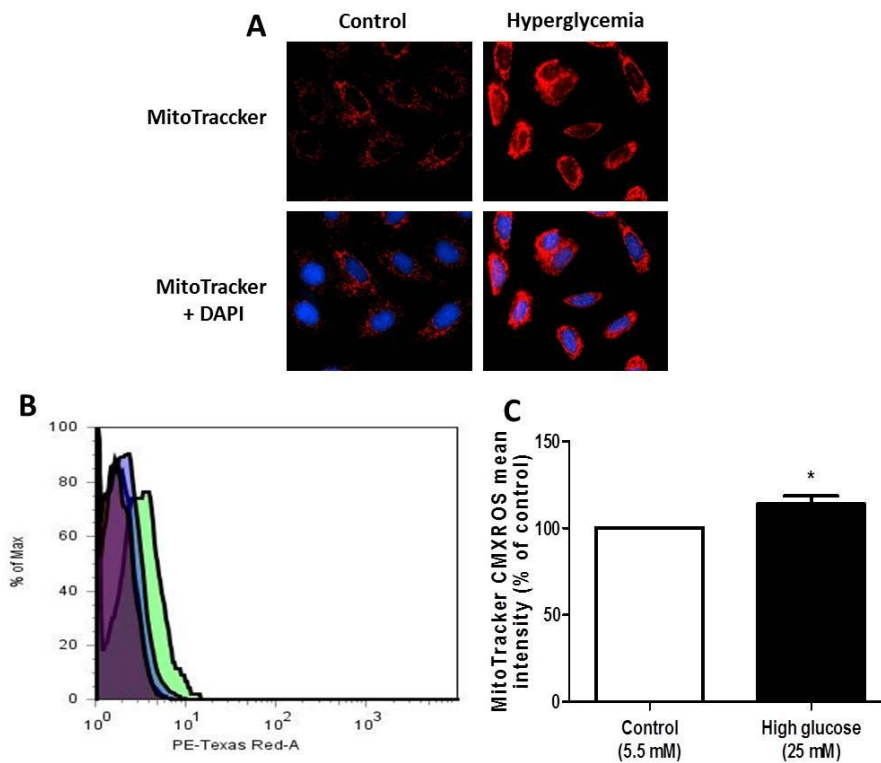


Figure 5.3 MitoTracker Red CMH2XROS staining of cells to indicate mitochondrial ROS sources. H9c2 cells were subjected to 24 h high glucose conditions vs. controls. (A) Fluorescence microscopy analysis of MitoTracker fluorescence intensity (Texas Red, top panel) with nuclei stained with DAPI (blue fluorescence, bottom panel); (B) Fluorescence intensity histogram indicating PE-Texas Red signal as measured by flow cytometry with controls indicated in the red peak, high glucose treated cells in the blue peak and a positive control (50 μM H_2O_2) in green; (C) Statistical analysis of flow cytometry population data (10,000 events analyzed per treatment condition), expressed as percentage (%) of control. Values are expressed as mean \pm SEM (n=3 for microscopy, n=9 for flow cytometry). *P<0.05 vs. control.

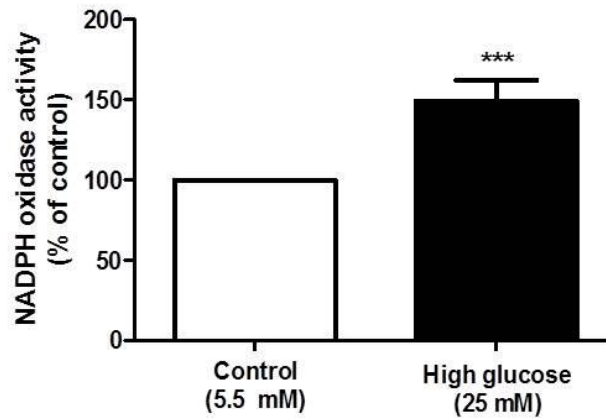


Figure 5.4 NADPH oxidase activity increased under high glucose conditions. H9c2 cells were subjected to 24 h high glucose conditions vs. controls. Values are expressed as mean \pm SEM (n=6). ***P<0.001 vs. controls.

The insulin-mediated uptake of glucose was determined by flow cytometry using the fluorescent glucose analog 2-NBDG. Here low glucose control cells rapidly upregulated glucose uptake upon insulin stimulation (red line on graph) from 10 – 30 min (P<0.001 vs. respective basal control indicated by the black line) (Fig 5.5A). Inhibition of insulin signaling by 100 nM wortmannin, a PI3K inhibitor (blue dotted line), blunted the stimulatory effect of insulin (P<0.05 vs. control insulin). Twenty minutes insulin stimulation was chosen to evaluate glucose uptake in subsequent experiments (Fig 5.5B). The insulin stimulatory effect on glucose uptake could be reproduced in control cells, however, this was markedly inhibited in cells treated with high glucose.

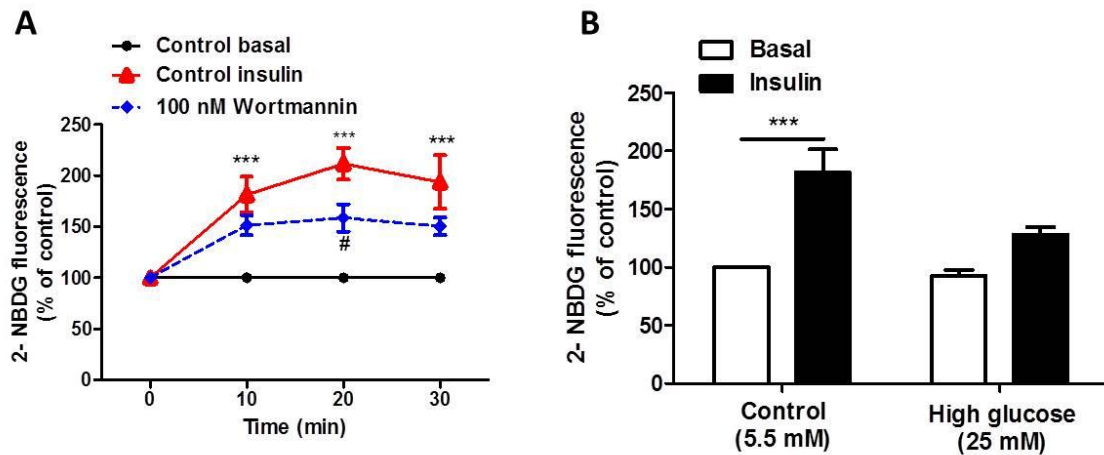


Figure 5.5 Impaired glucose uptake in response to high glucose conditions. H9c2 cells were subjected to 24 h high glucose conditions vs. controls. Flow cytometry analysis of 2-NBDG fluorescence intensity in viable cells. (A) Preliminary optimization to evaluate insulin-mediated glucose uptake over time (basal controls – black line; insulin treated groups – red line; 100 nM wortmannin treated groups – blue dotted line). (B) H9c2 cells were subjected to 24 h high glucose conditions vs. controls and glucose uptake evaluated after 20 min insulin exposure vs. basal controls. Values are expressed as mean \pm SEM (n=8). ***P<0.001 vs. basal control; #P<0.05 vs. 20 min insulin.

To confirm our findings, we repeated these experiments in the presence of a HA-GLUT4-GFP construct. Assessment of GLUT4 translocation revealed similar findings to the glucose uptake data (Fig 5.6), i.e. inhibited insulin stimulation in the HG group, while insulin increased GLUT4 translocation in the control condition (P<0.001 vs. basal)

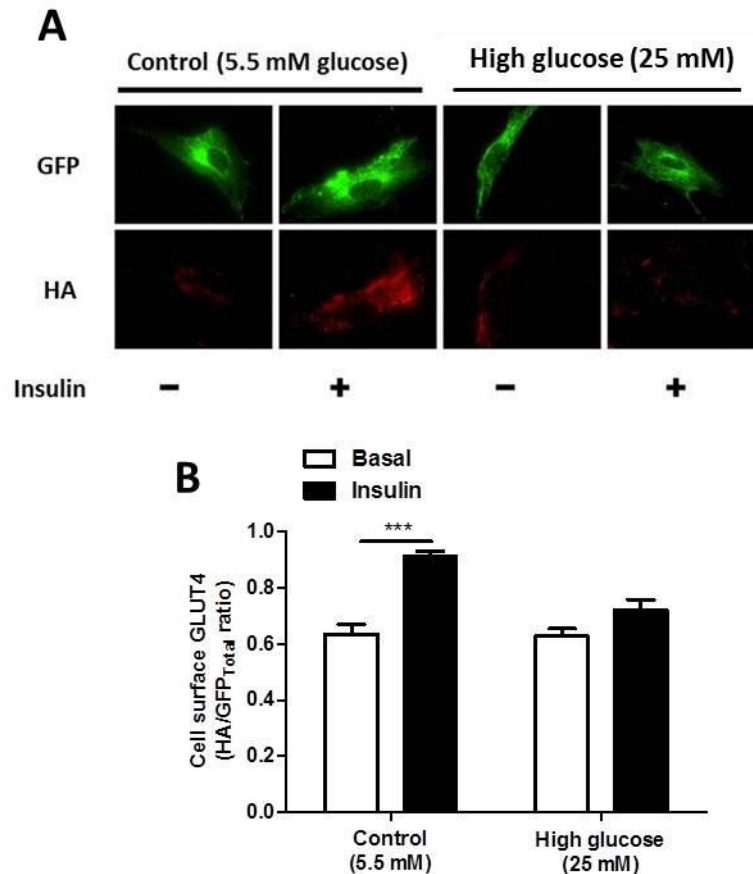


Figure 5.6 High glucose treatment suppressed the translocation of HA-GLUT4-GFP to the sarcolemma. H9c2 cells were subjected to 24 h high glucose conditions vs. controls. (A) Fluorescence microscopy analysis of H9c2 cells expressing GFP (green fluorescence, top panel) stained with Texas Red-conjugated anti-HA antibody (red fluorescence, bottom panel). The anti-HA antibody binds to an HA target sequence in the first exofacial loop, which is exposed upon translocation and fusion at the sarcolemma in response to insulin. (B) Quantification of the HA:GFP ratio as a measure of GLUT4 translocation. Values are expressed as mean \pm SEM ($n \geq 150$ cells from five independent experiments) *** $P < 0.001$ vs. unstimulated (basal) control.

Further analysis of insulin action revealed downregulation of Akt activity under high glucose conditions ($P < 0.001$ vs. control) (Fig 5.7).

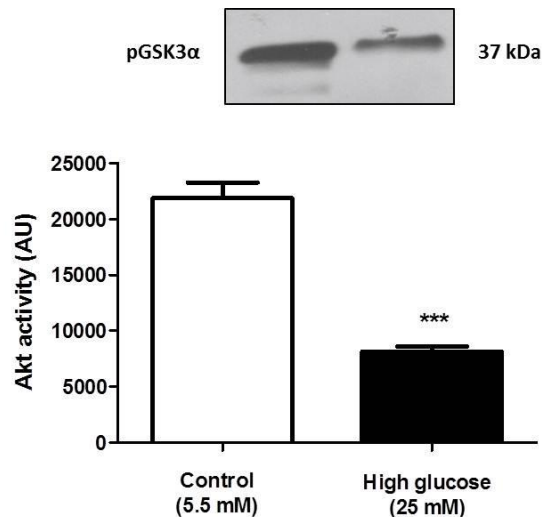


Figure 5.7 Acute hyperglycemia downregulated the kinase activity of Akt. Cell free *in vitro* kinase activity of Akt was assessed by immunoprecipitation of Akt from H9c2 cells that were subjected to 24 h high glucose conditions vs. controls. Equal concentrations of the isolated Akt was exposed to the Akt substrate GSK3 α and ATP at 30°C, resulting in the Akt-catalyzed formation of phosphorylated GSK3 α and analysis of pGSK3 α by Western blotting (refer Section 4.5.3 for methodology). Values are expressed as mean \pm SEM (n=3). ***P<0.001 vs. control.

5.4.2. Mitochondrial and NOX-derived ROS mediates insulin resistance

Our next aim was to determine whether the higher ROS levels produced by the mitochondria and NOX play a role in the induction of insulin resistance under high glucose conditions. We employed the modulators of mitochondrial and NOX-derived ROS (discussed in Section 5.3). The elevated intracellular ROS levels as determined by DCF fluorescence were markedly reduced by 4-OHCA ($63.1 \pm 13.9\%$) ($P<0.01$ vs. HG), while NOX inhibition (by DPI) attenuated it by $78.6 \pm 16\%$ ($P<0.01$ vs. HG) (Fig 5.8A). Mitochondrial ROS levels were reduced with 4-OHCA treatment ($P<0.001$ vs. HG). However, DPI treatment did not result in any significant changes (Fig 5.8B). As expected, treatment with DPI markedly decreased NOX activity (by $124.6 \pm 8.4\%$) ($P<0.001$ vs. HG) (Fig 5.8C). Surprisingly, 4-OHCA administration also lowered NOX activity ($33.1 \pm 8.6\%$, $P<0.05$ vs. HG). The difference between 4-OHCA and DPI

(~91%) was statistically significant ($P < 0.001$), indicating that DPI more specifically inhibited NOX activity

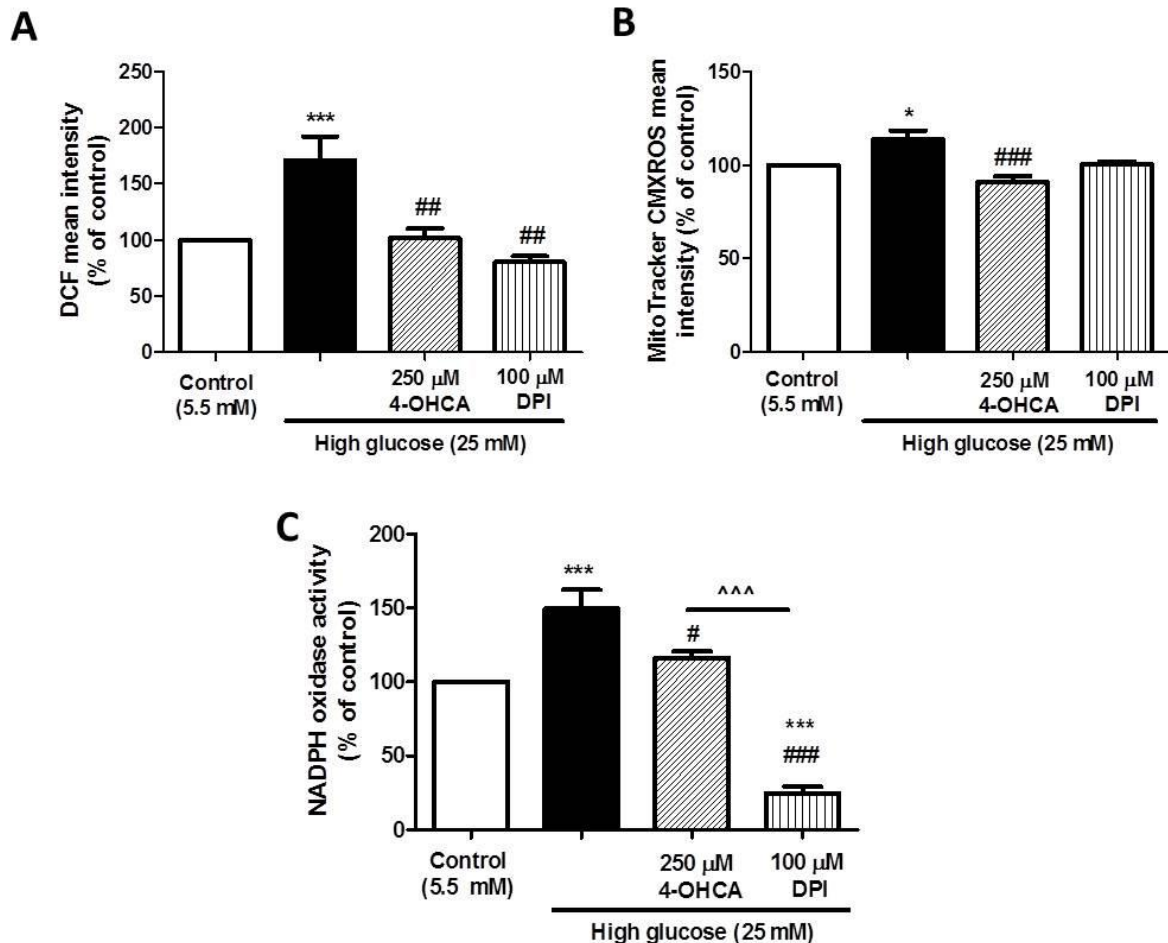


Figure 5.8 Pharmacological attenuation of mitochondrial- and NOX-derived ROS. H9c2 cells were subjected to 24 h high glucose conditions vs. controls \pm 1 h treatment with a) 250 μ M 4-OHCA (inhibits mitochondrial ROS), and b) DPI (NOX inhibitor). Flow cytometry analysis of (A) DCF fluorescence and (B) MitoTracker Red fluorescence. (C) Assay of NOX activity. Values are expressed as mean \pm SEM (n=6-9). * $P < 0.05$, *** $P < 0.001$ vs. control; ## $P < 0.01$, ### $P < 0.001$ vs. high glucose; ^^^ $P < 0.001$ vs. indicated treatment.

We next employed the ROS modulators in the analysis of insulin action. Both antioxidant treatments (4-OHCA and DPI) restored glucose uptake ($P < 0.05$ and $P < 0.01$ vs. basal, respectively) after insulin stimulation (Fig 5.9). The respective 4-OHCA and DPI treatments also significantly increased the recruitment of HA-GLUT4-GFP to the sarcolemma ($P < 0.001$ vs. basal) (Fig 5.10). Furthermore, 4-OHCA and

DPI treatment reversed the inhibitory effect of high glucose on Akt activity (Fig 5.11). Together, these data point toward the involvement of both mitochondrial and NOX-derived ROS in the hyperglycemia-induced attenuation of insulin action and consequently, glucose uptake.

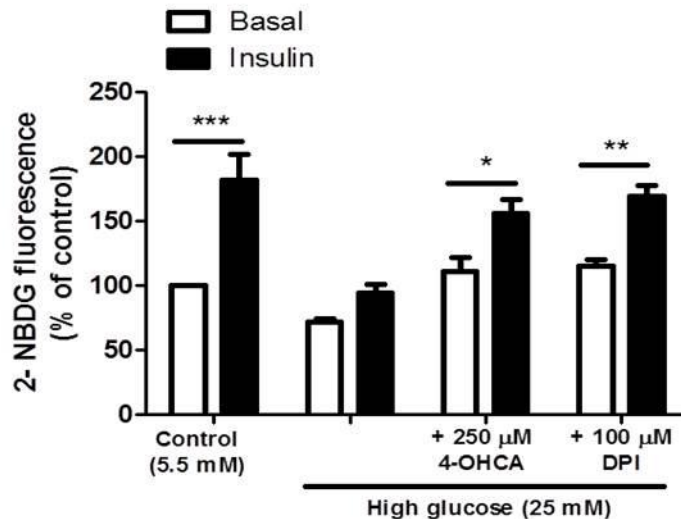


Figure 5.9 Enhanced glucose uptake upon inhibition of mitochondrial and NOX-derived ROS. H9c2 cells were subjected to 24 h high glucose conditions vs. controls \pm 1 h treatment with a) 250 μ M 4-OHCA (inhibits mitochondrial ROS), and b) DPI (NOX inhibitor). Flow cytometry analysis of 2-NBDG fluorescence. Values are expressed as mean \pm SEM (n=4). *P<0.05; **P<0.01; ***P<0.001 vs. indicated basal controls.

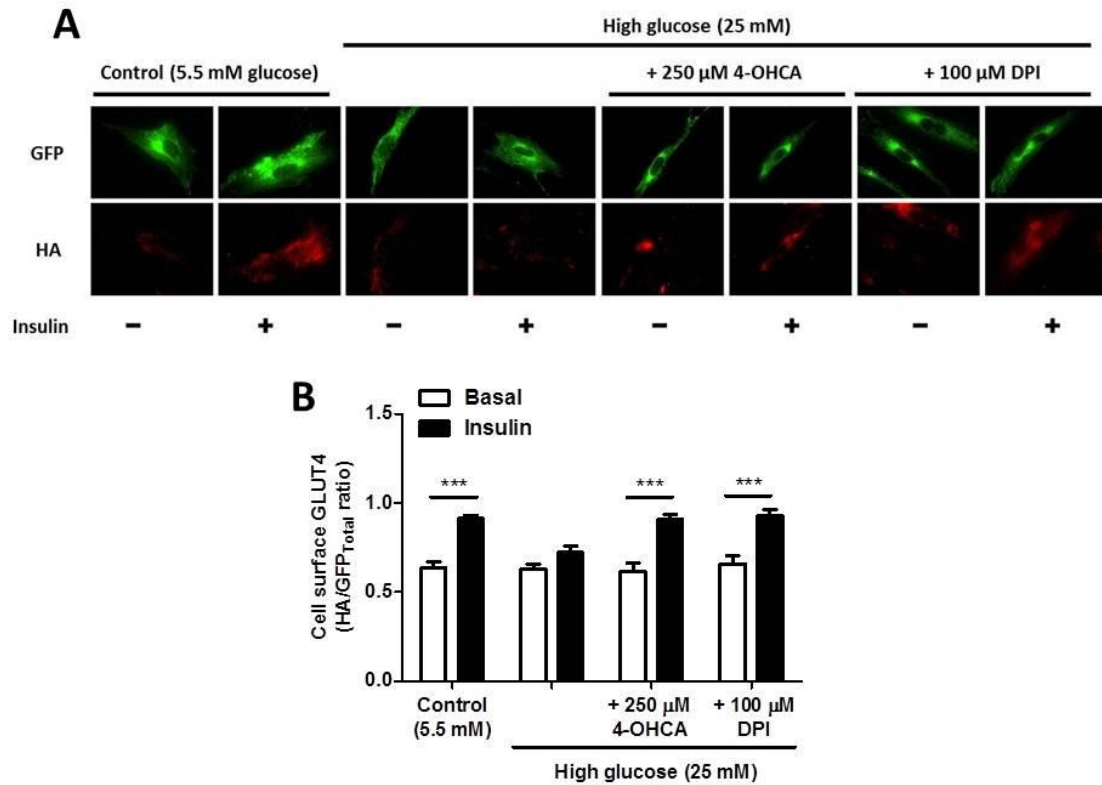


Figure 5.10 Attenuation of ROS (mitochondrial and NOX-derived) restored GLUT4 translocation. H9c2 cells were subjected to 24 h high glucose conditions vs. controls \pm 1 h treatment with a) 250 μ M 4-OHCA (inhibits mitochondrial ROS), and b) DPI (NOX inhibitor). (A) Fluorescence microscopy images of cells expressing HA-GLUT4-GFP with and without insulin stimulation. (B) Quantification of HA:GFP ratios. Values are expressed as mean \pm SEM ($n \geq 150$ cells from five independent experiments). *** $P < 0.001$ vs. respective basal control.

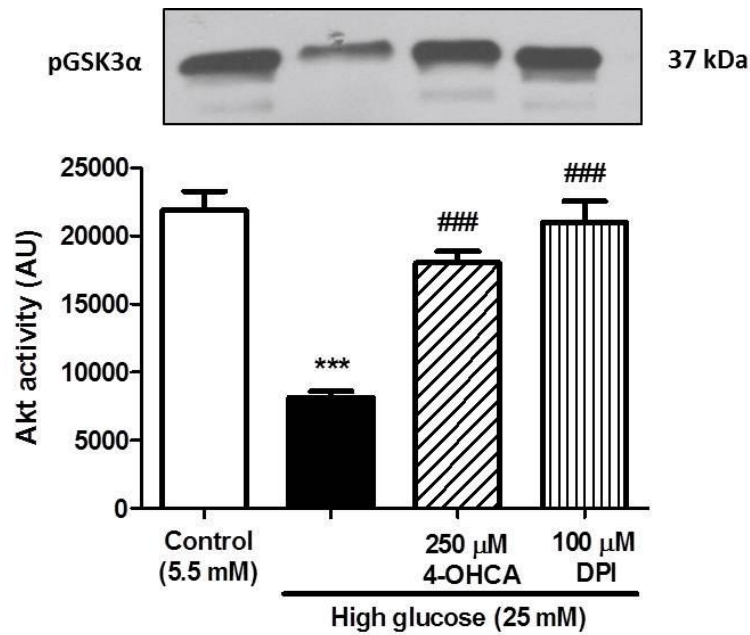


Figure 5.11 Regulation of Akt activity by mitochondrial and NOX-derived ROS. Cell free *in vitro* kinase activity of Akt was assessed by immunoprecipitation of Akt from H9c2 cells that were subjected to 24 h high glucose conditions vs. controls \pm 1 h treatment with a) 250 μ M 4-OHCA (inhibits mitochondrial ROS), and b) DPI (NOX inhibitor). Equal concentrations of the isolated Akt was exposed to the Akt substrate GSK3 α and ATP at 30°C, resulting in the Akt-catalyzed formation of phosphorylated GSK3 α and analysis of pGSK3 α by Western blotting (refer Section 4.5.3 for methodology). Values are expressed as mean \pm SEM (n=3). ***P<0.001 vs. control; ###P<0.001 vs. high glucose.

5.4.3. Attenuation of endogenous antioxidant systems under hyperglycemic conditions

To gain further understanding of the intracellular redox status, we next investigated the activity of intrinsic antioxidant defense systems. Superoxide dismutase (SOD) activity was reduced by high glucose by $42.4 \pm 6.7\%$ (P<0.001 vs. control), but this effect was markedly reversed by 4-OHCA (~2.6 fold) and DPI (~2.4 fold), respectively (P<0.001 vs. HG) (Fig 5.12).

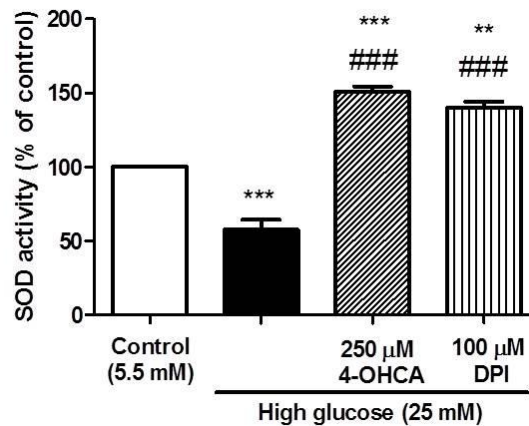


Figure 5.12 High glucose attenuated superoxide dismutase (SOD) activity. H9c2 cells were subjected to 24 h high glucose conditions vs. controls \pm 1 h treatment with a) 250 μ M 4-OHCA (inhibits mitochondrial ROS), and b) DPI (NOX inhibitor). Values are expressed as mean \pm SEM (n=6). **P<0.01, ***P<0.001 vs. control; ###P<0.001 vs. high glucose.

Total GSH levels were also lowered by high glucose (P<0.01 vs. control) (Fig 5.13B). The 4-OHCA treatment failed to increase GSH levels, while it was upregulated by DPI (P<0.001 vs. high glucose and P<0.001 vs. 4-OHCA). NADPH is an essential substrate to NOX (to produce ROS), and to the glutathione system (to replenish GSH pools and increase antioxidant defenses) (Fig 5.13A). The fate of intracellular NADPH and its role in the cell's redox status is a subject of much controversy. In light of our NOX and GSH data, we next determined the effects of high glucose \pm 4-OHCA \pm DPI on G6PD (a major producer of intracellular NADPH) activity, NADPH levels and the ratio of NADP⁺:NADPH. G6PD activity remained unaltered by high glucose and 4-OHCA treatment, while DPI increased it modestly (P<0.01 vs. 4-OHCA) (Fig 5.13C). Furthermore, inhibition of G6PD activity by treatment with 6-aminonicotinamide (6-AN, 100 μ M) mirrored the effect of high glucose on GSH levels (Fig 5.13D). In parallel, NADPH levels (Fig 5.13E) and the NADP⁺:NADPH ratio (Fig 5.13F) were unchanged by high glucose and 4-OHCA treatment, while DPI decreased NADPH levels (P<0.01 vs. HG). DPI treatment also increased the

NADP⁺:NADPH ratio (P<0.01 vs. 4-OHCA), indicative of higher NADPH turnover (Fig 5.13F).

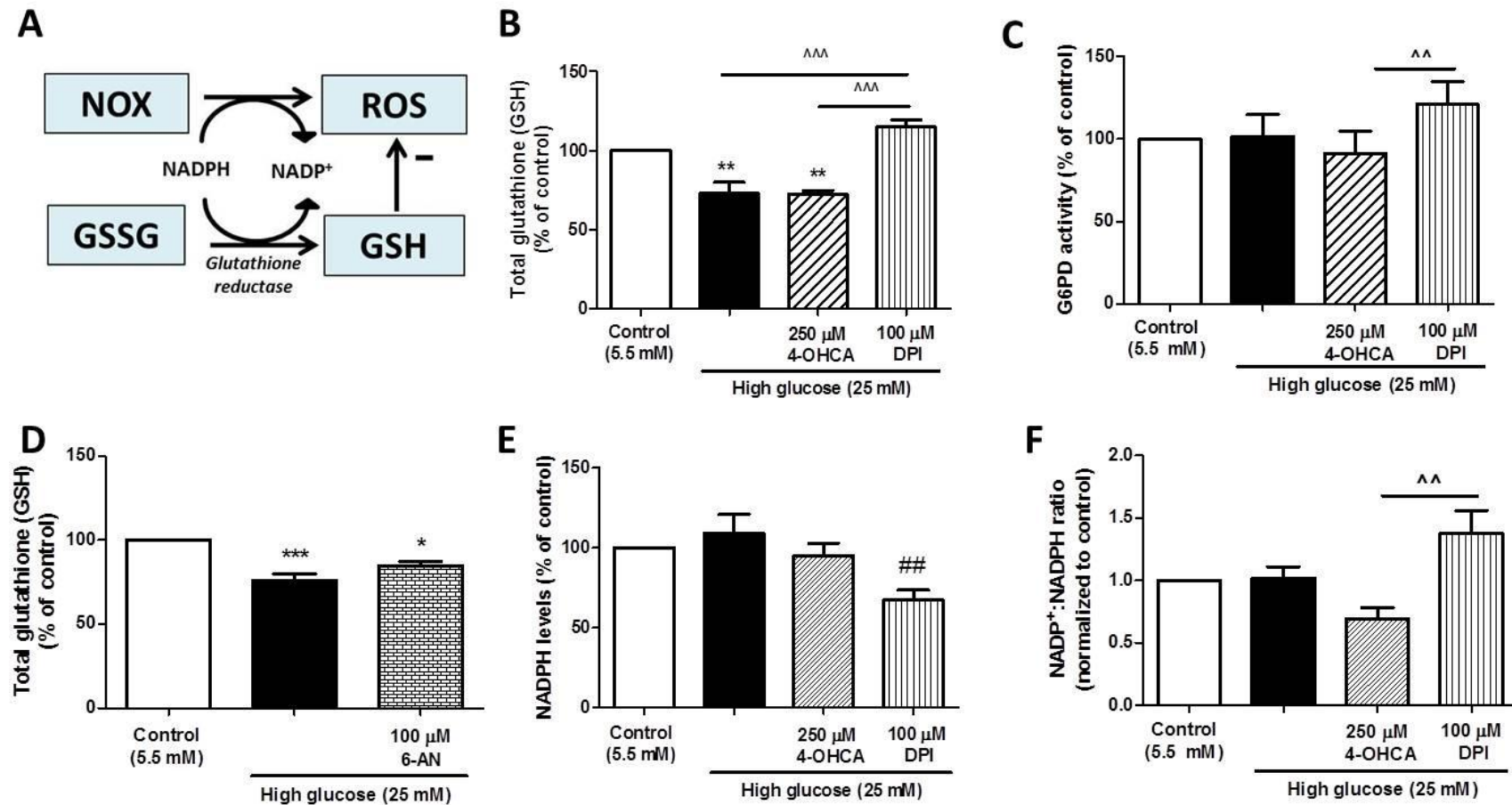


Figure 5.13 Attenuation of the glutathione replenishment system under high glucose conditions. H9c2 cells were subjected to 24 h high glucose conditions vs. controls ± 1 h treatment with a) 250 μM 4-OHCA (inhibits mitochondrial ROS), b) DPI (NOX inhibitor), 100 μM 6-aminonicotinamide (6-AN: G6PD inhibitor employed to test relevance of G6PD-mediated NADPH production). (A) Schematic representation of the reactions of NOX (leading to ROS formation) and replenishment of reduced glutathione (GSH; an intrinsic antioxidant), both requiring NADPH; (B and D) Glutathione levels; (C) G6PD activity; (E) NADPH levels; (F) NADP⁺:NADPH ratio. Values are expressed as mean ± SEM (n=6-9). *P<0.05, **P<0.01, ***P<0.001 vs. control; ##P<0.01, ###P<0.001 vs. high glucose; ^^P<0.01, ^^P<0.001 vs. indicated treatment.

Interestingly, markers of intracellular damage resulting from oxidative stress evaluated here, i.e. aconitase activity and the levels of malondialdehyde adducts, were unaltered in all experimental conditions (Fig 5.14).

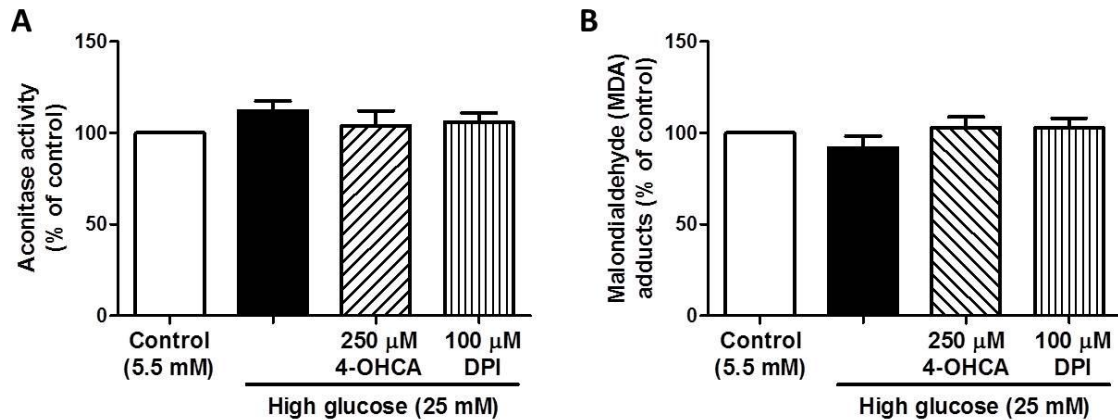


Figure 5.14 Intracellular markers of oxidative damage were unaltered. A: Aconitase activity; B: Malondialdehyde adducts.

5.5. Discussion

Excess nutrients (e.g. hyperglycemia) are key features of the metabolic syndrome and can play a significant part in the etiology of insulin resistance (de Moura *et al.*, 2009; Sharma *et al.*, 2007). Furthermore, myocardial insulin resistance can elicit detrimental consequences that eventually impact on cardiac metabolism and function (Barr *et al.*, 2007; Liao *et al.*, 2002; Rubin *et al.*, 2012; Tian and Abel, 2001). Acute hyperglycemic episodes *per se* may also contribute significantly to unfavorable outcomes after stroke and to impaired endothelial function in humans (Parsons *et al.*, 2002; Williams *et al.*, 1998). Furthermore, acute hyperglycemia may induce apoptosis in perfused rat hearts (Ceriello *et al.*, 2002; Mapanga *et al.*, 2013), while it is correlated with mortality in patients undergoing cardiac surgery (Doenst *et al.*, 2005).

However, a mechanistic link between acute hyperglycemic episodes and the etiology of insulin resistance is an important consideration that indeed warrants further attention.

Although oxidative stress is implicated in the etiology of insulin resistance, the mechanisms involved and its role in the acute hyperglycemic setting remain poorly understood. The current paradigm suggests that mitochondrial ROS function as a central mediator to link hyperglycemia-mediated defects to diabetic complications (Brownlee, 2005). This notion has, however, recently been revisited and new information raise additional questions regarding its validity (reviewed in Schaffer *et al.*, 2012). In light of this, we undertook to further investigate these concepts in an *in vitro* model of acute hyperglycemia. We used a novel, holistic approach to interrogate various pathways and mechanisms at one time point and under the same condition. The major finding of study I (outlined in this Chapter) is that *both* mitochondrial- and NOX-derived ROS are upregulated and may act in tandem to blunt cardiac insulin-mediated glucose uptake in response to acute hyperglycemia. Our findings therefore support a modification of the classic “unifying hypothesis” and sheds novel insights into the onset of acute hyperglycemia-mediated insulin resistance.

We initially set up an *in vitro* model of acute hyperglycemia where cardiomyoblasts displayed elevated ROS levels (total, mitochondrial and NOX-derived), and defective insulin action (glucose uptake, GLUT4 translocation and Akt kinase activity). These findings are in agreement with previous research, e.g. optimization of *in vitro* glucose levels reversed insulin resistance in skeletal muscle and adipose cells isolated from type 2 diabetic patients, demonstrating that hyperglycemia itself or in the presence of

high insulin levels is a potent initiator of insulin resistance (Burén *et al.*, 2003; Zierath *et al.*, 1994). Moreover, others established decreased glucose uptake accompanied by lower insulin receptor substrate 1 (IRS1) protein levels in adipocytes exposed to high glucose and insulin levels (Renström *et al.*, 2007). Isolated rat ventricular cardiomyocytes exposed to high glucose also displayed decreased glucose uptake and impaired insulin signaling and contractile function *in vitro* (Ren *et al.*, 1996, 2003).

Our data are also in agreement with studies done in our laboratory that showed increased ROS levels under hyperglycemic conditions (Mapanga *et al.*, 2012; Rajamani and Essop, 2010), while oxidative stress is associated with metabolic dysfunction in animals and humans *in vivo* (Furukawa *et al.*, 2004). Furthermore, previous studies determined that increased ROS production due to chronic hyperglycemia can lead to damaging cardio-metabolic complications. For example, elevated levels of 4-hydroxy-2-nonenal and protein/lipid peroxidation were found in patients and animal models of diabetes, while micro- and macrovascular complications can also arise from oxidative stress-induced alterations in vascular endothelial cells (Kawahito *et al.*, 2009; King and Loeken, 2004; Stentz *et al.*, 2004). Recent studies from our laboratory also showed higher levels of myocardial apoptosis and reduced cardiac function associated with hyperglycemia-mediated oxidative stress (Mapanga *et al.*, 2012; 2013, Rajamani and Essop, 2010; Rajamani *et al.*, 2011).

Oxidative stress is also implicated in the induction of insulin resistance in target tissues (e.g. adipose, skeletal muscle and liver) (Costford *et al.*, 2009; Gao *et al.*,

2010; Grimsrud *et al.*, 2007; Messner *et al.*, 2013; Ruskovska and Bernlohr, 2013). Here hyperglycemia-induced ROS can reduce GLUT4 translocation in 3T3-L1 adipocytes (Grimsrud *et al.*, 2007; Ruskovska and Bernlohr, 2013), and decrease insulin synthesis and secretion in pancreatic β -cells (Futamura *et al.*, 2012). Meigs and colleagues (2007) recently showed an association between oxidative stress and insulin resistance in participants at risk for diabetes in the Framingham offspring study (Meigs *et al.*, 2007). Tissue levels of oxidative stress markers were upregulated prior to the development of insulin resistance in rodents exposed to high fat feeding (Matsuzawa-Nagata *et al.*, 2008). Furthermore, employment of antioxidants *N*-acetyl cysteine, taurine and α -lipoic acid resulted in protection against oxidative stress-mediated insulin resistance and sensitized tissues and L6 myocytes to insulin action (Haber *et al.*, 2003; Maddux *et al.*, 2001).

The intracellular source(s) of ROS production - at the center of hyperglycemia-induced detrimental effects - is gaining considerable attention (as recently reviewed in Schaffer *et al.*, 2012). Hyperglycemia-mediated ROS production is generally proposed to have strong mitochondrial origins, i.e. the inhibition of mitochondrial respiratory complexes triggers excess superoxide generation, with deleterious downstream outcomes (known as the unifying hypothesis of hyperglycemic damage) (Brownlee, 2005; Giacco and Brownlee, 2010). Indeed, mitochondrial ROS production is associated with insulin resistance, with hydrogen peroxide playing a major role in disrupting several key mediators of insulin action (Anderson *et al.*, 2009; Fisher-Wellman and Neuffer, 2012). Mitochondrial dysfunction and defects in its morphology were reported in muscle tissue of diabetic patients and animal models (reviewed in Cheng *et al.*, 2010; Rabøl, 2011). Whether defects at the mitochondrial

level are causative factors, or a consequence of insulin resistance, is not yet clear (reviewed in Rabøl, 2011). Furthermore, additional sources of ROS may also play a significant role in the etiology of insulin resistance.

Since the NOX complex also acts as a key source of ROS production in cardiomyocytes (Balteau *et al.*, 2011; Brewer *et al.*, 2011; Li *et al.*, 2006; Santos *et al.*, 2011; Serpillon *et al.*, 2009), it emerges as another important regulator that may also orchestrate the detrimental effects of acute hyperglycemia. Our findings revealed that 4-OHCA and DPI treatment reversed the inhibitory effect of high glucose on insulin-stimulated glucose uptake, GLUT4 translocation and Akt activity, suggesting involvement of both mitochondrial and NOX-derived ROS. Intriguingly, NOX-derived ROS constituted the overwhelming majority of overall ROS generated by acute hyperglycemia. Furthermore, the mitochondrial ROS inhibitor (4-OHCA) also blunted NOX activity suggesting that the relatively low mitochondrial ROS levels can cross-talk with, and activate the NOX system in response to acute high glucose exposure. We propose that the initial modest increase in mitochondrial ROS may act as a trigger for downstream activation of NOX. This is further evident in the relatively equal effects of 4-OHCA and DPI treatment on total ROS, glucose uptake, GLUT4 translocation and Akt activity, despite the modest contribution of mitochondrial ROS. In support, a recent study determined that mitochondrial ROS (superoxide, hydrogen peroxide, peroxynitrite) can trigger NOX activation in phagocytic cells and vascular/cardiac tissues (Kröller-Schön *et al.*, 2013). NOX-mediated ROS can subsequently mediate detrimental effects, e.g. playing a role in cardiac contractile dysfunction leading to heart failure, while also promoting myocardial apoptosis (Balteau *et al.*, 2011; Serpillon *et al.*, 2009). Further investigation is warranted to

evaluate the validity of such a mechanism and to ascertain the molecular basis. Nevertheless, NOX activation alone may also play a significant role in the etiology of insulin resistance. For example, others found that Ang II- and high glucose-mediated NOX activation may play a role in diminishing insulin signaling events and reduce insulin-mediated glucose uptake and GLUT4 translocation (Ogihara *et al.*, 2002; Sloniger *et al.*, 2005; Wei *et al.*, 2006)

Since the overall degree of intracellular oxidative stress depends on both the production and removal of ROS, we next assessed intracellular antioxidant defense systems and found diminished SOD activity and GSH levels following high glucose treatment. Inhibition of both mitochondrial- and NOX-derived ROS markedly upregulated SOD activity, while only DPI (NOX inhibitor) increased GSH levels. We are unclear how exactly high glucose levels attenuate SOD activity. We propose that this may be the result of oxidative damage to the SOD enzyme, but further studies are required to confirm this.

Although replenishment of GSH pools (anti-oxidative) and NOX activity (pro-oxidative) are processes with opposite effects, both require NADPH as substrate (Serpillon *et al.*, 2009). However, the fate of intracellular NADPH with hyperglycemia is a subject of contention. Our data show higher NOX activity, oxidative stress and decreased GSH while activity of G6PD (a major source of NADPH), NADPH levels and the NADP⁺:NADPH ratio remained unaltered in response to acute high glucose exposure. However, NOX inhibition increased G6PD activity and GSH levels, while concomitantly attenuating NADPH levels. Thus our findings indicate that acute high glucose exposure drives NOX activation (and NADPH consumption) over

replenishment of GSH pools by G6PD and the PPP. Indeed, NOX-derived superoxide production is fueled by G6PD-mediated NADPH in Zucker fa/fa rats, a model of severe hyperglycemia and hyperlipidemia (Serpillon *et al.*, 2009). Although our data showed unchanged G6PD levels with acute hyperglycemia, previous studies found reduced G6PD, NADPH and GSH levels accompanied by oxidative stress in kidneys of streptozotocin-induced diabetic rats (Xu *et al.*, 2005). Furthermore, G6PD deficient (G6PDx) mice exposed to different obesogenic diets displayed metabolic dysfunction, however this was coupled to reduced oxidative stress (Hecker *et al.*, 2012).

We therefore postulate that the acute hyperglycemia in our system may reduce G6PD-mediated NADPH production, however, the limited NADPH levels may be utilized exclusively for NOX activation *versus* GSH formation. This mechanism may act as important cycle to promote oxidative stress, along with reduced SOD activity and increased ROS output by mitochondria and NOX. The markers of oxidative damage analyzed in this study (aconitase activity and MDA levels) were unchanged. This is in contrast to data showing its dysregulation with acute hyperglycemia (33 mM glucose) in *ex vivo* rat heart perfusion experiments (Mapanga *et al.*, 2013). We suggest that the ROS levels induced by high glucose (25 mM) in our *in vitro* system may be less severe to induce the reduction in aconitase activity and elevation in MDA levels indicative of damage by oxidative stress. The differences may also be attributable to the distinct models utilized to assess such markers. Together our findings demonstrate that greater oxidative stress with acute high glucose exposure occurs due to both higher ROS generation (mitochondrial- and NOX-derived) and an

impairment of defense mechanisms, that ultimately blunts insulin-mediated glucose uptake.

In conclusion, our data support the hypothesis that oxidative stress related to acute hyperglycemia may play a significant role in the dysregulation of insulin action in cardiac-derived cells. We propose that *both* mitochondrial and NOX-derived ROS play a role here. Furthermore we describe two mechanisms that may considerably contribute to the observed levels of intracellular ROS. Firstly, a modest increase in mitochondrial ROS may act as a triggering mechanism leading to the activation of downstream events, including NOX activation which may result in further upregulation of ROS levels. Secondly, the increased activation of NOX may favor NADPH utilization, leading to decreased replenishment of GSH pools. This mechanism together with decreased SOD activity will further promote intracellular oxidative stress. The molecular link(s) between hyperglycemia-mediated ROS production and diminished insulin action are beyond the scope of this chapter, but will be addressed in the next chapter.

5.6. References

- Anderson, E.J., Lustig, M.E., Boyle, K.E., Woodlief, T.L., Kane, D.A., Lin, C.-T., Price, J.W., Kang, L., Rabinovitch, P.S., Szeto, H.H., Houmard, J.A., Cortright, R.N., Wasserman, D.H., Neuffer, P.D., 2009. Mitochondrial H₂O₂ emission and cellular redox state link excess fat intake to insulin resistance in both rodents and humans. *J Clin Invest* 119, 573–81.
- Balteau, M., Tajeddine, N., De Meester, C., Ginion, A., Des Rosiers, C., Brady, N.R., Sommereyns, C., Horman, S., Vanoverschelde, J.-L., Gailly, P., Hue, L., Bertrand, L., Beauloye, C., 2011. NADPH oxidase activation by hyperglycaemia in cardiomyocytes is independent of glucose metabolism but requires SGLT1. *Cardiovasc Res* 92, 237–46.
- Barr, E.L.M., Zimmet, P.Z., Welborn, T.A., Jolley, D., Magliano, D.J., Dunstan, D.W., Cameron, A.J., Dwyer, T., Taylor, H.R., Tonkin, A.M., Wong, T.Y., McNeil, J., Shaw, J.E., 2007. Risk of cardiovascular and all-cause mortality in individuals with diabetes mellitus, impaired fasting glucose, and impaired glucose tolerance: the Australian Diabetes, Obesity, and Lifestyle Study (AusDiab). *Circulation* 116, 151–7.
- Brewer, A.C., Murray, T.V.A., Arno, M., Zhang, M., Anilkumar, N.P., Mann, G.E., Shah, A.M., 2011. Nox4 regulates Nrf2 and glutathione redox in cardiomyocytes in vivo. *Free Radic Biol Med* 51, 205–15.
- Brownlee, M., 2005. The pathobiology of diabetic complications: a unifying mechanism. *Diabetes* 54, 1615–25.
- Burén, J., Lindmark, S., Renström, F., Eriksson, J.W., 2003. In vitro reversal of hyperglycemia normalizes insulin action in fat cells from type 2 diabetes patients: is cellular insulin resistance caused by glucotoxicity in vivo? *Metabolism* 52, 239–45.
- Ceriello, A., Quagliaro, L., D'Amico, M., Di Filippo, C., Marfella, R., Nappo, F., Berrino, L., Rossi, F., Giugliano, D., 2002. Acute hyperglycemia induces nitrotyrosine formation and apoptosis in perfused heart from rat. *Diabetes* 51, 1076–82.
- Chavali, V., Tyagi, S.C., Mishra, P.K., 2013. Predictors and prevention of diabetic cardiomyopathy. *Diabetes Metab Syndr Obes* 6, 151–60.
- Cheng, Z., Tseng, Y., White, M.F., 2010. Insulin signaling meets mitochondria in metabolism. *Trends Endocrinol Metab* 21, 589–98.
- Chiha, M., Njeim, M., Chedrawy, E.G., 2012. Diabetes and coronary heart disease: a risk factor for the global epidemic. *Int J Hypertens* 2012, 697240.
- Costford, S.R., Crawford, S.A., Dent, R., McPherson, R., Harper, M.-E., 2009. Increased susceptibility to oxidative damage in post-diabetic human myotubes. *Diabetologia* 52, 2405–2415.
- Cross, A.R., Jones, O.T., 1986. The effect of the inhibitor diphenylene iodonium on the superoxide-generating system of neutrophils. Specific labelling of a component polypeptide of the oxidase. *Biochem J* 237, 111–6.

- De Moura, R.F., Ribeiro, C., de Oliveira, J.A., Stevanato, E., de Mello, M.A.R., Moura, R.F. De, Oliveira, J.A. De, Alice, M., Mello, R. De, 2009. Metabolic syndrome signs in Wistar rats submitted to different high-fructose ingestion protocols. *Br J Nutr* 101, 1178–84.
- Doenst, T., Wijeyesundera, D., Karkouti, K., Zechner, C., Maganti, M., Rao, V., Borger, M.A., 2005. Hyperglycemia during cardiopulmonary bypass is an independent risk factor for mortality in patients undergoing cardiac surgery. *J Thorac Cardiovasc Surg* 130, 1144.
- Du, X., Matsumura, T., Edelstein, D., Rossetti, L., Zsengellér, Z., Szabó, C., Brownlee, M., 2003. Inhibition of GAPDH activity by poly(ADP-ribose) polymerase activates three major pathways of hyperglycemic damage in endothelial cells. *J Clin Invest* 112, 1049–57.
- Eriksson, J.W., 2007. Metabolic stress in insulin's target cells leads to ROS accumulation - a hypothetical common pathway causing insulin resistance. *FEBS Lett* 581, 3734–42.
- Fisher-Wellman, K.H., Neuffer, P.D., 2012. Linking mitochondrial bioenergetics to insulin resistance via redox biology. *Trends Endocrinol Metab* 23, 142–53.
- Furukawa, S., Fujita, T., Shimabukuro, M., Iwaki, M., Yamada, Y., Nakajima, Y., Nakayama, O., Makishima, M., Matsuda, M., Shimomura, I., 2004. Increased oxidative stress in obesity and its impact on metabolic syndrome. *J Clin Invest* 114, 1752–61.
- Futamura, M., Yao, J., Li, X., Bergeron, R., Tran, J.-L., Zycband, E., Woods, J., Zhu, Y., Shao, Q., Maruki-Uchida, H., Goto-Shimazaki, H., Langdon, R.B., Erion, M.D., Eiki, J., Zhou, Y.-P., 2012. Chronic treatment with a glucokinase activator delays the onset of hyperglycaemia and preserves beta cell mass in the Zucker diabetic fatty rat. *Diabetologia* 55, 1071–80.
- Gao, D., Nong, S., Huang, X., Lu, Y., Zhao, H., Lin, Y., Man, Y., Wang, S., Yang, J., Li, J., 2010. The effects of palmitate on hepatic insulin resistance are mediated by NADPH Oxidase 3-derived reactive oxygen species through JNK and p38MAPK pathways. *J Biol Chem* 285, 29965–73.
- Giaccari, A., Sorice, G., Muscogiuri, G., 2009. Glucose toxicity: the leading actor in the pathogenesis and clinical history of type 2 diabetes - mechanisms and potentials for treatment. *Nutr Metab Cardiovasc Dis* 19, 365–77.
- Giacco, F., Brownlee, M., 2010. Oxidative stress and diabetic complications. *Circ Res* 107, 1058–70.
- Grimsrud, P.A., Picklo, M.J., Griffin, T.J., Bernlohr, D.A., 2007. Carbonylation of adipose proteins in obesity and insulin resistance: identification of adipocyte fatty acid-binding protein as a cellular target of 4-hydroxynonenal. *Mol Cell Proteomics* 6, 624–37.
- Gustafsson, I., Brendorp, B., Seibaek, M., Burchardt, H., Hildebrandt, P., Køber, L., Torp-Pedersen, C., 2004. Influence of diabetes and diabetes-gender interaction on the risk of death in patients hospitalized with congestive heart failure. *J Am Coll Cardiol* 43, 771–7.
- Haber, C.A., Lam, T.K.T., Yu, Z., Gupta, N., Goh, T., Bogdanovic, E., Giacca, A., Fantus, I.G., 2003. N-acetylcysteine and taurine prevent hyperglycemia-induced insulin resistance in vivo: possible role of oxidative stress. *Am J Physiol Endocrinol Metab* 285, E744–53.

- Halestrap, A.P., Denton, R.M., 1975. The specificity and metabolic implications of the inhibition of pyruvate transport in isolated mitochondria and intact tissue preparations by alpha-Cyano-4-hydroxycinnamate and related compounds. *Biochem J* 148, 97–106.
- Hecker, P.A., Mapanga, R.F., Kimar, C.P., Ribeiro, R.F., Brown, B.H., O'Connell, K.A., Cox, J.W., Shekar, K.C., Asemu, G., Essop, M.F., Stanley, W.C., 2012. Effects of glucose-6-phosphate dehydrogenase deficiency on the metabolic and cardiac responses to obesogenic or high-fructose diets. *Am J Physiol Endocrinol Metab* 303, E959–72.
- Kawahito, S., Kitahata, H., Oshita, S., 2009. Problems associated with glucose toxicity: role of hyperglycemia-induced oxidative stress. *World J Gastroenterol* 15, 4137–42.
- King, G.L., Loeken, M.R., 2004. Hyperglycemia-induced oxidative stress in diabetic complications. *Histochem Cell Biol* 122, 333–8.
- Kröller-Schön, S., Steven, S., Kossmann, S., Scholz, A., Daub, S., Oelze, M., Xia, N., Hausding, M., Mikhed, Y., Zinßius, E., Mader, M., Stamm, P., Treiber, N., Scharffetter-Kochanek, K., Li, H., Schulz, E., Wenzel, P., Münzel, T., Daiber, A., 2013. Molecular mechanisms of the crosstalk between mitochondria and NADPH oxidase through reactive oxygen species - studies in white blood cells and in animal models. *Antioxid Redox Signal* 214, 311–312.
- Li, J., Stouffs, M., Serrander, L., Banfi, B., Bettioli, E., Charnay, Y., Steger, K., Krause, K., Jaconi, M.E., 2006. The NADPH oxidase NOX4 drives cardiac differentiation: role in regulating cardiac transcription factors and MAP kinase activation. *Mol Biol Cell* 17, 3978–3988.
- Liao, R., Jain, M., Cui, L., D'Agostino, J., Aiello, F., Luptak, I., Ngoy, S., Mortensen, R.M., Tian, R., 2002. Cardiac-specific overexpression of GLUT1 prevents the development of heart failure attributable to pressure overload in mice. *Circulation* 106, 2125–2131.
- Maddux, B.A., See, W., Lawrence, J.C., Goldfine, A.L., Goldfine, I.D., Evans, J.L., 2001. Protection Against Oxidative Stress-Induced Insulin Resistance in Rat L6 Muscle Cells by Micromolar Concentrations of α -Lipoic Acid. *Diabetes* 50, 404–410.
- Mapanga, R.F., Joseph, D., Symington, B., Garson, K.-L., Kimar, C., Kelly-Laubscher, R., Essop, M.F., 2013. Detrimental effects of acute hyperglycaemia on the rat heart. *Acta Physiol (Oxf)* n/a–n/a.
- Mapanga, R.F., Rajamani, U., Dlamini, N., Zungu-Edmondson, M., Kelly-Laubscher, R., Shafiullah, M., Wahab, A., Hasan, M.Y., Fahim, M. a, Rondeau, P., Bourdon, E., Essop, M.F., 2012. Oleanolic acid: a novel cardioprotective agent that blunts hyperglycemia-induced contractile dysfunction. *PLoS One* 7, e47322.
- Matsuzawa-Nagata, N., Takamura, T., Ando, H., Nakamura, S., Kurita, S., Misu, H., Ota, T., Yokoyama, M., Honda, M., Miyamoto, K., Kaneko, S., 2008. Increased oxidative stress precedes the onset of high-fat diet-induced insulin resistance and obesity. *Metabolism* 57, 1071–1077.
- Meigs, J.B., Larson, M.G., Fox, C.S., Keaney, J.F., Vasan, R.S., Benjamin, E.J., 2007. Association of oxidative stress, insulin resistance, and diabetes risk phenotypes: the Framingham Offspring Study. *Diabetes Care* 30, 2529–35.

- Messner, D.J., Rhieu, B.H., Kowdley, K. V, 2013. Iron overload causes oxidative stress and impaired insulin signaling in AML-12 hepatocytes. *Dig Dis Sci* 58, 1899–908.
- Nishikawa, T., Edelstein, D., Du, X.L., Yamagishi, S., Matsumura, T., Kaneda, Y., Yorek, M.A., Beebe, D., Oates, P.J., Hammes, H.P., Giardino, I., Brownlee, M., 2000. Normalizing mitochondrial superoxide production blocks three pathways of hyperglycaemic damage. *Nature* 404, 787–90.
- O'Donnell, B. V, Tew, D.G., Jones, O.T., England, P.J., 1993. Studies on the inhibitory mechanism of iodonium compounds with special reference to neutrophil NADPH oxidase. *Biochem J* 290, 41–9.
- Ogihara, T., Asano, T., Ando, K., Chiba, Y., Sakoda, H., Anai, M., Shojima, N., Ono, H., Onishi, Y., Fujishiro, M., Katagiri, H., Fukushima, Y., Kikuchi, M., Noguchi, N., Aburatani, H., Komuro, I., Fujita, T., 2002. Angiotensin II-induced insulin resistance is associated with enhanced insulin signaling. *Hypertension* 40, 872–9.
- Parsons, M.W., Barber, P.A., Desmond, P.M., Baird, T. a, Darby, D.G., Byrnes, G., Tress, B.M., Davis, S.M., 2002. Acute hyperglycemia adversely affects stroke outcome: a magnetic resonance imaging and spectroscopy study. *Ann Neurol* 52, 20–8.
- Rabøl, R., 2011. Mitochondrial function in skeletal muscle in type 2 diabetes. *Dan Med Bull* 58, B4272.
- Radke, P.W., Schunkert, H., 2008. Glucose-lowering therapy after myocardial infarction: more questions than answers. *Eur Hear J* 29, 141–143.
- Rajamani, U., Essop, M.F., 2010. Hyperglycemia-mediated activation of the hexosamine biosynthetic pathway results in myocardial apoptosis. *Am J Physiol Cell Physiol* 299, C139–47.
- Rajamani, U., Joseph, D., Roux, S., Essop, M.F., 2011. The hexosamine biosynthetic pathway can mediate myocardial apoptosis in a rat model of diet-induced insulin resistance. *Acta Physiol* 202, 151–7.
- Ren, J., Dominguez, L.J., Sowers, J.R., Davidoff, A.J., 1996. Troglitazone attenuates high-glucose-induced abnormalities in relaxation and intracellular calcium in rat ventricular myocytes. *Diabetes* 45, 1822–5.
- Ren, J., Duan, J., Hintz, K.K., Ren, B.H., 2003. High glucose induces cardiac insulin-like growth factor I resistance in ventricular myocytes: role of Akt and ERK activation. *Cardiovasc Res* 57, 738–48.
- Renström, F., Burén, J., Svensson, M., Eriksson, J.W., 2007. Insulin resistance induced by high glucose and high insulin precedes insulin receptor substrate 1 protein depletion in human adipocytes. *Metabolism* 56, 190–8.
- Rubin, J., Matsushita, K., Ballantyne, C.M., Hoogeveen, R., Coresh, J., Selvin, E., 2012. Chronic hyperglycemia and subclinical myocardial injury. *J Am Coll Cardiol* 59, 484–9.
- Ruskovska, T., Bernlohr, D.A., 2013. Oxidative stress and protein carbonylation in adipose tissue - Implications for insulin resistance and diabetes mellitus. *J Proteomics* 1820, 1–9.

- Santos, C.X.C., Anilkumar, N., Zhang, M., Brewer, A.C., Shah, A.M., 2011. Redox signaling in cardiac myocytes. *Free Radic Biol Med* 50, 777–93.
- Schaffer, S.W., Jong, C.J., Mozaffari, M., 2012. Role of oxidative stress in diabetes-mediated vascular dysfunction: unifying hypothesis of diabetes revisited. *Vasc Pharmacol* 57, 139–49.
- Serpillon, S., Floyd, B.C., Gupte, R.S., George, S., Kozicky, M., Neito, V., Recchia, F., Stanley, W., Wolin, M.S., Gupte, S.A., 2009. Superoxide production by NAD(P)H oxidase and mitochondria is increased in genetically obese and hyperglycemic rat heart and aorta before the development of cardiac dysfunction. The role of glucose-6-phosphate dehydrogenase-derived NADPH. *Am J Physiol Hear Circ Physiol* 297, H153–62.
- Sharma, N., Okere, I.C., Duda, M.K., Chess, D.J., O’Shea, K.M., Stanley, W.C., 2007. Potential impact of carbohydrate and fat intake on pathological left ventricular hypertrophy. *Cardiovasc Res* 73, 257–68.
- Sloniger, J.A., Saengsirisuwan, V., Diehl, C.J., Dokken, B.B., Lailerd, N., Lemieux, A.M., Kim, J.S., Henriksen, E.J., 2005. Defective insulin signaling in skeletal muscle of the hypertensive TG(mREN2)27 rat. *Am J Physiol Endocrinol Metab* 288, E1074–81.
- Stentz, F.B., Umpierrez, G.E., Cuervo, R., Kitabchi, A.E., 2004. Proinflammatory cytokines, markers of cardiovascular risks, oxidative stress, and lipid peroxidation in patients with hyperglycemic crises. *Diabetes* 53, 2079–86.
- Tian, R., Abel, E.D., 2001. Responses of GLUT4-Deficient Hearts to Ischemia Underscore the Importance of Glycolysis. *Circulation* 103, 2961–2966.
- Wei, Y., Sowers, J.R., Nistala, R., Gong, H., Uptergrove, G.M.-E., Clark, S.E., Morris, E.M., Szary, N., Manrique, C., Stump, C.S., 2006. Angiotensin II-induced NADPH oxidase activation impairs insulin signaling in skeletal muscle cells. *J Biol Chem* 281, 35137–46.
- Williams, S.B., Goldfine, A.B., Timimi, F.K., Ting, H.H., Roddy, M.A., Simonson, D.C., Creager, M.A., 1998. Acute hyperglycemia attenuates endothelium-dependent vasodilation in humans in vivo. *Circulation* 97, 1695–701.
- Xu, Y., Osborne, B.W., Stanton, R.C., 2005. Diabetes causes inhibition of glucose-6-phosphate dehydrogenase via activation of PKA, which contributes to oxidative stress in rat kidney cortex. *Am J Physiol Renal Physiol* 289, F1040–7.
- Zierath, J.R., Galuska, D., Nolte, L.A., Thörne, A., Kristensen, J.S., Wallberg-Henriksson, H., 1994. Effects of glycaemia on glucose transport in isolated skeletal muscle from patients with NIDDM: in vitro reversal of muscular insulin resistance. *Diabetologia* 37, 270–7.

CHAPTER 6

Study II: Metabolic alterations of acute hyperglycemia – role of non-oxidative glucose pathways in insulin resistance.

6.1. Introduction

Insulin resistance has a complex and multifactorial etiology with many factors contributing to its induction (Petersen and Shulman, 2006). Dietary fuel overabundance and excess lipid and glucose availability associated with metabolic dysfunction, may all play a role in its onset (Kawahito *et al.*, 2009; Sharma *et al.*, 2007a, 2007b; Tappy and Lê, 2010). The impact of chronic diabetes-associated hyperglycemia in the long term is known to have far reaching pathophysiologic effects (Brownlee, 2005; Du *et al.*, 2001; Kawahito *et al.*, 2009; King and Brownlee, 1996; King and Loeken, 2004; Rösen *et al.*, 2001). Of particular importance here are the adverse cardio-metabolic defects associated with diabetes. The mechanisms of myocardial insulin resistance and its impact on cardiac function is not completely understood. Moreover, it is important to consider the mechanisms at the center of insulin resistance onset in order to assess and implement preventative therapeutic strategies before too much damage is done. On a broader scale, metabolic dysregulation in obesity, metabolic syndrome, pre-diabetes and poor dietary and lifestyle habits may all contribute to the etiology of insulin resistance (Stumvoll *et al.*, 2005). It is our opinion, that acute hyperglycemia is a common downstream factor at the center of detrimental outcomes in this case. In light of this, we therefore undertook to investigate the effects of acute hyperglycemia on insulin resistance in

cardiac-derived cells, and to elucidate metabolic mechanisms that may orchestrate this.

In Chapter 5 we described an important role for both mitochondrial- and NOX-derived ROS production, along with mechanisms contributing to overall oxidative stress, in the impairment of glucose uptake under acute hyperglycemic conditions. We now aimed to further evaluate downstream mechanisms that may play important roles in mediating the damaging outcomes of high glucose. A widely held model is that elevation of mitochondrial-derived ROS causes DNA damage, and the subsequent release of PARP (as a restorative mechanism) can also inhibit GAPDH, thereby reducing glycolytic flux (Du *et al.*, 2003; Nishikawa *et al.*, 2000). Glucose metabolites are subsequently diverted into NOGPs (AGE, PKC, polyol pathway and HBP). This unifying hypothesis is proposed as a central mediator of harmful vascular complications associated with diabetes (reviewed in Brownlee, 2005; Giaccari *et al.*, 2009; Giacco and Brownlee, 2010). The contribution of additional mechanisms can, however, not be overlooked. Indeed, the unifying hypothesis is currently under the spotlight and alternative mechanisms also put forward (reviewed in Schaffer *et al.*, 2012). In agreement, our data from Chapter 5 show the importance of *both* mitochondrial- and NOX-derived ROS in exerting high glucose-mediated insulin resistance. In this chapter we aim to evaluate the contribution of ROS (from the sources identified before) in the induction of NOGPs and its downstream effects. We hypothesized that ROS from mitochondria and NOX, and specifically the cross-talk mechanisms identified in Chapter 5, contribute significantly to NOGP induction. Furthermore, this may serve as a molecular link to the diminished insulin action observed under acute hyperglycemic conditions.

6.2. Aims

The aims for this study were to determine the effect of hyperglycemia-induced ROS production (both mitochondrial- and NOX-derived) on NOGP induction and to assess possible links between NOGP induction and insulin resistance. Furthermore, we aimed to evaluate mechanisms of pathway cross-talk, the role of NOGP induction, and possible downstream molecular events linking ROS, NOGP induction and diminished insulin action.

6.3. Modulators

The involvement of the four NOGPs was assessed using pharmacological inhibitors to target key mediators of each respective pathway (Fig 6.1). Here we employed 100 μ M aminoguanidine (AMG; inhibits AGE precursors), 5 μ M chelerythrine (CHE; PKC inhibitor), 40 μ M 6-diazo 5-oxo-L-norleucine (DON; HBP inhibitor), and 10 μ M zopolrestat (ZOP; polyol pathway inhibitor) (refer Section 4.3 and Figs 4.1 and 4.2 for description of the methodology employed). The transketolase co-factor and activator benfotiamine (BFT) was employed to evaluate the influence of the pentose phosphate pathway (PPP) (Hammes *et al.*, 2003). This served as an additional means of collectively diminishing NOGP induction as shown in previous studies (Babaei-Jadidi *et al.*, 2003; Balakumar *et al.*, 2010; Beltramo *et al.*, 2008; Berrone *et al.*, 2006; Ceylan-Isik *et al.*, 2006; Hammes *et al.*, 2003; Katare *et al.*, 2010a, 2010b; Lin *et al.*, 1998; Wu and Ren, 2006). Inhibitor concentrations were selected based on previous studies (Chmura *et al.*, 2000; Davidoff *et al.*, 2004; Kador *et al.*, 2009; Rajamani and Essop, 2010; Rohr *et al.*, 1999; Wang *et al.*, 2010).

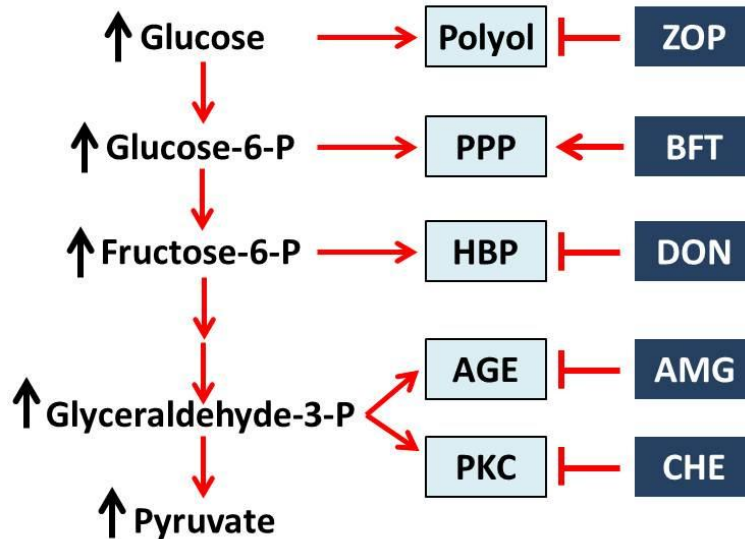


Figure 6.1 Modulators used to inhibit NOGPs. Zopolrestat (ZOP) – polyol pathway inhibitor, benfotiamine (BFT) – activates PPP, 6-diazo-5-oxo-L-norleucine (DON) – inhibits HBP, aminoguanidine (AMG) – AGE inhibitor, chelerythrine (CHE) – PKC inhibitor.

6.4. Results

6.4.1. Glucose metabolic alterations are mediated by mitochondrial and NOX-derived ROS

To gain an understanding regarding the intracellular metabolic milieu, we first set out to determine intracellular ATP levels as a measure of the cell's ability to couple fuel availability to energy production. High glucose treatment had no significant effect on total intracellular ATP levels (Fig 6.2). On the other hand, inhibition of both mitochondrial ROS (4-OHCA) and NOX activity (DPI) significantly reduced ATP levels by $82.7 \pm 2.7\%$ ($P < 0.001$ vs. high glucose) and $39.4 \pm 2.7\%$ ($P < 0.001$ vs. high glucose) respectively. These effects were also lower than the control values ($P < 0.001$ for 4-OHCA and $P < 0.05$ for DPI), while the more pronounced inhibitory

effect of 4-OHCA treatment resulted in a ~43% difference compared to DPI treatment ($P < 0.001$).

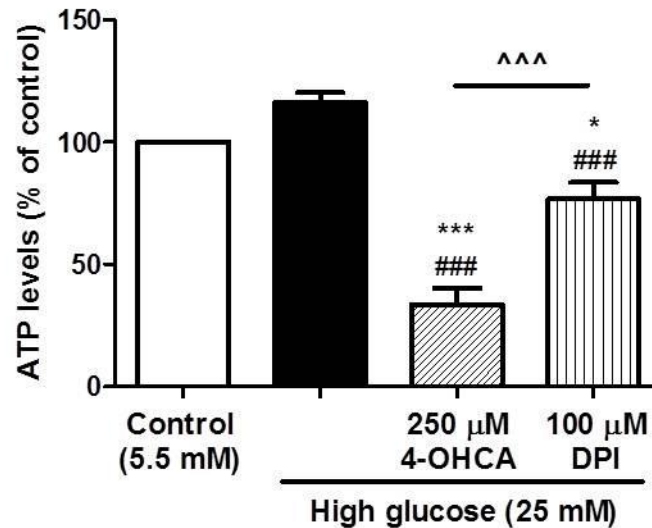


Figure 6.2 Intracellular ATP levels were reduced by ROS modulation. H9c2 cells were treated acutely with a) 4-OHCA and b) DPI under acute high glucose conditions. Values are expressed as mean \pm SEM (n=6). * $P < 0.05$, *** $P < 0.001$ vs. control; ### $P < 0.001$ vs. high glucose; ^^^ $P < 0.001$ vs. indicated treatment.

We next determined the effects of acute high glucose on NOGP activation. Acute high glucose treatment increased NOGP markers, i.e. methylglyoxal and sorbitol levels ($P < 0.001$ vs. controls, Fig 6.3A and B), and PKC activity ($P < 0.01$ vs. control, Fig 6.3C). However, transketolase activity remained unchanged under high glucose conditions, but was reduced following 4-OHCA ($P < 0.01$ vs. control, $P < 0.05$ vs. high glucose) and DPI administration ($P < 0.001$ vs. control, $P < 0.001$ vs. high glucose) (Fig 6.3D). We also found higher levels of intracellular O-GlcNAc modification [$P < 0.01$ vs. control, Fig 6.3E (ii and iv)]. Here, we employed fluorescence microscopy analysis of O-GlcNAc stained cells [Fig 6.3E (i and ii)], and Western blot analysis of total O-GlcNAc moieties from crude cell lysates [Fig 6.3E (iii and iv)]. Both 4-OHCA and DPI reduced methylglyoxal levels, PKC activity ($P < 0.001$ vs. high glucose), sorbitol levels

($P < 0.01$ vs. control, $P < 0.001$ vs. high glucose) and O-GlcNAc modification ($P < 0.001$ vs. high glucose – fluorescence microscopy; $P < 0.01$ vs. high glucose – Western blots).

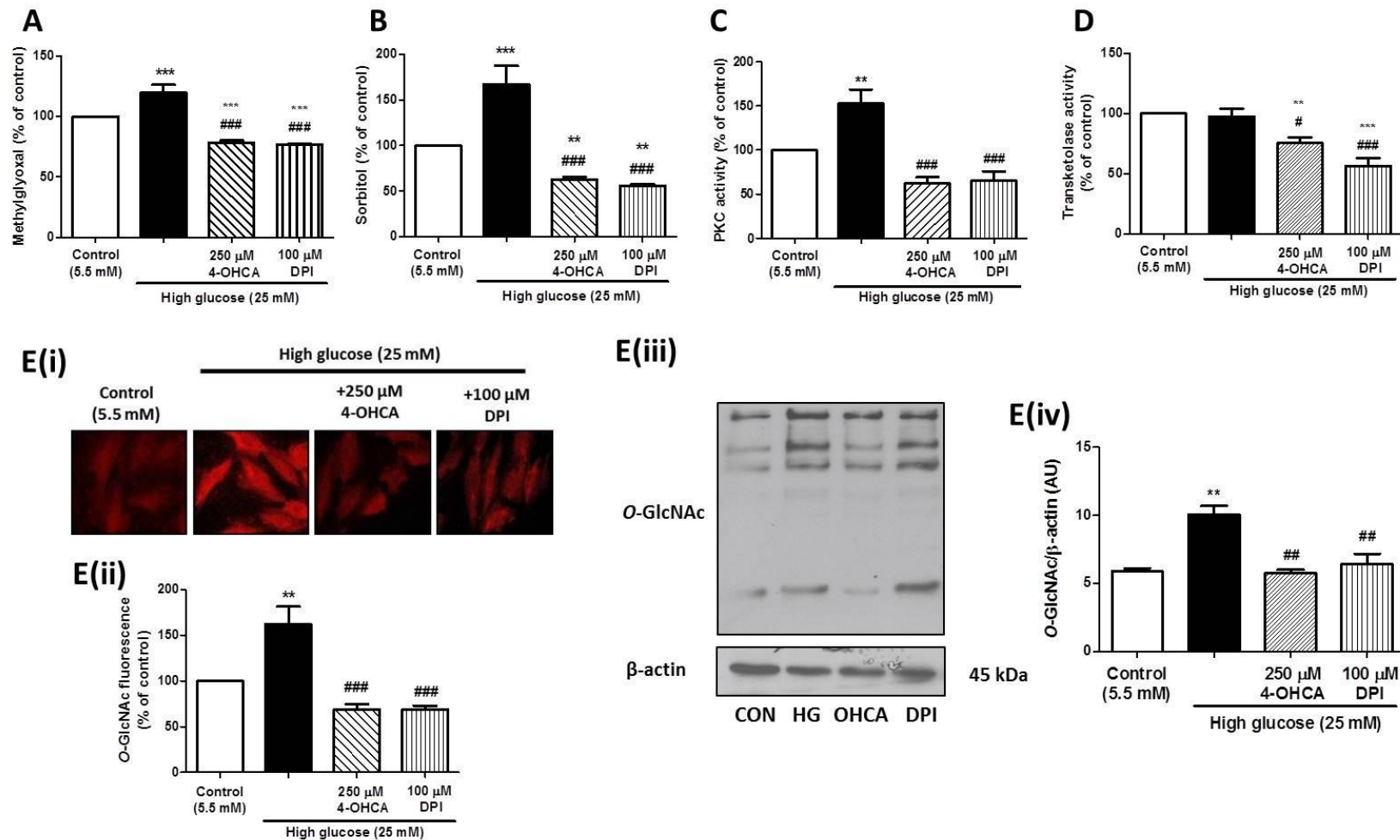


Figure 6.3 Metabolic alterations under acute high glucose conditions were mediated by ROS. H9c2 cells were subjected to 24 h high glucose conditions vs. controls ± a) 250 μM 4-OHCA (inhibits mitochondrial ROS), and b) DPI (NOX inhibitor). (A) Methylglyoxal levels (AGE pathway), (B) Sorbitol levels (polyol pathway), (C) PKC activity, (D) Transketolase activity (non-oxidative PPP), (Ei and ii) Immunofluorescence microscopy and quantification of total intracellular O-GlcNAc-modified proteins, (Eiii and iv) Western blot and quantification of O-GlcNAc-modified proteins (HBP), with densitometry values normalized to respective β-actin. Values are expressed as mean ± SEM (n=4-6). **P<0.01, ***P<0.001 vs. control; #P<0.05, ##P<0.01, ###P<0.001 vs. high glucose.

In an effort to understand the relative pathway induction under high glucose conditions, we next calculated the mean difference between controls and high glucose treated groups for each NOGP marker analyzed above (Fig. 6.4). The approximate percentage induction of each pathway according to the markers evaluated is expressed. Here, the polyol, PKC and HBP were more rigorously upregulated, with approximately 67%, 63% and 57% induction, respectively. AGE induction was increased by approximately 19%, while PPP (transketolase activity) was unaltered.

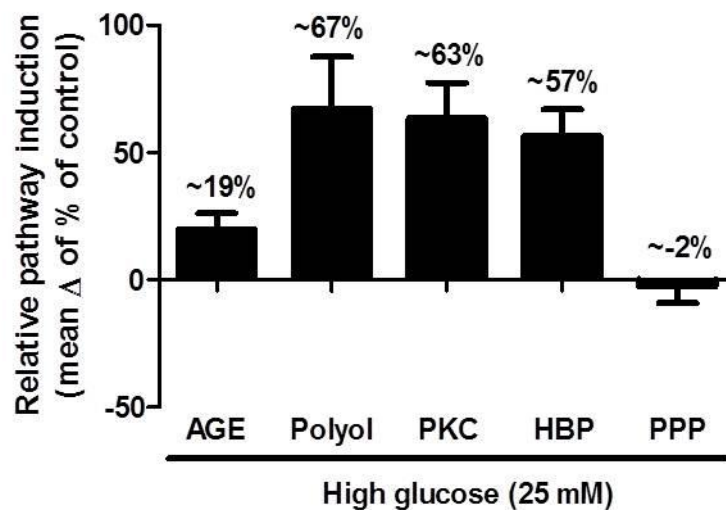


Figure 6.4 Relative percentage induction of NOGP markers by high glucose treatment. The mean difference (Δ) between control and high glucose treated samples were analyzed for each NOGP marker tested above (refer Fig. 6.3). Values are expressed as the approximate mean percentage Δ between high glucose and controls.

6.4.2. The role of NOGP modulation on insulin and ROS signaling events

In light of the previous data indicating ROS-mediated NOGP induction under high glucose conditions, we next set out to determine the influence of each NOGP on insulin action. We employed the individual pathway inhibitors as earlier described.

Our first aim was to evaluate the effect of each inhibitor on its respective pathway. Each individual inhibitor significantly blunted the hyperglycemia-mediated induction of its respective NOGP (Fig 6.5). Treatment with AMG significantly reduced methylglyoxal levels by $35.4 \pm 2.2\%$ ($P < 0.001$ vs. high glucose) (Fig 6.5A). ZOP and CHE respectively blunted sorbitol levels ($122.4 \pm 15.1\%$) and PKC activity ($102.2 \pm 9.8\%$) ($P < 0.001$ vs. high glucose) (Fig 6.5B and C). Fluorescence microscopy analysis of intact cells ($P < 0.001$ vs. high glucose) (Fig 6.5 Di) and Western blot analysis of cell lysate ($P < 0.05$ vs. high glucose) (Fig 6.5 Dii) both showed significant downregulation of O-GlcNAc moieties with DON treatment.

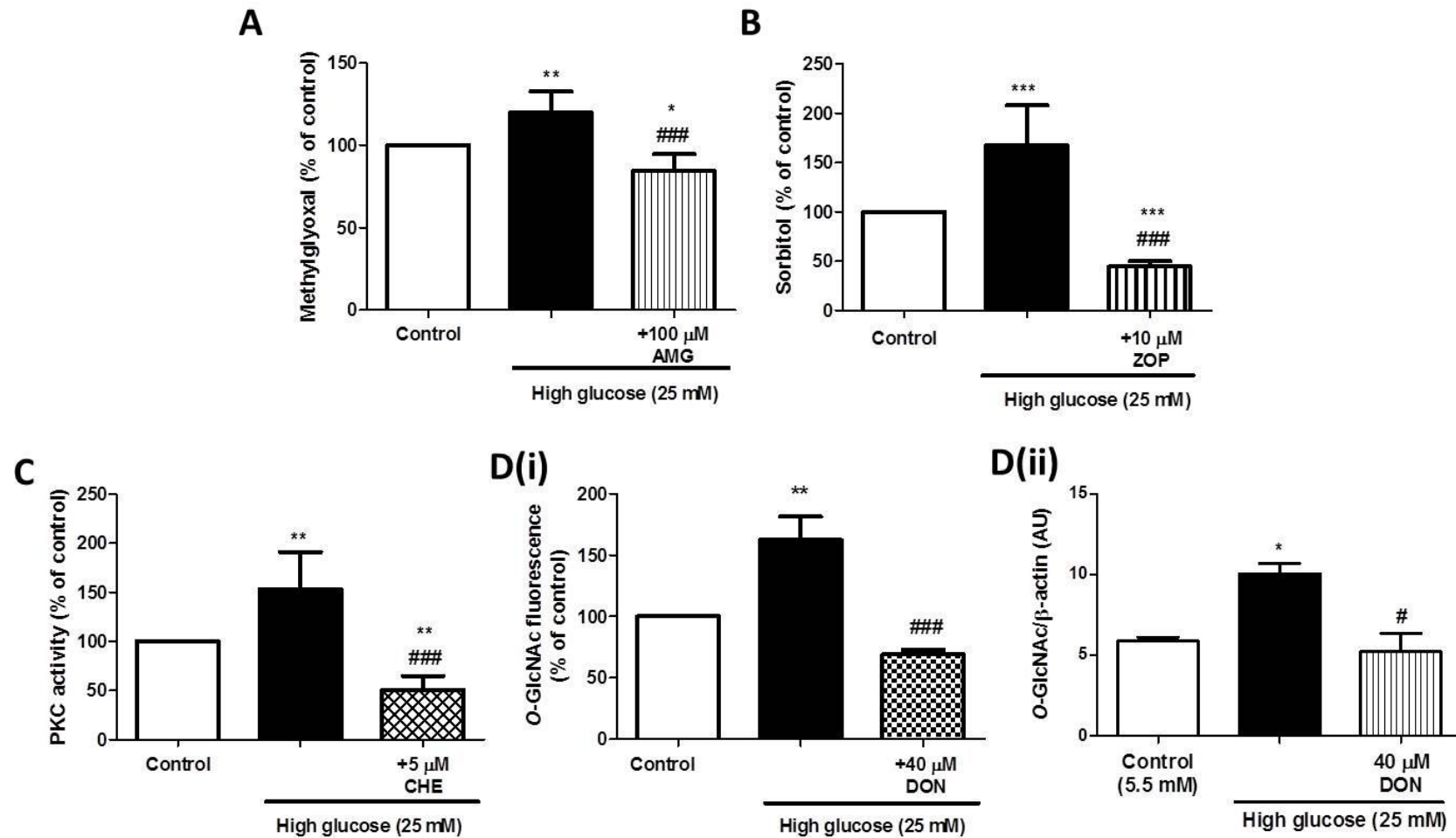


Figure 6.5 Inhibitory effect of NOGP inhibitors used in this study. H9c2 cells were subjected to 24 h high glucose conditions vs. controls \pm respective NOGP inhibitors as follows: 100 μ M AMG (for AGE pathway), 5 μ M CHE (for PKC pathway), 40 μ M DON (for HBP), 10 μ M ZOP (for polyol pathway). (A) Methylglyoxal levels (AGE pathway), (B) Sorbitol levels (polyol pathway), (C) PKC activity, (Di) Immunofluorescence microscopy data of total intracellular O-GlcNAc-modified proteins, (Bii) Western blot quantification of O-GlcNAc-modified proteins (HBP), with densitometry values normalized to respective β -actin. Values are expressed as mean \pm SEM (n=4-6). *P<0.05, **P<0.01, ***P<0.001 vs. control; #P<0.05, ###P<0.001 vs. high glucose.

We next evaluated the effect of each NOGP on glucose uptake by employing the respective inhibitors in separate experiments (Fig 6.6). All four modulator treatments significantly reversed the inhibitory effect of high glucose on insulin-stimulated glucose uptake. Cells treated with AMG, ZOP and DON increased insulin-stimulated glucose uptake by ~39, 40 and 49% under high glucose conditions, respectively ($P < 0.05$ vs. respective basal controls) (Fig 6.6A, B and D). On the other hand, CHE treatment had a more pronounced effect, i.e. it elevated glucose uptake by ~84% ($P < 0.001$ vs. basal control) (Fig 6.6C).

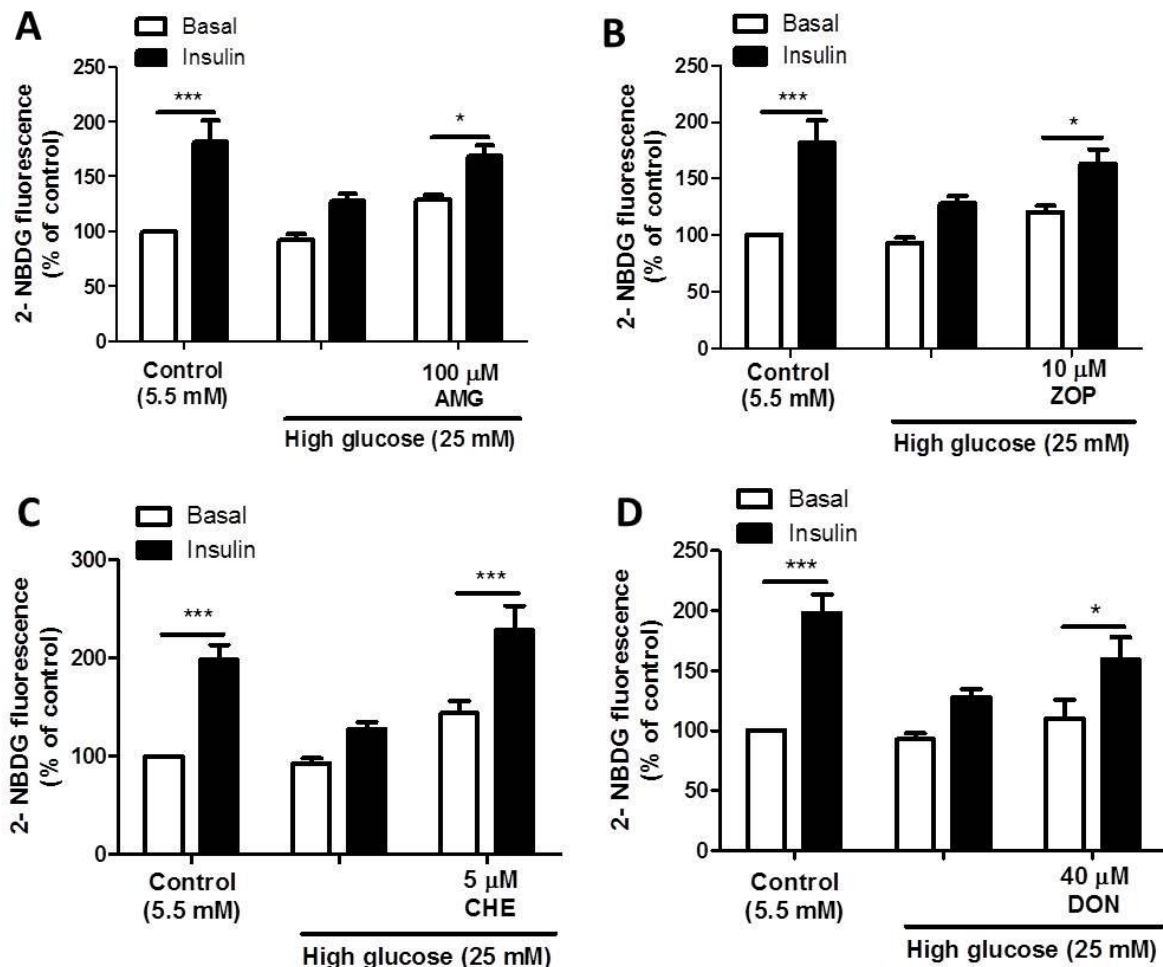


Figure 6.6 NOGP inhibition reversed high glucose-mediated inhibition of glucose uptake. H9c2 cells were subjected to 24 h high glucose conditions vs. controls \pm respective NOGP inhibitors as follows: (A) 100 μ M AMG (for AGE pathway), (B) 10 μ M ZOP (for polyol pathway), (C) 5 μ M CHE (for PKC pathway), (D) 40 μ M DON (for HBP). Values are expressed as mean \pm SEM (n=4). * $P < 0.05$, *** $P < 0.001$ vs. respective basal control.

In order to determine the relative contribution of each NOGP to glucose uptake, and to draw a statistical comparison between the pathways, we evaluated the effect of individual NOGP inhibitors on glucose uptake within the same experiment (Fig 6.7). Glucose uptake in cells treated with AMG, DON and ZOP were not significantly changed when comparing the four NOGP inhibitors together. However, PKC inhibition markedly increased glucose uptake upon insulin stimulation ($P < 0.01$ vs. respective basal control). These results mirrored the individual inhibitory studies showing PKC inhibition resulted in a more pronounced increase of glucose uptake. Although the AGE, polyol and hexosamine pathways may contribute to the observed insulin resistance associated with high glucose, the data suggest that PKC activation may outweigh that of the other pathways in this regard.

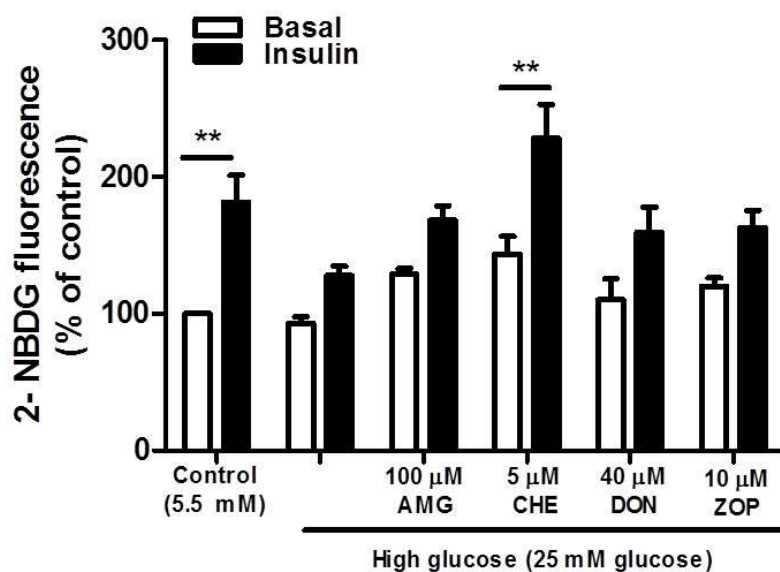


Figure 6.7 PKC inhibition outweighs that of the other NOGP inhibitors – upregulation of glucose uptake. H9c2 cells were subjected to 24 h high glucose conditions vs. controls \pm respective NOGP inhibitors as follows: 100 μ M AMG (for AGE pathway), 5 μ M CHE (for PKC pathway), 40 μ M DON (for HBP), 10 μ M ZOP (for polyol pathway). Values are expressed as mean \pm SEM (n=4). ** $P < 0.01$ vs. respective controls.

In the earlier part of this thesis (Chapter 5), we determined that oxidative stress plays a significant role in the modulation of high glucose-induced insulin resistance. These data demonstrate that imbalanced intracellular redox status plays a major role in driving high glucose-induced alterations and that altered NOGP flux and ROS production may act in concert to reduce glucose uptake. Since ROS-dependent changes resulted from both higher ROS levels (total; mitochondrial and NOX-derived) and attenuated antioxidant defenses, we further pursued molecular events that may be implicated in this process. In light of this, we employed the NOGP inhibitors to determine the impact of NOGP induction on mitochondrial and total intracellular ROS levels, as well as NOX activity under high glucose conditions (Fig 6.8). Mitochondrial ROS was attenuated by AMG, DON ($P < 0.05$ vs. high glucose) and CHE ($P < 0.001$ vs. high glucose), while ZOP treatment had no significant effect (Fig 6.8A). NOX activity was significantly downregulated by AMG ($P < 0.01$ vs. high glucose) (Fig 6.8B). Moreover, CHE treatment dramatically reduced NOX activity by ~4 fold ($P < 0.001$ vs. high glucose), resulting in significantly lower NOX activity compared to AMG ($P < 0.01$) and DON ($P < 0.001$). ZOP treatment also had a pronounced inhibitory effect (by ~86%) on NOX activity ($P < 0.01$ vs. high glucose). DON administration resulted in no significant difference. Total intracellular ROS levels were reduced by AMG, CHE, DON ($P < 0.01$ vs. high glucose) and ZOP ($P < 0.05$ vs. high glucose) (Fig 6.8C).

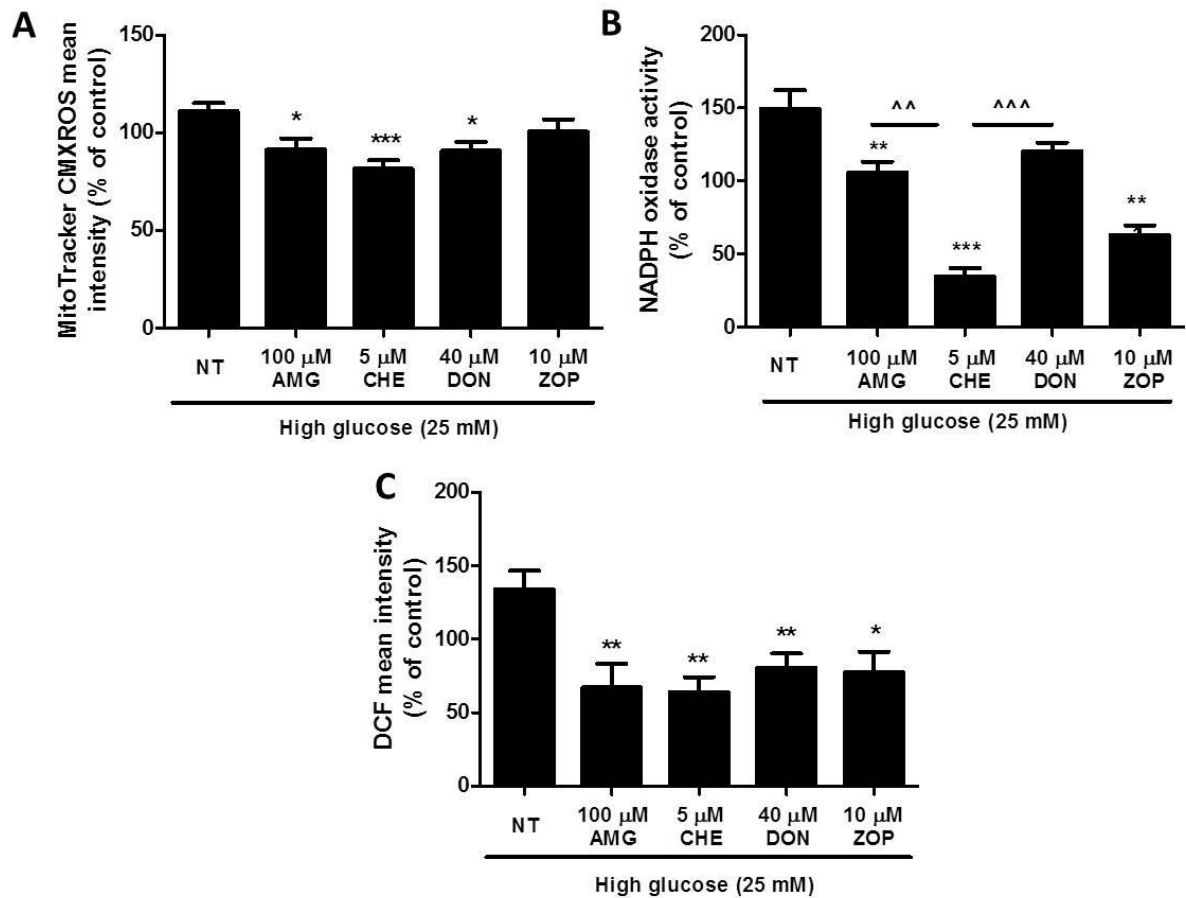


Figure 6.8 NOGP modulation attenuated high glucose-induced ROS production. H9c2 cells were subjected to 24 h high glucose conditions vs. controls \pm respective NOGP inhibitors as follows: 100 μ M AMG (for AGE pathway), 5 μ M CHE (for PKC pathway), 40 μ M DON (for HBP), 10 μ M ZOP (for polyol pathway). (A) MitoTracker Red analysis by flow cytometry; (B) NOX activity; (C) total intracellular ROS analyzed by DCF fluorescence using flow cytometry. Values are expressed as mean \pm SEM (n=6-9). *P<0.05, **P<0.01, ***P<0.001 vs. non-treated high glucose (NT); ^^P<0.01, ^^P<0.001 vs. indicated treatment.

The NOGP inhibitor treatments significantly reversed the downregulation of SOD under high glucose conditions (Fig 6.9). AMG (P<0.01 vs. control; P<0.001 vs. high glucose; P<0.05 vs. DON; P<0.01 vs. ZOP) and CHE (P<0.01 vs. control; P<0.001 vs. high glucose; P<0.05 vs. DON; P<0.05 vs. ZOP) induced a more pronounced effect compared to DON (P<0.001 vs. high glucose) and ZOP (P<0.01 vs. high glucose) treatments.

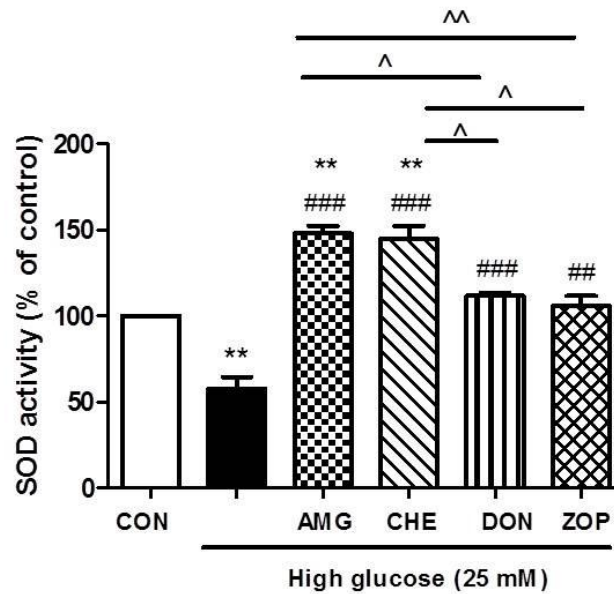


Figure 6.9 High glucose-mediated inhibition of SOD activity was reversed by NOGP inhibition. H9c2 cells were subjected to 24 h high glucose conditions vs. controls \pm respective NOGP inhibitors as follows: 100 μ M AMG (for AGE pathway), 5 μ M CHE (for PKC pathway), 40 μ M DON (for HBP), 10 μ M ZOP (for polyol pathway). Values are expressed as mean \pm SEM (n=6). **P<0.01, vs. control; ##P<0.01, ###P<0.001 vs. high glucose; ^P<0.05, ^^P<0.01 vs. indicated treatment.

In the previous chapter we showed that dysregulation of the replenishment of GSH under high glucose conditions may be an important mechanism contributing to the overall increase in ROS levels. We next aimed to assess the influence of NOGPs on this mechanism. GSH levels were increased by AMG (P<0.01 vs. HG), CHE (P<0.001 vs. HG) and ZOP (P<0.001 vs. HG) treatment, while DON had no significant effects (Fig 6.10A). ZOP increased G6PD activity (P<0.001 vs. control) while the other modulators elicited no significant effects (Fig 6.10B). NADPH levels were significantly lowered by CHE treatment (P<0.05 vs. control), while ZOP treatment upregulated it (P<0.05 vs. HG, P<0.05 vs. DON and P<0.001 vs. CHE) (Fig. 6.10C). The ratio of NADP⁺:NADPH was markedly upregulated by CHE treatment (P<0.01 vs. control, high glucose, AMG and DON; P<0.001 vs. ZOP). The other NOGP inhibitors had no significant effects.

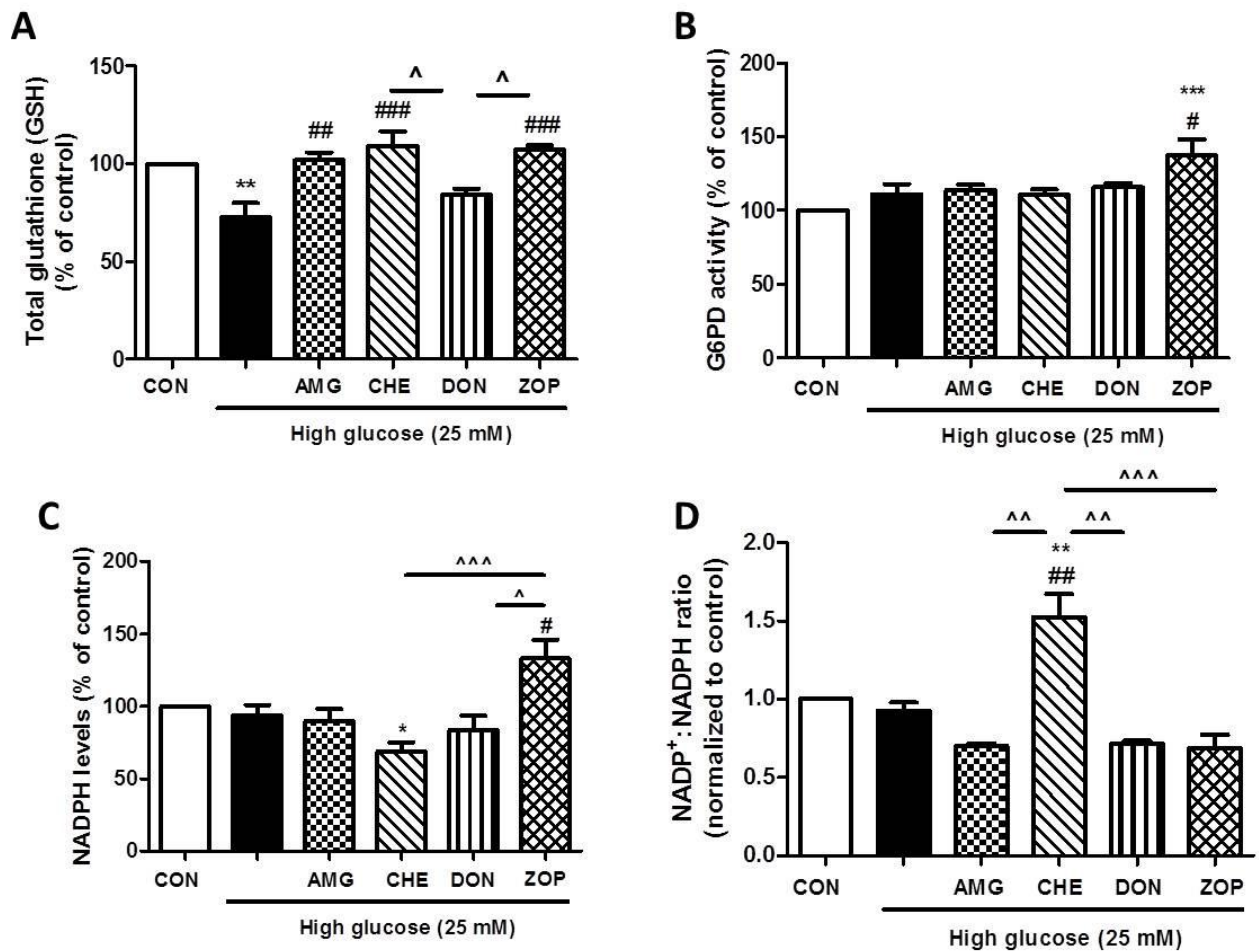


Figure 6.10 Regulation of the glutathione system by NOGP modulation. H9c2 cells were subjected to 24 h high glucose conditions vs. controls \pm respective NOGP inhibitors as follows: 100 μ M AMG (for AGE pathway), 5 μ M CHE (for PKC pathway), 40 μ M DON (for HBP), 10 μ M ZOP (for polyol pathway). (A) GSH levels, (B) G6PD activity, (C) NADPH levels, (D) NADP⁺:NADPH ratio. Values are expressed as mean \pm SEM (n=6-9). *P<0.05, **P<0.01, ***P<0.001 vs. control; #P<0.05, ##P<0.01, ###P<0.001 vs. high glucose; ^P<0.05, ^^P<0.01, ^^^P<0.001 vs. indicated treatment.

In an effort to assess the possible interplay between NOGPs, we investigated the effects of the NOGP inhibitors on all the other respective pathway markers under hyperglycemic conditions (Fig 6.11). Methylglyoxal levels (the AGE marker) were significantly decreased by CHE, ZOP (P<0.01 vs. high glucose) and DON (P<0.001 vs. high glucose). Sorbitol levels were markedly reduced by AMG, CHE and DON treatment (P<0.001 vs. high glucose) (Fig 6.11B). AMG treatment did not exert a significant effect on O-GlcNAc levels, however it was decreased by CHE (P<0.05 vs

high glucose) and ZOP ($P < 0.01$ vs. high glucose) administration (Fig 6.11C). PKC activity was markedly reduced by AMG, DON and ZOP treatment ($P < 0.001$ vs. high glucose).

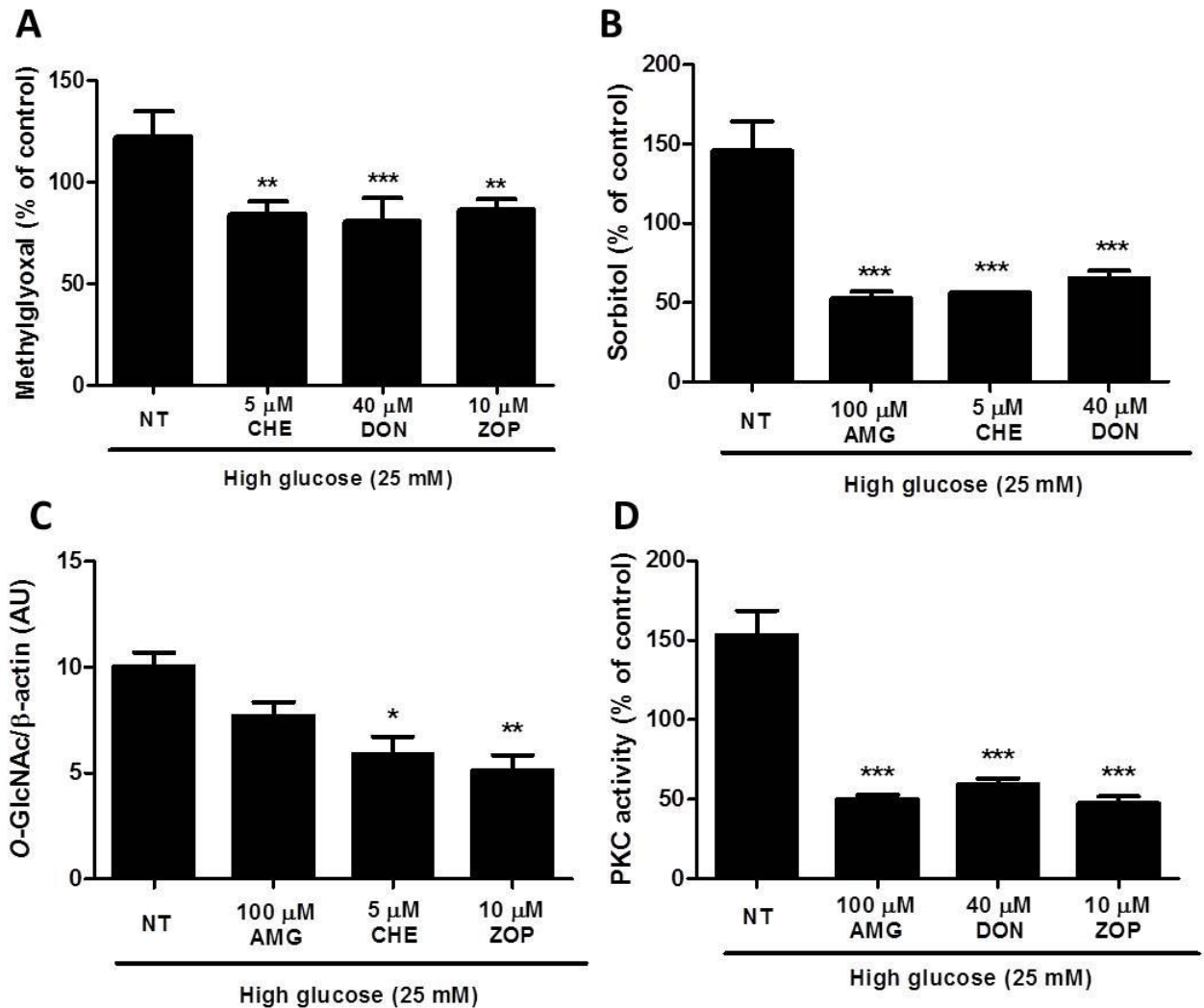


Figure 6.11 Levels of NOGP markers in high glucose treated cells subjected to pathway inhibition. H9c2 cells were subjected to 24 h high glucose conditions \pm respective NOGP inhibitors as follows: 100 μ M AMG (for AGE pathway), 5 μ M CHE (for PKC pathway), 40 μ M DON (for HBP), 10 μ M ZOP (for polyol pathway). (A) Methylglyoxal levels (AGE pathway), (B) Sorbitol levels (polyol pathway), (C) O-GlcNAc modified proteins (HBP), (D) PKC activity. Values are expressed as mean \pm SEM (n=6-9). *P < 0.05, **P < 0.01, ***P < 0.001 vs. non-treated high glucose (NT).

These data point toward NOGP interplay and their involvement in eliciting oxidative stress mechanisms and reduced glucose uptake. PKC activation may play a prominent role here. Our data further show no difference in PPP activity upon high

glucose treatment. The regulation of transketolase may, however, increase PPP flux and result in improved glucose metabolism. Indeed, thiamine or benfotiamine (BFT) administration (an important co-factor of transketolase) may have beneficial outcomes on dysregulated glucose metabolism (Katare *et al.*, 2010a; Mapanga *et al.*, 2013; Marchetti *et al.*, 2006; Schupp *et al.*, 2008; Stirban *et al.*, 2006; Winkler *et al.*, 1999; Wu and Ren, 2006). Thiamine and BFT are proposed to redirect flux away from the NOGPs by upregulating glycolytic intermediates and enzymes (Hammes *et al.*, 2003; Nishikawa *et al.*, 2000). We therefore aimed to further assess the role of NOGPs in our system by employing BFT *in vitro* and thiamine *in vivo*. The rationale here is that the reversal of NOGP induction by BFT or thiamine would confirm our inhibitor data and shed more light on the importance and impact of NOGPs and their role in oxidative stress-mediated insulin resistance under acute high glucose conditions.

6.4.3. Modulation of PPP diverts flux away from NOGPs – the role benfotiamine *in vitro* and thiamine *in vivo*

H9c2 cells were exposed to 24 h high glucose ± two concentrations of BFT (50 and 100 µM) for the final hour of the hyperglycemic period. Both concentrations of BFT robustly increased insulin stimulated glucose uptake – 50 µM (P<0.05 vs. basal) and 100 µM (P<0.01 vs. basal), with the 100 µM concentration exerting a greater effect (Fig 6.12).

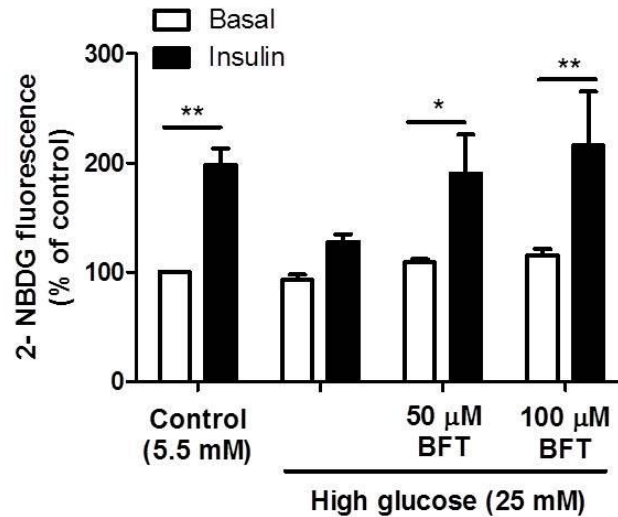


Figure 6.12 Benfotiamine administration increased glucose uptake. H9c2 cells were subjected to 24 h high glucose conditions \pm 50 and 100 μ M BFT. Values are expressed as mean \pm SEM (n=4). *P<0.05, **P<0.01 vs. respective basal control.

Compared to the other NOGP inhibitors, BFT (100 μ M) had a similar pronounced effect on glucose uptake as CHE treatment (P<0.01 vs. basal control). This suggests that PPP induction and PKC inhibition represents two major mechanisms resulting in the reversal of hyperglycemia-mediated insulin resistance.

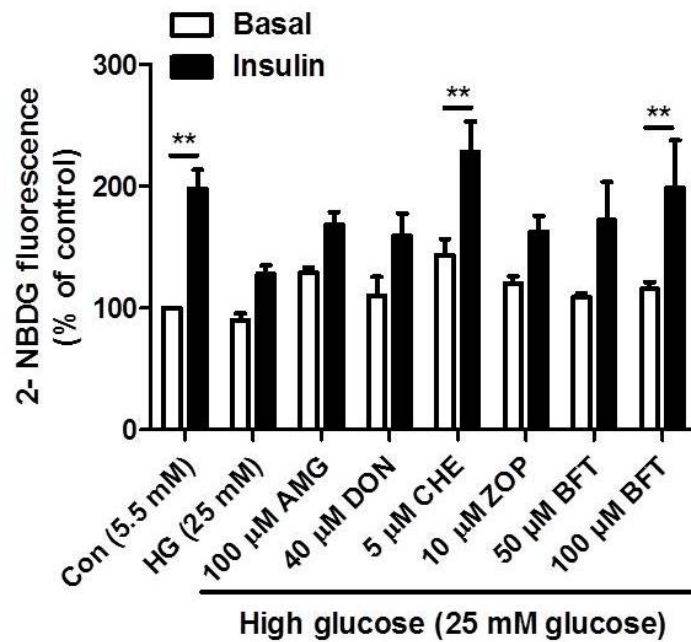


Figure 6.13 Comparison of BFT versus the other NOGP inhibitors – effect on glucose uptake. H9c2 cells were subjected to 24 h high glucose conditions vs. controls \pm respective NOGP inhibitors as follows: 100 μ M AMG (for AGE pathway), 5 μ M CHE (for PKC pathway), 40 μ M DON (for HBP), 10 μ M ZOP (for polyol pathway) and 50 and 100 μ M BFT (activates transketolase, non-oxidative PPP). Values are expressed as mean \pm SEM (n=4). **P<0.01 vs. respective controls.

Treatment of H9c2 cells exposed to acute high glucose and 100 μ M BFT increased transketolase activity (P<0.01 vs. control, P<0.01 vs. high glucose) (Fig 6.14A). On the contrary, BFT had no significant effect on G6PD activity (Fig 6.14B).

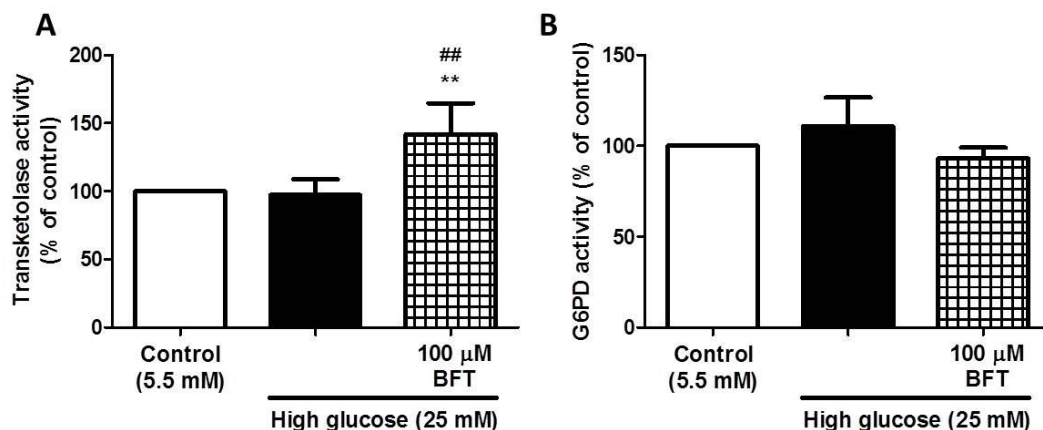


Figure 6.14 BFT increased transketolase activity. H9c2 cells were subjected to 24 h high glucose conditions vs. controls \pm 100 μ M BFT (activates transketolase, non-oxidative PPP). (A) Transketolase activity, (B) G6PD activity. Values are expressed as mean \pm SEM (n=6). **P<0.01 vs. control, ###P<0.01 vs. high glucose.

Since BFT promotes glucose metabolic flux (glucose oxidation) and may shift flux away from the detrimental NOGPs (Nishikawa *et al.*, 2000), we next endeavored to assess NOGP markers and ATP levels (as a marker of metabolic flux coupled to energy production) in cells treated with 100 μ M BFT during the last hour of hyperglycemia. BFT treatment markedly reduced methylglyoxal ($P < 0.01$ vs. control, $P < 0.001$ vs. high glucose) (Fig 6.15A) and sorbitol levels ($P < 0.01$ vs. high glucose) (Fig 6.15B). PKC activity was also significantly decreased ($P < 0.01$ vs. high glucose) (Fig 6.15C), along with O-GlcNAc levels ($P < 0.01$ vs. high glucose) (Fig 6.15D). Surprisingly, ATP levels were also diminished upon BFT treatment ($P < 0.05$ vs. control, $P < 0.01$ vs. high glucose) (Fig 6.15D).

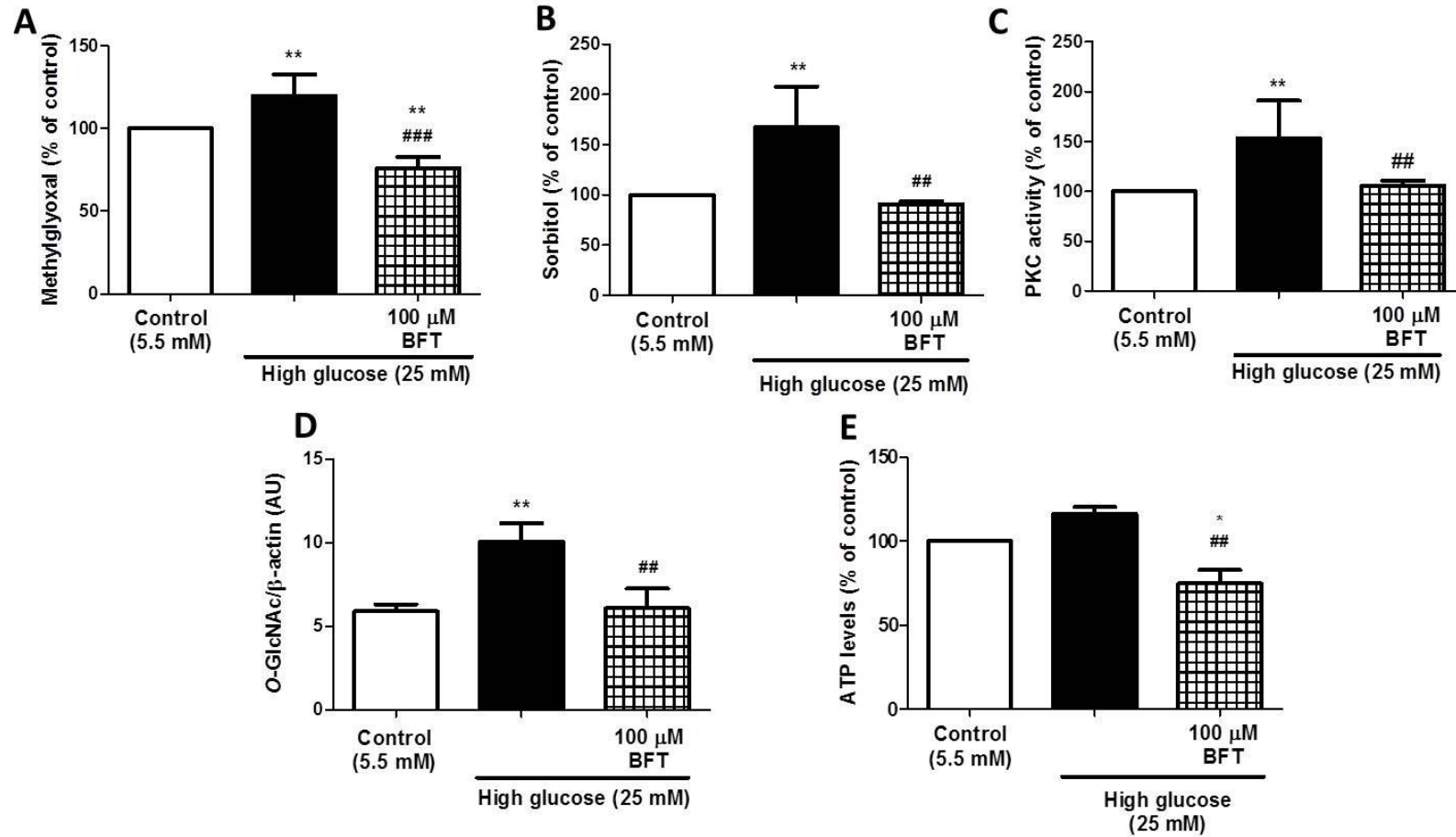


Figure 6.15 BFT treatment reduced NOGP markers and ATP levels. H9c2 cells were subjected to 24 h high glucose conditions vs. controls \pm 100 μ M BFT (activates transketolase, non-oxidative PPP). (A) Methylglyoxal levels (AGE pathway), (B) Sorbitol levels (polyol pathway), (C) PKC activity, (D) O-GlcNAc-modified proteins (HBP), (E) ATP levels. Values are expressed as mean \pm SEM (n=4-6). Values are expressed as mean \pm SEM (n=6). *P<0.05, **P<0.01 vs. control, ##P<0.01, ###P<0.001 vs. high glucose.

The relative NOGP induction under high glucose \pm BFT treatment conditions is depicted in Fig 6.16 below. This represents the mean difference in NOGP markers between BFT treated samples and high glucose treatments. BFT reduced markers of the AGE (~44%), polyol (~77%), PKC (~59%) and HBP pathways (~68%), and increased transketolase activity (PPP marker (~58%) compared to high glucose treatments.

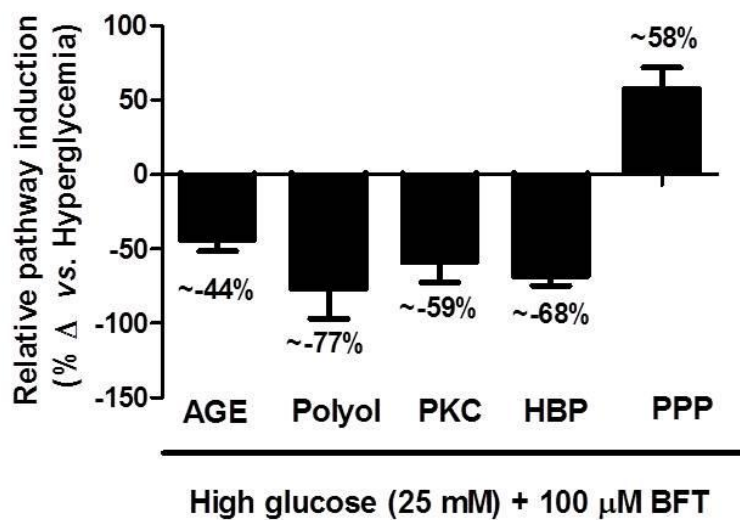


Figure 6.16 Relative NOGP induction with BFT treatment compared to high glucose. The mean difference (Δ) between high glucose and BFT treated samples were analyzed for each NOGP marker tested above (refer Fig. 6.15). Values are expressed as the approximate percentage Δ between high glucose and controls.

Our next aim was to evaluate the role of BFT treatment on ROS production (mitochondrial- and NOX-derived) and to elucidate whether it plays a role in the regulation of antioxidant defense systems under high glucose conditions. BFT treatment mitigated mitochondrial ROS ($P < 0.01$ vs. high glucose) (Fig 6.17A), NOX activity ($P < 0.05$ vs. control, $P < 0.01$ vs. high glucose) (Fig 6.17B) and total intracellular ROS ($P < 0.05$ vs. high glucose) (Fig 6.17 C).

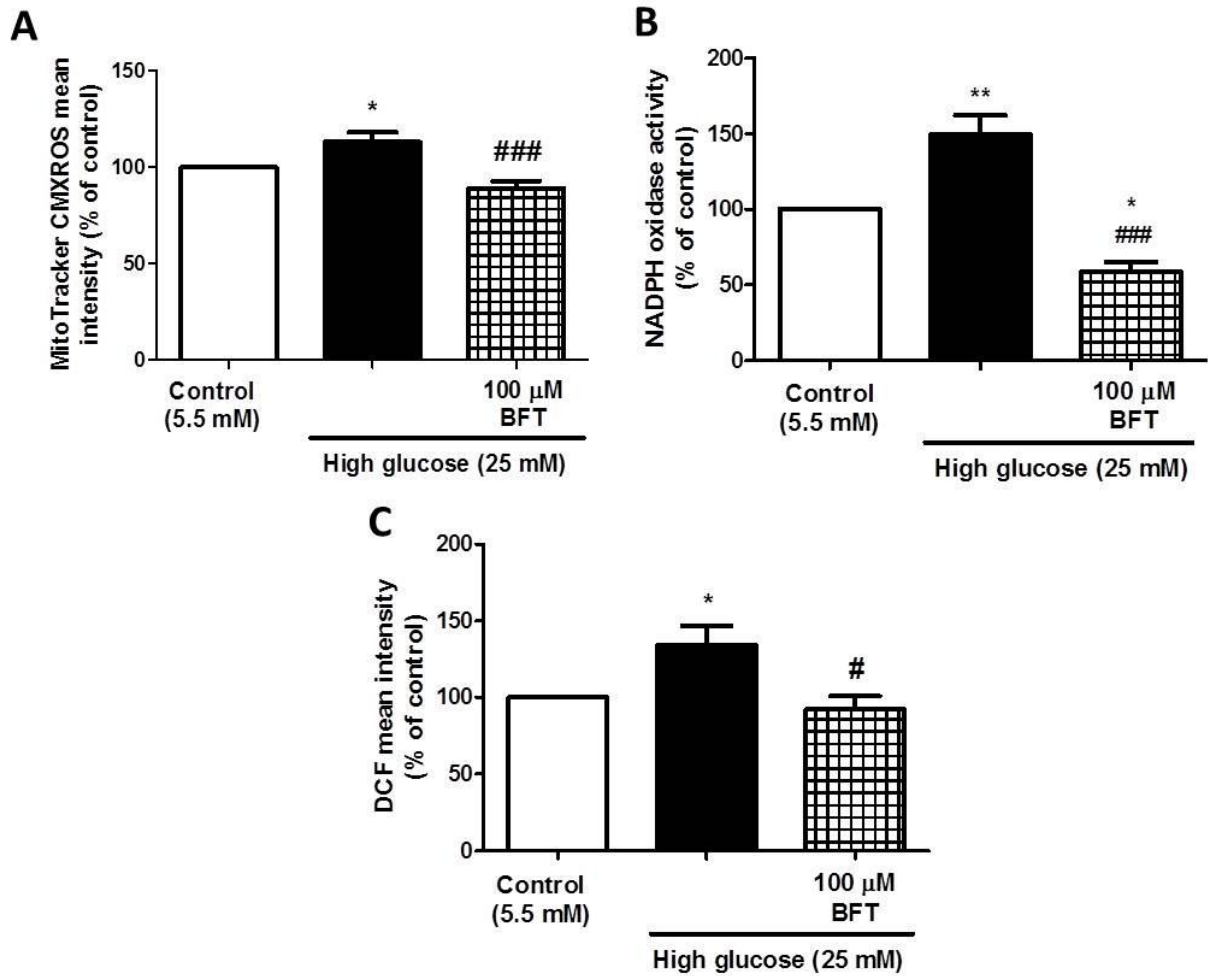


Figure 6.17 BFT attenuated ROS production. H9c2 cells were subjected to 24 h high glucose conditions vs. controls \pm 100 μ M BFT (activates transketolase, non-oxidative PPP). (A) MitoTracker Red analysis by flow cytometry; (B) NOX activity; (C) total intracellular ROS analyzed by DCF fluorescence using flow cytometry. Values are expressed as mean \pm SEM (n=6-9). *P<0.05, **P<0.01, vs. control; #P<0.05, ###P<0.001 vs. high glucose.

SOD activity was also markedly upregulated by BFT treatment ($P < 0.01$ vs. high glucose) (Fig 6.18).

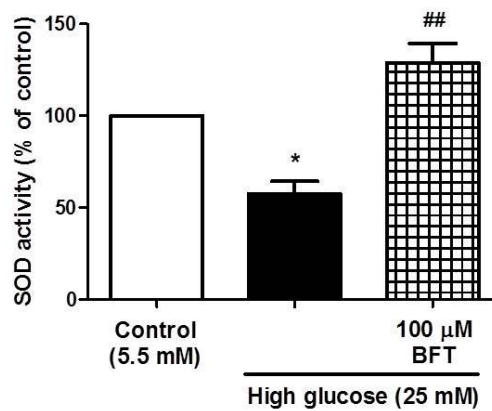


Figure 6.18: BFT administration increased SOD activity. H9c2 cells were subjected to 24 h high glucose conditions vs. controls \pm 100 μ M BFT (activates transketolase, non-oxidative PPP). Values are expressed as mean \pm SEM (n=6). * $P < 0.05$ vs. control; ## $P < 0.01$ vs. high glucose.

Our data further show that BFT treatment increased GSH levels ($P < 0.05$ vs. high glucose) (Fig 6.19A). Although such treatment had no effect on NADPH levels (Fig 6.19B), it resulted in a marked increase in the $\text{NADP}^+:\text{NADPH}$ ratio ($P < 0.01$ vs. control, $P < 0.01$ vs. high glucose) (Fig 6.19C). This suggests increased NADPH utilization by processes that are activated with BFT treatment.

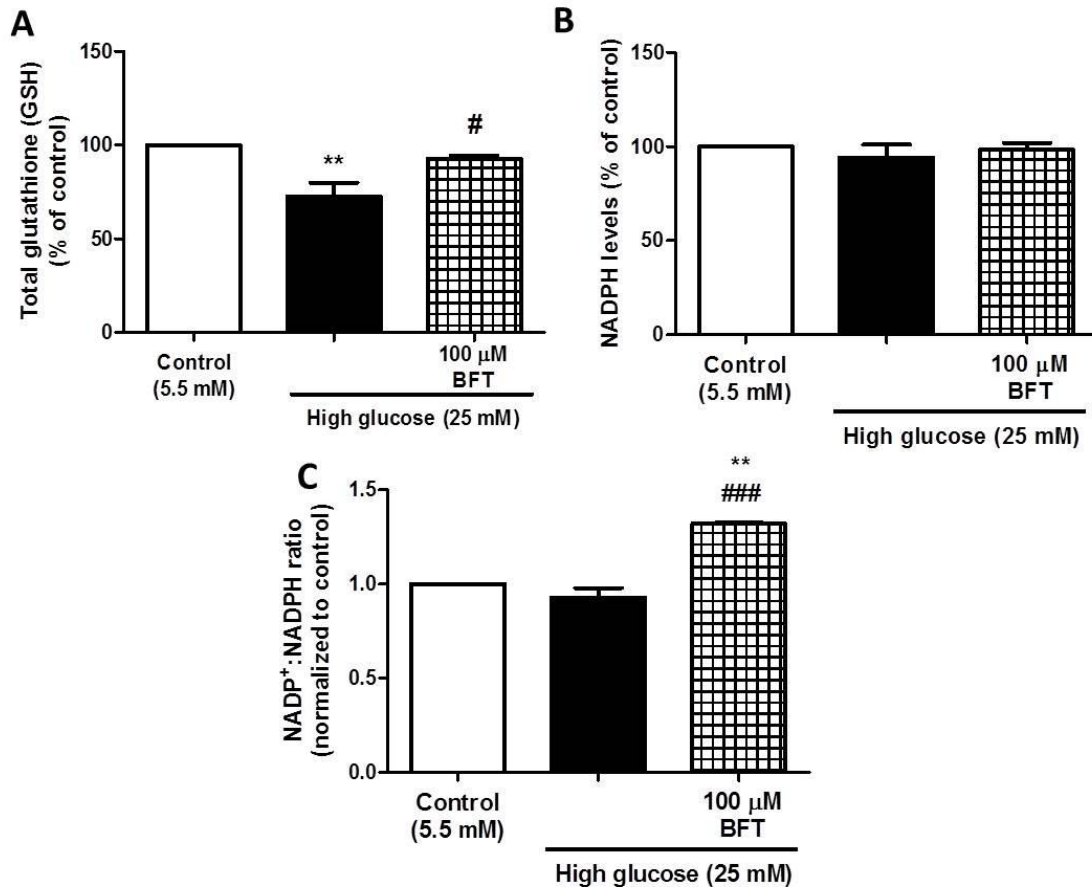


Figure 6.19 BFT upregulated GSH levels and increased NADPH utilization. H9c2 cells were subjected to 24 h high glucose conditions vs. controls \pm 100 μ M BFT (activates transketolase, non-oxidative PPP). (A) GSH levels; (B) NADPH levels; (C) NADP⁺:NADPH ratio. Values are expressed as mean \pm SEM (n=6-9). **P<0.01 vs. control; #P<0.05, ###P<0.001 vs. high glucose.

Since our previous data point toward interplay between NOGPs under high glucose conditions (refer Fig 6.11), we therefore postulated that transketolase activity may be regulated by NOGPs under high glucose conditions. We found that DON treated cells drastically decreased transketolase activity (P<0.001 vs. control, P<0.05 vs. high glucose; P<0.01 vs. CHE) (Fig 6.20). Although AMG and ZOP decreased transketolase activity by ~17 and ~24% (compared to high glucose) respectively, these effects were not significant. CHE resulted in an opposite effect to the other NOGPs, i.e. ~16% upregulation compared to high glucose; however this effect was

also not significant. Of note, CHE triggered a different effect compared to the other NOGPs.

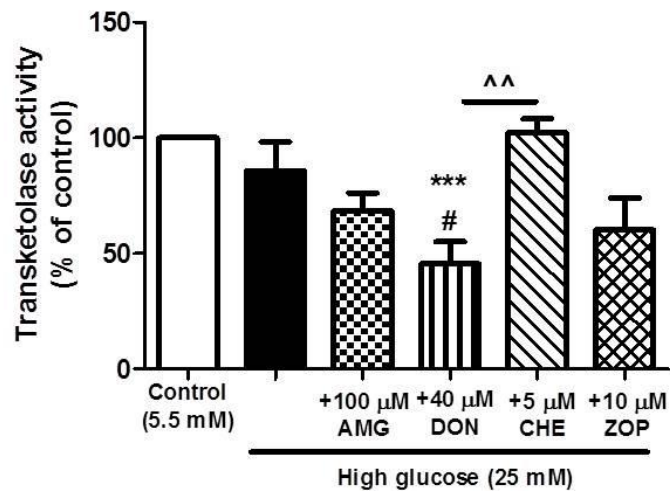


Figure 6.20 DON administration downregulated transketolase activity. H9c2 cells were subjected to 24 h high glucose conditions vs. controls \pm 100 μ M BFT (activates transketolase, non-oxidative PPP). (A) GSH levels; (B) NADPH levels; (C) $\text{NADP}^+:\text{NADPH}$ ratio. Values are expressed as mean \pm SEM (n=6-9). * P <0.05, ** P <0.01, *** P <0.001 vs. control; # P <0.05, ### P <0.001 vs. high glucose.

Our *in vitro* BFT studies in a simulated acute hyperglycemic setting showed that upregulation of the PPP may play an important role in diminishing high glucose-mediated insulin resistance. We now turned our attention to evaluating the effects of thiamine in an *in vivo* model of metabolic dysregulation – the OLETF rat. Previously collected heart tissues were kindly provided by Dr. Takao Tanaka (Osaka University of Pharmaceutical Sciences, Osaka, Japan). A description of the model and experimental protocol is provided in Section 4.4 (also refer Tanaka *et al.*, 2010). For this study, 25-week old OLETF rats displayed a “pre-diabetic” phenotype characterized by high glucose and high insulin levels, while 55-week old rats exhibited a diabetic phenotype (diminished plasma insulin levels accompanied by β -

cell damage and severe hyperglycemia). Moreover, thiamine treatment reversed the detrimental metabolic effects in this model.

We next aimed to assess the role of *in vivo* hyperglycemia in the two different states of glucose metabolic dysregulation (i.e. 25 weeks “pre-diabetes” and 55 weeks “overt diabetes”) and to evaluate the molecular mechanisms underlying the thiamine-induced reversal of metabolic dysfunction in collected heart tissues. More specifically, we aimed to evaluate the role of NOGPs and their regulation by thiamine treatment in each condition. We initially aimed to gain an understanding of insulin signaling. This was achieved by employing an ELISA-based Akt kinase activity assay. Akt activity was ~2.4 fold increased by thiamine treatment in the 25 week group ($P < 0.001$ vs. 25 week control) (Fig 6.21). Conversely, the 55 week old control animals displayed markedly reduced myocardial Akt activity ($P < 0.05$ vs. 25 week control, $P < 0.001$ vs. 25 week thiamine) at baseline and in response to thiamine treatment.

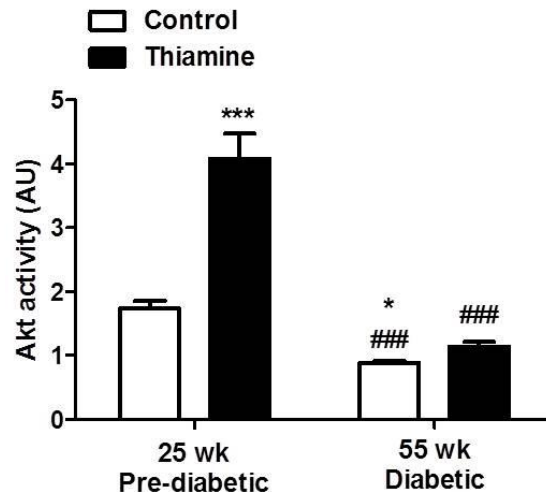


Figure 6.21 Myocardial Akt activity is upregulated by thiamine in 25 week old OLETF rats. Four week old OLETF rats were subjected to 2 g/L thiamine for 21 and 51 weeks, respectively. Animals were sacrificed at 25 and 55 weeks and heart tissues collected for Akt activity analysis. Values are expressed as mean \pm SEM (n=8). *P<0.05, ***P<0.001 vs. 25 week control; ###P<0.001 vs. 25 week thiamine.

We next aimed to determine NOGP activity in the pre-diabetic and diabetic states, as well as the effect of thiamine administration on NOGP activity. We started by assessing the activity of two key regulatory PPP enzymes, G6PD and transketolase (Fig 6.22). Thiamine treatment had no effect on G6PD activity compared to the respective controls in the 25 week or the 55 week groups (Fig 6.22A). It was, however, markedly reduced in the 55 week controls (P<0.01 vs. 25 week control, P<0.001 vs. 25 week thiamine). G6PD activity was also significantly lower with thiamine treatment in the 55 week old animals compared to thiamine treatment in the 25 week group. Transketolase activity was markedly upregulated with thiamine treatment in both the pre-diabetic (P<0.001 vs. 25 week control) and the diabetic groups (P<0.001 vs. 55 week control) (Fig 6.22B). Moreover, transketolase activity was reduced in heart tissue of the 55 week old animals (P<0.001 vs. 25 week control).

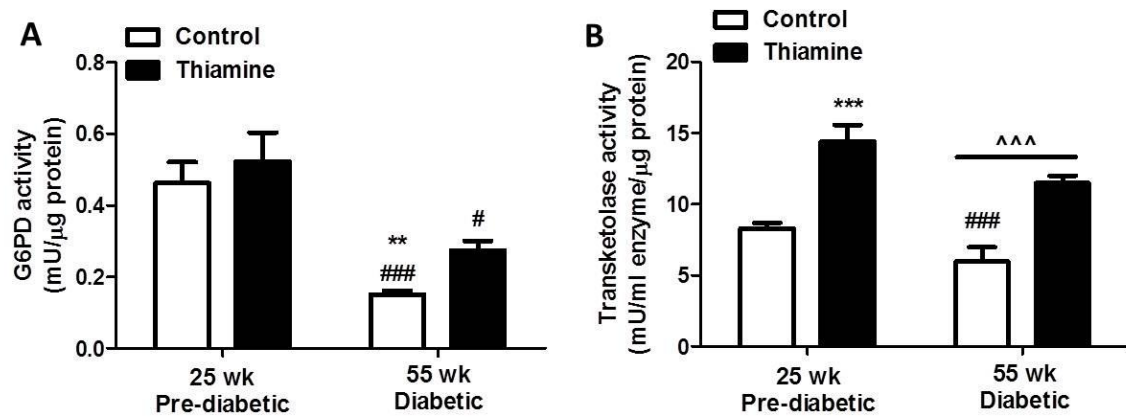


Figure 6.22 PPP enzymes are reduced in the 55 week old (diabetic) hearts and transketolase upregulated by thiamine *in vivo*. Four week old OLETF rats were subjected to 2 g/L thiamine for 21 and 51 week respectively. Animals were sacrificed at 25 and 55 week and heart tissues collected for analysis of (A) G6PD and (B) transketolase enzyme activity. Values are expressed as mean ± SEM (n=8). **P<0.01, ***P<0.001 vs. 25 week control; #P<0.05, ###P<0.001 vs. 25 week thiamine; ^^P<0.001 vs. indicated treatment.

Myocardial methylglyoxal levels were decreased with thiamine treatment in the pre-diabetic state (P<0.001 vs. 25 week control) (Fig 6.23). Furthermore, the older OLETF rats displayed lower methylglyoxal levels compared to the 25 week old rats (P<0.001 vs. 25 week control). However, thiamine treatment in the 55 week old diabetic animals did not have a significant effect compared to the controls, but remained lower vs. the 25 week controls (P<0.001).

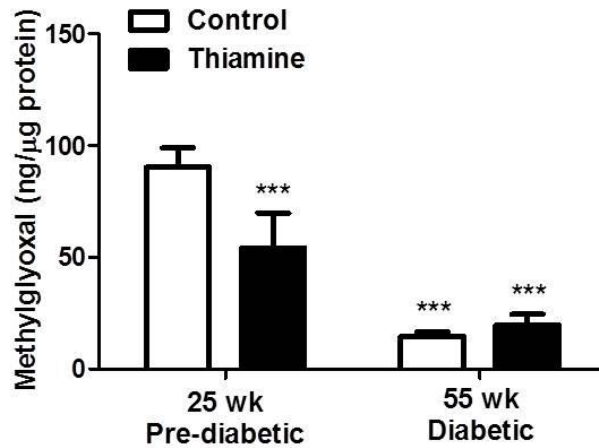


Figure 6.23 Methylglyoxal levels (marker of the AGE pathway) were decreased by thiamine treatment in pre-diabetic hearts *in vivo*. Four week old OLETF rats were subjected to 2 g/L thiamine for 21 and 51 week respectively. Animals were sacrificed at 25 and 55 week and heart tissues collected for analysis of methylglyoxal levels. Values are expressed as mean \pm SEM (n=8). ***P<0.001 vs. 25 week control.

Sorbitol levels were markedly reduced by thiamine administration in the pre-diabetic state (P<0.001 vs. 25 week control), while it was also lower in the older diabetic animals (P<0.01 vs. 25 week control). Thiamine treatment did not significantly alter sorbitol levels in the 55 week old group.

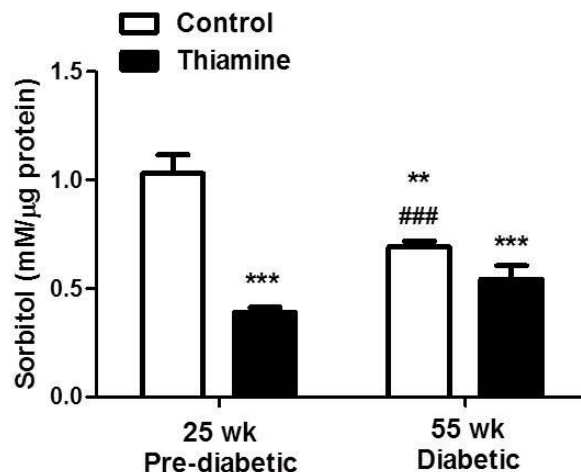


Figure 6.24 Sorbitol levels were decreased in the 25 week old animals. Four week old OLETF rats were subjected to 2 g/L thiamine for 21 and 51 week respectively. Animals were sacrificed at 25 and 55 week and heart tissues collected for analysis of sorbitol levels. Values are expressed as mean \pm SEM (n=8). **P<0.01, ***P<0.001 vs. 25 week control; ###P<0.001 vs. 25 week thiamine.

Similar trends were observed for PKC activity in heart tissues compared to the markers for the AGE and polyol pathways, i.e. reduced PKC activity in the 25 week thiamine-treated and 55 week control and thiamine groups vs. the 25 week controls ($P < 0.001$) (Fig 6.25). Thiamine treatment did not significantly change PKC activity in the 55 week old animals compared to controls, but resulted in a modest reduction compared to the 25 week old control ($P < 0.001$) and thiamine-treated animals ($P < 0.05$).

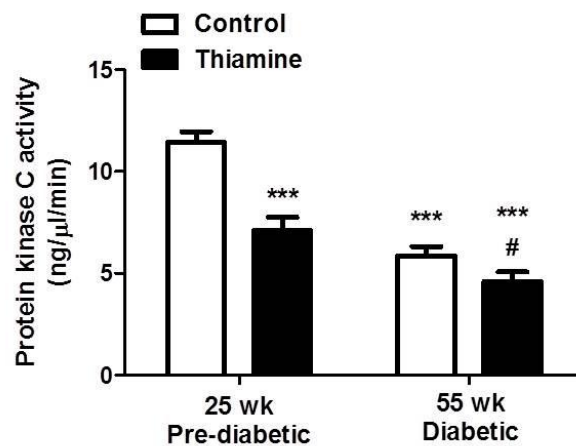


Figure 6.25 Thiamine treatment decreased PKC activity in the pre-diabetic OLETF rats. Four week old OLETF rats were subjected to 2 g/L thiamine for 21 and 51 week respectively. Animals were sacrificed at 25 and 55 week and heart tissues collected for PKC kinase activity assay. Values are expressed as mean \pm SEM (n=8). *** $P < 0.001$ vs. 25 week control; # $P < 0.05$ vs. 25 week thiamine.

Myocardial O-GlcNAc levels were assessed by Western blotting (Fig 6.26). Thiamine treatment decreased O-GlcNAc levels in the 25 week ($P < 0.001$ vs. 25 week control) and 55 week ($P < 0.001$ vs. 55 week control) heart samples. It was also modestly decreased in the diabetic control groups compared to the pre-diabetic control groups ($P < 0.001$).

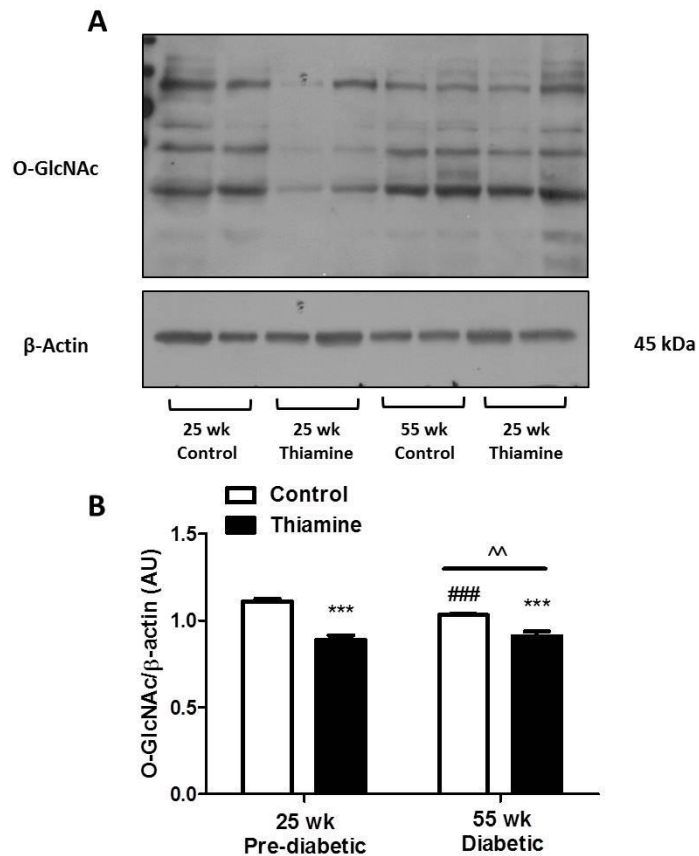


Figure 6.26 Thiamine treatment diminished O-GlcNAc levels in the pre-diabetic and diabetic OLETF rat hearts. Four week old OLETF rats were subjected to 2 g/L thiamine for 21 and 51 week respectively. Animals were sacrificed at 25 and 55 week and heart tissues collected for O-GlcNAc analysis by Western blotting. (A) Representative Western blots of O-GlcNAc and corresponding β -actin. (B) Quantification of Western blotting data with values normalized to respective β -actin. Values are expressed as mean \pm SEM (n=8). ***P<0.001 vs. 25 week control; ###P<0.001 vs. 25 week thiamine; ^^P<0.01 vs. indicated treatment.

6.4.4. Molecular events downstream of NOGP activation in *in vitro* simulated hyperglycemia

Collectively our data provides a strong metabolic link between high glucose-induced ROS production, activation of NOGPs and subsequent dysregulation of insulin action, including decreased insulin-mediated glucose uptake. Our next aim was to explore possible molecular mechanisms to link the observed upstream detrimental events to decreased insulin responsiveness. Upregulation of PKC isoforms may play an important role in regulation of insulin signaling mechanisms (Bandyopadhyay *et*

al., 1999a, 1999b; Hennige *et al.*, 2010; Itani *et al.*, 2000; Quagliaro *et al.*, 2003; Ragheb *et al.*, 2009). PKC β II may be a central effector of various detrimental outcomes under hyperglycemic conditions (Amadio *et al.*, 2010; Geraldles and King, 2010; Voris *et al.*, 2010), while it may also regulate NOX activity and the resultant ROS production (Quagliaro *et al.*, 2003). We therefore evaluated the protein levels of this isoform in our *in vitro* model of acute hyperglycemia, and assessed the role of mitochondrial and NOX-derived ROS by employing 4-OHCA and DPI treatments. Here PKC β II protein levels were upregulated by acute high glucose when compared to controls ($P < 0.001$) (Fig 6.27), and downregulated by both 4-OHCA and DPI treatment.

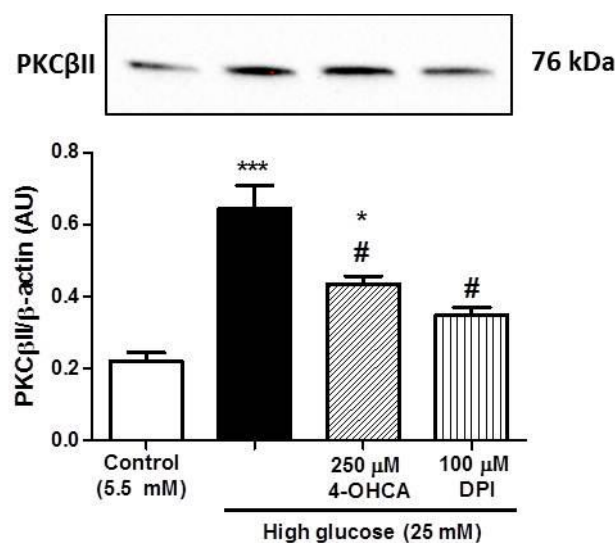


Figure 6.27 Upregulation of PKC β II by acute hyperglycemia was reduced by 4-OHCA and DPI treatment. H9c2 cells were treated acutely with a) 4-OHCA and b) DPI under high glucose conditions. Values are expressed as mean \pm SEM ($n=6$). * $P < 0.05$, *** $P < 0.001$ vs. control; # $P < 0.05$ vs. high glucose.

The post-translational modification of kinases involved in insulin signaling is key to their regulation. Phosphorylation is a major modification resulting in effective insulin action. However, several signals lead to downregulation of insulin signaling intermediates. O-GlcNAcylation of several insulin signaling intermediates, including

Akt, is proposed to effect downregulation of insulin action and may be involved in insulin resistance when HBP flux is elevated (Gandy *et al.*, 2006; Kang *et al.*, 2008; Park *et al.*, 2005; Vosseller *et al.*, 2002). Our data showed that Akt and O-GlcNAc co-localized in H9c2 cells, and this was increased ~3.3 fold in the high glucose treated group ($P < 0.05$ vs. control) (Fig 6.28). Treatment with 4-OHCA and DPI reduced this.

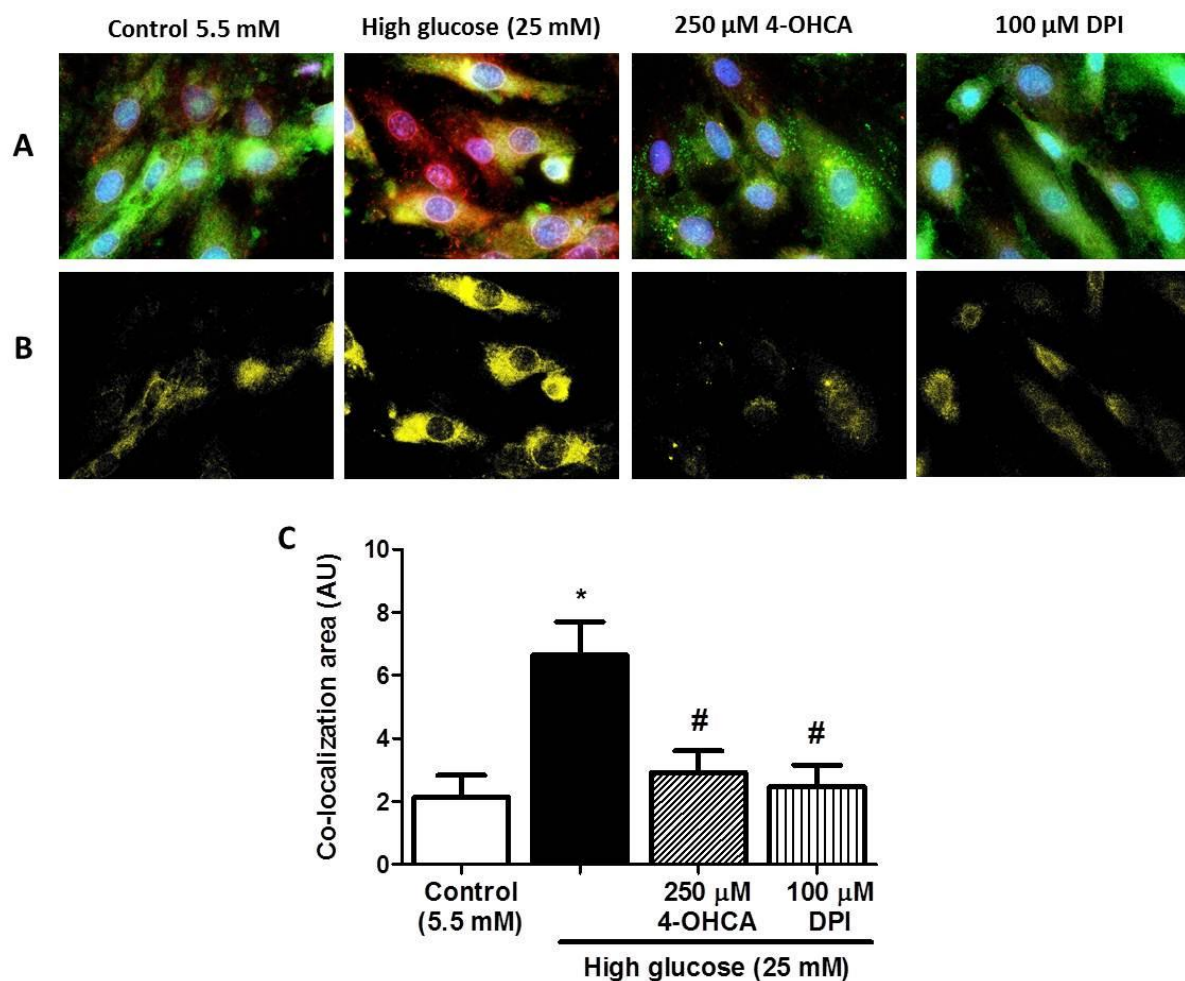


Figure 6.28 Co-localization of Akt and O-GlcNAc was elevated under high glucose conditions and reduced by inhibition of mitochondrial and NOX-derived ROS. H9c2 cells were treated acutely with a) 4-OHCA and b) DPI under high glucose conditions. (A) Fluorescence microscopy analysis of H9c2 cells co-stained with antibodies to detect Akt (FITC-green) and O-GlcNAc (Texas Red) with nuclei stained with DAPI (blue). (B) Co-localization of Akt and O-GlcNAc indicated in the yellow color. (C) Quantification of the area of co-localization expressed in arbitrary units (AU). Values are expressed as mean \pm SEM ($n=4$). * $P < 0.05$ vs. control; # $P < 0.05$ vs. high glucose.

Similar trends were observed when we analyzed AS160 and O-GlcNAc co-localization, i.e. a ~2.7 fold increase under hyperglycemic conditions ($P < 0.05$ vs. control) which was blunted by 4-OHCA ($P < 0.01$ vs. high glucose) and DPI treatment ($P < 0.05$ and vs. high glucose), respectively. Although further analysis warranted to confirm the co-localization results (e.g. co-immunoprecipitation experiments), our preliminary data suggest that increased modification of Akt and AS160 under acute hyperglycemic conditions is regulated by mitochondrial and NOX-derived ROS.

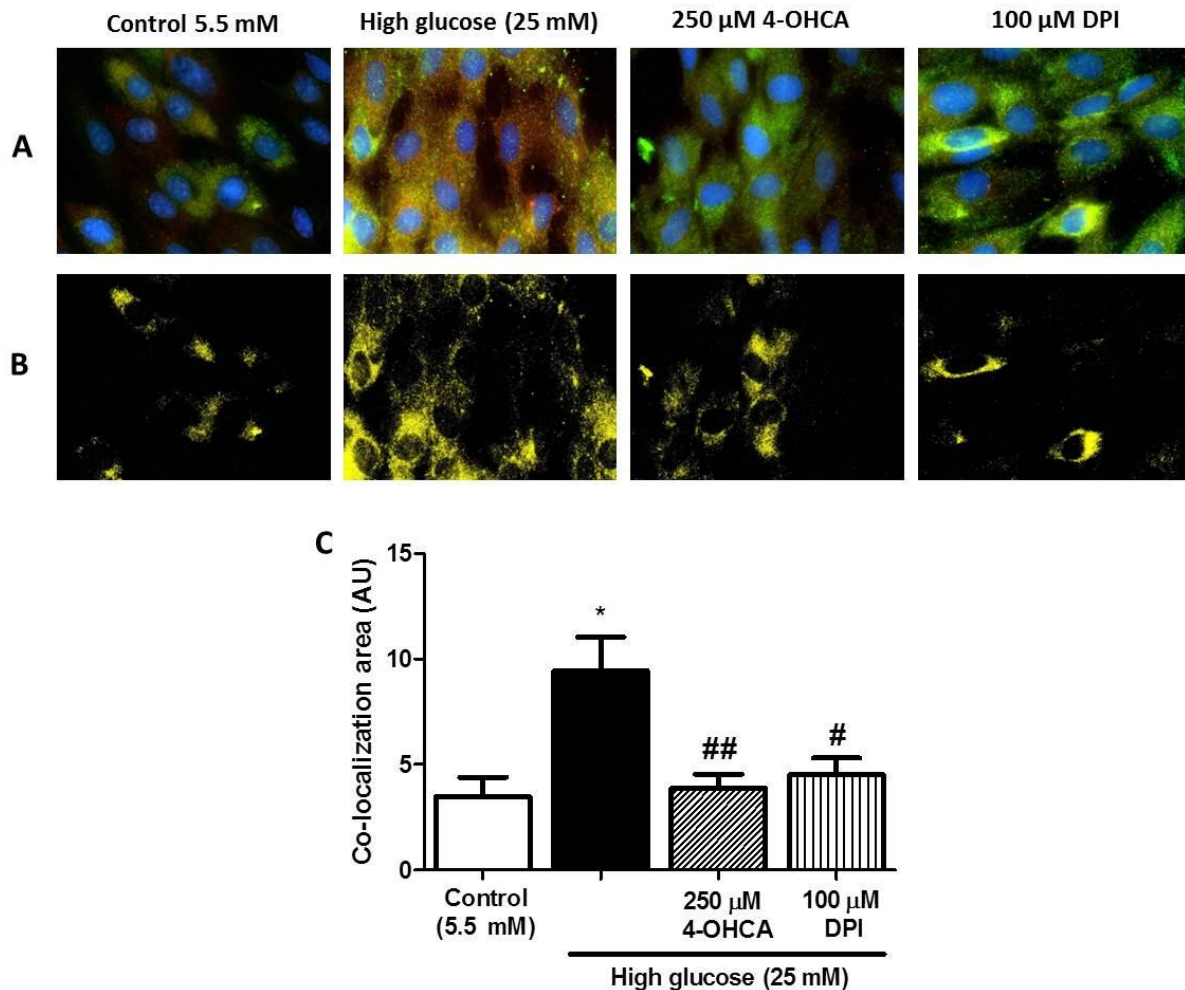


Figure 6.29 Co-localization of AS160 and O-GlcNAc was elevated under high glucose conditions and reduced by inhibition of mitochondrial and NOX-derived ROS. H9c2 cells were treated acutely with a) 4-OHCA and b) DPI under high glucose conditions. (A) Fluorescence microscopy analysis of H9c2 cells co-stained with antibodies to detect AS160 (FITC-green) and O-GlcNAc (Texas Red) with nuclei stained with DAPI (blue). (B) Co-localization of AS160 and O-GlcNAc indicated in the yellow color. (C) Quantification of the area of co-localization expressed in arbitrary units (AU). Values are expressed as mean \pm SEM (n=4). *P<0.05 vs. control; #P<0.05 vs. high glucose.

6.5. Discussion

The etiology of insulin resistance is complex and multifaceted. For example, it may result from metabolic alterations associated with multiple conditions of metabolic dysregulation (e.g. obesity and the metabolic syndrome), while increased consumption of energy rich food coupled to sedentary lifestyle may also fuel this

process (Petersen and Shulman, 2006; Stumvoll *et al.*, 2005). We are of the opinion that nutrient excess may be at the core of the detrimental causal effects of insulin resistance. More specifically, excursions of acute hyperglycemia - associated with excess nutrient intake or elevated postprandial glycaemic spikes in non-diabetic, pre-diabetic or diabetic individuals - can play a significant role in insulin resistance and its complications (Ceriello *et al.*, 2002; Kawahito *et al.*, 2009; Mapanga *et al.*, 2013, 2012; Williams *et al.*, 1998; Wisneski *et al.*, 1990; Yang *et al.*, 2009). The detrimental link between acute hyperglycemic episodes and the etiology of insulin resistance is thus an important factor to consider and explore. In Chapter 5 we identified a role for both mitochondrial- and NOX-derived ROS in the setting of acute hyperglycemia *in vitro*. Our data showed a link between oxidative stress and downstream disruption of insulin action with high glucose treatment. Furthermore, we proposed that mitochondrial ROS (although only modestly increased) may participate in cross-talk mechanisms and even trigger downstream activity of NOX and other molecular events. As a result we next turned our attention to investigate possible molecular events linking mitochondrial- and NOX-derived ROS production to the observed downregulation of glucose uptake.

Our first aim was to evaluate metabolic function under high glucose conditions and to assess the possible role(s) of mitochondrial- and NOX-derived ROS in this process. The first step was to measure ATP levels as an indicator of metabolic flux coupled to energy production. High glucose treatment had no significant effect on intracellular ATP levels. This is in accordance with the data showing lower glucose uptake (refer Fig 5.5), as one would expect a strong increase in ATP production when the glucose transport machinery would be functional and in the context of elevated extracellular

glucose availability. Conversely, it may also point towards alternate utilization of glucose metabolic intermediates, e.g. diversion into NOGPs (discussed below). Glucose uptake by alternative means (other than via GLUT4) may indeed be upregulated when extracellular glucose is high. For example, Balteau and colleagues recently showed increased glucose uptake via SGLT1 with damaging downstream effects (Balteau *et al.*, 2011). Administration of 4-OHCA inhibits the mitochondrial uptake of pyruvate (Halestrap, 1975), thereby limiting reducing equivalent production by the citric acid cycle, decreasing electron flow via the electron transport chain, and hence limiting mitochondrial ROS production. Thus a 4-OHCA-mediated reduction of mitochondrial pyruvate uptake may translate into lower mitochondrial ATP production. We are unclear how DPI treatment reduced ATP levels, but speculate that the inhibition of NOX may lead to activation of ATP consuming processes. These processes may be particularly increased in the period following acute DPI administration. Additional studies are required to further delineate a molecular basis for our observations. It may also be useful to determine the exact role on glucose-derived (glycolytic/glucose oxidation) ATP production.

To further evaluate the downstream effects of hyperglycemia-induced ROS, we subsequently determined the degree of NOGP activation in our experimental system. Exposure to acute high glucose coordinately induced the NOGP markers (AGE, polyol pathway, PKC, HBP) evaluated. These elevations were reduced by acute treatment with 4-OHCA and DPI. Our findings are in agreement (in part) with the unifying hypothesis that proposes that hyperglycemia-mediated oxidative stress may be a common upstream factor that elevates NOGP flux (Brownlee, 2005). Here mitochondrial-derived superoxide results in GAPDH inhibition and subsequent PARP

activation, leading to the diversion of upstream glycolytic intermediates into the NOGPs (Du *et al.*, 2003).

The current study now extends this paradigm since the data demonstrate that both mitochondrial and NOX-derived ROS coordinately upregulated all four NOGPs. Moreover, inhibition of both mitochondrial- and NOX-derived ROS generation lowered NOGP activation to the same extent, despite NOX-derived ROS constituting the bulk of ROS generated by acute high glucose exposure. These findings therefore support cross-talk between mitochondrial ROS and the downstream activation of the NOX system in our model (discussed in Chapter 5). The activity of transketolase (non-oxidative PPP) was, however, unaltered by high glucose conditions. Surprisingly, inhibition of ROS production (both mitochondrial- and NOX-derived) resulted in diminished transketolase activity. This suggests that transketolase activation may be linked to mitochondrial and NOX signaling events. However, further studies are needed to investigate this intriguing observation. It is also important to consider the contribution of attenuated antioxidant defense mechanisms to the overall intracellular oxidative stress as it forms another part of the extension to the original unifying hypothesis. Pharmacological studies aiming to delineate the role of oxidative stress should take these factors into account.

To ascertain the functional effects of NOGP activation, we employed various NOGP inhibitors. Initial optimization experiments showed that each individual inhibitor markedly reduced the hyperglycemia-mediated induction of their respective pathways. Furthermore, insulin-mediated glucose uptake was improved to varying degrees by each inhibitor. For example, PKC inhibition (CHE) resulted in the most

substantial reversal of high glucose effects compared to the other NOGP inhibitors. This indicates that PKC is the major downstream target of hyperglycemia-induced ROS that impairs insulin-stimulated glucose uptake with acute hyperglycemia. Indeed, PKC activation may exert a negative regulatory effect on insulin signaling (Bollag *et al.*, 1986; Takayama *et al.*, 1988). In support, Davidoff and colleagues (2004) found that high glucose-induced insulin resistance and diminished *in vitro* contractile function could be reversed by CHE treatment in rat ventricular cardiomyocytes isolated from diabetic animals. They concluded that PKC is a central modulator of hyperglycemic damage (Davidoff *et al.*, 2004).

The PKC family is composed of numerous isoforms with different subcellular localizations (reviewed in Cosentino-Gomes *et al.*, 2012). Oxidative stress can result in direct PKC activation that is usually associated with its translocation to the sarcolemma (Konishi *et al.*, 1997). The PKC enzyme family also plays an important role in the activation of NOX isoforms, e.g. the plasma-localized NOX2 (reviewed by Fisher, 2009). Since PKC β II is strongly implicated in the onset of insulin resistance (Hennige *et al.*, 2010), we next assessed its expression in our experimental system. Here PKC β II was upregulated by acute hyperglycemia and this induction was ROS-dependent (mitochondrial- and NOX-derived), indicating that it is a downstream target of mitochondrial and NOX signaling, respectively. Together, we show that acute hyperglycemia-induced ROS triggers coordinate NOGP activation, but that PKC β II is the key regulator responsible for attenuation of insulin-mediated glucose uptake in this instance. However, we cannot rule out the possibility that other PKC isoforms (not evaluated in this study) may also contribute to this effect.

Increased HBP flux may impair insulin-mediated glucose transport by acting as an upstream activator of PKC activation under high glucose conditions (Filippis *et al.*, 1997). Indeed, high glucose-mediated activation of the HBP is implicated as an important mechanism in the downregulation of insulin sensitivity (Chen *et al.*, 1997; Cooksey *et al.*, 1999; Marshall *et al.*, 1991; Robinson *et al.*, 1995), and insulin signaling intermediates (e.g. IRS1 and Akt) may be post-translationally modified by O-GlcNAc, resulting in reduced phosphorylation and activity (Arias *et al.*, 2004; Gandy *et al.*, 2006; Nelson *et al.*, 2002; Park *et al.*, 2005; Vosseller *et al.*, 2002). Our laboratory previously established that impaired cardiac function, increased infarct size and myocardial apoptosis were associated with oxidative stress and elevated HBP activation in various *in vitro*, *ex vivo* and *in vivo* models of experimental hyperglycemia (Mapanga *et al.*, 2012; Rajamani and Essop, 2010; Rajamani *et al.*, 2011). However, others found that acute elevation of HBP flux may be cardioprotective against ischemia-reperfusion damage and that this may be attributable to an adaptive response (reviewed in Chatham and Marchase, 2010; Fülöp *et al.*, 2007; McLarty *et al.*, 2013). Data from the current study suggest that HBP flux may not play a prominent role under our experimental conditions. We cannot, however, rule out pathway cross-talk as our preliminary data indicate reducing effects of each pathway inhibitor on markers of the other pathways, while co-localization studies revealed that Akt and its downstream substrate AS160, may both be modified by O-GlcNAcylation. Mitochondrial- and NOX-derived ROS may both be effectors of the O-GlcNAcylation of these intermediates, as 4-OHCA and DPI treatments markedly reduced the co-localization effect of high glucose. The prominence of such mechanisms deserves further attention.

We further aimed to elucidate whether any cross-talk exists between NOGP activity and oxidative stress mechanisms. NOX activity was markedly reduced and GSH levels enhanced by inhibition of the PKC (CHE) and polyol (ZOP) pathways. Inhibition of the AGE pathway (AMG) also increased GSH levels. Furthermore, PKC inhibition (CHE) lowered NADPH supply, while the latter was elevated with polyol pathway inhibition (ZOP). Polyol pathway inhibition also led to increased G6PD activity. These data indicate that there is cross-talk between the NOGPs but especially between the polyol and PKC pathways, with NADPH availability a key common metabolite determining which pathway will predominate under specific circumstances. Our data show that acute high glucose conditions increased polyol pathway flux, a process that utilizes NADPH (Asbun and Villarreal, 2006; King and Loeken, 2004; Sato *et al.*, 1999; Tracey *et al.*, 2000). The concomitant upregulation of PKC and subsequent activation of NOX further diminishes intracellular NADPH levels, while the activity of G6PD (a chief NADPH producing enzyme) is not altered. This results in attenuation of the glutathione replenishment reactions. The concomitant reduction in SOD activity, NOX activation and increased mitochondrial ROS production results in a global intracellular oxidative stress milieu. We propose that this may result in a vicious cycle of further NOGP activation and ROS production, all contributing to reduced insulin action. Others found that the elevation of AGEs may directly induce oxidative stress (Li *et al.*, 2007). In agreement, our data show involvement of AGEs in NOX activation and upregulation of mitochondrial ROS, as well as disruption of SOD activity and GSH levels. The precise mechanisms and possible interplay is not clear and needs further evaluation.

Upregulation of the PPP by BFT treatment may divert flux from the four NOGPs into the PPP and is associated with beneficial outcomes in the setting of hyperglycemia/diabetes (Hammes *et al.*, 2003). We therefore employed BFT to further evaluate the validity of our NOGP inhibitor data. Our data showed that BFT administration markedly reduced each of the NOGPs evaluated, and increased the activity of transketolase. BFT treatment (100 μ M) also prominently increased insulin-stimulated glucose uptake, and generally reversed the effects of acute hyperglycemia here described. This likely represents an attenuation of effects largely exerted by PKC, and to a lesser extent the polyol pathway. We were surprised that DON treatment reduced transketolase activity and it is our opinion that this may represent additional regulation of the PPP by HBP activation. We speculate that transketolase may be O-GlcNAc modified, however, this has not been shown before. The regulatory mechanism(s) and downstream outcome(s) need to be further evaluated.

We also evaluated NOGP activation in the setting of *in vivo* pre-diabetes and overt diabetes by employing the OLETF rat model of metabolic dysfunction (Tanaka *et al.*, 2010). This model develops mild obesity and insulin resistance associated with late onset hyperglycemia (Kawano *et al.*, 1992, 1994). We analyzed molecular derangements in heart tissues from rats treated with thiamine from the age of 4 week and rats developed hallmarks of a pre-diabetic state at the age of 25 week (elevated blood glucose accompanied by high insulin levels). By 55 week of age the rats were diabetic, displaying low insulin and chronic hyperglycemia accompanied by β -cell destruction and associated diabetic complications (Tanaka *et al.*, 2010). We evaluated Akt kinase activity as a marker of insulin action and found it was reduced over time. However, thiamine treatment markedly upregulated it in the pre-diabetic

rat heart. This is in accordance with our *in vitro* data showing normalized glucose uptake by BFT treatment in an acute hyperglycemic setting. Thiamine treatment also markedly increased transketolase activity in both age groups (25 and 55 weeks). However, G6PD activity (reduced in the diabetic vs. pre-diabetic tissues) could only be increased by thiamine in the 55 week group. These data further support our *in vitro* results showing that G6PD activity is relatively unaltered by BFT, but that transketolase is markedly increased during acute hyperglycemic conditions. NOGP markers (AGE, polyol pathway, PKC activity) were generally reduced in the diabetic tissues. This is in contrast to studies showing drastically elevated NOGP markers associated with diabetes (Brownlee, 2005; Giacco and Brownlee, 2010; Hammes *et al.*, 2003; King and Brownlee, 1996). However, these studies focused on tissues and cell types that are not insulin dependent (e.g. pancreatic β -cells and endothelial cells). We therefore conclude that overt diabetes, specifically the reduced insulin levels accompanied by severe insulin resistance, may result in decreased intracellular glucose in insulin responsive cells (e.g. cardiomyocytes) resulting in reduced glycolytic and NOGP flux. This is, however, not the case in the pre-diabetic/acute hyperglycemic phase, and the elevated intracellular glucose concentrations may in fact drive insulin resistance via the mechanisms described in this study. The original study by Tanaka and colleagues (Tanaka *et al.*, 2010), did unfortunately not include a LETO group (control for OLETF) meaning that conclusions regarding the effects observed in untreated OLETF rats vs. a normal metabolic state cannot be readily made. Nonetheless, their study showed differences in the metabolic parameters between OLETF rats included and from the breeder colony vs. LETO breeders (refer Tanaka *et al.*, 2010). In accordance with the *in vitro*

BFT data, thiamine administration reduced markers of all four NOGPs, mainly in the 25 wk group.

In summary, this study demonstrates that acute hyperglycemia triggers an 'unfortunate series of events' that contribute to decreased insulin-mediated cardiac glucose uptake (Fig. 6.30). We propose that acute hyperglycemia generates a relatively small amount of mitochondrial ROS (as a trigger event) that results in the direct activation of PKC isoforms in proximity and/or localized to the mitochondrion. Interestingly, others found that PKC β II was localized to mitochondria in melanomas (Voris *et al.*, 2010) making it an ideal candidate in this instance. However, further studies are required to determine whether this is indeed the case in the heart. PKC β II in turn can activate NOX that will result in substantially higher ROS production, thus amplifying the initial mitochondrial ROS trigger effect. Increased ROS levels can decrease antioxidant defenses (e.g. lower SOD activity) and its activation of the polyol pathway will lower GSH availability. Subsequently, intracellular oxidative stress triggers activation of the NOGPs, particularly PKC β II, leading to impaired insulin-mediated glucose uptake. We also propose that high glucose availability may increase these effects in a more direct fashion (i.e. high substrate supply, direct NOX activation). Thus repeated, acute hyperglycemic episodes may contribute to the onset of insulin resistance and subsequent detrimental effects on the heart.

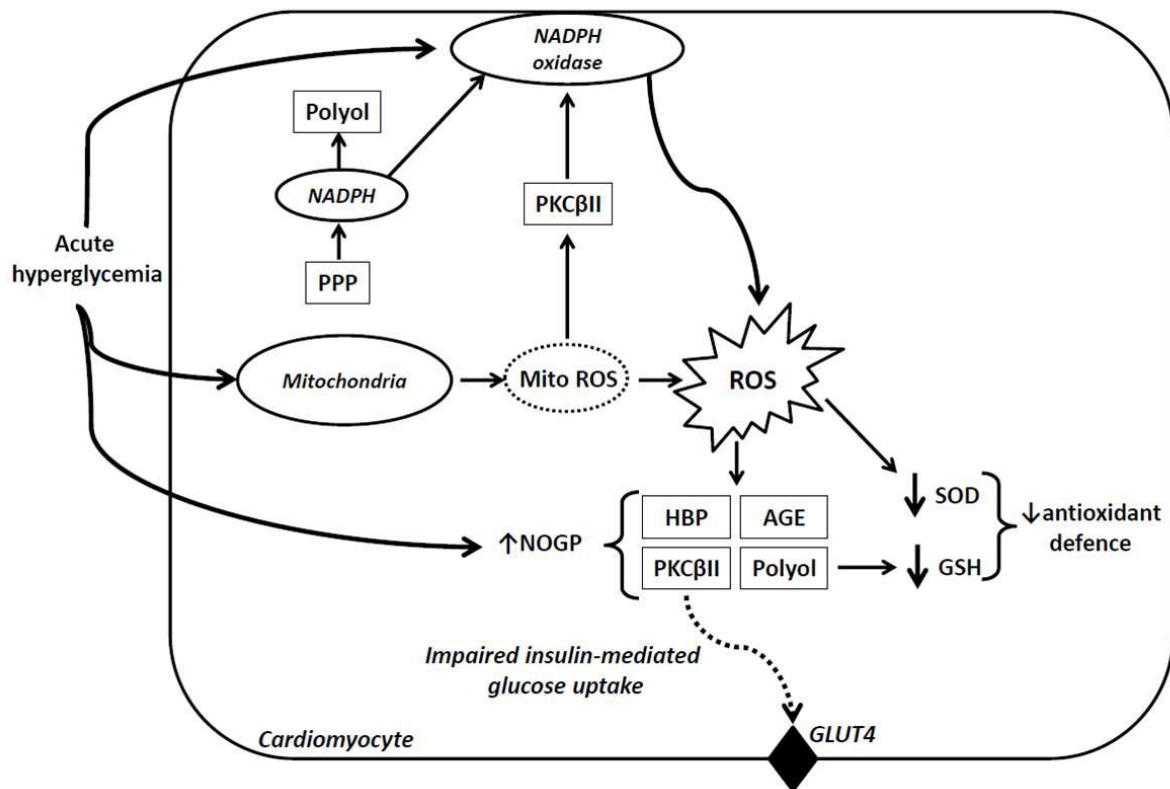


Figure 6.30 Our proposed model for acute hyperglycemia-induced myocardial insulin resistance.

6.6. References

- Amadio, M., Bucolo, C., Leggio, G.M., Drago, F., Govoni, S., Pascale, a, 2010. The PKCbeta/HuR/VEGF pathway in diabetic retinopathy. *Biochem Pharmacol* 80, 1230–7.
- Arias, E.B., Kim, J., Cartee, G.D., 2004. Prolonged incubation in PUGNAc results in increased protein O-Linked glycosylation and insulin resistance in rat skeletal muscle. *Diabetes* 53, 921–30.
- Asbun, J., Villarreal, F.J., 2006. The pathogenesis of myocardial fibrosis in the setting of diabetic cardiomyopathy. *J Am Coll Cardiol* 47, 693–700.
- Babaei-Jadidi, R., Karachalias, N., Ahmed, N., Battah, S., Thornalley, P.J., 2003. Prevention of incipient diabetic nephropathy by high-dose thiamine and benfotiamine. *Diabetes* 52, 2110–20.
- Balakumar, P., Rohilla, A., Krishan, P., Solairaj, P., Thangathirupathi, A., 2010. The multifaceted therapeutic potential of benfotiamine. *Pharmacol Res* 61, 482–8.
- Balteau, M., Tajeddine, N., De Meester, C., Ginion, A., Des Rosiers, C., Brady, N.R., Sommereyns, C., Horman, S., Vanoverschelde, J.-L., Gailly, P., Hue, L., Bertrand, L., Beauloye, C., 2011. NADPH oxidase activation by hyperglycaemia in cardiomyocytes is independent of glucose metabolism but requires SGLT1. *Cardiovasc Res* 92, 237–46.
- Bandyopadhyay, G., Standaert, M.L., Kikkawa, U., Ono, Y., Moscat, J., Farese, R. V, 1999a. Effects of transiently expressed atypical (zeta, lambda), conventional (alpha, beta) and novel (delta, epsilon) protein kinase C isoforms on insulin-stimulated translocation of epitope-tagged GLUT4 glucose transporters in rat adipocytes: specific intercha. *Biochem J* 337 (Pt 3, 461–70.
- Bandyopadhyay, G., Standaert, M.L., Sajan, M.P., Karnitz, L.M., Cong, L., Quon, M.J., Farese, R. V, 1999b. Dependence of insulin-stimulated glucose transporter 4 translocation on 3-phosphoinositide-dependent protein kinase-1 and its target threonine-410 in the activation loop of protein kinase C-zeta. *Mol Endocrinol* 13, 1766–72.
- Beltramo, E., Berrone, E., Tarallo, S., Porta, M., 2008. Effects of thiamine and benfotiamine on intracellular glucose metabolism and relevance in the prevention of diabetic complications. *Acta Diabetol* 45, 131–41.
- Berrone, E., Beltramo, E., Solimine, C., Ape, A.U., Porta, M., 2006. Regulation of intracellular glucose and polyol pathway by thiamine and benfotiamine in vascular cells cultured in high glucose. *J Biol Chem* 281, 9307–13.
- Bollag, G.E., Roth, R.A., Beaudoin, J., Mochly-Rosen, D., Koshland, D.E., 1986. Protein kinase C directly phosphorylates the insulin receptor in vitro and reduces its protein-tyrosine kinase activity. *Proc Natl Acad Sci U S A* 83, 5822–4.
- Brownlee, M., 2005. The pathobiology of diabetic complications: a unifying mechanism. *Diabetes* 54, 1615–25.

- Ceriello, A., Quagliaro, L., D'Amico, M., Di Filippo, C., Marfella, R., Nappo, F., Berrino, L., Rossi, F., Giugliano, D., 2002. Acute hyperglycemia induces nitrotyrosine formation and apoptosis in perfused heart from rat. *Diabetes* 51, 1076–82.
- Ceylan-Isik, A.F., Wu, S., Li, Q., Li, S.-Y., Ren, J., 2006. High-dose benfotiamine rescues cardiomyocyte contractile dysfunction in streptozotocin-induced diabetes mellitus. *J Appl Physiol* 100, 150–6.
- Chatham, J.C., Marchase, R.B., 2010. Protein O-GlcNAcylation: A critical regulator of the cellular response to stress. *Curr Signal Transduct Ther* 5, 49–59.
- Chen, H., Ing, B.L., Robinson, K.A., Feagin, A.C., Buse, M.G., Quon, M.J., 1997. Effects of overexpression of glutamine:fructose-6-phosphate amidotransferase (GFAT) and glucosamine treatment on translocation of GLUT4 in rat adipose cells. *Mol Cell Endocrinol* 135, 67–77.
- Chmura, S.J., Dolan, M.E., Cha, A., Mauceri, H.J., Kufe, D.W., Weichselbaum, R.R., 2000. In vitro and in vivo activity of protein kinase C inhibitor chelerythrine chloride induces tumor cell toxicity and growth delay in vivo. *Clin Cancer Res* 6, 737–42.
- Cooksey, R.C., Hebert, L.F., Zhu, J.H., Wofford, P., Garvey, W.T., McClain, D.A., 1999. Mechanism of hexosamine-induced insulin resistance in transgenic mice overexpressing glutamine:fructose-6-phosphate amidotransferase: decreased glucose transporter GLUT4 translocation and reversal by treatment with thiazolidinedione. *Endocrinology* 140, 1151–7.
- Cosentino-Gomes, D., Rocco-Machado, N., Meyer-Fernandes, J.R., 2012. Cell signaling through protein kinase C oxidation and activation. *Int J Mol Sci* 13, 10697–721.
- Davidoff, A.J., Davidson, M.B., Carmody, M.W., Davis, M.E., Ren, J., 2004. Diabetic cardiomyocyte dysfunction and myocyte insulin resistance: role of glucose-induced PKC activity. *Mol Cell Biol* 262, 155–63.
- Du, X., Matsumura, T., Edelstein, D., Rossetti, L., Zsengellér, Z., Szabó, C., Brownlee, M., 2003. Inhibition of GAPDH activity by poly(ADP-ribose) polymerase activates three major pathways of hyperglycemic damage in endothelial cells. *J Clin Invest* 112, 1049–57.
- Du, X.L., Edelstein, D., Dimmeler, S., Ju, Q., Sui, C., Brownlee, M., 2001. Hyperglycemia inhibits endothelial nitric oxide synthase activity by posttranslational modification at the Akt site. *Methods* 108, 1341–1348.
- Filippis, A., Clark, S., Proietto, J., 1997. Increased flux through the hexosamine biosynthesis pathway inhibits glucose transport acutely by activation of protein kinase C. *Biochem J* 324, 981–5.
- Fisher, A.B., 2009. Redox signaling across cell membranes. *Antioxid Redox Signal* 11, 1349–56.
- Fülöp, N., Marchase, R.B., Chatham, J.C., 2007. Role of protein O-linked N-acetylglucosamine in mediating cell function and survival in the cardiovascular system. *Cardiovasc Res* 73, 288–97.

- Gandy, J.C., Rountree, A.E., Bijur, G.N., 2006. Akt1 is dynamically modified with O-GlcNAc following treatments with PUGNAc and insulin-like growth factor-1. *FEBS Lett* 580, 3051–8.
- Geraldes, P., King, G.L., 2010. Activation of protein kinase C isoforms and its impact on diabetic complications. *Circ Res* 106, 1319–31.
- Giaccari, A., Sorice, G., Muscogiuri, G., 2009. Glucose toxicity: the leading actor in the pathogenesis and clinical history of type 2 diabetes - mechanisms and potentials for treatment. *Nutr Metab Cardiovasc Dis* 19, 365–77.
- Giacco, F., Brownlee, M., 2010. Oxidative stress and diabetic complications. *Circ Res* 107, 1058–70.
- Halestrap, B.A.P., 1975. Mitochondrial Pyruvate 85–96.
- Hammes, H.P., Du, X., Edelstein, D., Taguchi, T., Matsumura, T., Ju, Q., Lin, J., Bierhaus, A., Nawroth, P., Hannak, D., Neumaier, M., Bergfeld, R., Giardino, I., Brownlee, M., 2003. Benfotiamine blocks three major pathways of hyperglycemic damage and prevents experimental diabetic retinopathy. *Nat Med* 9, 294–9.
- Hennige, A.M., Heni, M., Machann, J., Staiger, H., Sartorius, T., Hoene, M., Lehmann, R., Weigert, C., Peter, A., Bornemann, A., Kroeber, S., Pujol, A., Franckhauser, S., Bosch, F., Schick, F., Lammers, R., Häring, H.-U., 2010. Enforced expression of protein kinase C in skeletal muscle causes physical inactivity, fatty liver and insulin resistance in the brain. *J Cell Mol Med* 14, 903–13.
- Itani, S.I., Zhou, Q., Pories, W.J., MacDonald, K.G., Dohm, G.L., 2000. Involvement of protein kinase C in human skeletal muscle insulin resistance and obesity. *Diabetes* 49, 1353–8.
- Kador, P.F., Randazzo, J., Blessing, K., Makita, J., Zhang, P., Yu, K., Hosoya, K.-I., Terasaki, T., 2009. Polyol formation in cell lines of rat retinal capillary pericytes and endothelial cells (TR-rPCT and TR-iBRB). *J Ocul Pharmacol Ther* 25, 299–308.
- Kang, E., Han, D., Park, J., Kyoung, T., Oh, M., Lee, S., Choi, S., Yong, Z., Kim, Y., Weon, J., 2008. O-GlcNAc modulation at Akt1 Ser473 correlates with apoptosis of murine pancreatic β cells 4.
- Katare, R., Caporali, A., Emanuelli, C., Madeddu, P., 2010a. Benfotiamine improves functional recovery of the infarcted heart via activation of pro-survival G6PD/Akt signaling pathway and modulation of neurohormonal response. *J Mol Cell Cardiol* 49, 625–38.
- Katare, R., Caporali, A., Oikawa, A., Meloni, M., Emanuelli, C., Madeddu, P., 2010b. Vitamin B1 analog benfotiamine prevents diabetes-induced diastolic dysfunction and heart failure through Akt/Pim-1-mediated survival pathway. *Circ Hear Fail* 3, 294–305.
- Kawahito, S., Kitahata, H., Oshita, S., 2009. Problems associated with glucose toxicity: role of hyperglycemia-induced oxidative stress. *World J Gastroenterol* 15, 4137–42.

- Kawano, K., Hirashima, T., Mori, S., Natori, T., 1994. OLETF (Otsuka Long-Evans Tokushima Fatty) rat: a new NIDDM rat strain. *Diabetes Res Clin Pract* 24 Suppl, S317–20.
- Kawano, K., Hirashima, T., Mori, S., Saitoh, Y., Kurosumi, M., Natori, T., 1992. Spontaneous long-term hyperglycemic rat with diabetic complications. Otsuka Long-Evans Tokushima Fatty (OLETF) strain. *Diabetes* 41, 1422–8.
- King, G.L., Brownlee, M., 1996. The cellular and molecular mechanisms of diabetic complications. *Endocrinol Metab Clin North Am* 25, 255–70.
- King, G.L., Loeken, M.R., 2004. Hyperglycemia-induced oxidative stress in diabetic complications. *Histochem Cell Biol* 122, 333–8.
- Konishi, H., Tanaka, M., Takemura, Y., Matsuzaki, H., Ono, Y., Kikkawa, U., Nishizuka, Y., 1997. Activation of protein kinase C by tyrosine phosphorylation in response to H₂O₂. *Proc Natl Acad Sci U S A* 94, 11233–7.
- Li, S.-Y., Sigmon, V.K., Babcock, S. a, Ren, J., 2007. Advanced glycation endproduct induces ROS accumulation, apoptosis, MAP kinase activation and nuclear O-GlcNAcylation in human cardiac myocytes. *Life Sci* 80, 1051–6.
- Lin, J., Alt, A., Liersch, J., Bretzel, R.G., Brownlee, M., Hammes, H., Giessen, J., 1998. Benfotiamine Inhibits Intracellular Formation of Advanced Glycation End Products in vivo. *Diabetologia* 1998–1998.
- Mapanga, R.F., Joseph, D., Symington, B., Garson, K.-L., Kimar, C., Kelly-Laubscher, R., Essop, M.F., 2013. Detrimental effects of acute hyperglycaemia on the rat heart. *Acta Physiol (Oxf) n/a–n/a*.
- Mapanga, R.F., Rajamani, U., Dlamini, N., Zungu-Edmondson, M., Kelly-Laubscher, R., Shafiullah, M., Wahab, A., Hasan, M.Y., Fahim, M. a, Rondeau, P., Bourdon, E., Essop, M.F., 2012. Oleanolic acid: a novel cardioprotective agent that blunts hyperglycemia-induced contractile dysfunction. *PLoS One* 7, e47322.
- Marchetti, V., Menghini, R., Rizza, S., Vivanti, A., Feccia, T., Lauro, D., Fukamizu, A., Lauro, R., Federici, M., 2006. Benfotiamine counteracts glucose toxicity effects on endothelial progenitor cell differentiation via Akt/FoxO signaling. *Diabetes* 55, 2231–7.
- Marshall, S., Bacote, V., Traxinger, R.R., 1991. Discovery of a metabolic pathway mediating glucose-induced desensitization of the glucose transport system. Role of hexosamine biosynthesis in the induction of insulin resistance. *J Biol Chem* 266, 4706–12.
- McLarty, J.L., Marsh, S.A., Chatham, J.C., 2013. Post-translational protein modification by O-linked N-acetyl-glucosamine: its role in mediating the adverse effects of diabetes on the heart. *Life sci* 92, 621–7.
- Nelson, B.A., Robinson, K. a, Buse, M.G., 2002. Defective Akt activation is associated with glucose- but not glucosamine-induced insulin resistance. *Am J Physiol Endocrinol Metab* 282, E497–506.

- Nishikawa, T., Edelstein, D., Du, X.L., Yamagishi, S., Matsumura, T., Kaneda, Y., Yorek, M.A., Beebe, D., Oates, P.J., Hammes, H.P., Giardino, I., Brownlee, M., 2000. Normalizing mitochondrial superoxide production blocks three pathways of hyperglycaemic damage. *Nature* 404, 787–90.
- Park, S.S.Y., Ryu, J., Lee, W., 2005. O-GlcNAc modification on IRS-1 and Akt2 by PUGNAc inhibits their phosphorylation and induces insulin resistance in rat primary adipocytes. *Exp Mol Med* 37, 220–9.
- Petersen, K.F., Shulman, G.I., 2006. Etiology of insulin resistance. *Am J Med* 119, 10S–16S.
- Quagliaro, L., Piconi, L., Assaloni, R., Martinelli, L., Motz, E., Ceriello, A., 2003. Intermittent high glucose enhances apoptosis related to oxidative stress in human umbilical vein endothelial cells: the role of protein kinase C and NAD(P)H-oxidase activation. *Diabetes* 52, 2795–804.
- Ragheb, R., Shanab, G.M.L., Medhat, A.M., Seoudi, D.M., Adeli, K., Fantus, I.G., 2009. Free fatty acid-induced muscle insulin resistance and glucose uptake dysfunction: evidence for PKC activation and oxidative stress-activated signaling pathways. *Biochem Biophys Res Commun* 389, 211–6.
- Rajamani, U., Essop, M.F., 2010. Hyperglycemia-mediated activation of the hexosamine biosynthetic pathway results in myocardial apoptosis. *Am J Physiol Cell Physiol* 299, C139–47.
- Rajamani, U., Joseph, D., Roux, S., Essop, M.F., 2011. The hexosamine biosynthetic pathway can mediate myocardial apoptosis in a rat model of diet-induced insulin resistance. *Acta Physiol* 202, 151–7.
- Robinson, K.A., Weinstein, M.L., Lindenmayer, G.E., Buse, M.G., 1995. Effects of diabetes and hyperglycemia on the hexosamine synthesis pathway in rat muscle and liver. *Diabetes* 44, 1438–46.
- Rohr, J.M., Truong, S., Hong, T., Yancey, P.H., 1999. Effects of ascorbic acid, aminoguanidine, sorbinil and zopolrestat on sorbitol and betaine contents in cultured rat renal cells. *Exp Biol Online* 4, 29–38.
- Rösen, P., Nawroth, P.P., King, G., Möller, W., Tritschler, H.J., Packer, L., 2001. The role of oxidative stress in the onset and progression of diabetes and its complications: a summary of a Congress Series sponsored by UNESCO-MCBN, the American Diabetes Association and the German Diabetes Society. *Diabetes Metab Res Rev* 17, 189–212.
- Sato, S., Secchi, E.F., Lizak, M.J., Fukase, S., Ohta, N., Murata, M., Tsai, J.Y., Kador, P.F., 1999. Polyol formation and NADPH-dependent reductases in dog retinal capillary pericytes and endothelial cells. *Invest Ophthalmol Vis Sci* 40, 697–704.
- Schaffer, S.W., Jong, C.J., Mozaffari, M., 2012. Role of oxidative stress in diabetes-mediated vascular dysfunction: unifying hypothesis of diabetes revisited. *Vasc Pharmacol* 57, 139–49.
- Schupp, N., Dette, E.M., Schmid, U., Bahner, U., Winkler, M., Heidland, A., Stopper, H., 2008. Benfotiamine reduces genomic damage in peripheral lymphocytes of hemodialysis patients. *Naunyn-Schmiedeberg's Arch Pharmacol* 378, 283–291.

- Sharma, N., Okere, I.C., Duda, M.K., Chess, D.J., O'Shea, K.M., Stanley, W.C., 2007a. Potential impact of carbohydrate and fat intake on pathological left ventricular hypertrophy. *Cardiovasc Res* 73, 257–68.
- Sharma, N., Okere, I.C., Duda, M.K., Johnson, J., Yuan, C.L., Chandler, M.P., Ernsberger, P., Hoyt, B.D., Stanley, W.C., 2007b. High fructose diet increases mortality in hypertensive rats compared to a complex carbohydrate or high fat diet. *Am J Hypertens* 20, 403–9.
- Stirban, A., Negrean, M., Stratmann, B., Gawlowski, T., Horstmann, T., Götting, C., Kleesiek, K., Mueller-Roesel, M., Koschinsky, T., Uribarri, J., Vlassara, H., Tschoepe, D., 2006. Benfotiamine prevents macro- and microvascular endothelial dysfunction and oxidative stress following a meal rich in advanced glycation end products in individuals with type 2 diabetes. *Diabetes Care* 29, 2064–71.
- Stumvoll, M., Goldstein, B.J., van Haeften, T.W., 2005. Type 2 diabetes: principles of pathogenesis and therapy. *Lancet* 365, 1333–46.
- Takayama, S., White, M.F., Kahn, C.R., 1988. Phorbol ester-induced serine phosphorylation of the insulin receptor decreases its tyrosine kinase activity. *J Biol Chem* 263, 3440–7.
- Tanaka, T., Kono, T., Terasaki, F., Yasui, K., Soyama, A., Otsuka, K., Fujita, S., Yamane, K., Manabe, M., Usui, K., Kohda, Y., 2010. Thiamine prevents obesity and obesity-associated metabolic disorders in OLETF rats. *J Nutr Sci Vitaminol (Tokyo)* 56, 335–46.
- Tappy, L., Lê, K.-A., 2010. Metabolic effects of fructose and the worldwide increase in obesity. *Physiol Rev* 90, 23–46.
- Tracey, W.R., Magee, W.P., Ellery, C. a, MacAndrew, J.T., Smith, a H., Knight, D.R., Oates, P.J., 2000. Aldose reductase inhibition alone or combined with an adenosine A(3) agonist reduces ischemic myocardial injury. *Am J Physiol Heart Circ Physiol* 279, H1447–52.
- Voris, J.P., Sitailo, L. a, Rahn, H.R., Defnet, A., Gerds, A.T., Sprague, R., Yadav, V., Caroline Le Poole, I., Denning, M.F., 2010. Functional alterations in protein kinase C beta II expression in melanoma. *Pigment Cell Melanoma Res* 23, 216–24.
- Vosseller, K., Wells, L., Lane, M.D., Hart, G.W., 2002. Elevated nucleocytoplasmic glycosylation by O-GlcNAc results in insulin resistance associated with defects in Akt activation in 3T3-L1 adipocytes. *Proc Natl Acad Sci U S A* 99, 5313–8.
- Wang, X.-L., Lau, W.B., Yuan, Y.-X., Wang, Y.-J., Yi, W., Christopher, T.A., Lopez, B.L., Liu, H.-R., Ma, X.-L., 2010. Methylglyoxal increases cardiomyocyte ischemia-reperfusion injury via glycative inhibition of thioredoxin activity. *Am J Physiol Endocrinol Metab* 299, E207–14.
- Williams, S.B., Goldfine, A.B., Timimi, F.K., Ting, H.H., Roddy, M.A., Simonson, D.C., Creager, M.A., 1998. Acute hyperglycemia attenuates endothelium-dependent vasodilation in humans in vivo. *Circulation* 97, 1695–701.
- Winkler, G., Pál, B., Nagybégyani, E., Ory, I., Porochnavec, M., Kempler, P., 1999. Effectiveness of different benfotiamine dosage regimens in the treatment of painful diabetic neuropathy. *Arzneimittelforschung*.

- Wisneski, J.A., Stanley, W.C., Neese, R.A., Gertz, E.W., Nose, R.A., 1990. Effects of Acute Hyperglycemia on Myocardial Glycolytic Activity in Humans. *J Clin Invest* 85, 1648–1656.
- Wu, S., Ren, J., 2006. Benfotiamine alleviates diabetes-induced cerebral oxidative damage independent of advanced glycation end-product, tissue factor and TNF-alpha. *Neurosci Lett* 394, 158–62.
- Yang, Z., Laubach, V.E., French, B. a, Kron, I.L., 2009. Acute hyperglycemia enhances oxidative stress and exacerbates myocardial infarction by activating nicotinamide adenine dinucleotide phosphate oxidase during reperfusion. *J Thorac Cardiovasc Surg* 137, 723–9.

CHAPTER 7

Concluding remarks

7.1. Summary of findings

So far, treatment of diabetes and its associated complications does not always achieve optimal results. This does not bode well for the alarming future projections regarding diabetes and similar metabolic diseases. Further fueling this is the strong association with cardio-metabolic complications, together contributing to the most significant percentage of non-communicable diseases. These complications affect young, working age adults from both developed and developing nations, resulting in a significant socio-economic burden. Obesity, metabolic syndrome and diabetes (undiagnosed, newly diagnosed or frank diabetes) are also highly prevalent in South Africa. A call for urgent measures to help curtail the growing disease burden is a global priority, however, the complex molecular mechanisms underlying the etiology of insulin resistance is not yet fully understood.

We are of the opinion that a thorough understanding of the pathophysiological mechanisms driving insulin resistance is of utmost importance to curb the disease progression at an early stage. Our study therefore evaluated the effects of acute hyperglycemia on insulin resistance in cardiac-derived cells. Our data reveal that acute hyperglycemia elicits oxidative stress mechanisms that are strongly implicated in mediating insulin resistance. We further describe cross-talk mechanisms between mitochondrial ROS and NOX activation with downstream induction of NOGPs. Here, PKC β II may play a central role in exerting downstream damaging effects. Such

pathway interplay can also amplify downstream activation of further detrimental effects. Collectively our data extend current hypotheses describing hyperglycemia-mediated derangements, specifically in the setting of insulin resistance. The findings of this study also point to ways how to confront the problem of insulin resistance and its complications, and lay a robust foundation for future work. Delineating the etiology of insulin resistance in more certain terms can greatly benefit identification of new pharmaceutical targets and the design of improved, more affordable medication and/or implementation of lifestyle intervention.

7.2. Limitations

Although we evaluated NOX activation in this study, we cannot comment on the specific NOX isoforms involved. Furthermore, we acknowledge that additional sources of ROS production (other than mitochondria and NOX) may also play a role and deserve further attention. The fluorescent probes used to detect ROS are not specific to any type, thus an analysis of specific ROS and reactive nitrogen species, and its impact on insulin action may provide additional insights. Additional methods to inhibit and enhance mitochondrial ROS, NOX and NOGPs (e.g. siRNA knockdown and/or overexpression of key regulatory enzymes) may also provide more specific means of controlling NOGP induction compared to the pharmacological inhibitors utilized here. For the current study, we focused on the expression levels of PKC β II in the hyperglycemic setting and its regulation by ROS. The role of additional PKC isoforms may also be important, and warrants further investigation. Furthermore, close attention should also be paid to the activity and intracellular localization of PKC isoforms, while specific means of isoform inhibition/activation should provide valuable

information. The use of H9c2 cells provides valuable model for the analysis of a wide variety of experimental assays. The cell line is easily maintained and can be experimentally manipulated by transfection or pharmacological treatments. The cells are, however, neonatal myoblasts and therefore prefer glucose as substrate *versus* the adult cardiomyocyte, which favors fatty acids. H9c2 cells also do not possess the ability to contract. These features mean that conclusions drawn from studies using H9c2 cells should be interpreted with caution when comparing to effects in the adult heart or cardiomyocyte. The lack of a LETO control in the OLETF study of thiamine treatment hampered our ability to draw firm conclusions and future *in vivo* studies should take this into account.

7.3. Future directions

For future studies we plan to further evaluate and clarify the molecular mechanisms involved in hyperglycemia-induced insulin resistance and perform additional studies to prove the unique model we here propose (refer Figure 6.30). We aim to employ more sophisticated *in vitro* techniques (including overexpression and siRNA transfections) and 'cause-and-effect' studies to rigorously evaluate the validity of this model. To further confirm these findings, we will also test our hypothesis in an *in vivo* context. Here we plan to perform additional studies on a genetically obese/insulin resistant (db/db) mouse model to evaluate the interplay between hyperglycemia, oxidative stress, NOGP activation and the onset of insulin resistance. Such investigations will be performed in a temporal manner to more precisely determine the sequence of events that lead to the development of insulin resistance, and related cardiac dysfunction in db/db mice. Successful completion of this study should

allow us to make valuable contributions toward understanding the etiology of insulin resistance/Type 2 diabetes and help identify novel therapeutic interventions to curb its onset. Moreover, our investigations in the heart should also contribute to an improved mechanistic understanding of the damaging link between insulin resistance and the onset of CVD, and point the way(s) ahead to disrupt this.

Appendix A – Modified radio-immunoprecipitation assay (RIPA) buffer

Modified radioimmunoprecipitation (RIPA) buffer – 100 ml

50 mM Tris-HCl, pH 7.4 (790 mg Tris dissolved in 75 ml dH₂O, add 900 mg NaCl, pH to 7.4 with HCl)

1% Nonidet-P40 (NP-40) – from 10% stock solution

0.25% sodium deoxycholate – from 10% stock solution

1 mM EDTA, pH 7.4 – from 100 mM stock solution

1 mM phenylmethylsulfonyl fluoride (PMSF) – from 200 mM stock solution (add just prior to use)

1 µg/ml leupeptin

4 µg/ml soybean trypsin inhibitor (SBTI)

1 mM benzamidine

1 mM sodium orthovanadate (Na₃VO₄)

1 mM sodium fluoride (NaF)

1 mM PUGNAc*

1% Triton X-100

All constituents, except PMSF, are added to a final volume of 100 ml, aliquoted and stored at -20°C

**PUGNAc is an O-GlcNAcase inhibitor and is added to blunt removal of O-GlcNAc moieties during the protein extraction procedure*

Appendix B – Bradford protein determination

Bradford stock solution (5X conc.)

Dilute 500 mg Coomassie Brilliant blue G250 in 250 ml 95% ethanol
 Add 500 ml phosphoric acid, mix thoroughly
 Adjust volume to 1 L with dH₂O
 Filter solution and store at 4°C

Bradford working solution

Dilute stock in a 1:5 ratio with dH₂O
 Filter with 2 filter papers

The filtered working solution should be a light-brown color – light sensitive!

Materials

1 mg/ml BSA stock solution (stored in freezer)
 Microcentrifuge tubes (7 for standards, 1 for each sample)
 dH₂O
 Ice
 Bradford working reagent
 Cuvettes
 Spectrophotometer

Protein determination:

1. Thaw the BSA stock solution
2. Thaw protein samples on ice if stored – keep on ice at all times
3. Make up a BSA working solution by diluting 100 µl BSA stock in 400 µl dH₂O, vortex thoroughly
4. Mark tubes – 7 for standards and 1 each for samples
5. Add BSA and dH₂O to standard tubes as indicated in the table below:

Protein standard (µg protein)	BSA (µl)	dH ₂ O (µl)
Blank	0	100
2	10	90
4	20	80
8	40	60
12	60	40
16	80	20
20	100	0

6. Add 95 μl dH_2O and 5 μl of each protein sample (cell or tissue lysate) to the appropriate tube
7. Vortex all tubes briefly
8. Add 900 μl Bradford working solution to each tube, vortex again
9. Incubate the tubes for at least 5 min at room temp. (*the reaction takes about two minutes to complete and is stable for up to 60 min*)
10. In the meantime, switch on the spectrophotometer, allow it to calibrate, and set the wavelength to 595 nm
11. Read absorbances, twice each, for each tube
12. If sample values fall outside the range of the highest protein standard, dilute with RIPA buffer
13. Use excel to draw a linear plot of standard absorbances, and calculate the protein concentration in each sample in order to make aliquots of equal protein amounts (in μg)

Appendix C – Western blotting protocol

Blue sample preparation

Laemmli sample buffer

dH₂O – 3.8 ml

0.5 M Tris-HCl, pH 6.8 – 1.0 ml

Glycerol – 0.8 ml

10% (w/v) SDS – 1.6 ml

0.05% (w/v) bromophenol blue – 0.4 ml

Materials

1.5 ml microcentrifuge tubes

Sharp tweezers

Ice

Heating block

β-mercaptoethanol

Microtube centrifuge

Vortex

Sample preparation:

1. Set the heating block to 95°C
2. Make up a working solution of sample buffer by combining 850 µl Laemmli buffer stock solution and 150 µl β-mercaptoethanol (*work in fume cabinet*), vortex thoroughly
3. Calculate the appropriate volume of each sample to give equal protein amounts (eg. 50 µg per sample) and calculate the number of sample sets needed
4. Label microcentrifuge tubes for each sample and sample set
5. Add a volume of working sample buffer equal to 1/3 of the total sample volume (2/3 protein + 1/3 sample buffer) as calculated, to each appropriate tube (*work in fume cabinet*)
6. Add the appropriate volume of protein sample to each tube
7. Punch small holes in the lid of each tube using the sharp tweezers
8. Heat samples on the heating block (95°C) for 5 min
9. Vortex each tube, spin down contents briefly (~10 seconds) and place on ice immediately
10. Samples can now be applied to gels for SDS-PAGE or stored at -20°C for future use

SDS-PAGE and Western blotting

Buffers:

10 X SDS running buffer (1 L)

10 g SDS

30.3 g Tris

144.1 g Glycine

Dissolve in 800 ml dH₂O

Adjust volume to 1 L using dH₂O

Store at room temperature

1X Transfer buffer (semi-dry blots) (1 L)

Dilute 100 ml of 10X stock solution (*from Bio-Rad*) in 500 ml dH₂O

Add 200 ml methanol (20% final conc.)

Adjust volume to 1 L with dH₂O

Store at 4°C

1X Transfer buffer (wet blots) (1 L)

2.9 g Glycine

5.8 g Tris

0.37 g SDS

200 ml methanol

Adjust volume to 1 L with dH₂O

Store at 4°C

Blocking buffer	Constituents
1% w/v BSA	1g BSA/100 ml 1X TBS-T
5% w/v BSA	5g BSA/100 ml 1X TBS-T
5% w/v fat-free milk	5g fat-free dried milk powder/100ml 1X TBS-T

Choice of suitable blocking buffer is dependent on specific antibody/antigen; blocking buffer must be filtered prior to use

SDS-PAGE:

1. Clean pairs of spacer plates and short plates, casting frames, casting stands and rubber gaskets
2. Place gaskets in grooves at the base of the casting stands

3. Assemble glass plates in green casting frames with the short plates facing to the front – push the clips outward to tighten the assembly and secure plates
4. Place the plate assembly onto the rubber gasket in the base of the casting stand, pushing down firmly while securing the clip
5. Add dH₂O between the plates to check for leakage
6. Get three small beakers, three disposable Pasteur pipettes and a small stirring bar
7. Label one beaker and add dH₂O to it, and label the other two beakers for the resolving and stacking gel respectively
8. Make up the required resolving gel according to the appropriate recipe:

Resolving gel recipes:

Gel constituent	6%	8%	10%	12%	15%
dH ₂ O	2.6	2.3	1.9	1.6	1.1
30% Acrylamide solution	1.0	1.3	1.7	2.0	2.5
1.5 M Tris-HCl, pH 8.8	1.3	1.3	1.3	1.3	1.3
10% w/v SDS	0.05	0.05	0.05	0.05	0.05
10% w/v APS	0.05	0.05	0.05	0.05	0.05
TEMED	0.004	0.003	0.002	0.002	0.002

Gel recipes are for 1 x 1 mm gel; values represent milliliter solution to be added to gel mixture

9. Add all constituents except the APS and TEMED, stir briefly and let solution stand for a few minutes to degas
10. Add APS and stir briefly (~30 seconds)
11. Add TEMED, stir briefly and quickly pour the gel mixture between the plates using a Pasteur pipette – be sure to avoid bubbles in the gel and leave enough space for the stacking gel (this can be checked beforehand by inserting a comb and marking the position)
12. Add a layer of dH₂O on top of the gel to prevent oxidation and bubbles
13. Allow gel to set for 1 hour while preparing 1:10 dilutions of SDS running buffer and TBS-T as well as the appropriate transfer buffer – place buffers in fridge to cool before use
14. After 45 min, start preparing the stacking gel:

4% stacking gel recipe:

Gel constituent	1 ml	2 ml	4 ml	8 ml
dH ₂ O	0.68	1.4	2.7	5.5
30% Acrylamide solution	0.17	0.33	0.67	1.3
1.0 M Tris-HCl, pH 6.8	0.13	0.25	0.5	1.0
10% w/v SDS	0.01	0.02	0.04	0.08
10% w/v APS	0.01	0.02	0.04	0.08
TEMED	0.001	0.002	0.004	0.008

Note: Different Tris-HCl buffers are used for stacking and resolving gels respectively

15. Once resolving gel has set, wash dH₂O off
16. Add APS and TEMED to the stacking gel solution and pour between plates
17. Gently insert appropriate combs, pushing down and avoiding bubble formation (make sure combs correspond to gel thickness)
18. Allow to set for 30 minutes
19. Retrieve standard protein marker from freezer and allow it to equilibrate to room temp
20. Retrieve samples from freezer (if previously stored) and equilibrate it to room temp (if samples have been prepared freshly, i.e. boiled, allow it to equilibrate to room temp)
21. Vortex each sample and spin down momentarily (~10 seconds)
22. Carefully remove combs from gels and gently wash wells with dH₂O
23. Remove plates from the casting stands and frames, and place in the U-shaped adaptor with the short plates facing inward
24. Insert assembly into the loading system and close the latches by pushing them inward while pushing down on the plates (the center will now form the buffer dam)
25. Fill the buffer dam with cold 1X running buffer until the buffer spills into the wells
26. Add 7.5 µl of the protein marker to the first lane on the far left of each gel
27. Add blue samples to the appropriate lane – use a micropipette and loading tips to apply the marker and samples
28. After loading of the gels, place the assembly inside a gel tank, fill the buffer dam to the top and add extra buffer into the tank – fill the tank to approximately 1 cm below the wells

29. Place the green lid with appropriate leads (black-to-black and red-to-red) on top of the tank and connect to the powerpack
30. Switch on the powerpack and perform an initial 10 min run at 100 V (constant) and 400 mA – this run will cause the samples to migrate through the stacking gel
31. Next, run the gels at 180 – 200 V until the sample dye front and smallest standard of the protein marker reaches the bottom of the gel – approximately 1 hour (running times may be adjusted according to the specific protein of interest)
32. Switch off power and disconnect electrodes before removing gel plates from the tank and assembly
33. Do not allow gels to stand at this point as proteins may dissolve from gels – move to electrotransfer step immediately

The choice of blotting procedure (wet vs. semi-dry) is mainly dependent on specific characteristics of the protein of interest, including size and solubility. Be sure to check these characteristics and employ suitable transfer method.

Electrotransfer (semi-dry blotting):

1. Cut two pieces of Bio-Rad extra thick blotting pads and one PVDF membrane per gel (cut these to the same size as the gel) – do this while the gels are running
2. Remove the prepared 1X transfer buffer from the fridge and get methanol ready – pour these solutions into separate tubs
3. Soak one blotting pad in transfer buffer and place on anode plate – role flat using a test tube to remove air bubbles
4. Soak the membrane in methanol for ~15 seconds, followed by soaking in transfer buffer
5. Place membrane on top of the pad and role flat
6. Carefully remove gels from glass plates using the green lifter – do so by holding the plates in one hand with your thumb on one side and other fingers on the other side, insert lifter between plates and gently lift the short plate with an upward motion, keeping both plates in

your hand – the gel should stick to one of the plates – place the plate with gel in transfer buffer and allow buffer to wash gel from the plate

7. Remove gel from the transfer buffer and place on top of the membrane – roll flat with the tube (be careful when handling gels as they are fragile)
8. Soak the second blotting pad in transfer buffer and place on top of the sandwich – roll flat
9. Insert the cathode plate and close the transfer system
10. Connect the electrodes and switch on the powerpack
11. Run at 0.5 A and 15 V for one to two hours (depends on size of protein of interest)
12. After transfer, remove membranes from system and place in 1X TBS-T to wash (see probing the membrane below) – gels may be stained using Coomassie blue to check transfer – membranes may also be stained with Poncaeu red before washing in TBS-T

Electrotransfer (wet blotting):

1. Cut two pieces of Whatman paper and one PVDF membrane per gel (8 X 6.3 mm)
2. Soak membrane in methanol for 5 – 10 min, and soak Whatman paper in transfer buffer
3. Retrieve 2 black fiber pads and soak in transfer buffer until use
4. Retrieve cassettes and assemble sandwich on black side as follows: black fiber pad, Whatman paper, gel (with marker on the right), membrane, Whatman paper, fiber pad – make sure to roll stack with a tube to remove bubbles
5. Close the cassette and place in the Transblot module (black side of cassette to black side of the module)
6. Place inside tank and fill with cold transfer buffer
7. Cover the tank with green lid (with electrodes inserted correctly)
8. Switch on powerpack and run at 160 mA (constant) for 90 min
9. Proceed to preparation of membrane

Preparing membranes for antibody probing

1. Remove membranes from transfer apparatus, place in a tub with TBS-T and wash 3X, 5 min each, on a bellydancer/shaker replacing TBS-T after each wash
2. Block membranes using suitable blocking buffer for 1 hour at room temp. (blocking buffer and time should be optimized depending on protein of interest)
3. Wash membranes 3 X 5 min each with TBS-T as before
4. Prepare primary antibodies by diluting in 5 ml TBS-T in a 50 ml falcon tube (the optimal dilution for each experiment should be determined, recommended dilutions for most antibodies are 1:1000 – 1:5000)
5. Incubate the membranes in the primary antibody overnight at 4°C while rotating on a tube roller
6. Wash membranes 3 X 5 min each with TBS-T as before
7. Prepare HRP-conjugated secondary antibodies by diluting in 5 ml TBS-T in a 50 ml falcon tube (the optimal dilution should be determined, recommended dilutions for most secondary antibodies are 1:4000 – 1:10 000)
8. Incubate membranes in secondary antibody for 1 hour at room temp. while rotating on a tube roller

Developing Western blots

1. Take ECL reagents from fridge and equilibrate to room temp., cut pieces of x-ray film (do so in the dark room), and prepare membrane cassettes by folding a booklet of transparencies on the inside
2. Wash membranes 3 X 5 min each with TBS-T as before
3. Prepare ECL substrate in a 1:1 ratio of reagent A and reagent B in a foil covered tube
4. Place membranes in a flat surface container and add ECL, spreading it evenly over the surface of the membranes
5. Incubate for 1 min at room temp.

6. Drain the ECL from the membranes and insert it between the two sheets of transparency, avoiding formation of air bubbles
7. Close the membrane cassette and go the dark room
8. Place a piece of film on the membrane to expose (best exposure time should be optimized, start off with 1 min and reduce or increase time accordingly)
9. Remove film from the cassette and place in developer solution until bands appear (this reaction takes about 7-10 seconds to occur)
10. Immediately remove film from the developer, wash thoroughly with water and place in fixer solution
11. Wash once more with water and allow film to dry